Dr. Sumit Kumar Jha
Harsh Shrivastava

RECENT TRENDS IN TRANSMISSION AND DISTRIBUTION

ALEXIS PRESS
JERSEY CITY, USA

RECENT TRENDS IN TRANSMISSION AND DISTRIBUTION

RECENT TRENDS IN TRANSMISSION AND DISTRIBUTION

Dr. Sumit Kumar Jha

Harsh Shrivastava

ALEXIS PRESS

ALEXIS PRESS

Published by: Alexis Press, LLC, Jersey City, USA
www.alexispress.us

First Published 2022

A catalogue record for this publication is available from the British Library

Library of Congress Cataloguing in Publication Data

Includes bibliographical references and index.

Recent Trends in Transmission and Distribution by *Dr. Sumit Kumar Jha, Harsh Shrivastava*

ISBN 978-1-64532-865-0

CONTENTS

CHAPTER 1

A COMPREHENSIVE STUDY ON DISTRIBUTION SYSTEM RESTORATION

Dr. Sumit Kumar Jha, Assistant Professor
Department of Electrical and Electronics Engineering, Presidency University, Bangalore, India
Email Id-sumitkumar.jha@presidencyuniversity.in

Abstract:

Because of advancements in infrastructure and the creation of cutting-edge measuring and communication technology, modern power systems are running more efficiently and consistently. However, power outages still happen and have a significant negative social and economic impact, particularly those brought on by natural disasters. In the paper author discusses the distribution system restoration, modified network radiality, and constraint of distribution.

Keywords:

Distribution System, Energy, Network, Power Flow, Transmission Line.

INTRODUCTION

The electrical energy utilized in commercial, industrial, and residential buildings is normally produced by a utility at such a central location, then transferred and delivered via the utilities power distribution system and transmission system to wherever it is needed. Electricity is managed, protected, transformed, and distributed securely to the customer through a utility power system of transmission and distribution. This building distribution system starts where the utilities power generation and transmission system terminate, which is often at a building regulated service entrance point. Transmission substations (also known as step-up transformers), transmission and distribution, distributions substations (sometimes known as step-down transformers), with distribution lines make up a utility power generation and transmission system. The many phases of transmitting energy across poles and cables from the supply to a residence or a place of business are referred to as generation and transmission. Electrical distribution and transmission are two different things. The voltage level during which electricity passes at each stage is the main distinction between the two. A network of electrical cables transports the power to both homes and businesses once it has been created from the resource, whatever the fuck that source may be. The electrical grid is made up of transmission and distribution system, which can be located above ground or buried.

Transmission: The interstate highway of power distribution is transmission. It refers to the component of energy distribution that involves transporting large amounts of power from the producing sites to substations located closer to locations where that electricity is needed. Larger, higher poles and towers known as transmission lines are used to transport numerous cables across longer distances. Large volumes of electricity are transported through transmission lines at high voltages; these levels are too high to be transmitted directly to a residence or place of business.

Distribution: Distribution is the grid's smaller population highway, if transmission is its interstate. The final stage of delivering electrical energy from the generator to the user is distribution. Transformers lower the voltage of power before it is transferred to the distribution system using transmission lines. A house or business can receive power from the distribution system at quite a voltage structure that meets for direct delivery. The lines that go down streets and up to your home, place of business, etc. were called distribution lines. Simply explained, in Table 1, transmission of electricity seems to be at a significantly greater voltage than distributing. Distribution lines are also the ones that are visible leading immediately to houses and businesses, whereas transmission lines are really the extremely large electric towers and cables people see.

Table 1: Illustrates the several parameters of transmission and distribution system.

Sl . No.	Parameters	Transmission	Distribution
1	Topology	Meshed	Radial
2	System Control	More Critical	
3	Electricity Market	Wholesale	Retail
4	Investments	Individual-more critical	Total- more critical
5	Quality of Supply		More Critical
6	Congestions	More Critical	

The interstate highway of power distribution is transmission. It refers to the portion of energy supply that involves transporting large amounts of power from the producing sites across great distances to substations located closer to the locations where electricity is most needed. Transmission lines can be identified by consumers as the larger, higher poles or towers carrying several cables over greater distances. Large volumes of power are sent via transmission lines at high voltages that are too high to be given directly to a building such as a house or office. Voltages exceeding 100 kV (100,000 volts) or higher are present in transmission system, transformers, power stations, and other equipment. Electricity distributors must often decrease the voltage of the power flowing through into the transmission line before delivering it to a home or place of business.

Transformers step down the electricity, especially the voltage level, transmitted over transmission lines and deliver it to distribution lines, which have been subsequently linked to households and businesses. Distribution is like the city street to transmission's major highway throughout the grid. It is the final stage of the transmission of electrical energy from the generator to the end user. Power can be sent directly to a house or business thanks to the distribution platform's voltage level. The lines that many people observe running along roadways are distribution lines. The electricity human’s use every day to keeping our food fresh, with us clothing clean, and our houses either cool or warm is known as distribution. Distribution lines, which many people see now in their communities, have a voltage of around 13 kV (13,000 volts), while a normal home uses 110 volts.

Main elements of a transmission line:

The three-phase, three-wire overhead technique is widely utilized to transmit electricity generation due to cost factors. Here are the primary basic components power system.

Conductors: six conductors for a double circuit's line and three conductors for a single circuit line. Conductors need to be the right size (i.e. cross-sectional area). This is dependent on its capability right now. Conductors with an aluminum-core steel reinforcement, or ACSR, are often utilized.

Transformers: Step-up and step-down models are used to increase and decrease the voltage level, respectively. Transformers make it possible to transport power more effectively.

Line Insulators: These devices mechanically support individual line conductors and electrically isolate them from of the support towers.

Towers of Support: to help the line conductors that are suspended in the air above.

Protective Devices: to safeguard the transmission system and guarantee reliability. Ground wires, lightning arrestors, circuit breakers, relays, and other components are among them.

Voltage Regulators: To maintain the voltage at the receiving end within allowable ranges.

LITREATURE REVIEW

Roofegari Nejad [1] et al. have explained resilient power system can quickly and effectively recover from outages brought either by natural disasters or man-made assaults. Transmission and distribution system operators (TSOs and DSOs) work together too quickly and reliably restore the system after a significant blackout. However, these two systems are often run independently without taking into account the strengths and weaknesses of each particular network or how they interact. This can cause the repair to take longer and provide less useful results. As a result, this research has established a distributed technique for integrated transmission and distribution systems restoration (ITDSR). By exchanging restricted boundary bus information in an iterative process, the distributed algorithm, which is based on the alternate direction method of multipliers (ADMM), may enable coordinated restoration for the both TSOs and DSOs. Convex AC Power Flow Model but also Three-Phase Unbalanced Branch Flow Model are both included in the ADMM-ITDSR model. In order to serve high priority loads across several networks, the ITDSR approach organizes the operation of dispersed energy resources. During testing of the integrated IEEE test cases, including such 14-bus transmission with 13-node distribution systems and 39-bus transmission having 123-node distribution systems, the usefulness and benefit of established models and algorithms are tested and proved.

Zhao Jin [2] et al. have to achieve effective coordinated restoration of the linked transmission and distribution (TS-DS) system, a novel decentralized restoration strategy has been developed. First, the TS-DS system is split into multiple subsystems according to their physical connection in order to account for the independent operations of the TS operator (TSO) and DS operators (DSOs) and to lessen the load on the TSO data processing. Then, using model decoupling but also iterative interaction between TS and DS, a decentralized decision-making framework is developed in order to implement the subsystems' autonomous but coordinated decision-making. Furthermore, a novel decentralized optimization technique is created to achieve the best coordinated restoration approach for the TS-DS system in order to ensure that the iterative procedure with non-convex models converges. The suggested decentralized restoration technique resolves the decentralized optimization method's non-convergence issue and allows the TSO and DSOs inside the coupled TS-DS system to make separate decisions. Utilizing two IEEE standardized test systems as well as an actual power system, the efficacy of the suggested technique is confirmed.

Nguyen [3] et al. have a software framework that is open-source and designed particularly to allow for rigorous dynamic performance assessment of trans active energy solutions for end-to-end electric power systems. The platform simulates a centrally controlled wholesale power market that operates over a transmission grid connected to one or even more distribution systems, with each distribution system made up of a group of grid-edge resources that operate over a distribution grid. Results from test cases are offered to show the platform's functionality. The test scenarios simulate a transmission system connected to a distribution system where homes are made up of both traditional loads and smart, price-responsive appliances. The Power Matcher, a well-known bid-based Tran's effective energy design, is used to perform transactions there at distribution level.

Wang [4] et al. have highlighted how the links between transmission networks (TNs) and distribution networks (DNs) are getting closer as a result of the widespread integration of distributed generators (DGs), particularly in the areas of reactive power and voltage. Problems with optimal reactive power flow (ORPF) for TN and DNs really aren't appropriate for independent solution. This research presents a distributed ORPF approach for global transmission and distribution (T&D) networks based upon heterogeneous decomposition (HGD) because of the fact that TN and DNs are run by various control centers. The global T&D-ORPF issue may be divided into the TN-ORPF master, DN-ORPF slave, and boundary consistency coordinating sub-problems by taking into account the features of the master-slave structure. The TN-ORPF or DN-ORPF sub-problems may be solved using any of those optimization techniques based on duality and gradients theory. The discrete control variables may be sequentially discretized and made differentiable by the addition of a punishment function towards the optimization method. The worldwide ORPF issue of T&D networks is decoupled using boundary sensitivities created by boundary dual multipliers. Transferring the boundary variables but also sensitivities between both the TN control center and DN central management results with the same result as the centralized optimization. The HGD algorithm's effectiveness is shown by the simulation results for IEEE 30-bus (TN) & modified IEEE 33-bus (DN) test systems with numerous DGs.

Tang [5] et al. have integrated operational risk assessment (I-ORA) method is suggested in order to address the needs of accurate operational threat assessment of integrated transmission and distribution networks (I-T&D). Examples show that I-ORA is required because it accurately handles the connection between the transmission and distribution networks, analyzes changes in significant customers' power supply modes (PSMs), and aids in enhancing the security and stability of the operation of the power grid. I-ORA method successfully satisfies two important technological requirements: integrated topology evaluation and interconnected power flow computation. The integrated power flow calculation, utilizing the self-adaptive Levenburg-Marquard technique and Newton method, can be utilized to assess risks of heavy load/overload and voltage discrepancy. In certain contingencies, integrated configuration analysis is employed to evaluate risks of substation power cuts, network splits, and PSM changes of significant users. Additionally, certain computation-intensive stages are concurrently processed using the graphics processing unit. The suggested I-ORA method can achieve accurate evaluation for the full I-T&D, according to numerical trials. Additionally, the efficiency and stability are satisfactory, indicating that the proposed I-ORA method may considerably improve future real-world I-T&D coordination operations.

Venkatraman [6] et al. discussed the development of techniques and software that really are numerically stable while also properly simulating dynamic events that may occur in real-world systems is necessary for combined transmission and distribution systems (CoTDS) modeling for power systems. The combined simulation is highly difficult since the time scales of the simulations might differ by orders of magnitude. This has prompted further study into the use of co-simulation approaches for simultaneous simulation of two systems. The transmission system but also distribution systems' parallel and series computations are used in this research to suggest two methodologies for the dynamic co-simulation of CoTDS. The influence of the integration time-step on the suggested CoTDS dynamic co-simulation techniques is investigated, and the convergence of numerical methods within co-simulation is addressed from a basic mathematical viewpoint. Inside a single time-domain simulation environment, the validity of both of these co-simulation techniques is tested against complete system simulation. Additionally, a commercial EMTP dynamic simulation is used to test the proposed CoTDS co-simulation approach. For a thorough fault-induced delayed amperage recovery simulation investigation, CoTDS dynamic co-simulation is even further proven on a New England 39-bus transmission network with ten load buses substituted with distribution systems, including a 5780-node distribution network on one load bus.

Müller [7] et al. have explained the shift to renewable energy and increasingly decentralized power generation necessitates the growth of the grid and of storage at all voltage levels. Planning for power systems nowadays focuses on certain voltage levels or spatial resolutions. In this paper, we introduce eGo, a top-down built open-source software solution that can maximize grid and storage growth across all voltage levels. Applying a multi-period linear optimum power flow while taking into account the grid infrastructure of extra-high and high-voltage (380 to 110 kV) level minimizes operation and investment expenses. As a result, the high-voltage level is integrated into the optimization issue, partially dissolving the common differentiation of the transmission and distribution grid. In order to reduce the medium and low voltage grid expansion demands that are subsequently identified, optimum curtailment and storage units are assigned in the medium voltage grid. Here, non-linear power flow-based heuristic optimization techniques were created. We came up with a cost-effective grid and storage expansion for any and all voltage levels in Germany by using the tool on future scenarios. Because of the integrated approach, grid expansion costs for medium and low voltage grids may be greatly reduced while storage growth and curtailment also contribute to the system's overall performance. However, the impact on costs throughout all of Germany was minimal. Instead, significant total reductions were achieved by taking into account genuine, geographically diverse time series.

Pilatte [8] et al. have explained how to create synthetic, mixed transmission and distribution network models using an open-source MATLAB toolkit. These can be used to analyze the relationships between transmission and various distribution systems, including the provision of ancillary services whilst also active distribution grids, the co-optimization of operations and planning the creation of emergency protection and control plans spanning various voltage levels, the analysis of aggregate market aspects, etc. Since the created test-system models may be readily customized, the user has the freedom to choose the required properties, such as the degree of renewable energy penetration, overall size of the finished system, etc.

According to the Lampropoulos [9] et al. hierarchical control architecture be used to allow aggregation entities to provide flexibility services in power systems. The day-ahead market optimization function of wholesale energy trading as well as ancillary services to the operators of

a transmission and distribution networks, such as the provision of automated frequency restoration reserves and peak shaving services, are the main areas of attention. The control structure is universal, expandable, and well-suited to handle all the various demands coming from lower levels, such as devices or users, up to distribution and transmission levels. In order to avoid disputes between operators of both the transmission and distribution networks when acquiring supplementary services with opposing goals, processes must be established. The framework is used on a case study that focuses on a collection of Dutch residential buildings that are outfitted with solar installations and battery-based energy storage devices. While the simulation scenarios consider the effects of various degrees of generation and consumption forecasting errors on economic performance, the yearly costs and benefits are derived using historical market data. The results of computer simulations provide a useful perspective on the variations in aggregator firms' business models and the possibilities of the marketplaces under investigation. The value calculation of peak shaving services there at distribution level is part of the economic evaluation. Increased procurement costs for these services are anticipated to encourage distribution system administrators to invest in expanding grid capacity.

Wang [10] et al. have introducing more vibrant and competitive power market is being incorporated into the Chinese power system. The business model and impact on the financial capability of the Chinese power-grid corporations have been modified by transmission and distribution tariff rules. This research examines the precise reform's substance, the calculations for each component of the financial capacity of a power grid, and the features of component interaction and feedback. They use the system dynamics theory to build a financial capacity model on top of this. In order to conduct empirical and sensitivity studies, they used a power-grid corporation as our case study. We then proposed management plans and policy suggestions.

Surana [11] et al. have highlighted that compensatory power generation and therefore unforeseen GHG emissions are caused by poor transmission and distribution (T&D) infrastructure that causes losses as energy goes from provider to consumer. Losses inside the T&D system from theft, inadequate planning, and management may also raise the overall amount of power produced. Mitigation efforts often concentrate on energy produced rather than delivered since the mix of electricity generating, combined heat and power production, and thermal plants account for nearly 40% of world GHG emissions1. In order to limit possible emissions from compensating generation following T&D aggregate losses (that is, technically and non-technical) in 142 countries, we integrate life cycle evaluations of power production with uncertainty analysis. According to our calculations, the losses from T&D infrastructure are responsible for roughly 1 billion metric tons of carbon dioxide equivalents in power each year (GtCO2e yr–1). Researchers estimate that improvements throughout technical losses and aggregate losses might result in emissions reductions of 411 and 544 million metric tons of carbon dioxide equivalents each year (MtCO2e yr-1), respectively. Not only could compensatory pollutants be decreased by lowering T&D losses, but more energy from investments in low-carbon power plants could also reach the intended users.

DISCUSSION

On the other hand, since there aren't enough stable power sources, distribution system outages brought on by transmission system problems are more difficult to repair. It is now feasible to power outage loads without the assistance of the transmission lines thanks to the increasing penetration of distributed energy resources (DERs) in distribution systems. In order to restore service in distribution networks, the idea of a micro grid was created. After natural catastrophes,

the outage distribution system was divided into several micro grids using a multiagent paradigm. The sectionalization of the outage distribution systems into radial islands via spanning tree search methods. To account for scattered generator characteristics, load pickup, etc., multi-stage and multi-time step DSR techniques were examined in and, respectively. Mixed-integer linear programming was used to develop the load restoration inside the distribution systems. In [24], the three-phase imbalanced distribution system was taken into consideration, and heuristic techniques were used to determine the best DSR approach. An approximate polyhedral method was used to linearize the three-phase power flow during the DSR step. A Tabu search technique was used to examine and resolve the problem of cold load pickup after a substation level outage. To examine the sequential restoration of three-phase unbalanced distribution systems with dispersed generators, a linearization approach was developed. It established a structure to organize the rehabilitation of the transmission system and distribution system in tandem. The following research gaps may be found despite the fact that the contributions of DERs towards accelerating DSR have been accurately predicted and quantified in the literature to date:

Although distribution networks are fundamentally imbalanced, the majority of DSR research concentrated on balanced distribution systems. We looked at three-phase power flows. A heuristic method was used;however, it cannot be guaranteed to find the best answer. Due to the test systems' existing radial nature, the topological limitation was disregarded in. To ensure the radially in but also to prevent the possibility of reconnecting islanded micro grids, sequential limitations were established. In works like, the dispatch of DERs is restricted to direct load control, but the optimum scheduling of DERs is included into DSR models. Therefore, only large-scale, utility-managed DERs are taken into account, disregarding the overwhelming majority of small-scale DERs with more varied features. In other words, system operators are permitted to regulate all DERs. DER flexibility, fault propagation, and other uncertainty variables like outage length are poorly characterized. In order to decrease complexity, robust optimization was used, although the DSR only takes into account one time slot. Based on the assumption that all potential line failures were known beforehand, scenario-based stochastic programming was applied. Existing DSR models may produce unworkable solutions if uncertainty considerations are not properly taken into account.

To fill up the gaps in current research, a DSR approach that can dynamically alter the topologies and DER schedules was presented. First, a model of the three-phase unbalanced distribution system as well as a correct linearization of the unbalanced power flow are performed. The established DSR model takes into account both local faults and breakdowns in the upstream transmission system, therefore it does not need electricity from substations. In light of certain outage conditions, the distribution system may be divided into one or more islands. Depending on outage information as well as the flexibility limits of DERs, the topological restrictions are re-designed in the created DSR model to construct a flexible number of radial islands. In this research, two DER kinds are taken into account: Rooftop photovoltaics (PVs) and energy-efficient home appliances are examples of aggregator-managed DERs. Utility-managed DERs include energy storage systems and medium-scale distributed generators. To get over the second obstacle, a hierarchical structure made up of a system operator and several load aggregators is used. Aggregators are in charge of planning customer and aggregator-managed DER energy consumption, whereas the system operator is in charge of keeping track of the distribution system's condition and carrying out the tasks required to reach DSR. The system operator and aggregators may work together to make the most of DERs' flexibility in order to speed up DSR without endangering consumers' privacy. Model predictive control (MPC) is used for uncertainty

modeling and is incorporated with the hierarchical DSR structure. As a result, the system operator as well as the aggregators may modify the DSR approach dynamically depending on the most recent prediction data to address forecast inaccuracies.

Modified Network Radiality

Constraints the typical radial operation of distribution networks, which has not been addressed, Existing studies have looked at the radiality limits. When a distribution system has to be reconfigured but only has one radial network, the spanning-tree restrictions and virtual power flow approach may be used to establish the radial topology. Although many radial subnetworks may be accommodated by radiality restrictions, the number of subnetworks is set and known beforehand. The islanded micro grid formulation should be adaptable to the system circumstances and DER capabilities, nevertheless, in distribution system restoration issues when the system failure scenarios and DER generating capacities are unclear. Therefore, without appropriate adjustment, the current approaches cannot be used directly. In order to guarantee the radiality of the reconfigured distribution system with a changeable number of islands, a novel set of radiality requirements that differ from the conventional spanning-tree constraints is devised in this study. The conventional spanning-tree restrictions are as follows:

$$\mu_{ij}^{+} + \mu_{ij}^{-} = \gamma_{ij}\ ,\ \forall ij \in \Omega^{\mathrm{L}}$$

$$\mu_{ij}^{+} \geq 0,\ \mu_{ij}^{-} \geq 0,\ \forall ij \in \Omega^{\mathrm{L}}$$

$$\sum_{j \in \Omega^{\mathrm{N}}} \mu_{ji}^{+} = 0,\ \forall i \in \Omega^{\mathrm{S}}$$

$$\sum_{j \in \Omega^{\mathrm{N}}} \mu_{ji}^{+} = 1,\ \forall i \in \Omega^{\mathrm{N}} \backslash \Omega^{\mathrm{S}}$$

The restriction prevents virtual traffic from passing via opened distribution lines. As illustrated, the virtual flow directions were nonnegative. The source nodes cannot have virtual flow injection, per the constraint. Virtual flow is injected from a certain feeder as limited for other nodes. The spanning tree restrictions, however, have the following drawbacks: Each split island has a different source node;thus, the number distinct restoration islands correspond to the amount of source nodes. This does not always happen when power generating capacity is insufficient to provide all the loads. Unrestored load nodes need to be enabled while optimizing the DSR for the first restriction. No virtual flow will indeed be injected into a node if it is not recovered.

$$\sum_{j \in \Omega^{\mathrm{N}}} \mu_{ji}^{+} = \kappa_i\ ,\ \forall i \in \Omega_{\mathrm{N}} \backslash \Omega_{\mathrm{S}}$$

To get around the second restriction, it should also be possible to vary the number of islands. According to graph theory, the number of linked nodes and the quantity of repaired lines may be correlated if a distribution system is split into NI radial sub networks:

$$\sum_{i \in \Omega^{\mathrm{N}}} \kappa_i - \sum_{ij \in \Omega^{\mathrm{L}}} \gamma_{ij} = N^{\mathrm{I}}$$

The number distinct formulated islands in a distribution system having NS source nodes at time step t should not be more than the number of source nodes.

$$1 \leq N^{\mathrm{I}} \leq N^{\mathrm{S}}$$

To provide power supply & maintain stability, substations and nodes with sizable controlled generating assets are often thought of as the source nodes. These days, inverter-based DERs may potentially be able to construct a grid with the right control methods. Substation nodes and all DERs administered by utilities are thus considered possible source nodes in this study. A DER will be omitted from S if it lacks the capacity to create grids. Since their capabilities are often constrained, aggregator-managed DERs are not included. An auxiliary binary variable I is added to change the initial spanning tree restrictions to account for the possibility of merging several source nodes into one island:

$$\sum_{j \in \Omega^{\mathrm{N}}} \mu_{ji}^{+} = \tau_i \, , \; \forall i \in \Omega^{\mathrm{S}}$$

$$\sum_{i \in \Omega^{\mathrm{N}}} \tau_i = N^{\mathrm{S}} - N^{\mathrm{I}}, \; \forall i \in \Omega^{\mathrm{S}}$$

$$\tau_i \in \{0, 1\} \, , \; \forall i \in \Omega^{\mathrm{S}}$$

At the source nodes, virtual flow injection is enabled. The number of source nodes using virtual flow injection is determined if NI islands are formed. The updated spanning tree restrictions for combining permit a configurable number of islands, each of which may have numerous source nodes. It should be noted that the updated virtual flow directions no longer represent the directions in which electricity really flows through the distribution system. To account for potential distribution line failures, a new limitation is established. The restriction mandates that distribution lines with faults won't be repaired.

$$\gamma_{ij} \leq 1 - \gamma_{ij}^{\mathrm{F}}, \; \forall ij \in \Omega^{\mathrm{L}}$$

However, even with numerous DERs functioning as source nodes, the updated spanning tree constraints by themselves do not ensure radiality at all islands. This study introduces a concept called virtual flow balancing to ensure connection throughout each separated island as mentioned below:

$$p_{i,t}^{\mathrm{VS}} - p_{i,t}^{\mathrm{VD}} = \sum_{ij \in \Omega^{\mathrm{L}}} \left(p_{ij,t}^{\mathrm{V}} - p_{ji,t}^{\mathrm{V}} \right)$$

$$0 \leq p_{i,t}^{\mathrm{VS}} \leq (1 - \tau_i) M$$

$$p_{i,t}^{\mathrm{VD}} \geq \kappa_i$$

$$0 \leq p_{ij,t}^{\mathrm{V}} \leq \gamma_{ij} M$$

Constraints

The restoration of a distribution network may be formulated as a restricted, non-differentiable multi-objective problem that is affected by power restrictions, topology constraints, the accessibility of RDGs, the frequency of the system, and other factors. The suggested SR issue has a number of limitations, which are classified and discussed.

Power Flow Constraints

Kirchhoff's rules and the Ohm law must agree in the DN, and this is ensured using power flow equations. For the repaired network to function reliably, the power flow equation must be met. Typically, the fundamental power flow equations are expressed in terms of powers for each node.

$$\begin{cases} P_{si} - P_{Li} = U_i \sum_{j=1}^{N} z_l U_j \left[g_l \cos(\theta_l) + b_l \sin(\theta_l) \right] \\ Q_{si} - Q_{Li} = U_i \sum_{j=1}^{N} z_l U_j \left[g_l \cos(\theta_l) + b_l \sin(\theta_l) \right] \end{cases}$$

In this equation, Psi and Qsi stand for the active and reactive power injected on node I PLDi and QLDi for the active and reactive power of connected load at node I zl stands for the binary nature of division l of the network connecting nodes I and j, as well as bl stands for the conductance and susceptance of branch l. N is the set of nodes in the network. Power flow calculations should handle additional RDG nodes correctly as a result of the introduction of RDG. Reference states that the typical handling strategy for various RDG node types is to simplify it into a negative load. If RDG nodes are operated in synchronism modes with a network, they are considered negative charges in this paper's power flow computation. The power flow balancing equations again for restored distribution system are altered as follows if the RDG integrates onto node i:

$$\begin{cases} P_{si} + P_{R\,DG\,i} - P_{Li} = U_i \sum_{j=1}^{N} z_l U_j \left[g_l \cos(\theta_l) + b_l \sin((\theta_l)) \right] \\ Q_{si} + Q_{R\,DG\,i} - Q_{Li} = U_i \sum_{j=1}^{N} z_l U_j \left[g_l \cos(\theta_l) + b_l \sin((\theta_l)) \right] \end{cases}$$

PRDGi and QRDGi stand for the reactive and active power of RDG at node I respectively. Once the network has been reorganized, the topological structure would have changed. It is important to continually compute the network power flow using the proper calculation techniques based on the power flow equation limitations. The forward-backward sweep approach has been used in this article to estimate the network power flow. The method's step-by-step procedure is described in represents Node I's maximum voltage for the recovered network.

$$V_{i\min} \le V_i \le V_{i\max},$$

Where Vi is the voltage amplitude of node i, Vimin, and Vimax are the lower limit and upper limit of node voltage.

CONCLUSION

In order for the envisioned smart grid to be self-healing, service restoration is crucial. When genuinely sized grids and multi-type defects are taken into account, this creates a massive and unsolvable challenge. For DN under various failure types, a hierarchical restoration approach is provided to address the SR issue. Four levels make up the restoration mechanism: dynamic topology analysis, RDG Island partitioning algorithms, reestablishing network connection via network reconfiguration, overall network optimization. The dynamic topology issue is solved in the first layer by the master problem, which also determines the service restoration plan and the out-of-service zones.

References:

[1] R. Roofegari nejad, W. Sun, and A. Golshani, "Distributed Restoration for Integrated Transmission and Distribution Systems With DERs," *IEEE Trans. Power Syst.*, vol. 34, no. 6, pp. 4964–4973, Nov. 2019, doi: 10.1109/TPWRS.2019.2920123.

[2] J. Zhao, H. Wang, Y. Liu, Q. Wu, Z. Wang, and Y. Liu, "Coordinated Restoration of Transmission and Distribution System Using Decentralized Scheme," *IEEE Trans. Power Syst.*, 2019, doi: 10.1109/TPWRS.2019.2908449.

[3] H. T. Nguyen, S. Battula, R. R. Takkala, Z. Wang, and L. Tesfatsion, "An integrated transmission and distribution test system for evaluation of transactive energy designs," *Appl. Energy*, 2019, doi: 10.1016/j.apenergy.2019.01.178.

[4] J. Zhao, Z. Zhang, J. Yao, S. Yang, and K. Wang, "A distributed optimal reactive power flow for global transmission and distribution network," *Int. J. Electr. Power Energy Syst.*, 2019, doi: 10.1016/j.ijepes.2018.07.019.

[5] K. Tang, S. Dong, J. Huang, and X. Ma, "Operational risk assessment for integrated transmission and distribution networks," *CSEE J. Power Energy Syst.*, 2019, doi: 10.17775/CSEEJPES.2020.02490.

[6] R. Venkatraman, S. K. Khaitan, and V. Ajjarapu, "Dynamic Co-Simulation Methods for Combined Transmission-Distribution System with Integration Time Step Impact on Convergence," *IEEE Trans. Power Syst.*, 2019, doi: 10.1109/TPWRS.2018.2874807.

[7] U. P. Müller *et al.*, "Integrated techno-economic power system planning of transmission and distribution grids," *Energies*, 2019, doi: 10.3390/en12112091.

[8] N. Pilatte, P. Aristidou, and G. Hug, "TDNetgen: An open-source, parametrizable, large-scale, transmission, and distribution test system," *IEEE Syst. J.*, 2019, doi: 10.1109/JSYST.2017.2772914.

[9] I. Lampropoulos, T. Alskaif, J. Blom, and W. van Sark, "A framework for the provision of flexibility services at the transmission and distribution levels through aggregator companies," *Sustain. Energy, Grids Networks*, 2019, doi: 10.1016/j.segan.2018.100187.

[10] Y. Wang *et al.*, "Chinese power-grid financial capacity based on transmission and distribution tariff policy: A system dynamics approach," *Util. Policy*, 2019, doi: 10.1016/j.jup.2019.100941.

[11] K. Surana and S. M. Jordaan, "The climate mitigation opportunity behind global power transmission and distribution," *Nature Climate Change*. 2019. doi: 10.1038/s41558-019-0544-3.

CHAPTER 2

OVERVIEW ON ELECTRICITY TRANSMISSION

Ms. Priyanka Ray, Assistant Professor
Department of Electrical and Electronics Engineering, Presidency University, Bangalore, India
Email Id-priyanka.ray@presidencyuniversity.in

***Abstract*:**

The large-scale transport of electrical energy from producing power plants to electrical substations is known as electric power transmission. High voltages are used to transfer electricity across long distances, reducing the amount of power lost. In this paper author is discusses the firm transmission right, efficient use of the electric power system, and requirements for firm transmission rights.

***Keywords*:**

Power,Energy, Substation, Transmission Tower, Electricity.

INTRODUCTION

Electric power transmission is the method used to convey massive quantities of energy generated from power plants, such commercial-scale solar installations, over vast distances for ultimate usage by customers. The North American complicated network, a huge network comprising electric power lines and related infrastructure across the United States, North, and Mexico, receives electricity from electricity generation plants throughout North America. Transmission often occurs at high voltage due to the large amount of power involved and the characteristics of electricity (69 kV or above). Typically, electricity is transported to a substation close to a metropolis. The high voltage power is reduced to lower voltages suited for consumer use at the substation before being distributed to end customers through (relatively) low-voltage electrical cables. If no acceptable transmission infrastructure were already in place, new transmission lines and related facilities would need to be built for newly built solar energy generating plants. A variety of environmental effects would result from the development, use, and abandonment of high-voltage transmission lines and related infrastructure. The size, kind, and length of both the transmission line, as well as a number of other site-specific criteria, will all have an influence on the type and extent of the impacts that come with its construction, operation, and dismantling. High-voltage electric transmission cables and related facilities' principal parts include:

Transmission Towers

The part of a power transmission system that is most noticeable is the transmission tower. They serve the purpose of maintaining the high-voltage conductors' (power lines') separation from the environment and from one another. There are several different tower designs that often use an open lattice work or a magnetic dipole, however they are all very tall metal constructions (a 500 kv tower may be 150 feet tall having cross arms as broad as 100 feet). An overhead wires line is supported by a tall structure known as a transmission tower, often referred to as a power transmission building, power tower, or energy pylon. Utility poles are often used to support lower-voltage sub-transmission and distribution lines which transport electricity from

distribution transformers to electric customer base in power grids. Overhead transmission lines are used to bring bulk electric power from generation facilities to electrical substations. The massive transmission cables must be carried by transmission towers at a suitable, safe height above the ground. Additionally, all towers must withstand a variety of natural disasters. Therefore, designing transmission towers is a crucial engineering task where civil, mechanical, and electrical engineering principles may all be used. One essential component of a system for transmitting electricity is a transmission tower. Figure 1 shows the components of a power transmission tower:

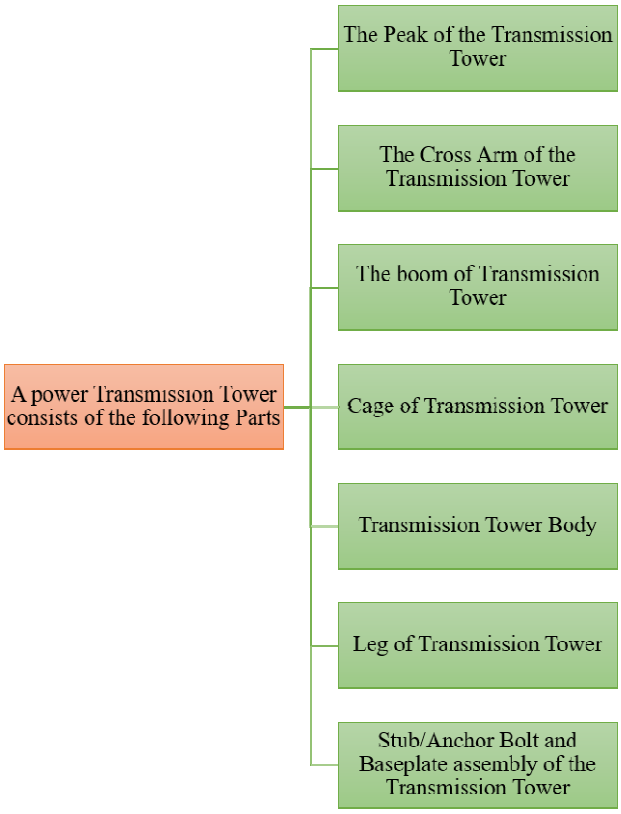

Figure 1: Illustrates the Power Transmission Tower consists of the following Parts.

Conductors (Power lines):

Electricity travels through and to customers along power lines known as conductors. For each electrical circuit, many wires are typically hung on a tower. The majority of conductors are made of twisted metal filaments, however more recent conductors may also include ceramic fibers in an aluminum matrix for increased strength and lower weight. Another of the most crucial parts of overhead cables is the conductor. As crucial as choosing a reasonable conductor size and reasonable transmission voltage is choosing the right type of conductor with overhead lines. The following characteristics a competent conductor need to possess:

- High electrical conductivity.
- High tensile strength to withstand mechanical stresses.
- Relatively lower cost without compromising much of other properties.
- Lower weight per unit volume.

Substations

Currently, there is a rising need for electricity, which can be met by power producing substations. Power producing substations come in a variety of forms, including thermal, atomic, and hydroelectric. Substations are being built at various places depending on the resources that are available, however these locations might not be closer towards load centers. The load center has the ability to do the real power use. Therefore, it is crucial to carry electricity from the substation towards the locations of the load centers. So, for this function, high-capacity, long-distance transmission networks are needed. Substations transform the extremely high voltages needed for electric transmission into lower voltages enabling consumer usage. Substations range in size and construction, although they can span a large area. They are usually cleared of vegetation and have a gravel surface. They are often walled and have a dedicated access road. Substations often have a variety of buildings, conductors, fences, lighting, and other elements that give the location a "industrial" aspect. Although power is reasonably produced at low voltage levels, supplying it at high voltage levels is less costly. Between the producing station and the consumer ends, a number of switching and transformation stations must be built in order to maintain high and low voltage levels. Those two stations are typically referred to as electrical substations.

LITERATURE REVIEW

Jiang Yu [1] et al. highlighted how China's uneven social-economic growth and resource endowments were overcome via the use of interprovincial energy transmissions. A bottom-up technology-based approach is used to project water consumption in the provinces that export power as well as potential water savings in the provinces that receive it. The findings show that, in 2014, owing to disparities in the water productivity of the electric power industry between exporting and importing provinces, energy transfers provided a co-benefit of saving 20.1 billion m3 of water nationwide. 10.98 billion M3 of the nation's precious water are saved via electrical transfers, accounting for regional water strains. Furthermore, it is anticipated that the provinces that export power would consume an extra 3.22 billion m3 of water for the 12 new transmission lines that China has suggested. A total of 16.97 billion m3 of water consumption will be saved nationwide when more water-intensive technologies, such as open-loop cooling, are used more often in the provinces that get power. In all locations, water use efficiency for electricity generation has to be increased. While electricity exports should be moved from water-stressed areas to water-abundant ones, transmitted power imports should still be promoted in water-scarce regions to reduce their water stressors. Energy transformation within Southern China's water-rich region might be enhanced by using gas-fired capacity and hydropower.

Chunyan Wang [2] et al. introduced 34–38% of Chinese citizens have lived in areas with severe water shortages for at least one month each year. However, owing to the mismatch between the population of the energy-receiving region living in water-abundant regions and the water shortage experienced in the region that exports power, the danger of water scarcity may be further increased by interregional electrical transmission. This research rigorously estimated this extra water shortage risk throughout China using specific thermal/hydropower plant data and a water scarcity index at the water basin size. Affected people, or those who reside in basins with lesser water scarcity but need energy produced in basins with greater water scarcity, are estimated to number 134 million, or 10% of China's total population. Over 60 million of these individuals, the bulk of whom resided in Southern China, were classified as severely impacted

population, meaning they relied on energy produced in areas of acute or extreme shortage to power their homes. If the planned transmission projects are carried out, this results in a 12% increase in the population that is water-stressed. On the other side, the inter-regional electrical transfers would serve a greater number of people, or 285 million. They depended on the power produced by basins with more plentiful water. It was discovered that hydroelectricity was more successful in reducing water shortage than intra-grid thermal energy transmission. It was found that the southern region of China had worse environmental performance when coordinating their water endowment with the production of power because it used energy from basins with low water tables instead of basins with adequate water tables.

Stadelmann-Steffen and Isabelle [3] have problem of how information provision impacts individuals' attitudes about various technical solutions centers on citizens' attitudes toward new technologies in energy transmission. Thus, it is thought that information's applicability depends on how it is presented and whether a technology is emerging or well-established. Transmission of electricity is related to the changeover of energy systems from nuclear and fossil fuels to renewable sources. As a result, the findings add to the current discussion on how to effectively incorporate new technology solutions in renewable energy policy. The study's experimental split ballot design for testing information effects on the basis of new data from a large-scale population survey performed in Switzerland is used in the paper's methodology. The findings show that although public perception of traditional technologies is mostly steady, information about new technology advancements is met with substantial popular reaction. This is especially true if the material highlights the drawbacks and unknowns of emerging technology. Furthermore, the simultaneous presentation of good information can hardly make up for such unfavorable information.

Peter [4] et al. have project investigates perceptions of enduring worry over high-voltage electrical overhead transmission lines (HVOTL). Homeowners' concerns about pertinent externalities may be thoroughly examined using psychometric, cultural, and more general risk analysis frameworks. The most important impressions, which were examined through a telephone poll in Queensland, Australia, are thought to relate to threats integrated with technology. The main externalities are noise and visual impacts, but they hide more serious concerns with electric and magnetic fields (EMFs). Less anxiety is felt about safety, environmental harm, and property concerns. According to regression research, gender, age, past exposure to HVOTLs, and one's living area all affect risk perception. The study offers important policy recommendations for infrastructure and related organizations while supporting the fundamental ideas of a risk society.

Neoptolemos [5] et al. goal is to give an integrated life cycle evaluation of Greece's electrical grid, taking into account the various power production technologies now in use there and the related energy transmission system. Semipro 7.1 Life Cycle Assessment software is used to examine the energy and environmental impact of the generating and transmission networks. The current study demonstrates that the electricity production industry, namely the system of mainland Greece, which would be dominated by centralized fossil fuel power plants, is responsible for the majority of the negative environmental consequences (>60%). When compared to production, transmission was shown to have a 70%–90% reduced life cycle effect. The largest source of GHG emissions is transmission power losses, but transformers and the infrastructure supporting transmission lines have far less of an influence during their lifetimes. Findings on the main energy demand show a similar pattern of behavior. While primary energy

consumption is anticipated to rise as a result of renewable energy sources' power-intensive building phase, future electricity supply mixes containing large proportions of renewable energy sources might result in much reduced GHG emissions. Also mentioned and addressed are findings on how power production and transmission affect environmental effects linked to human toxicity, ecosystem quality, resource shortages, etc.

Alexander [6] et al. discussed how government-granted monopoly advantages in energy transmission and required ownership unbundling impact power costs. Utilizing a priori mathematical modeling, possible rivalry is taken into consideration. The models taken into account demonstrate that only when the transmission monopoly is subsidized or its expenses are much lower than its potential income can consumers profit from its control. It has been shown that even in markets with significant entry barriers, prospective competition and the lack of monopolistic rights may lead to lower prices for energy transmission. Mandatory ownership unbundling has been proven to almost completely negate the impact of hypothetical competition in transmission.

Edward [7] et al. In-depth studies of space weather events have been published in peer-reviewed scientific journals. Despite a growing body of gray literature from various country research with differing degrees of methodological rigor, there has arguably been little examination of the possible socioeconomic implications of space weather. To estimate the possible socioeconomic effects of critical infrastructure failure brought on by geomagnetic disturbances, we provide a broad framework in this research and apply it to the British high-voltage power transmission network. The overall geophysical risk, asset vulnerability, and network structure of critical infrastructure systems have not yet been taken into account in socioeconomic analyses of this hazard. Our solution involves a three-step process that includes I calculating the likelihood of powerful magnetosphere sub storms, (ii) examining the susceptibility of electricity transmission assets to geomagnetic ally induced currents, and (iii) evaluating the socioeconomic effects under various levels of space weather forecasting. This has necessitated a multidisciplinary approach and contributed to the standardization of risk assessment for space weather. We conclude that the UK's gross domestic product loss from a Carrington-sized 1-in-100-year event without space weather forecasting capabilities may reach £15.9 billion, with this value falling to £2.9 billion based on present forecasting capability. However, the present forecasting capacity will deteriorate over the next several years as the life of the current satellites draws to a close. Therefore, essential infrastructure will be increasingly exposed to space weather if no further expenditure is made. Enhancing forecasting with further effort might lower the economic damage from a Carrington-scale, once-every-100-year catastrophe to £0.9 billion.

Petar Sabev [8] et al. an electricity transmission network's primary duty is to deliver electrical energy from producers and importers to all consumers in a reliable, economical, and environmentally responsible manner. The regional or national networks often include several nodes and redundant subnetworks, and they are heavily linked. The network is powered by a variety of power facilities. They are mostly based on nuclear, fossil, or renewable energy. The cost, availability, and sustainability parameters of the various power production systems vary. In the current study, the cost, availability, and sustainability indicators are used to undertake a systems analysis of power transmission networks. The P-graph framework, which lists all practical structural choices, has been employed. These metrics naturally rely on one another; for instance, increasing the proportion of renewable energy sources in the total energy supply for improved sustainability may decrease the system's availability. Based on the ongoing research, it

should be possible to increase transmission network sustainability without sacrificing overall availability. To demonstrate the suggested technique, the electrical transmission network in Hungary has been analyzed.

Dawei Chen [9] et al. the integrated coordination scheduling framework for just an integrated electricity-natural gas system (IEGS), which is discussed in this paper, is security-constrained and fully takes into account both the close interdependence between electricity and natural gas transmission systems as well as their unique dynamic properties at various timescales. Two linear programming models are included in the suggested framework. The first one focuses on hour-based steady-state synchronized economic scheduling on the mass flow rates of natural gas suppliers and power outputs of electricity producers while taking N 1 contingencies into account. The second one studies second-based slow hydrocarbon dynamics and optimizes gas source pressures to make sure that the inlet compressed gasses of the gas-fired generator is within the higher-pressure range anywhere at time between two consecutive steady-state schedule changes. It starts with the steady-state mass flow rate solutions of the gas sources as the initial value. An IEGS, which consists of an IEEE 24-bus electrical network as well as a 15-node 14-pipeline natural gas network connected by gas-fired generators, is used to verify the proposed architecture. The efficiency of the suggested framework in coordinating the natural gas and electricity systems and establishing the efficient and dependable functioning of IEGS is shown by numerical data.

James [10] et al. have the coordination and finance of transmission infrastructure, as well as liberalized power markets, provide persistent difficulties. Establishing transmission rates that indicate the need for more network capacity as well as optimal use of the current network is difficult. The liberalized energy market in Mexico is a good example of how transmission planning's roles are evolving. The Mexican market is very well positioned to collect congestion costs and encourage efficient behavior thanks to the implementation of locational marginal pricing. We draw attention to some of the possible issues that Mexico's proposed strategy and transmission fees may bring up for generating site incentives. Having generation following transmission investment rather than the other way around, a long-term transmission strategy may assist network optimization.

DISCUSSION

Firm Transmission Rights

It is simple to see the benefits of the electrical grid as a freeway for transporting inexpensive electricity from far sources. Low-cost hydro or coal plants that are remote from urban load centers transfer electricity through the grid and ease the challenge of building new facilities in more ecologically sensitive places. However, despite the allure of cheap energy, the fundamental duties of the electric power transmission grid remain to be upholding dependability and bringing down the price of generating capacity via system variety and capacity sharing. The dependability advantages alone would be enough to justify a large portion of the current electric power infrastructure, even without the allure of cheap energy from far-off sources. Multiple usage so drives the grid operator's priorities and processes.

Demanding on Transmission Rights

Regarding the interstate highway system, maintaining surplus capacity everywhere and removing any worries about access and congestion may be the greatest transmission strategy. But because of the issues caused by excessive demand for a common property, the transmission system is starting to resemble the city streets more and more. Unfortunately, the system as a whole risk collapsing if traffic on this route becomes stuck. A new formulation of the laws of the road is required since capacity constraints and the ensuing congestion are predicted to persist. With an emphasis on dependability in the past, managing the grid via a system of committees, a club of insiders who could establish and would follow informal "gentlemen's agreements" to share the financial costs and advantages, could and did function well. However, the shifting economic landscape has placed this club under duress recently. The significance of the grid has grown, as have the financial stakes, with the emergence of continuous long-distance economy power sales. The club meetings have become increasingly tense since faults in the informal arrangements now have significant economic consequences. Electric utilities, the typical club members, are looking for alternatives.

Efficient Utilization of Electric Power System

The objective is to encourage the usage of the electric power system in a cost-effective manner. A obvious place to start when talking about effective energy markets is with the economic dispatch of electric power plants linked by a transmission infrastructure. Economic dispatch, subject to plant availability and transmission network limits, optimizes benefits while minimizing costs. Prices are established at marginal costs, which take into account both the direct costs of production and the opportunity costs experienced by the whole system. With this viewpoint in mind, the theory of spot pricing is developed, taking into account the unique features of electric power transmission networks. Economic dispatch is compatible with efficient short-run pricing, and in theory, short-run equilibrium in a competitive market would replicate both these prices and the corresponding power flows. The availability of effective short-run pricing may provide a potent instrument for controlling how the electric power system is used. The competitive price at each bus is determined by the spot pricing hypothesis. The cost of efficient electricity transmission between buses would not be more than the difference between the spot prices at the individual buses. A matrix of spot price disparities across buses provides the basis for effective transmission pricing, and this difference serves as the natural equilibrium definition of the price of transmission. In order to manage the proper financial transfers among the players, efficient prices might stimulate the use of a short-run market or, more likely, central dispatch could be employed in combination with an efficient pricing model and a settlement system. The well-developed foundation for an effective utilization of the transmission system is provided by the notion of efficient short-run power pricing. Whatever the short-term use price strategy, it has to be combined with a long-term access policy and stable transmission service contracts. According to one viewpoint, the long-term market for electricity transmission might function as a series of successful short-term spot markets if certain pretty bold assumptions were made.

The main prerequisite for the transmission system would be diminishing or, at the very least, consistent returns to scale. Even the specific technical criteria of consistent returns to scale is unlikely to be reached in most situations, despite the potential appeal of relying only on short-term markets to define long-term rights. We would thus only be likely to depend exclusively on

the ideal long-run result resulting from a sequence of short-run pricing choices in an ideal environment. Consequently, developing a competitive long-term market brings with it additional challenges. And the secret to total efficiency is the long-term market. To locate and build new producing facilities and load centers, the most crucial necessity is to provide the proper incentives. Any failure to adopt a flawless short-run transmission pricing model would probably result in minor operational inefficiencies compared to the costs of making incorrect judgments about these significant plant investment decisions. The effective extension of the transmission system, particularly in the presence of economies of scale, poses its own set of difficulties in addition to allocating rights to the current transmission system. The extension of a centralized grid utilized by several relatively small market players would, in theory, need a cost-benefit analysis that would result in a solution that would not be reproduced in a completely decentralized market if users of the system lacked property or contract rights. Furthermore, effective usage of the transmission infrastructure may potentially result in prices that do not cover the cost of the extension if there are significant economies of scale. 3 The most effective planning and growth of the transmission network is a crucial matter that may be made simpler by the establishment of a system of contract rights, but it is distinct from the main theme of the current debate. We handle the issue of defining rights and pricing system usage in the short and long terms by assuming that there is some method for choosing the system's design and paying all expenses (usually via "club membership" or access fees).

Requirements for Firm Transmission Rights

In terms of long-term agreements, our focus is on creating a structure that specifies strong rights to the transmission system. Experience implies that investors will be hesitant to make commitments with nothing more than the promise of being able to participate in a short-term spot market for transmission services for long-lasting, permanent assets of the kind and size of big electric power plants. A clear entitlement to power transmission must be included in all long-term agreements that include capacity and energy payments. The accompanying use price system should strengthen the incentives for open access, effective secondary markets, and long-term firm rights with economic dispatch. Any system for transmission rights must also adhere to other, just as crucial requirements. Preserving the dependability of power system operations comes first. Any plan for changing the present system must acknowledge and appreciate the actual difficulties involved in running a power network on a daily basis. Investment and price policies must respect the controllers' unfettered operational autonomy, much as they do with airlines and the air traffic control system. 4 A plan that would significantly alter how the short-term system is now operated would likely encounter insurmountable institutional obstacles. A fair transmission allocation and price scheme should also be definable by firm and area, and it must pass the administrative feasibility test. The FERC's concern regarding the presence and potential misuse of market power must also be addressed in any transmission proposal. A transmission protocol should ideally be compatible with a competitive market and at the very least be unaffected by the use of market power. The status quo is under attack, particularly in regards to the open access and economic efficiency standards, and no existing solution satisfies all of the requirements. Defining transmission rights, however, offers a variety of conceptual challenges when departing from the status quo.

Rights to Transmission in a Contract Network the concept of rights and contracts requires a better approximation than the contract route if electric power flows along every parallel line. A

development of the contract route, the contract network offers a framework for specifying long-term rights while keeping the system's ability to be used effectively in the near term.

Competitive Pricing

The short-term loop flow issue demands a method that will control how the transmission system is used. To capture the shifting economics of power loads and power production, the transmission protocol for just a competitive market should, in particular, I preserve long-term capacity rights, (ii) make short-run users aware of opportunity costs, and (iii) encourage efficient trades. The short-term concerns of transmission congestion shouldn't penalize people with long-term rights; those who cause loop-flow congestion should pay the full cost incurred by their usage of the system; and those with inexpensive power should be allowed to exchange with those with costly power. Short-term transmission costs should be set using existing methods for determining appropriate spot rates. Although these spot prices might fluctuate a lot over time, our attention is on the locational pricing variations. The contribution margin of generation, the marginal cost of losses, and the opportunity cost brought on by system congestion are all taken into account when calculating the transmission prices in accordance with the optimum spot-pricing theory. The first two cost groupings are simple. The most affordable mix of power units required to fulfill the current demand must be used, according to economic dispatch. The plants would be transported from lowest to greatest marginal cost if all the loads and plants were in the same location. The economic dispatch calculation should account for power transmission losses if facilities are spread out and electricity must travel across a transmission infrastructure. However, if losses are taken into account, economic dispatch dictates that the cheapest plants be used first, and ideal spot prices will be equal to marginal costs.

However, if the transmission system is widely used, bottlenecks may result in congestion, which will limit the full utilization of all the least expensive plants. The restricted utilization of the plants generates what is usually referred to as "out-of-merit" dispatch, which may be attributed to the limits that cause the congestion. The pricing should reflect this opportunity cost. There are two main ways that congestion limits arise. The restriction on the flow of electricity on a single line is the simplest and simpler restriction. The maximum rate of electricity flow on a transmission line is determined by its thermal capacity. Additionally, a line limitation has an impact on every other flow in the network due to Kirchhoff's laws' interactions. As a result, the limitation may have an impact on the opportunity costs at each bus. A change in generation or load at any bus will have a small impact on the flow on the restricted line. Any thermal limitation may cause congestion, which can be calculated to determine how it would affect network-wide optimum spot pricing. A key component of the theory of spot pricing is the conclusion for thermal restrictions. Voltage magnitude restrictions at buses are a second significant cause of grid congestion. Voltage restrictions set operational limitations that may restrict the amount of power flowing through transmission lines during normal operations or as an approximation of the more complex worst-contingency analysis. Voltage restrictions may limit the transfer capacity even when power flows do not reach the thermal limits of the system and the transmission lines seem to have surplus capacity; thus, they must be taken into account when calculating the costs associated with congestion. The actual and reactive power loads and transfers in the alternating current (AC) transmission system must unavoidably be taken into consideration due to voltage limits. Remember that reactive power is measured in voltage-amperes-reactive, or Vars and MegaVars, while actual power—the power that illuminates our lamps—is measured in watts or Megawatts (MVars). Both actual and reactive power components

are separated into power production, load, and flowing in an AC system. Real power flow is something we naturally talk about, but reactive power is a different story for everyone save the electrical engineer. Even engineers have been known to avoid giving reactive power demands a physical interpretation: Without voltage restrictions, the actual power flow is the main issue, and it is customary to disregard the related reactive power analysis. The relationship between the two, however, is crucial in setting both the induced restrictions on real power flows and the corresponding spot prices. Voltage may be impacted both by real and reactive power loads. Since both real and reactive electricity are now subject to spot pricing, it is necessary to establish the related transmission rates for both kinds of power.

CONCLUSION

The system's availability might drop to an unacceptable level if solar power production is completely relied upon to meet the rising demand for electricity in the next years. As a result, if the availability is known, a crucial factor in the building of transmission networks is the proportion of renewable energy sources in overall power production. The work being done now shows how PSE tools may be effectively used in transmission networks. However, the chosen network and its characteristics have a significant impact on the outcomes. It represents the two systems' unique time constants. Due to gas source flow restrictions, it may not be possible to create a balance between supply and demand for mass flow rates. In this case, pressure scheduling may be used to address the discrepancy while maintaining the input pressures of gas-fired generators inside the acceptable operating range.

References

[1] X. Liao, L. Chai, Y. Jiang, J. Ji, and X. Zhao, “Inter-provincial electricity transmissions’ co-benefit of national water savings in China,” *J. Clean. Prod.*, 2019, doi: 10.1016/j.jclepro.2019.05.001.

[2] C. Wang, R. Wang, E. Hertwich, Y. Liu, and F. Tong, “Water scarcity risks mitigated or aggravated by the inter-regional electricity transmission across China,” *Appl. Energy*, 2019, doi: 10.1016/j.apenergy.2019.01.120.

[3] I. Stadelmann-Steffen, “Bad news is bad news: Information effects and citizens’ socio-political acceptance of new technologies of electricity transmission,” *Land use policy*, 2019, doi: 10.1016/j.landusepol.2018.11.022.

[4] D. A. Wadley, J. H. Han, and P. G. Elliott, “Risk hidden in plain sight: Explaining homeowner perceptions of electricity transmission infrastructure,” *Energy Policy*, 2019, doi: 10.1016/j.enpol.2019.06.022.

[5] N. Orfanos, D. Mitzelos, A. Sagani, and V. Dedoussis, “Life-cycle environmental performance assessment of electricity generation and transmission systems in Greece,” *Renew. Energy*, 2019, doi: 10.1016/j.renene.2019.03.009.

[6] A. Filatov, M. Vasilyev, and R. Zaika, “Ownership Unbundling and Monopoly Privileges in Electricity Transmission,” *Int. J. Public Adm.*, 2019, doi: 10.1080/01900692.2019.1672727.

[7] E. J. Oughton *et al.*, "A Risk Assessment Framework for the Socioeconomic Impacts of Electricity Transmission Infrastructure Failure Due to Space Weather: An Application to the United Kingdom," *Risk Anal.*, 2019, doi: 10.1111/risa.13229.

[8] R. Lakner, P. S. Varbanov, and F. Friedler, "Systems analysis of electricity transmission networks for improved sustainability," *Chem. Eng. Trans.*, 2019, doi: 10.3303/CET1976104.

[9] D. Chen, Z. Bao, and L. Wu, "Integrated coordination scheduling framework of electricity-natural gas systems considering electricity transmission N − 1 contingencies and gas dynamics," *J. Mod. Power Syst. Clean Energy*, 2019, doi: 10.1007/s40565-019-0511-z.

[10] J. Bushnell, A. Ibarra-Yúnez, and N. Pappas, "Electricity transmission cost allocation and network efficiency: Implications for Mexico's liberalized power market," *Util. Policy*, 2019, doi: 10.1016/j.jup.2019.100932.

CHAPTER 3

DEVELOPMENT OF OPTIMAL POWER FLOW MODEL

Mr. Sunil Kumar AV, Assistant Professor
Department of Electrical and Electronics Engineering, Presidency University, Bangalore, India
Email Id-sunilkumar.av@presidencyuniversity.in

Abstract:

The difficulty of choosing the appropriate operating levels operating electric power plants to fulfill demands supplied across a transmission network is represented by the Optimal Power Flow (OPF) concept, often with the goal of reducing operating cost. In this paper author discusses optimal power flow model, transmission right, prices and rents of electricity and contingencies of power system.

Keywords:

Cost, Optimal Power Flow Model, Network, Transmission Line, Frequency Ratio.

INTRODUCTION

Transmission lines generically refers to subterranean cables and overhead transmission lines. A transmission line's main job is to move large amounts of power between power plants and load centers. Electra Net is the owner, operator, and manager of 275kV, 132kV, and 66kV transmission and distribution. Poles, lattice structures, conductivity, cables, insulators, substructure, and earthing systems are only a few of the parts that make up transmission lines. Throughout this document, these elements are covered in further detail. On a plot of property known as the right-of-way, transmission lines are often built. On a right-of-way, a single form of construction is often utilized. Nevertheless, there are other cases where several structures and line types are used.

A right-of-way may take a direct route or, more frequently, it may veer off course to avoid obstructions. Constructions are put under pressure by the direction shift, and new types of transmission line structures have to be developed in order to compensate. Generally speaking, timber poles, concrete poles, aluminum or steel poles, as well as lattice towers are the types of structures utilized on transmission lines. Depending on how they are employed in a line, these constructions can be categorized as tangent, angled, or dead-end structures. Electrical transmission structures serve primarily as mechanical supports for conductors. This is accomplished by conserving structure geometry that maintain operational electricity clearances under specified serviceability and maximum stress levels while maintaining mechanical integrity avoiding irreversible structural deformation during ultimate load circumstances. Figure 1 illustrates the secondary purposes of transmission line architecture:

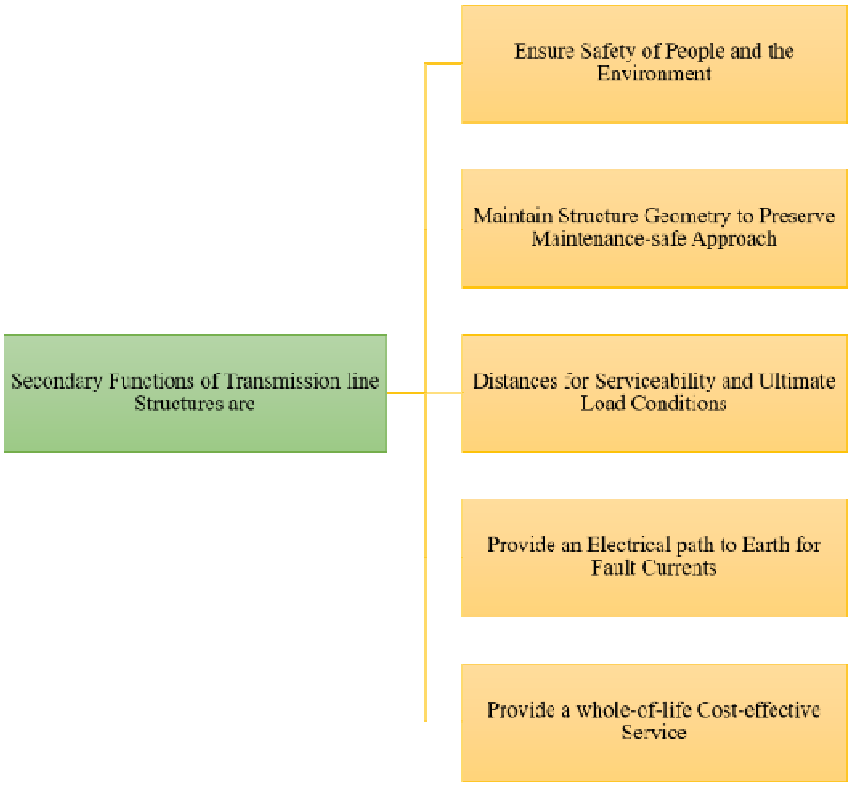

Figure 1: Illustrates the Secondary functions of transmission line structures.

Dead-End Structures

Everywhere a transmission line terminates, dead-end structures, also known as strain-termination structures, are employed. It is purposefully made to tolerate somewhat more stress and strain. Insulator strings throughout the strain insulators are typically used to identify dead-end constructions at the termination of transmission lines. Transmission lines could also include dead-end construction at any location when the structure or any of its parts is subjected to excessive strain. A double dead-end is an instance of one of these, which accommodates the strain on each phase of the line in both directions.

Angle Structures

At locations when a transmission line experiences a considerable shift in direction, this structural type is employed. Angle structures are strengthened specifically to withstand the stress exerted on them by direction changes.

Tangent Structures

On a transmission line, this style of construction is the most prevalent. It is also known as along-the-line or straight-through architecture. Typically, it is found along very straight stretches of a right-of-way. A transmission line must be able to support each component when it transitions from one tangent construction to the next. The insulator strings are often installed in the suspension configuration on the tangent constructions.

Factors Affecting Transmission Line Design

Almost every transmission line contains one of those many sorts of transmission line structures. There are various variables that affect where and how specific structures are employed. Building new transmissions is what is meant by transmission improvements. The load-serving entities in each zone are charged for the cost of transmission improvements. All clients in each zone are allocated a percentage of this fee based on their use. In conclusion, even if certain aspects (such transmission) are outside your control as a customer, one may still protect against cost increases by locking in rates and consistently attempting to cut use. Constellation's pricing options might assist customers in maintaining control over your electricity expenses even when transmission prices are predicted to increase. Our energy management specialists can assist customers in deciding how much of your use company should lock in with a fixed rate, how much business should purchase on the open market, and the best time to do so to protect against fluctuating market costs. The following are some of the most crucial elements in Figure 2:

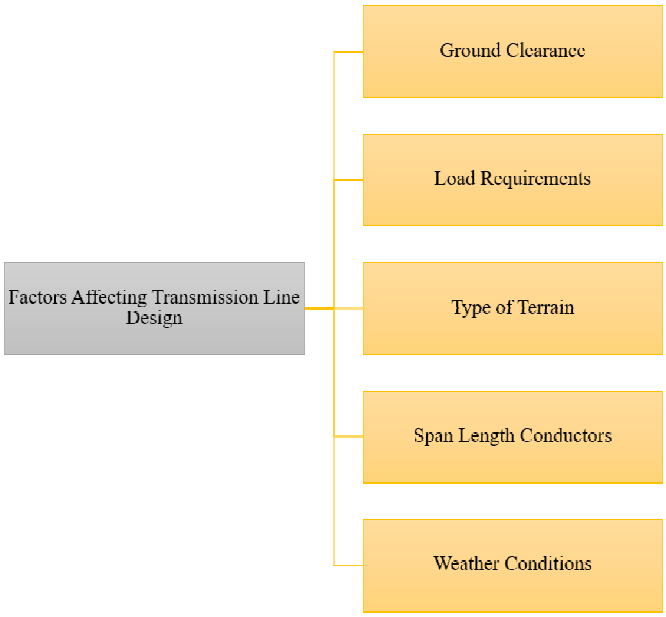

Figure 2: Illustrates the Factors Affecting Transmission Line Design.

LITERATURE REVIEW

Mukherjee [1] et al. stated various concepts for re-conductoring overhead wires have been put up in recent decades to increase power transmission capacity in light of the rising demand for energy. The traditional process of re-conductoring used to take a few weeks, but the ability to shut down for an extended length of time is a significant barrier to line uprating. Such a difficult process may be completed by an emergency restoration structure (ERS) in about 4-5 hours after line closure. The ERS is adaptable for restoration even after any natural catastrophes because to its rapid repair and mobility qualities. A case study of 132 kV restorations is used as a conceptual proof of concept in this paper. Due to a 132 kV single circuit transmission line interrupting its path, a 400 kV transmission line obstruction between Atur and Indira Puram that had existed since March 2017 was successfully rectified by the completion of this project.

Wang [2] et al. have explained that quantum-information science has a lot to gain from superconducting metamaterials. They provide a way to design on-chip dispersion relations and a band structure in the environment of circuit QED, which might then be used to create intricately entangled states of quantum circuits, to design quantum reservoirs, and as a component of quantum simulation architectures. Here, we report on the creation and measurement of a specific kind of circuit metamaterial resonator that is compatible with circuit QED designs and made of planar superconductivity lumped-element reactance's in the shape of a discrete left-handed transmission system at millikelvin temperatures. We go into great depth on this system's design, construction, and circuit characteristics. Additionally, we provide a thorough characterization of the dense mode spectrum within those metamaterial resonators, of the kind that we carry out by taking measurements of microwave transmission and by utilizing laser scanning microscopy. An analytical model based on current-voltage relationships for just a discrete transmission line is used to analyze the results, which are found to be in excellent quantitative agreement with both models. Humans specifically show that the damping due to external loading, spatial characteristics of current and charge densities, and metamaterial mode frequencies can be easily modeled and understood, making this framework a possess relevant for use in the future in quantum-circuit applications and for research into complex quantum systems.

Wenjie [3] et al. have explained that a low-temperature microwave-driven atmospheric pressure plasma jet (MAPPJ) is described along with its design, performance, and characteristics. The gas is released via a continuous-wave microwave, and the MAPPJ is based on a sophisticated coaxial transmission line topology. The gas flow may be controlled by feeding two channels of gas into the inner and outer coaxial transmission lines, respectively, allowing the plasma jet exposed to the atmosphere to be long and straight without a quartz tube. In the experiment, a 28.6 mm long straight low-temperature plasma jet is seen. This MAPPJ device has great efficiency across a broad operating range, and in the experiment without the need for a microwave matching network, a maximum efficiency of 89.6% is recorded. This strategy could be the first step towards the commercialization of MAPPJs at low temperatures.

Dongfeng [4] et al. have explained that on a balanced structure and a co-directional diode pair, this study suggests a unique 220-GHz third-harmonic mixer that uses a hybrid waveguide-fin-coplanar waveguide-microstrip line transmission line as the carrier circuit. In order to accomplish third-harmonic mixing, the mixing signals must be inputted into the hybrid transmission line in the proper direction. The balanced structure's mode orthogonality allows for strong isolation between both the radio-frequency (RF) port as well as the local oscillator (LO) port. To allow the RF signal to enter the diode pair with little loss, the metal slots just on fin line are employed as the RF signal's matching network. The results of the experimental tests demonstrate that the third-harmonic mixer's conversion loss is better than 18.5 dB inside the range of 210-230 GHz and only slightly varies in the wide range of intermediate frequency (IF).

Rambabu [5] et al. have explained that a wide frequency ratio dual-band quadrature branch line coupler (BLC) has been recommended. Here, closed-form design equations for a dual-band quarter wave transmission line structure operating at a broad frequency ratio are also provided. Additionally, an investigation of the fluctuations in the frequency ratio of the BLC circuit characteristics with respect to implementation was done. A dual-band BLC has been created, implemented, and evaluated for long-term evolution (LTE) 0.7GHz and public safety band (PSB)

4.9GHz in order to the experimental verification. The unique feature of the suggested design is the dual-band operation's broad frequency ratio, which may go as high as 11.8.

Ibrahim [6] et al. have introduced a systems for transmitting electric power have played a significant role in the development of our contemporary society. The construction of transmission line constructions that can survive severe natural hazards is necessary to ensure the constant supply of electric power. The present research focuses on the operation of conductor line systems under downburst stress, which accounts for 80% of weather-related transmission line failures, along with other kinds of wind occurrences. A unique failure mechanism of transmission line constructions may be discovered to damage the cross-arms of the supporting towers as a consequence of the development of longitudinal forces in the conductor lines due to the unusual arrangement of downburst wind fields. Examining the dynamic impact of downburst loading on these longitudinal forces and determining the applicability of employing quasi-static analysis are the major goals of the present work. Model-scale and full-scale analyses are used to accomplish this. In order to overcome the complexity brought on by time-varying aerodynamic damping coefficients, a simulation approach that can anticipate the dynamic response of conductor systems owing to downburst loading is initially proposed using the model-scale analysis. An original experiment performed at the WindEEE dome testing facility at The University of Western Ontario in Canada is used to verify the suggested concept. A wind field produced by a Computational Fluid Dynamics (CFD) model is utilized in conjunction with the verified model to carry out analysis at the full-scale level. The conductor system's longitudinal forces are dynamically insensitive, according to the results, and may thus be handled in a quasi-static manner. Finally, a comparison between the CFD wind field and full-scale recordings was done to assess the applicability of the wind field employed. Two variables that might have an impact on the quasi-static response—the first linking the peak velocity towards the post peak velocity and the second determining the ramping period—were used to make the comparison. The comparison revealed that altering the specified parameters would only produce a maximum 5% variation in the calculated responses. The comparison revealed that altering the specified parameters would only produce a maximum 5% variation in the calculated responses.

Mukul [7] et al. have used the Co-Planar Waveguide (CPW) transmission line using Periodic Defected Ground Structures is updated in this study and is suggested for usage as a high-speed microwave channel supporting embedded antennas. Slots of different forms are carved into the CPW ground surface to alter it. Wi-MAX applications are found to be compatible with the modified CPW channels, and a certain form of DGS unit cell may be chosen based on the bandwidth demand. It is constructed and tested because the CPW transmission line with circular-shaped DGS cells in two columns offers an impressive transmission coefficient of 0.89022 (1.01 dB). It is shown that the outcomes of the tests and the simulations are consistent.

Soyoung [8] et al. have the radio frequency interference (RFI) between high speed data transmission lines here on flexible printed circuit board (FPCB) and nearby Wi-Fi antennae grows as the space available for installing components within mobile devices decreases. In order to lessen the RFI influence on a smartphone's antenna, this research suggests trombone line topologies on the FPCB utilized in the camera module. Comparing the trombone construction to traditional meander lines, RFI is said to be reduced. Using a 3D full-wave electromagnetic simulator, the E-field, H-field, coupling S-parameter, and coupling voltages are obtained. In comparison to a conventional construction, the findings demonstrate the usefulness of the

trombone in enhancing RFI performance. With the aid of a 3D full-wave electromagnetic simulator, all simulation results were produced. The trombone structure's coupling S-parameter is decreased by up to 5 dB at the antenna's resonance frequency (@2.4 GHz). The receiver antenna's sensitivity is often less than -100 dB, therefore even a tiny amount of RFI reduction has a significant positive impact on the system.

Vyas [9] et al. have install new transmission lines in a country with a dense population like India. The nation is also in a fast-track growth phase, which contributes to the constant need for power brought on by the process of industrialization. The corridor width for transmission lines may be greatly decreased with the introduction of Extra and Ultra High Voltage transmission lines. The use of a unique objective function for improving the structural design of extra high voltage transmission lines is described in this work. Decisions about the right of way for transmission lines are made based on electromagnetic field and corona effects nearby. The objective function defined here optimizes the design of the transmission line tower structure by taking into consideration the combined effects of electromagnetic fields. Right of way decreases when towers are further compacted, which lowers costs associated with buying property. For the purpose of verifying the outcomes of the authors' optimization technique, a real-world instance involving a transmission line located in Gujarat is taken into account. A GUI that enables the display of fields along transmission lines in a 2D and 3D environment has been developed using MATLAB as a programming platform for mathematical modeling. The optimization issue is resolved through genetic algorithm coding. As is evident from the findings presented in this work, significant cost advantages and compactness in transmission tower construction are feasible. It is possible to adapt this optimization approach to Ultra High Voltage lines as well.

Guang Ming [10] et al. have acclaimed that you create a unique composite right/left transmission line with an interdigital structure and a double-spiral-defected resonant cell. The suggested structure is a composite right/left-handed structure since the double-spiral-defected resonance cell and the interdigital structure both provide the perception of the negative-. Then, using the suggested transmission line, a miniature branch-line coupler is created. The suggested composite right/left-handed transmission line's left-handed bandwidth is where the planned coupler operates, which results in a 66% size reduction over the conventional branch-line coupler.

DISCUSSION

An electrical network that employs alternating current (AC) may be thought of as a collection of buses linked by transmission lines that transport both active and reactive power streams. Reactive power flows usually measured in megavolt amps (MVA), whereas actual power flows were measured in megawatts (MWs) (MVars). The Var, which has the same unit as the watt and is the product of voltage and current, maintains the notational distinction between actual and reactive power. A set of nonlinear equations known as that of the AC load flow model may be used to explain the power flow in an AC electric network. Let y = g - d, or generation minus demand, become the 2 * nB vector of bus net reactive and real power injections when there are nB buses. This notation reflects how the "DC" Load Flow model evolved. According to the sign convention, rising y either results in higher expenses or lower net benefits. The actual power component of a nonlinear AC load flow model is referred to as the DC load flow. The connection between the reactive power and actual power half of the whole issue is weak under the prevailing assumptions. Additionally, the direct current flow equations inside a completely resistive network have the same basic form as the actual power flow equations, therefore the term DC

Load Flow. We need the whole AC model and spot pricing theory if voltage limitations and the related reactive power are significant. The constraints on net injections that maintain system generation, losses, L(y), the flow on each line, K(y), as well as the voltage at each bus are determined by Kirchhoff's laws and the conservation of power at each bus given the configuration of a structure composed of a buses and lines, with both the associated resistances but also reactances assumed fixed for the period (y). The goal of the ideal dispatch problem is to determine the net injections or loads that will provide the greatest net benefits, often through managing the dispatching of power plants. For the time being, we define an abstract benefit function, B(d), along with a cost function, C(g), and we make the assumption that the Kirchhoff's laws, the maximum voltage at the buses, Vmax, and the maximum average power tends to flow through into the lines, Zmax, can be used to characterize the able to operate constraints of the system. For the sake of simplicity, disregard any lower boundaries or further restrictions on power injections that may be tolerated. Therefore, the general optimum dispatch issue is if E is the 2 by 2*nB elementary matrix that adds the actual and reactive loads:

$$\underset{d,g}{Max}\, B(d) - C(g)$$

$$Eg - Ed - L(g-d) = 0,$$
$$K(g-d) \le z_{\max},$$
$$J(g-d) \le V_{\max}.$$

When this issue is resolved, a related pricing issue that links marginal costs, traffic, and the marginal benefits, or equilibrium prices, arises. The pricing model derives from the first-order conditions of the optimum dispatch problem using the relevant constraint multipliers, 0, IX, and x, respectively, under the normal regularity requirements, including continuous linear differential equations of B and C. The first-order conditions for the restricted optimization problem, also known as the first order Kuhn-Tucker conditions, are those derived from the local linear programming outward linearization,

$$\nabla C^t = \nabla B^t = (E - \nabla L)^t \theta - \nabla K^t \mu - \nabla J^t \tau.$$

The bus prices are equivalent to the marginal costs, VC t, or p A_ VB t. As a result, the price for marginal generation, inpa = EtO, the impact of losses, withpL = - VLtO, but also congestion, inpc = -(VKtl.t + V Jr'c), are included in the decomposition of bus pricing, with the negative signs being defined by the sign convention used to define net injections. Thus, the bus costs are reasonable.

$$p = p_G + p_L + p_C.$$

As a result, the dual prices occur in the normal manner when the optimum dispatch problem is solved, taking into account the constraint multipliers. The essential dual variables will be made accessible as a byproduct of the best solution if a formal optimization is used with a complete and clear definition of the benefit and cost functions. In theory, a atonement procedure in a live auction may provide this result. The functions B and C are often not explicitly accessible and no

such formal optimization is offered. Even though they may be challenging to include into the current computer systems, system operators often apply the appropriate judgment during the actual dispatch to respect limits and costs that are fairly real. Intertemporal interactions, for instance, might have a complex effect on the generation cost function, which is only roughly captured in the standard static optimum dispatch model. Transmission pricing may take use of the implicit prices compatible with the actual dispatch, as established after the fact, to avoid the potentially catastrophic requirement to construct a more sophisticated dispatch model or interfere with the current dispatch process. The dispatching process often results in a wealth of data that may be used to define constraints on the marginal costs for certain buses. For instance, if optimality is assumed, the operating cost of every plant in operation sets a lower constraint on the marginal cost and, therefore, the price, at that time. It is simple to calculate the multiplier values and characterize ex post the connections between the prices using these boundaries and a little amount of other information. There will often be only one consistent set of pricing since there will only ever be one unique solution to the limitations. For instance, if there are no enforceable limitations, the circumstances surrounding marginal losses completely dictate the cost of buses. Choose the multipliers as well as the prices p through into the linear program which minimizes the resulting rents in the event that there are multiple feasible solutions for the multipliers, which are typically produced by a piece-wise linear approximation of a cost function and result in a vertical segment on the supply curve. This will clear up any confusion. Finding the bare minimum of data required to determine such pricing is one objective. Examining the pricing equation makes it abundantly evident that in order to compute the different derivatives, we need a description of the network, together with the accompanying reactance's and resistances, as well as the net loads at each bus. Additionally, we must determine the binding network constraints for which the multipliers may not be zero due to complementary slackness. We need a binding higher or lower limit on the bus fare costs for each binding constraint. The dispatch method may make this information easily accessible as a consequence, which is the contract network framework's pragmatic operational assumption. The necessary data is comparable to that generated regularly in split-savings settlement systems often used in power pools, notably for the anticipated boundaries on prices at critical buses. The ex-post pricing may be easily obtained with this information. The fundamental components for establishing transmission costs and rights inside the contract network are provided by these bus pricing.

Transmission Rights, Prices, and Rents

Define the bus prices for real and reactive power in terms of a price representing the cost of generation, pG, marginal losses, pL, and a congestion price representing the marginal rents upon capacity constraints, Pc, given the system loads with the appropriate set of optimum constraint prices (0,g,x). Transmission is the simultaneous output of the exact amount of electricity at one bus and the input of that same quantity at another bus. Using the price differential between the two buses, determine the short-term cost of transmission. In order to balance out the common cost of generating and include solely the impact of losses and congestion, the price of power transmission is a matrix with the usual element enabling transmission from bus I to bus j as tij = pj - Pi. This specification of a transmission price allows for movement from bus to bus while eliminating the need to specify the network's route arbitrarily. Consequently, a contract network exists without the need of a contract route. The transmission analogs towards the bus power pricing decompositions are that if T is the matrix of actual power transmission prices,

$$T = T_L + T_C.$$

The transmission prices T are paid by all consumers of the transmission, either directly for the "transmission" or indirectly via the buying and selling of electricity at the different buses. To put electricity in one bus and pull the same amount from another bus inside the network is referred to as a transmission capacity struggle. They presume that it is possible to utilize all of the granted privileges concurrently. However, they modify the concept of a capacity right inside the contract network to permit either specified performance or the receipt of an equal rental payment. Holders of long-term transmission rights were effectively assumed to have purchased the right to use the system and ex post pay just the short-run cost of losses or to be paid a rental fee for the utilization of their rights by others. This rental payment is calculated using the network transmission price, TC, capacity congestion components based on the capacity right but instead of actual consumption. This is the core concept of the transmission line "shareholding" model when applied to a network and ex post pricing. For the sake of clarification, assume the capacity-fight holder does have the transmission rights for 300 MWs between buses I and j. The payment towards the right-holder is thus 300tcij for each term. The fight holder must pay LOOtij to the degree that the right-holder also utilizes the transmission system, such as when transmitting 100 MWs. In accordance with the capacity right, the net cost for these 100 MWs is merely the cost of losses (100tL/). The rental payment is offered to cover the cost of acquiring 200 MWs at bus j in order to complete a delivery contract for the remaining 200 MWs. Apparently, this rental payment will render the capacity-fight holder merely indifferent between I purchasing power at busj or (ii) specific performance throughout actually shipping this same additional power from bus I to busj there at current transmission prices if indeed the system is economically dispatched as well as the prices of any and all transmission and power sales seem to be short-run efficient. The transmission charge, which would also cover any damages and the rental payment, would be paid by the shipper with defined performance. However, if the shipper chooses to buy electricity locally at a competitive rate, the rental payment as specified just makes up for the higher cost of the power.

Curtailments, Contingencies, and Other Extensions

The general optimum dispatch model definition leads to the ex-post pricing model. This model can take into account a range of unusual circumstances that make operational management of the transmission grid difficult, thanks to restrictions on actual power flows and voltage magnitudes. Here, we explore particular examples or interpretations for curtailments, contingency analysis, and displacement, which seem to be, in theory, included under the general formulation, in order to show such expansions.

Curtailments

When the grid is operating normally, load patterns may cause bottlenecks that are so significant that the best dispatch option may include stopping or reducing service to consumers in a particular area. Although service curtailment is often a last choice, the pricing structure need to be able to handle this load situation. The economic consequence of placing a high emphasis on meeting total load is the use of curtailments only as a last option. Determining the opportunity cost of the curtailment by setting a high price for any such interruption is the logical technique for accounting for the impact of transmission-induced curtailments. The ex-post spot price at the

bus with the reduced load would include this outage penalty as a lower limit in the pricing model. The assessment of the marginal values of the limitations that created the bottleneck would be impacted by this high curtailment price in turn. And all of the prices would change as a result of these constraint values spreading across the network. If the users who are being restricted are owners of transmission capacity rights, the congestion payments would make up for the restrictions in accordance with the estimated outage penalty value.

Contingencies

The transmission grid's ability to function normally is dependent on worst-case contingency analysis. Under normal operating circumstances, the voltages at buses and the power flow on the lines are both much over any sustained limitations for the network's existing architecture. The system operators are worried about the circumstances that will exist if the worst-case scenario occurs, as opposed to the circumstances as they are right now. Consider the case when a line is cut. For this new network with both the missing line, all the processes on the system would immediately reorganize in accordance with Kirchhoff's rules. The basic operating requirement is, roughly speaking, to maintain the dispatch in such a way that, given the current loads on the buses, the line flows but also voltages resulting from the worst-case scenario will be within acceptable bounds. It is a challenging and complicated undertaking to determine the worst-case scenario and to solve the optimum dispatch issue ex ante in real time. But once the answer is found, it should be simple to express the general pricing issue and, by definition, identify the restrictions and flows. All that is necessary is to find the common barriers in the worst-case case scenario that ostensibly established the dispatch's restrictions and then utilize this scenario's network description to estimate the appropriate pricing. Consequently, it will be required to identify the predicted contingency that limited the actual delivery in in addition to the data on pricing limits.

CONCLUSION

The operator of the transmission grid acts as a go-between, collecting congestion fees from system users and paying congestion rents to the owners of both the capacity rights. Determining whether the money is sufficient to pay the capacity-right holders' obligations is consequently important to the grid operator. The rental obligations will be covered by the overall congestion payments inside the contract network. This is a specific instance of the more general issue of whether any transmission pricing plan would generate sufficient overall income. Transmission construction is widely known to benefit from economies of scale, and these economies indicate that at the ideal size, the short-run marginal cost might be lower than the average cost. Therefore, a one-part, marginal-cost pricing scheme would not bring in enough money to pay for growth. Restoring enough income would need a multi-part pricing structure with fixed and variable costs. However, this comprehensive analysis is beyond of the scope of our discussion; instead, we focus on the more specific issue of whether the transmission congestion payments system's short-term income is enough.

References:

[1] S. Mukherjee, S. Chattaraj, M. Irfan Khan, D. Prasad, P. Barua, and H. Agarwal, “Transmission line restoration using ERS structure,” *Adv. Sci. Technol. Eng. Syst.*, 2019, doi: 10.25046/aj040551.

[2] H. Wang *et al.*, "Mode Structure in Superconducting Metamaterial Transmission-Line Resonators," *Phys. Rev. Appl.*, 2019, doi: 10.1103/PhysRevApplied.11.054062.

[3] W. Fu, C. Zhang, C. Nie, X. Li, and Y. Yan, "A high efficiency low-temperature microwave-driven atmospheric pressure plasma jet," *Appl. Phys. Lett.*, 2019, doi: 10.1063/1.5108538.

[4] D. Ji, B. Zhang, Y. Yang, Z. Niu, F. Yong, and X. Chen, "A 220-GHz Third-Harmonic Mixer Based on Balanced Structure and Hybrid Transmission Line," *IEEE Access*, 2019, doi: 10.1109/ACCESS.2019.2910170.

[5] A. M. Zaidi, M. T. Beg, B. K. Kanaujia, K. Srivastava, and K. Rambabu, "A Dual Band Branch Line Coupler With Wide Frequency Ratio," *IEEE Access*, 2019, doi: 10.1109/ACCESS.2019.2896646.

[6] I. Ibrahim, A. El Damatty, and A. Elawady, "The dynamic effect of downburst winds on the longitudinal forces applied to transmission towers," *Front. Built Environ.*, 2019, doi: 10.3389/fbuil.2019.00059.

[7] R. C. Mahajan, V. Parashar, V. Vyas, and M. Sutaone, "Design and implementation of defected ground surface with modified co-planar waveguide transmission line," *SN Appl. Sci.*, 2019, doi: 10.1007/s42452-019-0245-6.

[8] S. Lee, H. A. Huynh, Y. Han, D. Choi, and S. Kim, "RFI enhancement technique for FPCB design using trombone transmission line structure," 2019. doi: 10.23919/EMCTokyo.2019.8893697.

[9] K. Vyas and J. G. Jamnani, "Cost effective design of extra high voltage transmission lines for minimizing transmission congestion problems," *Int. J. Innov. Technol. Explor. Eng.*, 2019, doi: 10.35940/ijitee.J9455.0981119.

[10] L. Geng, G. M. Wang, P. Peng, and Y. W. Wang, "Design of Miniaturized Branch-Line Coupler Based on Novel Composite Right/Left-Handed Transmission Line Structure," 2019. doi: 10.1109/COMPEM.2019.8779071.

CHAPTER 4

INSPECTION OF INSULATORS ON HIGH-VOLTAGE POWER TRANSMISSION LINES

Dr. V Joshi Manohar, Professor
Department of Electrical and Electronics Engineering, Presidency University, Bangalore, India
Email Id-joshimanohar@presidencyuniversity.in

Abstract:

A test voltage there at designated wet power frequency withstand potential is applied to the insulating material. In the event that neither a flashover nor a puncture occurs during the test, the results will be good. In this paper author discusses the inspection of insulator with types of insulators, wave inspection via electronic of insulator, and robot for electronic wave inspection.

Keywords:

High-Voltage Power, Insulator, Electricity, Robot, Transmission Lines.

INTRODUCTION

An insulator is a substance that prevents heat and electricity from passing through it. Many electrical components are connected using electrical insulators, a protector and protective device. It contributes significantly to the creation of several electrical and electronic circuits as well as overhead power systems. An Insulator supports the overhead line components upon that poles and stops current passage to the ground. The transmission lines need to operate correctly. An insulator can be made from many different materials, including rubber, wood, plastics, mica, and many others. Manufacturers, wholesalers, and a range of Suppliers and Organizations all sell insulators. Porcelain is frequently used to make the insulators for high voltage transmission lines. Although many other specific composition materials, including glass, polymer, steatite, and many others, are also employed in the production of overhead line insulators. Porcelain outperforms glass in terms of mechanical strength, leakage resistance, and temperature sensitivity. Insulators differ from other electrical devices in Figure 1 in a number of distinct ways. Here are a few characteristics of insulators:

Due to the widespread presence of transmission lines in our area, continuous human exposure to electromagnetic fields through high voltage transmission lines has been a major issue for people. Based on the standards established by various organizations such as the International Commission on Non-Ionizing Radiation Protection, so every nation has its own criteria for exposure to electric fields (ICNIRP). For the general population at a frequency of 50 Hz, the ICNIRP has proposed a continuous electric field exposure limit of 5 kV/m. Given the potential health risks induced by the electric fields radiated by very high voltage power lines, the introduction of electric fields to human bodies has become a crucial topic of concern. The closeness of current-carrying conductors in industrial settings presents the maximum exposure to this emitted electromagnetic environment. Numerous studies have investigated the generated current in a human body caused by a high voltage transmission line's 50 Hz electric field. This is a crucial factor in the likelihood that electric fields will have an impact on biology. The body current or current density produced by the magnetic field is substantially less than the maximum body current created by the electric field from such a transmission line.

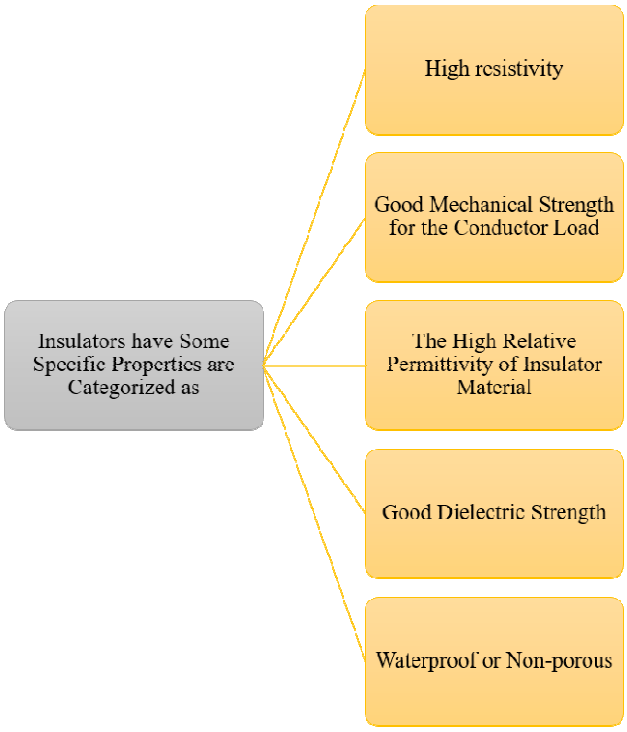

Figure 1: Illustrates the Insulators have some specific properties that make them different from other electrical devices.

Type of Insulators Used in Transmission lines

There are 5 types of insulators used in transmission lines as overhead insulation.

Pin Insulator

Although pin insulators were the first overhead insulators to be created, they are still often employed in power networks down to 33 kV systems. Depending on the application voltages, pin type insulators might be single part, two part, or three part types. Usually often employ one component type insulators in an 11 kV system, where the entire pin insulator is made of one piece of appropriately formed glass or porcelain. Since an insulator's leakage channel runs over its surface, it is preferable to maximize the vertical length of the insulator's surface area. And provide a lengthy leakage channel, it provides one, two, or more rain shields or petticoats upon that insulator body. Additionally, petticoats or rain gutters on an insulator have another use. The exterior surface of these rain sheds, also known as petticoats, becomes wet when it rains, while the inside surface stays dry and non-conductive. As a result, the conducting channel via the damp pin insulator surface would occasionally stop.

Post Insulator

Post insulators are comparable to pin insulators;however, post insulators are better suited for applications requiring higher voltage. In comparison to pin insulators, post insulation materials are taller and feature more petticoats. This kind of insulator can be mounted vertically or horizontally on either a supporting structure. The insulator includes clamp arrangements in both the top and bottom ends for fastening, and it is composed of a single piece of porcelain.

Suspension Insulator

Beyond 33KV, increasing voltage makes using pin insulators uneconomical due to the insulator's increased bulk and weight. Larger single unit insulators are challenging to handle and replace. Suspension insulators were created as a solution to these problems. In suspension insulation, a string of insulators is formed by joining them in series, with the lowest insulator carrying the line conductor. Because of its disc-like form, each suspension string's insulator was known as a disc insulator.

Strain Insulator

String insulators are employed when suspension strings are needed to support exceptionally high conductor tensile loads. A transmission line must withstand a significant conductor tensile stress or strain when it encounters a dead end or a sharp corner. A strain insulator should possess both the requisite electrical insulating qualities as well as substantial mechanical strength.

Stay Insulator

The stays for low voltage wires must be elevated and insulated from the ground. The stay insulators, which is used in stay wires and is often made of porcelain, is meant to prevent the guy-wire from falling to the ground in the event that it breaks.

Shackle Insulator

Low voltage distribution networks typically employ spool insulators, commonly referred to as shackle insulators. It may be applied either horizontally or vertically. Following a rise in the usage of subterranean cable for distribution, the utilization of such insulators has lately declined. The spool insulator's tapering hole distributes the weight more evenly and reduces the risk of fracture under heavy strain. Soft binding wire is used to secure the conductor throughout the groove of a shackle insulator. Due to the subterranean cable utilized for distribution, these insulator is currently less frequently employed. It has a conductor inside the groove and may be fastened using a flexible binding wire.

LITERATURE REVIEW

Xinbo [1] et al. have explained that A factor that is directly connected to the insulating qualities of composite insulators is their hydrophobicity. The hydrophobicity grade of a composite insulator must be correctly and objectively determined in order to decide if the insulator inside the transmission line has to be removed. This work proposes detailed research on the hydrophobicity detection for composite insulators of transmission lines using image analysis, allowing for rapid measurement of the hydrophobicity of composite insulators. The hydrophobic pictures undergo sequential grayscale, median filtering, and histogram equalization processes. The water drop (or water mark) area is segmented using binary large object analysis, and four water repellency-related metrics are recovered. The enhanced support vector machine approach is also used to determine how hydrophobic composites insulators are. The findings demonstrate that the suggested hydrophobicity detection technique, which has an accuracy of more than 91%, can identify sample composed hydrophobic levels of insulators.

Chen Rui [2] et al. have explained that Identifying Insulator defects is a crucial step in the high-voltage transmission line inspection process. However, the accuracy and robustness of present approaches are often lacking. Additionally, these techniques can only find a single problem in

the insulator string and cannot find multiple faults. In this research, a unique approach for insulator one fault and multi-fault detection in UAV-based aerial photos is provided. These images often include complicated interference in their backgrounds. Due to the variations in recording angle and distance, the forms of the insulators also fluctuate clearly. We make full use of such a deep neural network to differentiate between insulators and background interference in order to lessen the effect of complicated interference on the identification of insulator failures. In order to build a standard insulator identification dataset called "InST detection," a large number of insulator aerial photos with manually labeled ground-truth are first gathered. In order to accurately determine the locations of the insulator strings in the aerial picture, a new convolutional network is also suggested. Finally, a fresh approach of fault identification is put forward that can recognize both single and multiple faults in aerial photographs. Our suggested technique outperforms state-of-the-art insulator defect identification methods, according to experimental findings on a large number of aerial pictures.

Gao Zishu [3] et al. have installed many insulators on the transmission line, and damage to these insulators will have a significant influence on the security of the power supply. A prerequisite and essential duty for power line inspection is image-based segmentation of a insulators inside the power transmission lines. For insulator pixel-level segmentation, a modified conditionally generative adversarial network was proposed in this research. The generator is rebuilt using encoder-decoder layers and an asymmetric convolution kernel, which may reduce the complexities of the network but also extract more varieties of feature data. The discriminator learns the loss to training the generator and is made up of a fully convolutional network predicated on patch GAN. Experiments show that the suggested technique outperforms Pix2pix, SegNet, and other cutting-edge networks in terms of mIoU performance and computational efficiency.

Samuri [4] et al. have presented an investigation of the distribution of space charges on high voltage (HV) insulators at various contamination levels. In this experiment, two different kinds of HV insulators were used, namely glass and porcelain insulators. Using QuickfieldTM software, a string of four glass and porcelain insulators with a 33 kV line voltage was constructed and simulated. To study the impact of space charge dispersion, four levels with contamination layers of varying thickness have been put to the surface of insulators. According to the findings of the simulation, the charge and voltage distribution are affected differently by the various kinds of insulators employed at transmission lines. Additionally, it is discovered that what a single porcelain insulator has a substantially larger charge amplitude than a single glass insulator. Furthermore, for a string of four insulators, porcelain insulators exhibit substantially larger voltage distribution throughout the creep age distance than glass insulators do at all degrees of contamination.

Roman [5] et al. have to achieve optimum operating performance, the high voltage transmission line design has to make careful insulator selections. The Cahora Bassa high voltage direct current (HVDC) transmission line throughout South Africa underwent in-situ tests of leakage current (LC) on composite and glass insulators over a six-month period. Investigated are the effects of temperature, humidity, moisture, rain, and the voltage and current of the HVDC line on LC. The findings indicate that, with the exception of conditions of high humidity or rain, the behavior of composite and glass insulators is identical. Glass insulators have higher LC levels when it starts to rain and the humidity is high (>90%), but composite insulators show lower LC levels in similar circumstances. The LC data show an essentially square-wave behavior under normal

weather circumstances of no rain and low humidity, with LC cycling between lower (20 A) and higher values (60 A) with reasonably brief transitions every day. Condensation here on insulators, which is a major factor in the LC levels on polluted insulators, may be blamed for this phenomenon. The LC level is unaffected by changes in line current and voltage.

Jiang Hao [6] et al. have presented the primary cause of power transmission accidents is insulator fault in the transmission lines. Images obtained during the aerial inspection can be used to identify insulator faults for future maintenance. Due to the complicated background and variety of insulators, insulator fault detection is an interesting and difficult task for automatic transmission line people inspection systems. A novel multi-level perception-based insulator fault detection method for aerial images. An ensemble architecture that incorporates multiple single-level perceptions implements the multi-level perception. The consideration to the insulator fault names the low level, middle level, as well as high level of these single-level perceptions. They distinguish between an insulator fault in one or more insulators, or in the entire image. An ensemble method is suggested for producing the results in order to address the filtering issue inside the combination of three single-level perceptions. A potent deep meta-architecture known as the single shot multi-box detector (SSD) is used to train the detection models used in the multi-level perception. The well-trained SSD models could indeed automatically extract high quality characteristics from aerial images instead of manually extracting characteristics. By employing the multi-level perception, the advantages of both global and local information could perhaps achieve a favorable balance. Furthermore, limited inspection images have been fully utilized by that of the proposed method. The proposed method successfully detected insulator faults under a variety of conditions inside the practical inspection data, with a recall and precision of 93.69% and 91.23%, respectively. The experimental findings demonstrate that the suggested method can significantly improve the accuracy and robustness.

Miao Xiren [7] et al. have because it is an difficult problem for an autonomous transmission line inspection system to locate insulators with crowded backgrounds in aerial photos. In this research, we offer a deep learning-based insulator detection approach for aerial photos that is efficient and trustworthy. The single shot multi-box detector (SSD), a potent deep meta-architecture, is combined with a two-stage fine-tuning technique in the proposed deep detection approach. Instead of manually extracting features from aerial photos, the SSD-based model may include an automated multi-level feature extractor. The use of a two-stage fine-tuning technique employing distinct training sets is motivated by transfer learning. In the first step, the COCO model is adjusted using aerial pictures that include numerous insulator kinds and backdrops in order to create the basic insulator model. The training sets of the individual insulator kinds and the specific conditions to be recognized are used to fine-tune the basic model in the second step. The well-trained SSD model can immediately and precisely detect the insulator by inputting the aerial photos after the two-stage fine-tuning. The findings demonstrate that, in aerial photos with complicated backgrounds, porcelain and composite insulators can both be promptly and precisely detected. The suggested method may greatly improve robustness, accuracy, and efficiency.

Lanlan Liu [8] et al. have presented the autonomously created live-operational robot for insulator replacement on 110–220 kV power transmission lines. The robot is designed to be composed of three platforms: a non-obstacle-surmounting platform that primarily consists of the robot body, 2 different robot arms, two robot hands, as well as two end-effectors; a control platform that consists of a motion control system, a communications network, an image capture system, and a ground base station that simulates the manual electric potential live working process of replacing

insulators. Additionally, the robot is constructed to be shielded from electromagnetic interference. The robotic device described in this study is a first for China.

Shenghui Wang [9] et al. have explained One of the key electrical components of the power grid is the insulator. The stability and safety of the power system are gravely threatened by pollution flashover of insulators. It is crucial to consider the insulating state of contaminated insulators inside a timely manner. In this study, a frame is taken from an ultraviolet video of such an insulator discharge, the image is segmented by ultraviolet spots, the area of the spots and their time series are calculated, as well as the relationship between both the spots and leakage current at various discharge stages is examined. Based on these findings, the insulator's insulating state is determined and flashover warning is implemented. It was built an artificial foggy chamber having continually changeable humidity. The UV imager captured video of disc insulator contamination being discharged. Extracts were made of the discharging's UV properties. The insulating condition of insulators was categorized into four stages: "safe," "warning," "alert," and "hazardous" using the naked eye observation, leakage current signal, and other associated factors. The sample data were processed and grouped, and the spot area sequence's arithmetic average, maximum, standard deviation, and discharge frequency were all retrieved. The project's practical application demonstrates that the spot region sequence is useful for determining the insulation state of insulators.

Xiaohui [10] et al. have a hypothetical dynamic model of multiple insulator-string-equipped two- and three-span transmission system is provided. The model has a significant chance of taking into account the impact of transmission line motion in the axial direction and insulator string swinging on adjacent spans, unlike conventional single-span models. By combining the moment equilibrium of insulators string swing as well as the free vibration calculation of the each span, which takes into account the longitudinal component with inertia resulting from motion of a support, the formulas of in-plane and out-of-plane motion of multi-span were constructed. The continuity of a displacement and force results in accurate and approximate resolutions for the equations controlling multi-span vibrations under self-weight. A wide range of asymmetrical and symmetrical dynamic aspects of neighboring spans interaction occurring in different transmission line parameters are explored based on theoretical formulations. According to the findings, span number, the ratio of structural performance, Irvine's parameter, and insulator string length all have a significant impact on the natural frequencies of the corresponding in-plane and out-plane modes. Additionally, the ABAQUS-based finite element findings are provided, demonstrating the validity of the theory.

DISCUSSION

The conductors of overhead electricity lines must be supported on poles or towers since they are not themselves insulated, preventing currents from the conductors from passing through the supports and into the soil (i.e., line conductors must be properly insulated from their supports). A piece of non-conducting equipment known as an insulator is used to support electrical cables and protect them from the earth or other conductors. They must have the proper distances between the line conductors, the conductors and the ground, and the conductors and the pole or tower. They are installed on an appropriate cross-arm. The line must have this clearance to be protected from the maximum voltage and worst atmospheric conditions that might possibly be present. In order to protect the conductor from the worst possible mechanical loading circumstances, the insulator must also supply the required mechanical supports. Porcelain and toughened glass are

the most often utilized materials in the building of insulators. At the start of the 20th century, as demand for high-voltage insulators rose, porcelain established its position as the better material. It has since undergone more than 100 years of process and technical development. Two or more suspension insulators linked in sequence to up a string insulator. The length of the string insulator increases with the operating voltage of a transmission line. The porcelain has to be completely vitrified before being glazed. In order to produce a surface that will be maintained mostly free from dust and moisture, glazing is required. Since the insulator's primary function is to maintain the weight of an overhead line conductors in all wind and weather situations, it must be mechanically sound. Since the beginning of the power business, system voltage levels and the distance over which electrical power is transferred have both been steadily rising. As a result, the quantity of suspension insulators utilized on power lines has significantly increased. For the 20- and 30-kV lines in Korea, a sizable number of suspension line insulators are utilized, the majority of which are of the porcelain kind. Unfortunately, the service life of the majority of porcelain insulators is only approximately 10 years, and many of the insulators in use in Korean utility networks have been in operation for much longer. A testing procedure is required to guarantee the porcelain insulator just on power lines. Or, in order to avoid deadly mishaps, technology that calls for changing the insulator has to be designed. Many professionals from all around the globe have been working on developing new kinds of porcelain insulator testers as a way to enhance field test procedures for porcelain insulators. For instance, it has been suggested and shown that an electric field may be used to evaluate an insulator's state and find inherent flaws. To find the insulator flaws, a computational electric-field measuring technique (CEFMM) has been created. Additionally popular is porcelain insulator checking based on infrared and ultraviolet pictures.

Types of Insulators

Insulators with pins have a pin that fastens to the cross arm of the pole or tower. A soft metal thimble must be employed to keep the porcelain from coming into direct contact with both the harsh metal pin. The conductor is housed in a groove on the insulator's top end. The conductor is secured with annealed wire made of the same material as that of the conductor as it goes through this groove. Typically, this is employed for voltages up to 33 kV.Post insulators: In the substation, they are used to support the bus bars and disconnect switches. The difference between a post insulator and a pin type insulator is that the former has a metal base and, more often than not, a metal cap that enables many units to be attached in series. The porcelain components of the insulator are in the shape of cones that fit tightly within one another and are joined together by specialized cement. Line post (LP), switch post (SP), and cut off switch (COS) insulators are the further divisions of the post insulator.

Insulators of the Suspension Type

With a rise in line voltage, the price of a pin insulator increases extremely quickly. For lines exceeding 33 kV, suspension insulators are thus used. They go by the names disc insulators and string insulators too though. The porcelain disc-shaped suspension insulator has grooves under the surface to lengthen the surface leakage route. It is equipped with a metal pin beneath and a metal cap just at top.

Wave Inspection via Electronic

The signal measuring device's hardware design. A radio-frequency receiver picks up signals first, followed by an ultrasonic receiver. For this study, a mobile robot going along a power transmission line has an inspection tool for insulators put on it. Within a very small angle of direction, an ultrasonic sensor may detect a signal at a distance of around 10 meters. As a result, it is used for directing and orienting the robot as well as finding the location of the insulator. The 29.4912-MHz RF signal is picked up by an electric wave receiver (MC3362) after the ultrasonic receiver pinpoints the precise position of the insulator. The 400-kHz IF signal may be demodulated using the 400-kHz filtering circuit and integrated intermediate frequency module. This IF signal is then amplified and calibrated by the gain offset controller and buffer amplifier. Here, a multiplier CA3091D-based automatic gain controller (AGC) circuit is used. The IF signal following amplification & calibration as well as the average voltage of a dc offset are the two inputs to the AGC. The low-frequency signal may be shown on the signal measuring board and via PC after additional low pass filtering and amplification. In terms of the on-board display, the signal must first be identified as an envelope before the low-frequency signal's strength is shown on a five-step LED. In order to get more precise data on the insulator quality, a low-frequency signal is also provided to Lab view enabling display and harmonic recovery.

Robot for electronic wave inspection

In order to implement the automated broad scope of application, the fundamental idea of detection, this monitoring robot is primarily made up of a detecting module, signal processing module, supportive mechanism, lifting mechanism, mobility mechanism, and other elements. The heart of the robot is its sensor and signal processing modules, which can constantly detect the strength and direction of electromagnetic waves. In addition, a lifting mechanism was created to address the issue of robot driving on various types of surfaces. It can carry out the following tasks: Electromagnetic wave signal intensity distribution, which includes the position of the robot, is also a particular range of band of electromagnetic wave that can quickly and reliably identify emission sources. It The strongest signal placement in the range direction (if any, for example, signal towers close to the launch tower and the robot's ability to measure distance) could be calculated by the ARM microcontroller program. From there, the strongest electromagnetic wave direction can be used to determine the strength of the strong electromagnetic vibration region. The robot must modify the foot's function using the wheels & tracks, two types of movable parts that can adjust to various types of road surfaces.

Infrared Imaging Inspection

Thermography uses infrared video and still cameras to measure surface temperatures. The light that these instruments observe is in the heat spectrum. Images upon that video or film capture the temperature changes throughout the surface of the structure, with white denoting warmer places and black denoting colder sections. The auditor may decide if insulation is required with the use of the resultant photos. In order to make sure that insulation has been laid properly, they also act as a quality control tool. An interior or exterior assessment is both possible with a thermographic examination. The energy assessor chooses the approach that, in a given weather scenario, would provide the greatest outcomes. Because warm air coming from a structure does not always pass through the walls in a straight line, interior scans are more typical. The source of heat loss that has been observed in one region of the outside wall may really be on the inside of the wall. Additionally, when it is windy outdoors, it is more difficult to distinguish temperature changes

on a building's outside surface. Since there is less air movement inside, interior surveys are often more accurate as a result of this challenge. A blower door test running is also often utilized in conjunction with thermographic scans.

The blower door makes air leaks from cracks in the building shell more noticeable. These air leaks show up as black streaks in the viewfinder of the infrared camera. Thermograms—images that depict fluctuations in surface heat—are created by thermography using specifically crafted infrared video or still cameras. This technology has a wide range of uses. Electrical system thermograms may identify excessively hot electrical connections or parts. Mechanical systems' thermograms may identify the heat produced by excessive friction. Thermography is a technology used by energy assessors to find heat losses and air leaks in building envelopes. Energy auditors may evaluate the efficiency of the insulation used in a building's construction using infrared scanning. The generated thermograms assist assessors in determining if insulation is required for a structure and where it should be installed. Thermographic scans of roofs may often find roof leaks because wet insulation transmits heat more quickly than dry insulation. You should have a scan performed before to buying a home in addition to employing thermography when in an energy evaluation; even brand-new homes may have flaws in their thermal envelopes. You could want to add a provision mandating a thermographic scan of the home in the contract. A qualified technician's thermographic scan is often accurate enough to serve as evidence in legal proceedings.

Spectrum Analysis in the Field of High-Voltage Power Transmission Line

The two types of high-voltage power lines are overhead transmission lines and subterranean cables. Overhead cable provides the advantages of cheap cost and high level of power compared to subterranean cable. As a result, it is often used for long-distance power transmission. Overhead transmission lines, as contrast to subterranean cables, are created as bare lines with no insulation. This sort of transmission line produces a powerful electric field that poses a risk to human life. The principal impacts of powerful electric fields on the human body, according to current research, are the weakening of the endocrine, cardiovascular, and central neurological systems. These will interfere with sleep and productivity and may potentially cause leukemia, cancer, and other severe illnesses. The "limit duration variable electric field, magnetic field, and electromagnetic field (300 GHz) exposure recommendations" were put out by the International Commission on Non-Ionizing Radiation Protection (ICNIRP) in 1998.

Harmonic Retrieval and Spectrum Analysis

It is believed that only harmonics are present and therefore the periodicity intervals are constant using typical harmonic analysis methods based on the Fourier transform, however the periodicity intervals inside the presence of inter-harmonics were variable and extremely lengthy. There are several domains where the harmonic retrieval problem (HRP) may be found. Prony's technique is just one of the well-known solutions to this issue. In reality, noise always taints the measured signals (or statistics) since Prony's approach is so sensitive to measurement noise. As a result, several strategies have been put forward to combat the impact of measurement noise. These include the state space realization technique, the Pisarenko harmonic decomposition approach, the maximum likelihood technique, and the linear prediction method. Both the high-order statistic (cumulants) approach and the poly-spectral analysis method were put forward. However, all of the test findings from the aforementioned studies were from simulations. The measuring circumstances in a real field test are imperfect due to multiplicative and additive disturbances,

which might be correlated or independent. Based on practical data for high-voltage electricity transmission lines, this work suggests a harmonic recovery approach inside the complex noise background that is solved using a slice of the sixth-order time-averaged momentary poly-spectra. A real-world field test has validated this method.

CONCLUSION

The manufacturers are in charge of creating the next generation of non-ceramic insulators, enhancing production processes and quality control, introducing new materials, etc. It is advised to do further study to improve knowledge of non-ceramic application and understanding of insulator behavior in various environmental circumstances. This would enable more precise prediction of long-term insulator performance. The findings ought to help utilities choose and dispose of insulation. The suggested network is relevant to real-time segmentation on embedding devices in the future since the trainable parameters are constrained. The method may also be used for other detecting jobs in power inspection.

References

[1] X. Huang, T. Nie, Y. Zhang, and X. Zhang, "Study on Hydrophobicity Detection of Composite Insulators of Transmission Lines by Image Analysis," *IEEE Access*, 2019, doi: 10.1109/ACCESS.2019.2922279.

[2] J. Han *et al.*, "A method of insulator faults detection in aerial images for high-voltage transmission lines inspection," *Appl. Sci.*, 2019, doi: 10.3390/app9102009.

[3] Z. Gao *et al.*, "Insulator Segmentation for Power Line Inspection Based on Modified Conditional Generative Adversarial Network," *J. Sensors*, 2019, doi: 10.1155/2019/4245329.

[4] N. A. Samuri, N. A. binti Othman, M. A. M. Piah, N. A. M. Jamail, and H. Rosli, "Comparison on space charge and voltage distribution of high voltage insulator subjected to different contamination levels," *Bull. Electr. Eng. Informatics*, 2019, doi: 10.11591/eei.v8i3.1585.

[5] M. Roman, R. R. van Zyl, N. Parus, and N. Mahatho, "In-Situ monitoring of leakage current on composite and glass insulators of the Cahora Bassa HVDC transmission line," *SAIEE Africa Res. J.*, 2019, doi: 10.23919/SAIEE.2019.8643145.

[6] H. Jiang, X. Qiu, J. Chen, X. Liu, X. Miao, and S. Zhuang, "Insulator Fault Detection in Aerial Images Based on Ensemble Learning with Multi-Level Perception," *IEEE Access*, 2019, doi: 10.1109/ACCESS.2019.2915985.

[7] X. Miao, X. Liu, J. Chen, S. Zhuang, J. Fan, and H. Jiang, "Insulator detection in aerial images for transmission line inspection using single shot multibox detector," *IEEE Access*, 2019, doi: 10.1109/ACCESS.2019.2891123.

[8] L. Liu, Y. Yan, Z. Zhou, H. Guo, W. Li, and Z. Cao, "Development of Live Working Robot for Replacing Insulators on Power Transmission Lines," 2019. doi: 10.1088/1742-6596/1168/2/022090.

[9] S. Wang, L. Niu, H. Li, and W. Hu, "Insulation Condition Evaluation of Contaminated Disc Insulator for Transmission Lines Based on the Characteristic of Discharge UV Imaging Characteristics," *Gaoya Dianqi/High Volt. Appar.*, 2019, doi: 10.13296/j.1001-1609.hva.2019.02.029.

[10] X. Liu, L. Liu, M. Cai, and B. Yan, "Free vibration of transmission lines with multiple insulator strings using refined models," *Appl. Math. Model.*, 2019, doi: 10.1016/j.apm.2018.10.021.

CHAPTER 5

CALCULATION OF PARAMETERS OF TRANSMISSION LINE WITH PHASOR MEASUREMENT UNITS

Mr. Bishakh Paul, Assistant Professor
Department of Electrical and Electronics Engineering, Presidency University, Bangalore, India
Email Id-bishakhpaul@presidencyuniversity.in

Abstract:

Electricity is transported by a transmission line from the producing substation to the different distribution facilities. The voltage and current waves are sent through it from one endpoint to the other. A conductor with a consistent cross-section along on the line makes up the transmission system. Between the conductors, air serves as just an insulating or dielectric medium. In this chapter author discusses calculation of parameters of transmission line with help of phasor measurement unit (PMU). In this chapter author is calculate parameters of transmission line with techniques of PMU.

Keywords:

Network, Phasor Measurement Unit, Power, Transmission Line.

INTRODUCTION

Different kinds of power plants produce various forms of electricity. These plants are also a long way from the load. Sending this power to both the outlying parts of all regions is therefore required. Moreover, the power produced at a voltage range of 11 to 15 kV. In a transmission line, there would be a significant loss of power if you transfer the electricity at this voltage level. Power is therefore transferred at a higher level of voltage in order to decrease the cost and transmission loss. The term "transmission line" refers to a conductor that carries electrical current from a power station to other locations in the system.

Parameters of transmission line

The specifications of a transmission line affect its performance. The four primary parameters of a transmission line are resistance, inductance, capacitance, as well as shunt conductance. Anywhere along line, these variables are spread equally. Consequently, it is also known as the transmission line's distribution parameter.

Transmission-line-mode

Series impedance is made up of inductance and resistance, however shunt admittance is made up of capacitance and conductance. The explanation of a few crucial transmission line parameters.

Line Inductance

Magnetic flux is produced by the transmission line's current flow. EMF is introduced into the circuit as a result of the magnetic flux changing together with the transmission line's current. The speed of flux change determines the size of the induced EMF. The quantity known as the line's

inductance measures how much resistance the EMF produced throughout the transmission line creates to current flow in the conductor.

Line Capacitance

Air performs the role of a dielectric medium in transmission lines. This dielectric material acts as a capacitor between both the conductors, storing electrical energy and raising the line's capacitance. The amount of charge that flows through a conductor per unit degree potential difference is known as capacitance. When comparing long transmission lines to short transmission lines, impedance is the most crucial factor. It has an impact on the system's efficiency, voltage control, power factor, and reliability.

Shunt Conductance

The dielectric between both the conductors is air. Due to dielectric flaws, some current flows throughout the dielectric medium whenever alternating voltage is applied in a conductor. Leakage current is the term for such current. Leakage current is influenced by atmospheric pollution, including moisture and surface encrustations.

Performance of Transmission Lines

The computation of sending end voltage, sending end current, sending end power factor, power failure in the lines, transmission losses, control, and restrictions of power flows under transient and steady state circumstances are all included in the definition of performance. Estimates of performance are useful for system planning. Several important factors are explained.

Voltage regulation –A current-carrying power transmission experiences a voltage drop as a result of the line's resistance, inductance, plus capacitance. As a result, the voltage at the receiving end is lower than the voltage at the sending end. Switching frequency is the difference in voltage strength between a transmission line's transmission and reception ends.

$$\text{percentage voltage regulation} = \frac{\text{Sending end voltage} - \text{receiving end volatge}}{\text{Sending end volatge}} * 100$$

Where;

VR = Receiving end voltage

VS = Sending end voltage

Reduce as much as feasible the transmission line's % voltage regulation value.

The proportion of the input power towards the output power is used to calculate the effectiveness of transmission lines.

$$\text{percentage transmission line efficiency} = \frac{\text{power delieverd at receiving end}}{\text{power sent from the sending end}} * 100$$

$$\eta_T = \frac{V_R I_R \cos \emptyset_R}{V_S I_S \cos \emptyset_s} * 100$$

Where;

VR = Receiving end voltage

VS = Sending end voltage

$\cos \emptyset_R$= Power factor at receiving end

IR = Receiving end current

IS = Sending end current

$\cos \emptyset_s$= Power factor at sending end

The line is significantly further out from the ground for safety reasons. The transmission line's conductors are supported by the electrical tower. Towers are composed of steel to give the conductor a high level of strength. High voltage direct current is sent across large distances via a transmission line. An electrical circuit's capacity to allow AC to pass through that without any obstructions, or the effectiveness of a transmission line, is measured by admission. The Siemens SI unit is indicated by the sign Y. The opposite of admittance is impedance. Whenever the AC flow is present, the transmission line's difficulty is measured. It is denoted by the sign z and is measured in ohms.

LITERATURE REVIEW

Asprou [1] et al. explained that the power system control center's monitoring and controlling tools make use of the transmission line characteristics in various ways. The situational awareness of a power system operators is favourably impacted by precise understanding of the power system model, including transmission lines' impedances. Additionally, it enhances the defense and corrective actions that may be used in the event of a disruption. However, because line parameters are often prone to inaccuracies when recorded in the control center database, they must be continually improved. When both ends of a transmission line include phasor measurement units (PMUs), it is possible to calculate the characteristics of the transmission line using synchronized current and voltage total harmonic distortion measurements. Although it is simple to determine the transmission line parameters using PMU measurements, the synchronized phasor measurements' uncertainty should be taken into account when determining the derived transmission line parameter values. In this study, an analytical equation is established, taking into account both instrument transformers but also PMU errors, for the boundaries of the transmission line parameters estimated from PMU measurements. Monte Carlo simulations are used to assess the estimated limits of uncertainty, and the relevance of understanding the boundaries of the computed line parameters is emphasized via the development of power-voltage curves that take into account the lower and upper ranges of the parameters. The IEEE 14-bus system is used to produce the simulation's findings.

Sun Zidan [2] et al. have explained that the ambient temperature, wind velocity, wind speed and direction, and other climatic factors have an impact on the transmission capacity for transmission lines. The installed measuring instruments may measure the environmental factors. However, given the high expense of the power grid, it is impractical to install environmental monitoring equipment all along the line. This paper first investigates the inverse distance normalized

interpolation and regular Kriging interpolation methods for estimating environmental parameters while taking into consideration the limited number of measurement equipment, distribution characteristics of temperature and humidity, and transmission lines. It is investigated how dynamic thermal rating of transmission lines, based on IEEE standard but also CIGRE standard thermal equivalence equation, affects the load capacity of overhead lines. Finally, utilizing information from China's environmental data network, the distributed thermal ratings of transmission lines is achieved. The price of the environmental measuring instrument drops, while the dynamic rating's accuracy rises.

Spalek [3] has there is the issue of selecting a transmission line criteria when a lumped parameter analysis is necessary. The formal presentation of the transmission line system comes first. Second, a fresh standard for transmission line lumped-parameter analysis is put out. The criteria has a straightforward mathematical formula and a clear physical interpretation. In addition to wave length, the suggested criteria also consider transmission line dissipation. It is simple to modify the criteria to meet certain needs, such as the required level of no-load output voltage variation.

Masayuki [4] et al. have to identify the causes of electromagnetic noise inside the time domain, we design a system of multi-conductor transmission lines and lumped parameter circuits (MTL). We provide a discretized method to handle all MTL systems and lumped parameter circuits, as well as the boundary conditions between these platforms. The MTL systems and lumped parameter circuits are each characterized by a set of linked partial differential equations. We may carry out a time-domain analysis that takes into account dependent sources and coupling devices within the context of the circuit theory thanks to the inclusion of the time-domain impedance as well as the element matrices. We are able to determine how the normal, uncommon, and antenna modes for three-line systems will couple together as well as strategies for noise reduction.

Yang Wu [5] et al. have to preserve the stability and dependability of the power system, real-time monitoring of both the line status is crucial. Overhead transmission lines have played a significant role in the transmission and distribution of electricity. The collection of dynamic line characteristics is crucial to maintaining the UAV's track and safety even as unmanned aerial vehicle (UAV) steadily evolves into an innovative and efficient instrument for inspection of transmission lines. An innovative parameter reconstruction technique for overhead transmission lines was put forward in this article. The issue was changed into a nonlinear optimization problem using a framework for the estimated transmission line inverse problem. The location and current characteristics of the lines were rebuilt from the magnetic field statistics based on the suggested comprehensive methodology, which incorporated the metaheuristic algorithm with interior point approach. Theoretical simulation showed that the method successfully prevented results being trapped in local optima. A dual-axial tunneling magneto-resistive magnetic field measuring device was created for the experimental implementation. The results of the measurements and calculations demonstrated the reliability and precision of the thorough reconstruction algorithm in conjunction with both the magnetic field measuring equipment, opening the door to a more promising method for controlling the trajectory of UAVs and monitoring transmission lines in real-time.

Reynaldo [6] has the thunder same Lightning Characteristic recorded in the subtropical region differs significantly from the parameters in the tropical area. In order to determine the characteristics of the lightning current at the tropics and how they affect the resistance of

transmission lines to lightning strikes, an eight-year measurement was conducted at the Lightning Measurement Station in Mount Tangkuban Perahu. High voltage and extra high voltage transmission lines are used to transmit energy to private companies and the Indonesian state electricity utility. Common lightning protection systems are used to shield these transmission cables from lightning strikes. There have been reports of power system failures caused by damage to insulators on transmission towers, earth wires, and transmission lines arresters due to differing lightning characteristics. The lightning protection on transmission lines has been improved with the installation of certain cutting-edge technologies based on studies conducted at the Lightning Measurement Station at Mount Tangkuban Perahu and other study locations in Indonesia. There have been several notable advancements documented.

Botong Li [7] et al. have explained that the geometrical parameters of the transmission line are prerequisite for precisely calculating frequency-dependent parameters as well as studying the electromagnetic transient process. Considering that the equivalent geometrical parameters are difficult to obtain directly, this paper proposes a method to calculate geometrical parameters of overhead transmission line using impedance and capacitance matrices measured at power frequency. By applying the inverse derivation of the Carson formula, the expressions of the average height of the line and the conductor radius can be obtained if the self-impedance of the line is known, while the distance between two conductors and that between one conductor and the image of another can be found with the mutual impedance. On this basis, if both the impedance and capacitance of the transmission line at power frequency are given, iteration can be used for higher accuracy. Finally, MATLAB- and PSCAD/EMTDC-based simulations are carried out verifying the effectiveness and sensitivity of the method.

Rafael Silva [8] et al. have investigated the impact of incorporating frequency-dependent soil parameters on transmission line models for the simulation of lightning transients on overhead transmission lines. Frequency-dependent soil parameters were considered using an alternative implementation of Marti's transmission line model. Results indicate that the consideration of frequency-dependent soil parameters on transmission line models can be relevant for the simulation of lightning over-voltages on high-voltage transmission lines if the ground is a poor conductor.

Chu Xu [9] have the current differential protection presently being used for high-voltage direct-current (HVDC) transmission lines requires increases in time delay and threshold to avoid mis-operation, which is induced from a distributed capacitance current along the transmission line, leading to low operation speed and disabling the device from distinguishing between internal and external faults. The unbalanced currents of the non-fault pole are studied in two cases: under an external fault as induced by the distributed characteristics and under a single-pole-to-ground fault as induced by the coupling characteristics of the transmission line parameter. To overcome its defects, this paper develops a new differential protection algorithm based on the distributed-parameter transmission-line model. The fault identification criterion using the compensated current of the common mode and fault pole selection criterion using the compensated current of the differential mode are introduced. Unaffected by the distributed capacitance current, this differential protection correctly operates with high sensitivity through the entire process during the fault. The feasibility and validity of the differential protection algorithm are verified.

Cavalcante [10] et al. have introduced a transmission line (TL) design involves complex mechanical parameters that require the use of software to process the calculation. Such

complexity makes teaching-learning of transmission line projects difficult. In this context, the present work aims to develop a user-friendly computational tool for educational application in the mechanical study of transmission lines. The tool was developed from MATLAB software based on mathematical models of the literature. Simulations in different conditions of an uneven span of TL, including the effect of the wind and, subsequently, the wind with temperature in the TL, is presented. As result, the acting forces and graphs obtained in the tool helped to observe the behavior of the mechanical parameters in the different simulated situations. Thus, the mechanical parameters of a TL studied on theory can be obtained for different conditions with the developed tool. For more, the tool demonstrates to be a facilitator for teaching-learning due to its user-friendly interface.

DISCUSSION

Modern power system control centers' software tools significantly depend on past knowledge of network structure and characteristics. The transmission line parameters were thought to be time invariant and are kept in the control center databases, unlike with the system topology, which may vary during the day. The manufacturers' statistics and common line configurations are often used to calculate the stored values for the transmission line parameters. Although such a process would provide impedance values that were very near to the real ones in a perfect environment, this is certainly not the case in the actual field. The values of a stored line parameters deviate from the actual ones due to environmental variables (including such temperature and soil resistivity), modeling errors (such as those made when designing parallel transmission lines and joint capsules of overhead transmission lines that could be connected to underground cables), and human elements (such as unreported changes in network connectivity or incorrectly calculated line length). According to some studies, there may be a 30% difference between the impedances that are actually measured and the recorded line characteristics (and vice versa). Such mistakes might have a detrimental effect on the operation of monitoring instruments (like the state estimator), providing false information to power system operators. The uncertainties connected to the computed parameters using PMU measurements have been addressed in several publications. In merely takes into account the uncertainty that the PMU introduces to the observed synchro phasors when solving a multivariable optimization model to estimate the range of the power transmission parameter change. It suggested a two-stage optimization issue to lessen the systematic errors supplied to the PMU measurements by the instrument transformers, which create variances in the estimated line parameters (from their nominal values). In the distribution grid, estimate of the line parameters also is receiving more attention. The parameters of the transformers and distribution lines were estimated using data from micro-PMUs, and any discrepancies between both the model and the computed parameters were found. Both systematic and random errors are taken into account for the estimation of a line parameters inside the distribution grid, including that of the uncertainties of an instrument transformers and PMUs. The modeling uncertainties inside the estimation problem of the distribution grids include the uncertainties of a line parameters. The uncertainties connected to the determined line parameters using PMU measurements are analytically expressed and obtained in this research. The formulas are produced by accounting for both the instrument transformers' and the PMU's maximum measurement errors. For the computation of an uncertainty near to the real one, the instrument transformers errors, particularly those of the current transformers, must be taken into account. It was specifically shown in that the inaccuracy of the line parameters determined by PMU measurements varied depending on the system loading circumstances. This is a result of the

current transformers' maximum error fluctuating according to the current that flows through them. Therefore, in order to determine the analytic solution of the uncertainties related to the computed line parameters, both current and voltage transformers errors in addition to PMU errors are taken into account in this article. When used to extract power-voltage (P-V) curves again for IEEE 14-bus system, the boundaries produced by the computed uncertainties are verified by Monte Carlo simulations.

Calculation of Line Parameters through PMU Measurements

Most of the power system control center's monitoring software depict transmission lines as an analogous pi model (i.e., state estimator, power flow analysis, and transient stability analysis). Four parameters, namely the series conductance (gsr), the series susceptance (bsr), this same shunt conductance (gsh), and the shunt susceptance, are used to characterize the corresponding model (bsh). It should be emphasized that the shunt conductance is insignificant and that the pi model often ignores it. The series admittance ysr (which includes both the series conductance and susceptance) as well as the shunt admittance ysh were computed as follows given that the synchronized current and voltage phasors being accessible from the two ends of the line via PMUs,

$$y_{\mathrm{sr}} = \frac{\tilde{I}_s \tilde{V}_r + \tilde{V}_s \tilde{I}_r}{\tilde{V}_s^2 - \tilde{V}_r^2}$$

$$y_{\mathrm{sh}} = \frac{\tilde{I}_s - \tilde{I}_r}{\tilde{V}_s + \tilde{V}_r}$$

Where Is seems to be the current phasor that originates from bus s and Is is the current phasor which reaches bus r as illustrated in Fig. 1, and V s and V r are the voltage phasors for buses s and r, correspondingly. The line parameters were calculated as a function of a voltage magnitude (V), the voltage angle (), the current magnitude (I), as well as the current angle () by expressing both voltage and current phasors into rectangular form and substituting those in (1) and (2),

$$g_{\mathrm{sr}} = \frac{A\left[V_s^2\cos(c) - V_r^2\cos(d)\right] + B\left[V_s^2\cos(h) - V_r^2\cos(l)\right]}{V_s^4 + V_r^4 - 2V_s^2V_r^2\cos(2\phi_s - 2\phi_r)} \tag{3}$$

$$b_{\mathrm{sr}} = \frac{A\left[V_s^2\sin(c) + V_r^2\sin(d)\right] + B\left[V_s^2\sin(h) + V_r^2\sin(l)\right]}{V_s^4 + V_r^4 - 2V_s^2V_r^2\cos(2\phi_s - 2\phi_r)} \tag{4}$$

$$b_{\mathrm{sh}} = \frac{I_s V_s \sin(\theta_s - \phi_s) - B\sin(h) - A\sin(d) + V_r I_r \sin(\phi_r - \theta_r)}{V_s^2 + V_r^2 + 2V_s V_r \cos(\phi_s - \phi_r)} \tag{5}$$

$$A = I_s V_r$$
$$B = I_r V_s$$
$$c = \theta_s + \phi_r - 2\phi_s$$
$$d = \phi_r - \theta_s$$
$$h = \theta_r - \phi_s$$
$$l = 2\phi_r - \theta_r - \phi_s$$

The transmitting and receiving buses of the transmission line are denoted by the subscripts s and r, respectively. Since PMUs may be utilized to collect all the data needed to calculate the transmission line characteristics, measurement uncertainties are included in Figure 1.

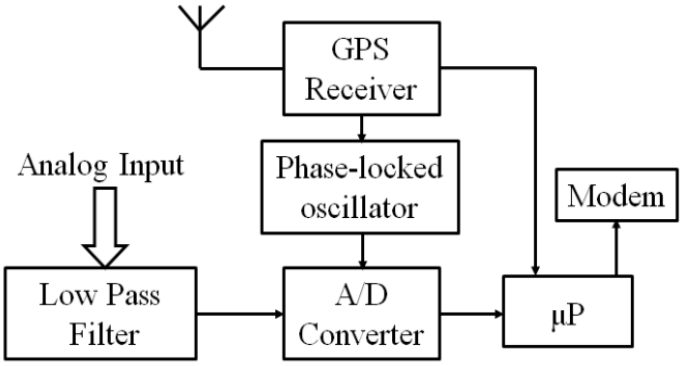

Figure 1: Illustrates the circuit diagram of PMU measurement of line parameters.

Calculation of Line Parameter Uncertainties

When the events follow the abstract model employed by the measurement system, the equipment used to get the measurement introduces the uncertainties that come with the measurement. In this study, only instrument uncertainties are taken into account and model uncertainties are disregarded. The pi model as well as the distributed line model are used to depict the line parameters of an IEEE 14-bus system in order to validate this premise. In order to recognize the modeling mistake, the magnitude and voltage angle of both the buses (extracted from of the simulation) for the two models of the lines are compared. While the greatest voltage angle variation (bus 3) is 0.037°, the maximum bus voltage magnitude divergence (bus 5) is 1.36 104 p.u. When all buses are taken into account, the average voltage magnitude deviation is 5.9105 p.u., whereas the average angle deviation is 0.023°. This demonstrates that the modeling uncertainties may be disregarded for the purposes of the study given in this publication. The instrument transformers as well as the PMU are the two key elements in the measurement chain for the PMU measurements, as illustrated in Fig. 2. Before entering the PMU, the grid electricity and voltage are stepped down to a safe level using the instrument transformers. Due to the need for instrument transformer inputs in the majority of PMU measurement chains using PMUs (except the ones that PMUs are connected to merging units). A voltage transformer and just a current transformer are always linked via wires to the PMU. The acquired measurement has an uncertainty introduced by both parts of the PMU measurement chain, which may be assessed using either the type A or type B assessment technique. In this kind of assessment approach, the measuring process is repeatedly observed under the same operating and environmental

circumstances, and the uncertainty is roughly calculated from those observations. However, since operational circumstances are constantly changing in the area of power systems, the type of assessment approach cannot be used. The makers of the measurement chain's component parts supply information that is used in the type B assessment approach to estimate the measurement uncertainty. In particular, the measurement errors are handled as random variables whose distribution for every component (i.e., instrument transformers and PMU) should be understood in order to accurately calculate the standard uncertainty linked to the measurement chain in Fig. 2. This is so because the variance of a error distribution represents the measurement uncertainty. The uncertainties of a computed quantity may be used to indicate the boundaries of that particular quantity, according to the Guide here on Expression of Uncertainty in Measurement (GUM). More precisely, the enlarged uncertainty may be used to provide an interval within which the computed amount resides, taking into account a significant percentage of the distribution of values that might be assigned to it. A coverage factor k that typically accepts values in the range of 2 to 3 is used to determine the enlarged uncertainty. The instrument transformer but also PMU manufacturer data sheets, however, only provide the error boundaries and no clear information on the error distribution. According to the GUM, in this situation, a uniform error distribution should really be presumptive.

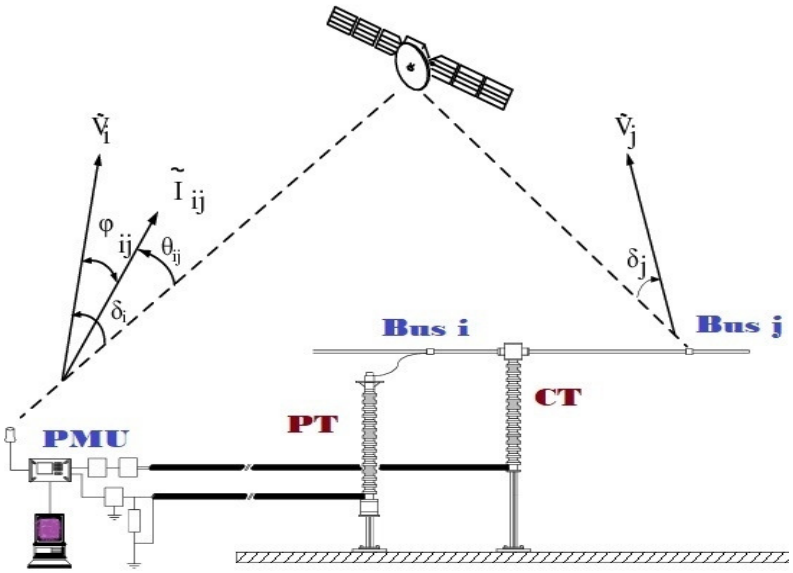

Figure 2: Illustrates the Trapezoidal distribution of the PMU measurement chain error.

Where unit f stands for a symmetric uniform distribution with such a mean value of zero, the bounds of which are given in parentheses. The formulas introduce random errors to the PMU measurements by selecting a random sample from such a uniform distribution. The voltage and current magnitude maximum errors were denoted by e V VT and e I CT, e V PMU, and e I PMU, whereas the voltage and current angle maximum errors are denoted by e VT, e CT, e PMU, and e PMU. The maximum voltage and current magnitude deviations are provided as percentages, it should be noted. As a result, the network's voltage and current magnitudes (V/Network), as shown in Figure 2 as the error-free numbers, are multiplied by a random sample drawn from each of the two uniform distributions (PMU and ITs). Additionally, the magnitudes of the observed voltage and current closely match the formulas. This is because a very tiny number that might be disregarded would come from the product of a uniform distributions which

should exist. This assumption is supported by the fact that the term produced by multiplying the IT error by the PMU is 200 times lower than that produced by simply adding the mistakes. Due to this, the measurements made by instrument transformers and PMUs are independent of one another and contribute to the total level of uncertainty. This independence of measurement chain components may not hold true, however, if a more intricate measurement chain is taken into account. However, it should be remembered that the measurement chain elements that cause the most mistake in the results are the instrument transformers but also PMUs.

CONCLUSION

As opposed to the customary one measurement every 2 to 4 seconds supplied by traditional SCADA systems, PMUs may deliver up to 60 measurements per second. PMUs provide a significant advantage over conventional methods of data collection since every PMU data is time-stamped utilizing GPS data.The capacity may be used to forecast and identify stress and instability upon that grid, improve the precision of modeling system conditions, and offer information enabling event analysis after one disturbance had occurred, among other things. To determine inefficiencies, anticipate, and control line congestion in transmission networks all throughout the globe, tens of thousands more PMUs having recently been deployed. They are sometimes used in distribution networks as well. PMU provide the chance to switch out the conventional manual adjustments needed by SCADA systems with an autonomous system that makes judgments and delivers control signals. These capabilities promise to make it possible to integrate renewable energy sources, distributed energy resources (DERs), but also micro grids more effectively and robustly. Our grid is becoming more dependable, robust, and ultimately cleaner thanks in large part to PMUs.

References:

[1] M. Asprou, E. Kyriakides, and M. M. Albu, “Uncertainty Bounds of Transmission Line Parameters Estimated from Synchronized Measurements,” *IEEE Trans. Instrum. Meas.*, 2019, doi: 10.1109/TIM.2018.2867966.

[2] Z. Sun, Z. Yan, L. Liang, R. Wei, and W. Wang, “Dynamic thermal rating of transmission line based on environmental parameter estimation,” *J. Inf. Process. Syst.*, 2019, doi: 10.3745/JIPS.04.0110.

[3] D. Spalek, “Proposal of the criterion for transmission line lumped parameters analysis,” *Bull. Polish Acad. Sci. Tech. Sci.*, 2019, doi: 10.24425/bpasts.2019.131571.

[4] M. Abe and H. Toki, “Theoretical Study of Lumped Parameter Circuits and Multiconductor Transmission Lines for Time-Domain Analysis of Electromagnetic Noise,” *Sci. Rep.*, 2019, doi: 10.1038/s41598-018-36383-3.

[5] Y. Wu *et al.*, “Overhead Transmission Line Parameter Reconstruction for UAV Inspection Based on Tunneling Magnetoresistive Sensors and Inverse Models,” *IEEE Trans. Power Deliv.*, 2019, doi: 10.1109/TPWRD.2019.2891119.

[6] R. Zoro, “Tropical lightning current parameters and protection of transmission lines,” *Int. J. Electr. Eng. Informatics*, 2019, doi: 10.15676/ijeei.2019.11.3.4.

[7] B. Li and M. Lv, “A calculation method of transmission line equivalent geometrical

parameters based on power-frequency parameters," *Int. J. Electr. Power Energy Syst.*, 2019, doi: 10.1016/j.ijepes.2019.04.013.

[8] R. S. Alípio, A. De Conti, A. Miranda, and M. T. Correia De Barros, "Lightning Overvoltages Including Frequency-Dependent Soil Parameters in the Transmission Line Model," 2019.

[9] X. Chu, "Unbalanced current analysis and novel differential protection for HVDC transmission lines based on the distributed parameter model," *Electr. Power Syst. Res.*, 2019, doi: 10.1016/j.epsr.2019.02.003.

[10] J. L. D. S. Silva *et al.*, "A computational tool for teaching-learning of mechanical parameters in transmission lines," 2019. doi: 10.1109/INDUSCON.2018.8627263.

CHAPTER 6

CLASSIFICATION FOR TRANSMISSION LINES BASED ON GROUP SPARSE REPRESENTATION TECHNIQUES

Dr. Sumit Kumar Jha, Assistant Professor
Department of Electrical and Electronics Engineering, Presidency University, Bangalore, India
Email Id-sumitkumar.jha@presidencyuniversity.in

***Abstract*:**

In an over complete dictionary, sparse representation (SR) is being used to represent data with the fewest number of atoms feasible. Using the SR, one can clearly describe the data and quickly identify the important information. In this chapter author has discusses sparse representation techniques for classification of transmission lines.

***Keywords*:**

Power, Sparse Representation Techniques, Transmission Line.

INTRODUCTION

The voltage and conductor length of transmission lines determine their categorization. Power is transported from the producing station towards the load center through the transmission line. It is mostly divided into two categories. The three variables R, L, and C affect how well a transmission line works. The distribution of these three variables is constant over the whole length of a line. Between both the line conductor as well as the ground conductor, there is capacitance in addition to the resistance, inductance, and series impedance. Because it is necessary to understand how capacitance was taken into consideration in order to understand transmission line performance, overhead transmission lines were divided into two categories: AC transmission lines and DC transmission lines.

AC Transmission Line

Power is transmitted from producing stations towards load centers through an AC transmission line using an alternating current. It consists of a series of wires that are carried from one location to another and are supported by transmission towers. These lines will display a consistent distribution of the three constants, resistance, inductance, and capacitance, over their whole length. Along the whole length of the line, capacitance serves as the shunt element while resistance, inductance, and resistance combine to produce a series impedance. The overhanging ac transmission lines are divided into three categories based on operating voltage and duration: short transmission lines, medium transmission lines, as well as long transmission lines.

Short Transmission Line

The term "Short Transmission Line" is used to describe an overhead transmission line that is less than 50 kilometers in length. The operating voltages for short transmission lines are often lower than 20kV. Since these lines are shorter and operate at lower voltages, the impact of capacitance

is overlooked. Therefore, while assessing the effectiveness of the short transmission line in Figure 1, the impacts of the line's resistance and inductance are taken into account.

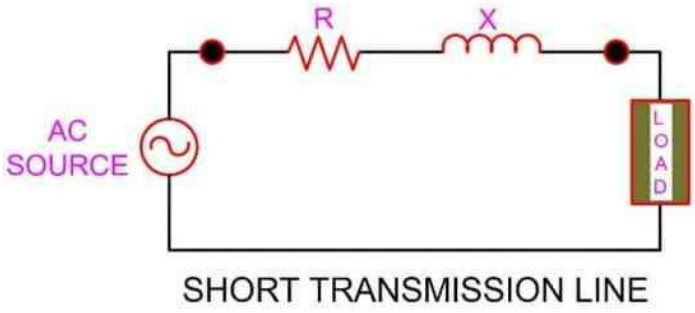

Figure 1: Illustrates the circuit diagram of short transmission line.

Medium Transmission Line

Medium transmission lines were overhead transmission lines that are between 50 and 150 km in length and have an operating voltage more than 20 kV. The impact of capacitance will indeed be taken into account since the charging current will have to be high due to the longer medium transmission lines. The shunt component is made up of the transmission lines' capacitance, which is dispersed throughout the whole length of the line. However, it will be considered in the analysis and calculations that perhaps the capacitance is grouped and concentrated at various tactical locations. The configurations of the medium transmission system vary depending on where the capacitance is located. These arrangements demonstrate the many methods in which the impact of capacitance was taken into account. According to where the capacitance is located, there are three configurations,

End condenser representation of medium transmission lines

In this layout, it is presumable that the transmission line's complete capacitance is focused on its receiving end side. The medium transmission line design for the end condenser.

Nominal-T representation of medium transmission lines

One of the localized capacitance techniques employed to assess the transmission line's efficiency is the nominal-T approach, commonly known as the middle condenser method. With this technique, transmitting end voltages are undercompensated (given low values). The midpoint (middle) of the whole transmission line is where it is believed that the overall capacitance of both the line will be concentrated when using the nominal-T approach. The charging current travels through half of the line because the whole line capacitance is considered to be in its center, and the series impedance (composed of impedance and inductive reactance) of a line was divided in half on each side of the capacitors.

Nominal-π representation of medium transmission lines

The split condenser method is another name for the nominal-method. Additionally, it is a localized capacitance approach that is effective in calculating the transmission line's performance. The transmitting end voltages are overcompensated (given greater values) using

this approach. The transmission line's capacitance is split in half and put at the receiving end and transmitting end, respectively, throughout the nominal-method.

Long Transmission Line

Long transmission lines are defined as overhead transmission lines that are longer than 150 km. These lines operate at a voltage greater than 100kV. Their line parameters are expected to be distributed uniformly over the length of the line for handling of this kind of line.

DC Transmission Line

In AC transmission lines, both cost of the transmission line associated loss rises for the transmission of electricity over long distances under higher voltages. Additionally, because to a rise in supply voltages and distance, the ac long transmission line has issued such stability limitations, voltage management, line compensation, connectivity of lines, grounding impedance, etc. The creation of HVDC (high voltage direct current) transmission, which is nothing more than a dc transmission line, was prompted by the many issues with long-distance ac transfer of data. Long transmission lines can be powered by direct current (DC), which provides a number of benefits including no stability issues, no charging current, minimal skin effect, no need for reactive correction, bulk power transfer, economic power transmission, etc. stringent techniques are employed for their solution, which is top of the line. Converters can be used to construct a dc transmission, but power generation and usage remain at ac levels. Two converters are needed, one at the transmitting end and a second on the receiving end. The converter at the receiving end side functions as the inverter whereas the converter at the sending end side functions as the rectifier (converts ac voltage to dc voltage) (converts dc to ac). However, using a dc transmission method across short and medium distances is ineffective.

LITERATURE REVIEW

Shenxing [1] et al. have introduced the protective relaying system for transmission lines includes the fault classification as a key component. The classification of faults in transmission lines using half-cycle superimposed current signals is addressed in this paper using a novel method based on group sparse representation. The proposed method described in this study reduces the need to manually design features when compared to traditional feature extraction methods. Signals are factorized over an overly-complete basis, where the fault signals themselves are the basis' elements. The classification algorithm is based on the notion that any test sample which belongs to a class can be roughly derived from the training samples of a specific fault type. The coefficient should be group sparely populated and its non-zero submissions correspond to a specific group of correlated training samples when it is solved by l2, 1 minimization. It is demonstrated that the suggested classification method can be appropriately adjusted to handle signals that contain noise. Moreover, the random mapping technique is used to reduce the dimensions. The results of many PSCAD/EMTDC simulations as well as field data from a genuine system show that the suggested technique is accurate, quick, and noise-resistant for fault classification.

Arouche Freire [2] et al. have managing the significant disturbances that might occur during generation, transmission, and distribution is essential for maintaining the quality of the power in electrical power systems. In order to aid in the management and upkeep of the electrical system,

several studies seek to analyze these disruptions by examining the behavior of a electrical signal via the categorization of short circuit faults within power transmission lines. Most fault classification methods, however, have a high computational cost and do not always produce satisfactory results; the above methods use front ends in data processing before being processed by traditional classification algorithms like Artificial Neural Network (ANN), Support Vector Machine (SVM), K-Nearest Neighbors (KNN), but also Random Forest (RF) which are adopted into to the Frame Based Sequence Classification (FBSC) architecture that uses the whole front ends Wavel. The UFPAFaults database and the Hidden Markov Model (HMM) algorithm, which directly handles the electrical signals in the form of multivariate time series are an alternative way for identifying faults without the usage of front ends. The HMM algorithm is suggested as a potential classifier by the results because it performs better than the traditional classifiers ANN, SVM, KNN, and RF when used with the FBSC architecture due to its comparably low error rate of 0.03%. Only the ANN and RF classifiers provide such a result that is close to what the HMM algorithm offers whenever the statistical test with such a significance of =5% is applied. Another important consideration is that the HMM algorithm significantly reduces computational costs by more than 90% of processing time when compared to the traditional classifiers of a FBSC architecture, demonstrating the algorithm's potential for direct fault classification in transmission lines for the electric power system.

Yanhai Wang [3] et al. have using the Basic computer vision tasks include image classification and object detection. In this study, we introduce transmission line fault detection. Noise and transient magnitude can have an impact on traditional fault detection techniques in transmission lines. Researchers propose a novel fault zone detection method that makes use of a quality-aware, fine-grained categorization model that is well encoded for the discovery of category cues in order to get around these limitations. Our method seeks to identify the most distinct image patches for categorization. Wavelet-support vector machine and quality-based discriminative feature extraction are the main methods used in our approach. By using Fast R-CNN based image samples decomposition, in which the quality module is used to choose the most discriminative areas, they are able to extract the characteristics of the line currents. The extracted features are then used to train an SVM to identify the fault. We carry out thorough research on transmission line fault detection to confirm the viability and superiority of with us suggested approach.

Balakrishnan, P and Sathiyasekar, K. [4] have approach Discrete Wavelet Transform (DWT) based Wavelet Transform (WT) is a new algorithm for defect detection, classification, and destination of overhead transmission lines that is proposed. The various system faults, including LG, LLG, and LLLG in transmission lines, should be quickly identified, categorized, and located. The voltage and current signal documentation from of the MATLAB power model is the foundation of the suggested technique, which generates transient voltage and current signals in both the time and frequency domains. To record transient current signals and extract relevant high frequency detail coefficient for identifying and categorizing the fault disturbance, DWT is utilized using "db6" as the mother wavelet. The ground threshold value provides the basis for the categorization process. By obtaining the fault data from the source terminal finish to the remote terminal end and the total length of the transmission line, faults can be located. Simulink model and the MATLAB/SIMULINK environment are used to test the proposed method. The suggested algorithm successfully detected, classified, and located all eleven categories of potential

transmission line faults during simulation, and the results were compared to those obtained using the AR and MED technique.

Yanpeng Hao [5] et al. have transmission line forecasting is crucial for power grid anti-icing strategies, but current prediction models have drawbacks like application restrictions, poor generalization, and just a lack of worldwide prediction capability. The classification of a icing process plays an important role in this paper's proposed segmental icing forecasting model for transmission lines, which aims to address these shortcomings. A hierarchical K-means clustering method is used to obtain the classification, and 11 characteristic parameters are suggested. Using this method, 97 icing processes from of the China Southern Power Grid's Icing Monitoring System have been grouped into six categories based on the shape of their curves, and abstracted icing evolution curves are created based on the clustering centroid. The findings support the notion put forth for the segmental icing forecasting model by demonstrating that the procedures of ice events are likely different and that the icing process can be thought of as a combination of various segments and nodes. The types of icing evolution that have been obtained through monitoring data and clustering are more detailed and specific, and this work lays the groundwork for building models as well as contributing to other fields.

Subodh Kumar [6] et al. have proposed a novel method for fault detection and classification that used the CNN (Convolution Neural Network) architectural style, primarily the VGG-16 and VGG-19, and the application of the DWT (db-8) and CWT filter banks. This method has been used for the fault current throughout three phases' detailed decomposition at seven levels in a transmission line with a 600 MVA capacity for 200 km, respectively, for different distance but also fault inception angle. The fault current, which is discovered using the transmission line throughout three phases for various times, distances, and fault inception angles, is comprehensive coefficient decomposed to use the db-8 wavelet at 12.5 kHz frequency response for six levels, and the resulting representation of time and frequency, known as a spectrogram, would then be computed by CWT filter banks. Then, for the purpose of classifying various faults and comparing the two architectures, we train those images and used the VGG-16 and VGG-19 architectures. Compared towards the ANN architecture, this method is much more robust and validates a lot of data in a short amount of time.

Mohammad Farshad [7] has using the K-means data description (KMDD) method, it was suggested a novel protection scheme again for detection and classification of fault conditions in bipolar HVDC transmission lines. The dc voltage and current signals here on inverter side are used in the proposed compensation scheme. For these signals, relatively brief time windows are taken into account, and the sum values of data windows are computed. The KMDD method is used to prepare some post-fault data generated under various circumstances for each dc fault type. Then, even in the presence of unknown conditions, new internal dc faults are detected and classified using the obtained centroids and thresholds. A 1000 km bipolar overhead HVDC transmission line is used to evaluate the effectiveness of the proposed method for 4320 internal and 2816 external fault situations under conditions that were not present during the planning phase. The results obtained show that now the proposed protection scheme has been stable during external ac faults as well as the pre-fault normal conditions through addition to being straightforward and requiring low sampling frequencies for internal dc faults.

Yuxuan Liu [8] et al. have used machine learning algorithms may be well suited for classifying LiDAR point clouds, but when they are employed to classify point clouds of power facilities,

many issues, including a high number of computational features and poor computational efficiency, may arise. This study suggests using the Adaboost algorithm and several topological restrictions to resolve these issues. The Adaboost algorithm is used to perform coarse classification and select the top five features for each object that have the best discrimination. These top five features are then combined together into strong classifier. The best scales are instantaneously chosen for power transmission lines, and even the rough classification results are improved. Because of the similarities of their proposed major characteristics, it is challenging to distinguish power towers from vegetation points when using only spatial features. In order to distinguish the power buildings from vegetation points, the topological association between both the power line and power tower has been introduced. The experimental outcomes demonstrate that our method can accurately and even more effectively classify power transmission lines and power towers than manual classification.

Osaji Emmanue [9] et al. have explained Technology advancement in the interconnection of Renewable Green Energy Sources (RGES) such as Photovoltaic (PV) systems and Wind Farm Generators (WFG) into conventional power systems as a potential future solution to meet the rising demand for energy globally in order to lower the cost of power generation and lessen the impact of climate change. Security protection of the power system is also put at risk by this innovation since injected fault current infeeds on existing facilities impair it. This infeedcauses a healthy section of a connection to trip unexpectedly and a failure of a protection system. This study uses extracted one-cycle fault signature of both voltage and current signals with wavelet statistical method in MATLAB to introduce an adaptive fault classification method on High Voltage Transmission Line (HVTL) both with and without RGES-WFG integration configurations. The results are distinct entropy energy principles on proposed network infrastructure but also distinct signatures between all fault types but also fault distances. With only an operation time of 0.01 seconds, the algorithm for supervised machine learning from of the Bayesian network generated the best-generalized model with just an RMS error value of 0.05 again for identification and classification of single line-to-ground (SLG) faults. Ideal for integrating an adaptive unit protection strategy.

Pradyumna Kumar [10] et al. have utilizing feed forward and radial basis component neural networks, a novel method for the identification and tracking of transmission line congestion in power systems is presented. To achieve the desired result of identifying the overloaded or congested lines, the neural network is trained to discover the complex mapping between such a variety of nonlinear multi-objective input functions and also the designated target during the detection stage. For classification of both the congested lines according to their severity, the cases indicating sentence congestion during in the detection phase are presented to the radial basis functions neural network. The proposed feed forward neural network with Levenberg-Marquardt back - propagation algorithm scheme provides the fastest convergence even though compared to other types of stochastic gradient descent schemes and also the conventional approach as well, according to the results of a MATLAB-based case study carried out on the IEEE 30-bus test system. Additionally, the severity classification stage of the radial basis functions neural network exhibits demonstrably quicker convergence.

DISCUSSION

Power systems need transmission lines as a critical component. Transmission line faults lead to equipment instability and damage. In order to prevent problems, the electric power system must

be protected. For effective protection, the defective line must be immediately isolated from the system when the issue has been found. To restore the system and hasten its recovery, fault categorization and placement must then be carried out. There are numerous algorithms for fault detection and classification that have been developed, according to fault transients. How transitory characteristics are recovered from the initial fault signal is a key concern in the proposed technique. As a result of its perfect time frequency localization capabilities, Wavelet Transform (WT) is chosen as the most effective tool to analyze the fault. It has been suggested to use wavelets to extract features effectively. It is discussed whether WT is appropriate for non-stationary signal analysis. With the aid of WT expressed, local analysis of the relaying signal. To identify defects and poor phase selection, WT is used to collect the high frequency components of traveling waves. For series compensated transmission lines, the fault classification tool is developed using the discrete wavelet transform (DWT). DWT is a web-based tool utilized by relaying applications. Despite the fact that WT is well suited for transient wave analysis, it still needs some improvements in order to find and categorize faults. There are some restrictions on how many fancy pictures can be displayed, and its transformed output even now contains a lot of data that needs to be processed further. This makes it more difficult to automatically extract features for defect detection and classification.

The transmission line is the part of the Electric Power System (EPS) that is most susceptible to failures, particularly as the line is prone to a variety of different sorts of natural phenomena from one end to the other, including atmospheric discharge, forest fires, windstorms, and much more. Such circumstances may result in disruptions (faults) inside the transmission line, which may subsequently stop the flow of electric energy. Short circuit type faults are indeed the ones which have the biggest effects on consumers among transmission line faults. According to studies, these faults are to blame for about 70% of power systems malfunctions and blackouts. As a result, it is clear that EPSs must implement methods for diagnosing and recognizing these problems. It is also essential to analyze the electrical signal behavior via short circuit fault categorization in order to help with power supply maintenance and restoration. There are two categories of transmission in-line fault classification systems are live classification systems and post-fault classification approaches. Online classification systems reach a decision (classification) quickly, with both the analysis segment (and frames) roughly coinciding with the moment the defect manifests itself. Post-fault classification varies from online classification within this entry is a vector of fixed size. Post-fault classification may be carried out offline, as well as its input is indeed a multivariate variable duration (length) series data. Problems that can be allowed to treat as problems of conventional classification and sequence are attempted to be solved by online and post-fault systems, respectively.

Sparse Representation Technique

Signals convey obscene quantities of data, where it is often impossible to detect the important information like a needle in a haystack. In a sparse representation, processing is quicker and easier since fewer coefficients disclose the desired information. Such representations may be created by breaking down signals across fundamental waveforms from a collection of waveforms known as a dictionary. However, the hunt for the Holy Grail of the perfect sparse transform tailored to all signals is fruitless. There is now a veritable forest of novel transforms available because to the discovery of wavelet orthogonal bases using local time-frequency dictionaries. Therefore, an essential survival strategy is to adapt sparse representations with signal features

and derive effective processing operators. If created with the intention of concentrating the signal energy across a small collection of vectors, an orthogonal basis is indeed a dictionary of the smallest possible size that may provide a sparse representation. A geometric signal description is provided by this collection. Then, using diagonal operators calculated using quick techniques, efficient signal compression and noise reduction procedures are used. However, it's not always the best. A more comprehensive dictionary aids in the construction of concise and precise statements in natural languages. Similar to this, creating sparse representations of complicated signals requires dictionaries containing vectors that are bigger than bases. However, selecting is challenging and calls for more sophisticated algorithms. The resolution of novel inverse issues may also be enhanced by sparse representations using redundant dictionaries, in addition to pattern identification, compression, and noise removal. This comprises compressive sensing, source reduction, and super resolution.

The relevant qualities of the sparse representation approach in signal representation and reconstruction have led to its significant success in the area of signal processing. The technique's fundamental concept is to mimic the original signal using only a few words from the dictionary. Sparse representation has seen significant growth in popularity in recent years across a variety of industries, including state estimation, face recognition, digital identification, objection detection, and picture classification. The creation of an efficient dictionary is a major problem for sparse representation, however. It suggested a sparse representation technique in which a dictionary is created straight from the training data. It will be feasible to represent these test samples as just a linear combination of only those training samples belonging to the same class provided sufficient training samples from each class are provided. However, it is not anticipated that training signals from other classes would enhance the representation of the test sample. Since only a tiny portion of the complete dictionary would be included, this depiction is meant to be minimalist. In addition, it is suggested to penalize the linear combination's coefficients' l 1 -norm. The correlation between the training samples is not taken into account by the sparsity in the amount of training data. The label information from training samples is taken into account, and the class sparsity—which causes group sparsity—is prioritized above the amount of training samples. Group sparse representation can be effectively recovered by l 2, 1 reduction thanks to recent advancements in the theory of sparse representation using compressed sensing. Notably, the sparse representation-based classification technique eliminates the need to create a separate classifier. Ideally, after computing the sparse solution, all nonnegative entries in the coefficient correspond to training samples from such a single class, making it simple to place the test sample in that class.

Representation of Fault Signals in Sparse Form Measured three-phase half-cycle superimposed current signals are therefore stacked in the sequence of phase-a, phase-b, and phase-c to create the training and testing samples, which are used to categorize faults. Assume that the length of the stacked signal, m, is represented by the symbol. The supplied ni training examples from the i-th class was put into a matrix called Ai = [i,1, i,2,..., ni] R mni, where the columns represent the given samples. Any testing signal y from the same class will roughly reside in the linear span of a training samples connected with signal I if the i-th signal class has enough training samples.

$$\boldsymbol{y} = \alpha_{i,1}\boldsymbol{v}_{i,1} + \alpha_{i,2}\boldsymbol{v}_{i,2} + \ldots + \alpha_{i,n_i}\boldsymbol{v}_{i,n_i},$$

I, J, and J are equal to 1, 2, ni for certain scalars. The matrix A = [A1, A2, Ak] R mn, where n = Pk i=1 ni, is used to represent the training samples for all k classes. After that, all training samples may be used to rewrite the linear representation of such a testing signal y as:

$$\boldsymbol{y} = A\boldsymbol{x}_0,$$

x0 = [0,..., 0, i,1, i,2,..., i,ni, 0,..., 0] The elements of the sparse vector T R n, with the exception of those connected to the i-th class, are all zeros. Each atom in dictionary A is normalized to also have unit l 2 -norm, which means that for an atom with the symbol, it is normalized to /kk2. This is done because the magnitude for fault components varies depending on the fault situation. Since m is often less than n in situations based on sparse representation, Equation is unknown, and its solution is indeed not unique. Studies in the literature on compressed sampling, however, reveal that the sparse solution is also distinct if the solution is recognized to be sparse. Only the training samples taken from the same class may adequately reflect a valid test sample y. If k is big, this representation is inevitably sparse. Equation is a linear inverse problem as a result, and its sparse solution is unique. The following optimization issue solves the coefficient x0:

$$(l^0): \ \hat{\boldsymbol{x}}_0 = \arg\min \|\boldsymbol{x}\|_0 \ s.t. \ A\boldsymbol{x} = \boldsymbol{y},$$

Where the l 0 -norm, which determines the number of nonzero entries in x, is denoted by ||x||0. Although it is theoretically conceivable to solve the NP-hard l 0 -minimization issue, doing so would be impractical since it calls for a thorough examination of all potential combinations. The following approximate answer is achieved by substituting the l 0 norm with the l 1 norm:

$$(l^1): \ \hat{\boldsymbol{x}}_1 = \arg\min \|\boldsymbol{x}\|_1 \ s.t. \ A\boldsymbol{x} = \boldsymbol{y},$$

Compressed sensing theory demonstrates that if certain sparsity requirements are met, i.e., the answer is sufficiently sparse and the solution of Equation is identical to the solution of Equation, it is possible to compute effectively. The l 1 -minimization issue may be solved quickly using one of five sample methods as follows: Homotopic, Iterative Shrinkage-Thresholding, Proximal Gradient, Gradient Projector, and Augmented Lagrange Multiplier (ALM).

Criterion of Classification: Minimal Reconstruction Error

The test signal y should be tagged to that class such that, after the test signal y is recovered, those nonzero elements in the estimate x1 are all connected to columns of A from the same object class. The coefficient x may, however, have a few minor non-zero entries related to many classes that are brought on by noise or modeling mistake. A simple classifier based on the reconstruction error was subsequently created. A function i(x) preserves the non-zero entries throughout x that are associated with each class I and sets the other coefficients to zero for each class i. Ai(x1) is a representation of a test signal y approximation for the i-th class. The Euclidean distance between the test signal y as well as the approximation signal Ai(x1) is the reconstruction error again for i-th class. The test signal may then be categorized by placing it in the fault class with the lowest reconstruction error:

$$\min r_i(\boldsymbol{y}) = \|\boldsymbol{y} - A\delta_i(\hat{\boldsymbol{x}}_1)\|_2$$

The complete sparse representation-based classification method is stated in Algorithm 1.

CONCLUSION

Sparse signal representation allows for the highly efficient acquisition, representation, and compression of high-dimensional signals. This success is primarily due to the innately sparse representations that important types of signals, such as audio and visual signals, have in relation to fixed bases (such as Fourier or Wavelet), or concatenations of these bases. Such representations may also be computed using optimistic pursuit-based methods or convex optimization without sacrificing high accuracy. These algorithms are reliable and efficient. Despite the fact that images (or their properties) are intrinsically very high dimensional, images from the same class exhibit degenerate structure in many applications, which adds to the ability of sparse representations to reveal semantic information. In other words, they are located on low-dimensional subspaces, sub manifolds, or stratifications or nearby them or inside them. If additional representative samples are collected for the distribution, it should be anticipated that a typical sample will present a rather sparse representation with relation to such a (perhaps learned) basis.

References:

[1] S. Shi, B. Zhu, S. Mirsaeidi, and X. Dong, "Fault Classification for Transmission Lines Based on Group Sparse Representation," *IEEE Trans. Smart Grid*, 2019, doi: 10.1109/TSG.2018.2866487.

[2] J. C. Arouche Freire, A. R. Garcez Castro, M. S. Homci, B. S. Meiguins, and J. M. De Morais, "Transmission Line Fault Classification Using Hidden Markov Models," *IEEE Access*, 2019, doi: 10.1109/ACCESS.2019.2934938.

[3] Y. Wang, Q. Li, and B. Chen, "Image classification towards transmission line fault detection via learning deep quality-aware fine-grained categorization," *J. Vis. Commun. Image Represent.*, 2019, doi: 10.1016/j.jvcir.2019.102647.

[4] P. Balakrishnan and K. Sathiyasekar, "Transmission line fault detection, classification and location using wavelet transform," *Int. J. Eng. Adv. Technol.*, 2019, doi: 10.35940/ijeat.F1337.0986S319.

[5] Y. Hao *et al.*, "A classification method for transmission line icing process curve based on hierarchical k-means clustering," *Energies*, 2019, doi: 10.3390/en12244786.

[6] D. Paul and S. K. Mohanty, "Fault Classification in Transmission Lines Using Wavelet and CNN," 2019. doi: 10.1109/I2CT45611.2019.9033687.

[7] M. Farshad, "Detection and classification of internal faults in bipolar HVDC transmission lines based on K-means data description method," *Int. J. Electr. Power Energy Syst.*, 2019, doi: 10.1016/j.ijepes.2018.07.044.

[8] Y. Liu, M. Aleksandrov, S. Zlatanova, J. Zhang, F. Mo, and X. Chen, "Classification of power facility point clouds from unmanned aerial vehicles based on adaboost and topological constraints," *Sensors (Switzerland)*, 2019, doi: 10.3390/s19214717.

[9] O. Emmanue *et al.*, "Hybrid signal processing and machine learning algorithm for adaptive fault classification of wind farm integrated transmission line protection," *Int. J. Integr. Eng.*, 2019, doi: 10.30880/ijie.2019.11.04.010.

[10] P. K. Sahoo and P. K. Satpathy, "Detection and Classification of Transmission Line Congestion by Feed Forward and Radial Basis Function Neural Networks," *J. Inst. Eng. Ser. B*, 2019, doi: 10.1007/s40031-018-0362-4.

CHAPTER 7

OVERVIEW ON FERRANTI EFFECT IN TRANSMISSION LINES

Mr. Ravi V Angadi, Assistant Professor
Department of Electrical and Electronics Engineering, Presidency University, Bangalore, India
Email Id-raviangadi@presidencyuniversity.in

Abstract:

Whenever an electrical transmission line being run in a no-load or low-load situation, the Ferranti Effect causes the voltage there at receiving end to rise. As a consequence, the voltage at the receiver end is greater than at the sending point. In this chapter author is discusses Detail explanation of the Ferranti effect by considering a nominal pi (π) model.

Keywords:

Electrical Transmission,Electricity, Ferranti Effect, Power, Transmission Line.

INTRODUCTION

Whenever an electrical transmission line was run in a no-load or low-load situation, the Ferranti Effect causes the voltage there at receiving end to rise. As a result, the voltage at the receiving end was higher than at the sending point. Sebastian Ziani de Ferranti, and electrical engineer, made this occurrence known. He initially noticed an increase in voltage in some locations of a London electricity supply in 1887. The interplay of the line's capacitance and inductance results in the effect. The voltage at the receiving end may be proportional to the applied voltage whenever the power line is used in no-load or low-load situations. This voltage may result in hazardous conditions and put stress on the cables and equipment if it exceeds the line's rated value. The Ferranti effect inside an electric transmission line was explained using the traditional T-scheme in Figure 1. The charging current of a line is what causes the Ferranti effect. The current that enters the capacitor whenever an alternating voltage was provided is referred to as the charging current. Capacitive current is another name for a charging current. Whenever the line's receiving end voltage is higher than its sending end, then charging current in the line rises.

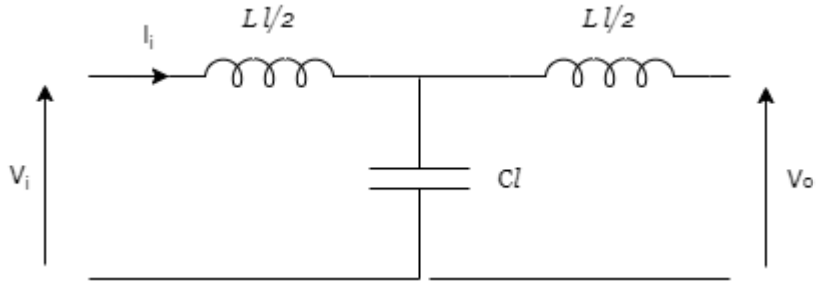

Figure 1: Illustrates the T Scheme of a transmission line.

Where,

L= is the longitudinal inductance of the line [H/km]

l= is the length of the line [km]

C =is the transversal capacitance of the line [F/km]

Vi= is the voltage at the input of the line

Ii= is the current at the input of the line

Vo= is the voltage at the output of the line.

The Kirchhoff principle is applied to the circuit above using the following equation, which assuming the line is in an "open circuit" (no-load) state:

$$I_i = \frac{V_i}{(j\omega L\frac{l}{2} - j\frac{1}{\omega Cl})}$$

$$V_o = -j\frac{l_i}{\omega Cl} = -j\frac{V_i}{\omega Cl\left(j\omega L\frac{l}{2} - j\frac{1}{\omega Cl}\right)} = \frac{V_i}{(1-\omega^2 CL\frac{l^2}{2})}$$

It is clear from the circuit model that the output voltage seems to be the voltage on the capacitor because there is no load present. It'll see where a crucial factor in the Ferranti effect is the line's longitudinal capacitance. In particular, calculating the differential between them, referring to the output voltage, has shown us that the output voltage Vo is greater than the input voltage Vi. This can be seen from the calculations above:

$$\frac{V_o - V_i}{V_o} = \omega^2 CL\frac{l^2}{2}$$

These observations lead us to various important conclusions, including the following: The Ferranti Effect is more likely to impact transmission lines for power systems running at higher frequencies. For instance, if two identical electrical lines were run at the same voltages but then at different frequencies, the line operating at the higher frequency would need to be shorter to prevent an unwanted potentially dangerous voltage increase through the other end. The Ferranti Effect will become more noticeable with cable lines since the frequency inductance inside a cable typically ranges from 0.5 to 0.7 times that of an overhead line. However, the capacitance values are typically 20 to 60 times greater.As a result, the line inductance and capacitance combination with a cable line might be 10 to 30 times greater. The line's length is quite important. However, whenever the line length approaches /4, the length becomes much more crucial. At the no-load situation, it is feasible to show that the trigonometric nomenclature of the transmission line formulas:

$$V_o = \frac{V_i}{\cos 2\pi\frac{l}{\lambda}}$$

Since we have 02l/2 for 0l/4 (and 0l1500 km at 50 Hz), the term at the denominator somewhere between 1 and 0. The voltage at the line's receiving end tends to really be infinite as even the line length approaching /4. The interplay of the line's inductance and capacitance is indeed the primary cause of the Ferranti Effect. Generally, it is well recognized that the Ferranti Effect should be properly considered when designing a power distribution system that prevents unexpected voltage rises that might result in failures and harmful circumstances.We must restrict the maximum length of both the electrical transmission cables in order to prevent the Ferranti Effect. Because of this, standard power transmission lines are limited to 600–700 km at 50 Hz (or 500-600 km at 60Hz).

Ferranti Effect Occurs:

The primary parameters of lines with a length of 240 km or more are capacitance and inductance. The capacitance is really not concentrated at specific locations on such transmission lines. It is evenly dispersed over the whole duration of the line. The current drawn by that of the line's capacitance when the voltage is supplied at the transmitting end is greater than the current voltage is measured. Therefore, compared to the usual voltage at the transmitting end, the voltage somewhere at receiving end is relatively high for no load or a low load. The inductance and capacitance of both the line might generate a resonance scenario by shortening it to reduce these phenomena, as a result of the line's inherent constructive characteristics. Installing an extra reactor is a frequent approach to prevent the Ferranti Effect (basically an inductance). This significantly lessens this issue and compensates again for line's transversal capacitance.

LITERATURE REVIEW

Hiremath [1] et al. have introducing Electrical Energy is transferred from a generating location, such as a power plant, to an electric substation via electrical power transmission lines. The transmission network refers to the network of interconnecting lines that makes this possible. These transmission lines are distinct from the distribution network, which connects high voltage substations to customers. The examination of transmission lines is a significant subject in the Electrical Engineering program's curriculum. This involves having a basic grasp of ideas like the Ferranti effect, ABCD parameters and their analysis, the efficiency of transmission lines and the computation of losses, modeling of transmission lines (T and Pi sections), surge impedance loading, and other related ideas. Transmission line simulations are often used to examine the aforementioned ideas. Students investigate these transmission lines in experiments. The experimental platforms on which various features of Transmission lines are examined are simulators that replicate the corresponding model of the actual Electrical Power Transmission Lines operating for many kilometers of lengths. These kinds of simulators are a limited resource in the setting of many engineering institutions; normally, a particular school would have no more than one such setup. This is due to these simulators' high price and large size.

Amreiz [2] et al. have several electrical engineering courses have included the teaching of transmission lines at both the undergraduate and graduate levels. These courses were taught using a strategy that included mathematical analysis and the identification of analogous circuits. When working with a large variety of electrical components within a circuit, such an approach will provide challenging difficulties for the pupils. Circuit simulation has been a significant aid in the teaching of transmission lines at any and all levels during the last ten or so years. A 180 km long HVAC transmission line was employed as the model transmission line for this study. The transmission line may be simulated as just a single-phase transmission line with a length of 540 km or as a three phase transmission line with a length of 180 km. Each segment of the 180 km transmission line was 30 km long, and the line is split into 6 pieces. Every 30 kilometers, the line inductance was taken into account, and every 15 km, the line capacitance. Actual values for the 400KV transmission line's line parameters (RLC) are 0.02978/km, 1.06 mH/km, and 0.0146 F/km, respectively. The transmission cable carries 250W of electricity.

Mukesh Nagpal [3] et al. have explained that over the course of three days, additional visits for line protection were required due to the 500-kV line corridor's heavy smoke from nearby wildfires. Shortly after the line was de-energized, a switchable line-connected reactor that was intended to manage Ferranti voltages tripped and locked out twice by its protection. Up until

visual inspections of the reactor were performed on both instances, lockout operation limited operating flexibility and prohibited speedy reactor reinsertion. The smoke increased the line capacitances, according to the results of the forensic examination into the incident. When the line tripped and the reactor and line both were de-energized, this resulted in the creation of a near-60-Hz zero sequence resonant circuit. The capacitive linked zero sequence 60-Hz voltage created by circuits that operate briefly next to the line was amplified by the resonant circuit. The sensitive ground overcurrent protection was tripped by the voltage amplification's sufficient current flow through the reactor. A comprehensive mitigation is intended to prevent a repeat of the incident and actually improve line dependability. Because this issue of unexpected activation of line shunt reactor protection has not before been disclosed, the purpose of this article is to share lessons gained from the event investigation with peer utilities.

Xiaohua Li [4] et al. represented there will be more installations of crossing AC and DC lines as a result of the benefits of DC in long-distance transmission and the lack of power transmission corridors. Line contact faults are common in AC/DC systems because of the close spacing between the lines. There is no unique defense provided by AC systems. Although DC systems have included AC/DC line contact protection, there hasn't been much study on how to use it. DC protection activities function erratically as a result of the arrival of the AC component. As a consequence, there are several ways for DC protection to operate. The fault-treating process in DC systems may be quite difficult since various DC protection trip strategies might vary greatly across companies. This study simulates an AC/DC line contact failure while taking into account important factors by developing an AC/DC crossover model with comprehensive AC and DC protection. Both AC and DC systems have potential dangers, as shown by the simulation study's conclusion. The AC line's direct current component will make it difficult to activate the circuit breaker, and at the location of ABB's block strategy, the Ferranti effect will cause a significant overvoltage. The hazards may be reduced by increasing AC protection's existing zero detection.

A. Divya Swarna Sri [5] et al. have explained that different components are used in a flexible AC transmission system to increase the stability and transfer capacity of the transmission system. When there is no load or a light load there at receiving end, this approach may be used to charge the transmission line. Shunt capacitance inside the transmission line would become dominant as a result of the low current flowing through the transmission line. Because of the electrical amplification caused by this (Ferranti Effect), the voltage at the receiving end would be higher than the voltage at the transmitting end (effect will be high in long transmission line). Shunt inductors are linked across the transmission line to counteract the Ferranti effect. This study uses an inductive circuit to lessen the Ferranti effect. Proposed circuit has been realistically tested in hardware system after being modelled using MATALB and Simulink.

Noureddine Hidouri [6] has investigated a 380 kV transmission line model connected to an experimental wind turbine simulator. The author first discusses a theoretical study focusing on the model of a wind turbine, the salient synchronous generator, and also the transmission system before presenting and evaluating the experimental results that deal with both the voltages, the Ferranti effect, the active and reactive powers there at sending end and even the receiving end with different kinds of loads. Additionally covered are the Ferranti effect and the power analysis. Theoretical research and experimental findings have advantages.

Kumarshanu Chaurasiya [7] et al. since most power quality concerns may be mitigated or resolved with sufficient control of reactive power, the idea of reactive power management encompasses a wide range of both system and customer problems. When large inductive loads

are connected into transmission lines, a poor power factor problem is often seen because of the trailing load current. Also occasionally, when there is little load on the transmission line, very little current flows through it, creating a leading shunt capacitance that amplifies voltage and causes the receiving end side voltage to sometimes double that of the sending end side voltage (the Ferranti effect) in long transmission lines. By combining a parallel configuration of a thyristor controlled reactor (TCR) and a thyristor switched capacitor (TSC), which would automatically provide a smooth current control wide variety from capacitive to inductive values by varying this same firing angle of a thyristor through with a microcontroller, we have a novel phenomenon of hybrid reactive power attempting to control model.

Miodrag Forcan [8] et al. have describes an enhanced teaching technique that has been created for the analysis of balanced functioning of overhead transmission lines. To attain higher-level knowledge accomplishment, the suggested educational strategy integrates theoretical, simulation, and experimental methodologies. There are a number of exercises that have been developed and used in the teaching process. Some typical steady state regimes for overhead transmission lines, including the Ferranti effect, natural load flow, and capacitive overhead line behavior, have been studied. To ascertain the fundamental properties of the switching transients, a specific investigation has been conducted. The simulation analysis and parameter estimate of the system were done using the MATLAB/Simulink software suite. The comparison of several overhead power transmission models led to the recommendation of practical modeling recommendations. In order to undertake experimental computations, a physically scaled system made up of numerous Pi sections that replicate a 400 kV overhead transmission line 100 km in length has been used. The suggested approach was tried in a high voltage electronics undergraduate course, and students provided insightful application comments.

Tuan Ngo and Tuyen Vu [9]presented our ongoing research on the use of low frequency AC (LFAC) in wind turbine applications. It is obvious to observe that the transmission reactance is greatly decreased when the operating frequency of the power system is dropped. As a consequence, the quantity of reactive power on the transmission line is significantly reduced. Additionally, low frequency operation helps reduce the Ferranti effect, or capacitive line charging, in an overhead line transmission system, preventing excessive voltage increasing problems. A two-bus power system is used to numerically illustrate the advantages of low frequency operation. The investigation of transformer behaviour at various operating frequencies is very crucial. In Ansys Maxwell 3D, a detail transformer model for a 2.0 MW wind turbine application is developed and tested. The simulation demonstrates that a transformer's core losses, or hysteresis but also eddy current losses, are lower in low frequency operation than those in 60 Hz operation. The transformer architecture should really be cautious for low frequency operation because the flux density within the core is larger under low operating frequency than it is during 60 Hz operation.

Nassim Guernoudj [10] has presented the Ferranti effect (line capacitive effect). In the area of power transmission across vast distances using relatively low frequencies, Ferranti effects are well-known (Ibrahim A et.al, 005). When using very long transmission lines, the voltage there at receiving end may often double that at the sending end (Walling J). It is essential to find a way to stop this effect from occurring in our network since it has the potential to be very damaging to network equipment, particularly for line and electric cable insulation. With the knowledge that this network has been powered by that of the gas turbine plants of Adrar and Also in Salah, interconnected through such a 220Kv network extending from In Salah to Timimoun via Aoulef

and Adrar, we performed several test results of MATLAB simulations upon that Algerian network ADRAR and particularly electrical transmission line segments (line ADRAR TIMIMOUNE 192Km and line ADRAR IN SALAH 409Km) with and without mobile self. Finally, this simulation research improves the grid's voltage setting. The benefit of employing the mobile self 220Kv for balancing the voltage there at end of high voltage cables is made clear.

DISCUSSION

It is possible to think of a lengthy transmission line as having a significant quantity of both inductance and capacitance dispersed throughout its whole length. The Ferranti Effect happens when the current pulled by the line's dispersed capacitance is higher than the current generated by the load at the line's receiving end (during light or no load). This capacitance charging current causes a voltage drop across the transmission system's line inductance, which is in phase with both the voltages at the sending end. As we approach closer to the loaded end of the line, this voltage drop continues growing additively, and as a result, the voltage at the receiving end tends to rise beyond the voltage being supplied, causing the phenomenon known as the Ferranti effect in the power system. Let's use the phasor graphic below to show this.

Detail explanation of the Ferranti effect by considering a nominal pi (π) model:

Let us consider the long transmission line in which OE represents the receiving end voltage; OH represent the current through the capacitor at the receiving end. The phasor FE represents the voltage drop across the resistance R. The voltage drops across the X (inductance). The phasor OG represents the sending end voltage under a no-load condition (Figure 2).

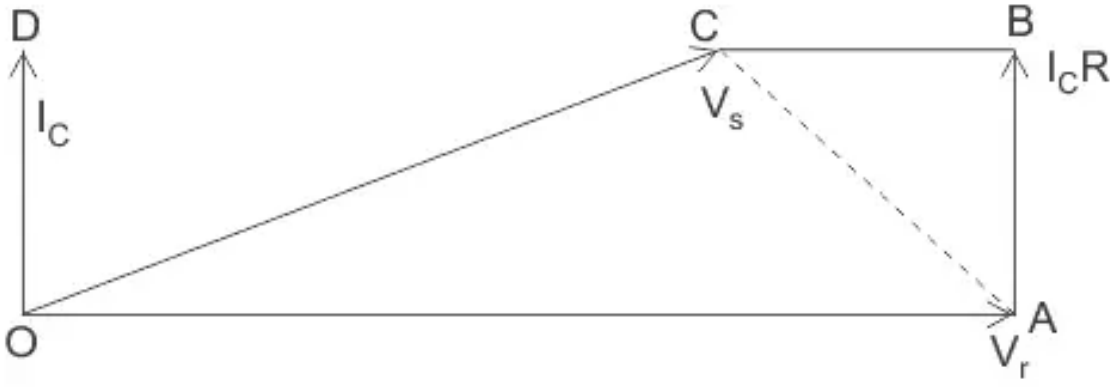

Figure 2: Ferranti effect by considering a nominal pi (π) model,

Therefore, this specific phenomenon is caused due to both the capacitance and inductor impact of the transmission line. As a result, the Ferranti effect is minimal in the instance of a short transmission line since the inductor of such a line is realistically thought of as being close to zero. The no-load receiving end voltage has indeed been observed to typically be 5% higher than that of the transmitting end voltage for just a 300 Km line running at a frequency of 50 Hz. Let's now analyze the Ferranti effect by taking a look at the phasor diagrams that were previously shown. In this case, Vr is regarded as the reference phasor and is represented by OA.

$$Thus\ V_r = V_r(1 + j0)$$
$$Capacitance\ current,\ I_c = j\omega CV_r$$
$$Now\ sending\ end\ voltage\ V_s = V_r + resistive + reactive\ drop.$$
$$= V_r + I_cR + jI_cX$$
$$= V_r + I_c(R + jX)$$
$$= V_r + j\omega CV_r(R + j\omega L)[Since\ X = \omega L]$$
$$Now\ V_s = V_r - \omega^2 CLV_r + j\omega CRV_r$$

For a nominal pi (π) model

$$V_s = \left(1 + \frac{ZY}{2}\right)V_r + ZI_r$$

At no load, Ir = 0

$$V_s = \left(1 + \frac{ZY}{2}\right)V_r$$

$$V_s - V_r = \left(1 + \frac{ZY}{2}\right)V_r - V_r$$

$$V_s - V_r = V_r\left[1 + \frac{YZ}{2} - 1\right]$$

If the resistance of the line is neglected,

$$Z = jwlS$$

$$V_S - V_r = \frac{1}{2}(jwlS)(jwcS)V_r$$

$$V_S - V_r = -\frac{1}{2}(w^2S^2)lcV_r$$

For overhead lines, 1/√lc = velocity of propagation of electromagnetic waves on the transmission lines = 3×10^8m/s.

$$\sqrt{lc} = \frac{1}{3 \times 10^8}$$

$$lc = \frac{1}{(3 \times 10^8)^2}$$

$$V_S - V_R = -\frac{1}{2} w^2 S^2 . \frac{1}{(3 \times 10^8)^2} V_r$$

$$w = 2\pi f$$

$$V_S - V_R = -\left(\frac{4\pi^2}{18} \times 10^{-16}\right) f^2 S^2 V_r$$

Above equation shows that (VS-Vr) is negative. That is Vr>Vs. This equation also shows that Ferranti effect also depends on frequency and the electrical length of the lines.

In general, for any line

$$I_r = 0, V_r = V_{rnl}$$

$$V_S = AV_{rnl}$$

$$|V_{rnl}| = \frac{|V_s|}{|A|}$$

$$V_S = AV_r + BI_r$$

At no load, for a long line, A is less than unity, and it decrease with the increase in the length of the line. Hence, the voltage at no load is greater than the voltage at no load (Vrnl > Vs). As the line length increases the rise in the voltage at the receiving end at no load becomes more predominant

Reduce Ferranti Effect

Electrical devices are designed to work at some particular voltage. If the voltages are high at the user ends their equipment get damaged, and their windings burn because of high voltage. Ferranti effect on long transmission lines at low load or no load increases the receiving end voltage. This voltage can be controlled by placing the shunt reactors at the receiving end of the lines. Shunt reactor is an inductive current element connected between line and neutral to compensate the capacitive current from transmission lines. When this effect occurs in long transmission lines, shunt reactors compensate the capacitive VAr of the lines and therefore the voltage is regulated within the prescribed limits. Voltage rise is directly proportional to the

square of the length of a line, and Ferranti effect is more occurs in short transmission cables because their capacitance is high. Specific electrical energy is used by electrical machinery. If the voltage at the consumer end is much above ground, the device becomes destroyed, and the gadget's windings burn from the intense electrical energy. When there is no load on long transmission lines due to the Ferranti effect, the voltage will rise at the collecting end. By positioning the shunt-reactors close to the transmission lines' collecting end, this may be limited. This reactor worked in conjunction with the lines and the neutral to restore the capacitive current as it existed in the transmission lines. These reactors pay off the transmission lines since this result occurs in long transmission lines, which keeps the voltage within the predetermined limits. According to the Ferranti effect and the length of the transmission line, the overvoltage may be determined. This happens when there is an energized transmission line but not enough load or when the load is disconnected. This result is brought about by the voltage drop across the line's inductance have been in phase with the voltages at the transmitting ends. Therefore, this event is caused by the inductance. The longer the line and the greater the applied voltage, the more pronounced this impact will be. The transmission line may be safeguarded by reducing the temporary overvoltage in the line by using the Ferranti effect's facts and compensating for it. Thus, everything here is about the Ferranti effect in a transmission line, including what it is, how to calculate it, etc. They believe that you understand this concept far better than do. In addition, if you have any questions about this concept.

Defense mechanisms and the Ferranti Effect

Switchgear and protection systems are often created for transferring end voltage in transmission lines. Circuit breakers as well as other protective mechanisms activate and shut off the circuit for safety when the Ferranti effect causes a spike in voltage in the transmission line. However, maintenance is necessary to restore the transmission line switchgears to their original condition. Given that more reactive power is created than is absorbed, reactive correction is necessary in transmission lines.

Paying no attention

If installed at the proper positions in the transmission line, shunt reactors and series capacitors may lower the voltage increase. Shunt reactors may be used to adjust the line's capacitance while series capacitors can be used to compensate for the transmission line's impedance. Along the length of the transmission line, series capacitors are positioned to lower the transmission line's effective reactance (inductive reactance and capacitive reactance). Low voltage at the receiving end in comparison to the sending end voltage occurs from the series insertion of capacitors to compensate for the transmission line inductance. Shunt reactors are put in place at the intersections wherever two or more lines converge as well as at the endpoints of the lines. In electrical transmission networks, shunt reactors may also be linked across the power transformers' tertiary winding. The shunt reactors are built similarly to power transformers, with the exception of non-magnetic spaces between the reactor core steel packets. Reactors with three or five legs are utilized in 3-phase systems alternately. These reactors' neutrals may either be left uncovered, earthed directly, or earthed through an earthling reactor.

Active Compensation

The Ferranti effect may be reduced by utilizing FACTS devices to compensate for reactive power. The right switching of these components may assist regulate the Ferranti effect affecting transmission lines? Thyristor-controlled reactors and variable resistor switched capacitors can

indeed be connected to the transmission line. Electrical transmission systems may include compensators for reactive power, which helps to lessen the Ferranti effect, such as STATCOM, dynamic voltage conservators, and unified power flow controllers (UPFC). Whenever it comes to ways to lessen the Ferranti effect on transmission lines, there are both passive and active options available. The software from Cadence may help power system engineers choose the best compensation strategy for a particular transmission system.

CONCLUSION

Due to the Ferranti effect throughout the transmission line length, the overvoltage may be verified. It happens when the line is powered up, but there is no load or a very mild load. The voltage drop across the line's inductance's alignment with the voltages at the transmitting end is what causes the effect. The cause of this occurrence is thus inductance. The longer the line and greater the applied voltage, the more noticeable the Ferranti effect will be. The momentary overvoltage inside the transmission line may be decreased thanks to the understanding of the Ferranti effect and adjusting for it, protecting the line.

References:

[1] K. B. Ram *et al.*, "Remote Labs for Electrical Power Transmission Lines Simulation Unit," in *Lecture Notes in Networks and Systems*, 2019. doi: 10.1007/978-3-319-95678-7_21.

[2] H. Amreiz, A. Janbey, and M. Darwish, "Simulation of HVAC Transmission Line," 2019. doi: 10.1109/UPEC.2019.8893642.

[3] M. Nagpal, R. P. Barone, T. G. Martinich, Z. Jiao, S. H. Manuel, and S. Merriman, "Wildfire Trips De-Energized Line Shunt Reactor," *IEEE Trans. Power Deliv.*, 2019, doi: 10.1109/TPWRD.2018.2882999.

[4] X. Li, J. Feng, Z. Liang, and Z. Cai, "Protection Operation Sequences and Risks in AC/DC Line Touch Fault," 2019. doi: 10.1109/POWERCON.2018.8601593.

[5] A. D. S. Sri, "Depiction and Compensation of Ferranti Effect in Transmission Line," *Int. J. Res. Appl. Sci. Eng. Technol.*, 2018, doi: 10.22214/ijraset.2018.3234.

[6] N. Hidouri, "An efficiency experimented wind turbine emulator linked to transmission line model 380 kV," *Electr. Eng.*, 2018, doi: 10.1007/s00202-016-0486-y.

[7] K. Chaurasiya, S. Rajput, S. Parmar, and P. A. Patel, "Reactive Power Management Using TSC-TCR," *Int. Res. J. Eng. Technol.*, 2018.

[8] M. Forcan, M. Banjanin, and G. Vuković, "Advanced teaching method for balanced operations of overhead transmission lines based on simulations and experiment," *Int. J. Electr. Eng. Educ.*, 2018, doi: 10.1177/0020720917750955.

[9] T. Ngo and T. Vu, "Study of Low Frequency AC Transmission for Wind Turbine Applications," 2018. doi: 10.1109/PESGM.2018.8585843.

[10] N. Guernoudj, "Ferranti effects in Algerian network adrar, simulation model using MATLAB," 2018. doi: 10.5220/0009770602310237.

CHAPTER 8

STUDY ON CORONA EFFECT IN TRANSMISSION LINE

Dr. Rahul Kumar, Assistant Professor
Department of Mechanical Engineering, Sanskriti University, Mathura, Uttar Pradesh, India
Email Id- rahulk.soeit@sanskriti.edu.in

Abstract:

There is a phenomenon called corona that all transmission lines experience. A small electric discharge or corona that causes the air molecules in the area to ionize or experience a little localized change throughout electric charge may sometimes be produced by the localized electric field close to electrified components and conductors under specific circumstances. In this chapter author discusses the causes of corona effect in transmission line and how to reduce corona effect in transmission line.

Keywords:

Corona, Corona Effect, Power, Transmission Line.

INTRODUCTION

The atmosphere around the conductors is subjected considerable electrostatic stresses when they provide an alternating potential difference between two conductors with considerable spacing's compared to their diameters. The air surrounding the conductors remains unchanged when low power is distributed among them. However, if we steadily raise the voltage, a point is reached where a hissing sound can be heard and a violet light can be seen surrounding the conductor. In transmission lines, such phenomenon is referred to as the corona effect. There is usually ozone gas generation in conjunction with it. Due to electrostatic tensions, the air from around conductor turns conducting, which causes the light. If power distribution is raised further, lighting and sound intensity will rise until flashover between both the conductors occurs as a result of the breakdown from air insulation.

The corona effect is the term used to describe the occurrence of hissing noise, violet illumination, and ozone gas generation in an overhead power transmission conductors. The corona glow will indeed be constant along the length if the conductors were homogeneous and smooth; if not, the rough places will look brighter. Voltage and current interactions between both the sending- and receiving-ends have been used up to this point to illustrate the transmission line performance formula. Dealing with transmission line formulas in the format of sending- and receiving-end complex electricity and voltages is easy since loads are much more frequently represented in terms of actual (watts/kW) and reactive (VARs/kVAR) energy. Although the issue of power flow through some kind of transmission line in a larger network will be covered later, the underlying concepts of power flow through transmission lines are demonstrated here using a single transmission line. The light caused by the corona effect within electrical transmission lines would differ in the phase conductive in the case of the DC system. Positive conductors shine uniformly and brightly, while negative conductors glow unevenly.

Causes of Corona Effect in Transmission Line

Smaller distance between the conductors increases the likelihood that flashover will occur between them without audible hissing noise or illumination. It's because there isn't enough time for the light to form due to the decreased distance between both the conductors. The main reasons for the corona effect within transmission lines in Figure 1 are as follows:

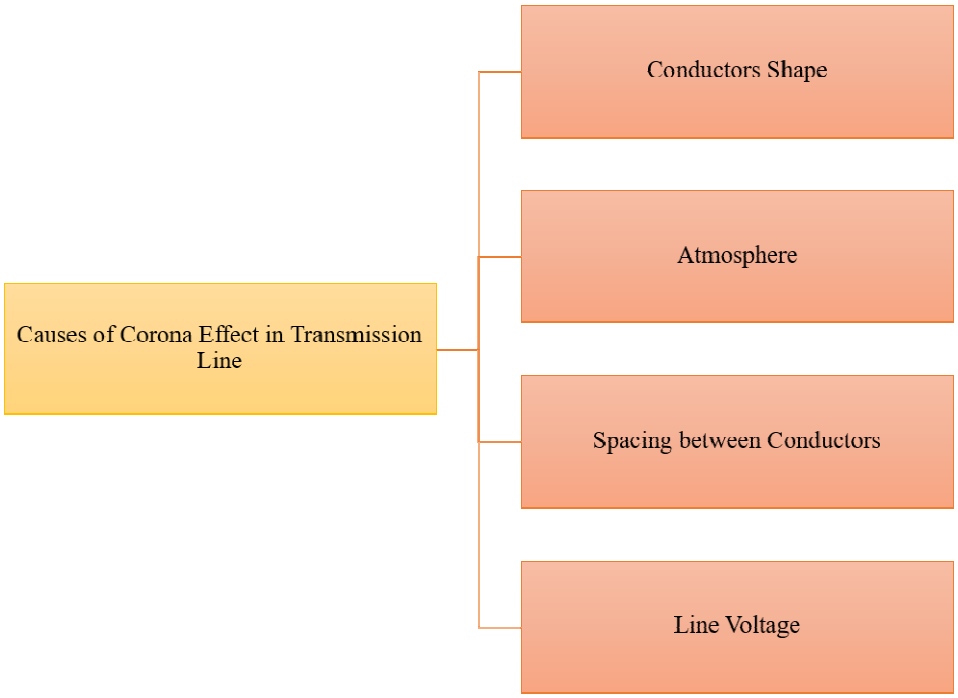

Figure 1: Illustrates the Causes of Corona Effect in Transmission Line.

Conductors Shape

The conductor's shape and environment have an impact on the corona effect in transmission lines. More corona will form due to the surface's roughness and irregularity. This is so because the dielectric strength is less due to the inhomogeneity of the surface. Similar to how a solid conductor with a smooth surface produces less corona than a grounded conductor with an uneven surface.

Atmosphere

Corona is impacted by the physical characteristics of the environment since it is created by ionizing the air around the conductor. When opposed to fair weather, corona develops at significantly lower voltage during storms because there are more ions present.

Spacing between conductors

There might not be a corona effect if the distance between the conductors was made very great relative to their radii (r). As a result, the electrostatic tensions there at conductor surface are decreased by wider separation.

Line Voltage

The corona effect is substantially impacted by line voltage. If it is low, the area surrounding the conductor does not shift, and a corona is not produced. The corona effect, on the other hand,

manifests when the line voltage is high enough to cause electrostatic tensions to build at the conductor surface and trigger the air surrounding the conductor to conduct.

Advantages of Corona Effect

The air around the conductor turns into a conductor as a result of the corona's creation. The conductor's imaginary diameter grows as a result. The electrostatic tensions between the conductors are reduced when the diameter is raised. Electrostatic tensions between the conductors are lowered via the corona effect. This lessens the chance of a flashover and enhances system functionality.

Lightning transients' impacts are lessened by corona:

Disadvantages of Corona Effect

Energy is lost as a result of the corona effect within electrical transmission lines and is radiated as light, heat, vibration, and chemical reaction. Ozone gas is created during the corona's creation, and it interacts chemically with the conductor to cause corrosion. Since the current taken by the line as a result of corona loss is not sinusoidal, the line experiences no sinusoidal voltage drop. This can cause the nearby communication cables to become unreliable.

Methods of Reducing Corona Effect

At a working voltage of 33 kV or greater, it has been shown that strong corona effects are present. In order to prevent any corona on substations or bus-bars rated at 33 kV or above, cautious designs should be devised. In any other case, highly ionized air might lead to flashover throughout the insulators and between the phases, seriously harming the apparatus. The corona effect within transmission lines can be minimized using the following techniques: By expanding the conductor's diameter: Because corona develops at higher voltages as conductor size increases, the impacts of corona are significantly diminished. This is the rationale for the adoption of bigger cross-sectional area ACSR conductors in transmission lines. As the distance between the conductors is expanded: Corona effect can be minimized by reducing the distance between conductors and raising the voltage during which corona develops. The cost of the structural support might climb too much if the spacing is raised too much.

LITERATURE REVIEW

Ahmed Abugalia [1] has the effects from corona on travailing waves via h. v. transmission lines are given using a constructed model that includes non-linear shunt capacitance and conductance in parallel. Its parameters are assessed by the use of a mathematical formula. To model the issue and resolve the associated line differential equations, including the corona component of those equations, the Simulink approach of the Mat Lab program is employed. A review of prior research using various models is provided. The difference between the new model's output and the old one.

Ikhlas Kitta [2] et al. have explained that electric current and loss of the corona phenomena have a significant impact on power losses. It is abundantly obvious that network characteristics, load patterns, and meteorological variables all affect losses. The climate of South Sulawesi is tropical. This industry must be able to withstand exposure to a variety of high tropical climatic variables, including temperatures between 23.40 and 33.30 degrees Celsius, sun exposure for more than 12 hours each day, relative humidity near to 100%, and average rainfall of 440 to 1322 millimeters. This climatic factor will convey the signal concurrently. The purpose of this book is to link

environmental variables to power losses on a 275 kV transmission line in South Sulawesi. The findings of this investigation revealed that corona power losses on a 275 kV transmission line in South Sulawesi were influenced by temperature and the length of sun exposure.

Kaustubh Vyas [3] et al. have difficult to install new transmission lines in a country with a dense population like India. The nation is also in a fast-track growth phase, which contributes to the constant need for power brought on by the process of industrialization. The corridor width for transmission lines may be greatly decreased with the introduction of Extra and Ultra High Voltage transmission lines. The use of a unique objective function for improving the structural design of extra high voltage transmission lines is described in this work. Decisions about the right of way for transmission lines are made based on electromagnetic field and corona effects nearby. The objective function defined here optimizes the design of the transmission line tower structure by taking into consideration the combined effects of electromagnetic fields. Right of way decreases when towers are further compacted, which lowers costs associated with buying property. For the purpose of verifying the outcomes of the authors' optimization technique, a real-world instance involving a transmission line located in Gujarat is taken into account. A GUI that enables the display of fields along transmission lines in a 2D and 3D environment has been developed using MATLAB as a programming platform for mathematical modeling. The optimization issue is resolved through genetic algorithm coding. As is evident from the findings presented in this work, significant cost advantages and compactness for transmission tower construction are feasible. This optimization approach may also be used to lines with ultra-high voltage.

Ke Zhu [4] et al. have a new era of renewable energy and smart grid growth, the high-voltage direct current (HVDC) transmission network has expected to expand further as an addition to AC transmission. Voltage monitoring of HVDC transmission lines is essential for determining the quality of the delivered power and implementing the management of the power system's stability. However, due to their intrusiveness or high cost, existing voltage sensors (such as Hall-effect voltage sensors and optical-fiber voltage sensors) continue to be practical for large-scale implementation for monitoring this same HVDC transmission lines. As a result, traditional potential transformers are limited to working with AC voltage. This research proposes a non-contact method for monitoring the voltages of HVDC transmission lines depending on electric coupling and magnetic field sensing. From detecting the induced voltage from induction bars, the voltages of HVDC transmission lines may be calculated, and their correlation coefficients were obtained by magnetic sensing using an optimization algorithm that establishes their respective spatial placements. The corona effect of a HVDC transmission lines and also the sensitivity and stability of a proposed platform are both explored. After being simulated on a system of around 100 kV HVDC transmission lines, the performance of the suggested sensing method was further experimentally confirmed on a scaled HVDC transmission-line testbed inside the lab. By using copper induction bars and magneto resistance sensors, this sensing approach may be accomplished at a minimal cost. This approach is appropriate for a broad deployment across HVDC transmission networks enabling wide-area monitoring due to its non-contact nature and affordability.

Sören Hedtke [5] et al. have explained that in comparison to current HVAC infrastructure, hybrid AC/DC overhead wires provide a substantial increase in transmission capacity. While audible noise and corona events are critical for gaining public acceptability, they are both impacted by mutual AC/DC coupling. Only a few experimental research exist, despite the fact that the

underlying phenomena must be thoroughly understood and precisely anticipated. Therefore, a substantial laboratory setup is used to study the corona effects in depth while subject to the impacts of electric field bias, ripple, and space charges. The findings demonstrate a distinct trend inside the phase resolved partial discharge (PRPD) pattern with repetition rate, which may be used to explain changes in audible noise.

Zhenyu Li [6] et al. have in that studied, iterative calculations are used to determine the effects of wind on the ion flow field of such a monopolar transmission line within the corona cage of a square cross-section. And used the charge simulation approach, the analytical distribution of the electric field is solved (CSM). For the distribution of space charge distribution, the upwind finite volume technique (UFVM) with second order precision is provided. In the computation domain, a dual mesh grid is also formed; this mesh's interwoven geometric design ensures a rapid convergence rate. The electrostatic attraction and ion current density upon that bottom side are measured using field mills and Wilson plates in the last section, which is intended to test the viability and accuracy of this technique. The numerically calculated data is well-aligned with the measurement-based data.

Kaustubh Vyas [7] have the need for electrical power inside the nation has increased dramatically, making technical advancements in transmission systems necessary for the long-distance transfer of large amounts of electricity. The magnitudes of the electric and magnetic fields throughout a transmission line's length have a significant impact on the decision about the corridor width. Thus, the accurate assessment of the electromagnetic fields and coronal impacts of overhead transmission lines, such as radio interference and Audible Noise, is of increased relevance. In this research, a unique GUI-based method for computing the fields produced by electricity transmission lines utilizing three dimensions is implemented. Study material includes an actual Ultra High Voltage AC (UHVAC) line case. Utilizing recently created software that makes it simple to compute and depict electromagnetic fields including corona effects in 3D coordinates, transmission lines are studied. To construct GUI-based software to assess the fields throughout the whole length of the investigated transmission lines, MATLAB is employed as the development platform. Along with the most basic Maxwell's potential coefficient theories and 3D integration methods, it makes use of the notion of charge simulation method (CSM).

Kaustubh Vyas [8] et al. Have explanation the primary factors that need to be taken into account while constructing any transmission line are electric and magnetic fields, as well as corona effects. These factors have an impact on the transmission corridor width and are thus crucial for determining right of way. This research develops a computational model and a functional GUI using the MATLAB programming environment. The program created here just needs the bare minimum of information about any transmission arrangement. This cutting-edge GUI can calculate the values of the electric and magnetic fields, radio interference, acoustic noise, and other factors for various tower designs, such as single circuit horizontal, doubled circuit vertical, etc. For the purpose of calculating the right of way for just a UHVAC transmission line, distinct field effects and corona effects may be plotted and studied on a lateral, longitudinal, and 3D profile.

Carlos Tejada-Martinez [9] et al. have in that studied,the radio interference (RI) lateral profiles caused by corona discharge in high voltage direct current (HVDC) transmission lines may be calculated using the approach that is described. The technique is based on a transmission line model that takes the skin effect into account in the conductors and the ground plane using the idea of complicated penetration depth. Modal decomposition theory is used to decouple the

bipolar system and calculate the attenuation constants from of the line parameters. Bipolar transmission lines of 500 and 600 kV were examined as application scenarios. Then, parametric sweeps of five factors that have an impact on the RI levels are shown. The sub-conductor radius, bundles spacing, and number of sub-conductors inside the bundle were used to compute both the maximum electric field and the RI. In addition, the soil resistivity and RIV (radio interference voltage) frequency were utilized to compute the RI values. The RI levels generated by the HVDC lines were then minimized using vector optimization, and discrepancies between both the designs with nominal and optimum values are explored.

Lanbo Wang [10] et al. have corona discharge, which often happens on transmission lines and has certain negative effects on the power transmission system, is a self-sustained discharge of gaseous medium hetero inhomogeneous electric fields. In order to mimic the development of charged particles with neutral species in humid air, a kinetic model for corona discharges is proposed in this research. Our model includes 69 species and 393 chemical reactions that take crucial processes comprising H_2O molecules and hydrates into account in order to examine the impact of humidity. In order to increase the reaction database's integrity, CO_2 molecules are also included. As an input, a time development of decreased electric field strengths E/N, which represent typical corona discharge experimental values, is employed. H3O+ represents one of the major positive ions, according to the modeling results, which are qualitatively consistent with earlier experimental findings. Also covered is the impact of humidity and pulse width upon plasma chemistry. It has been discovered that humidity has an impact on the maximum density and lifespan of the particular species. Meanwhile, varying pulse widths of an input electric field may have an impact on the plasma chemistry.

Ignjatović, Milan [11] et al. have explained that in an inhomogeneous electric field, the partial discharge that surrounds wires and edges is known as a corona. In dry air, the electric field must be at least 2.6 MV/m in strength for the gas to be ionized by collision. The corona is an unwelcome side effect of overvoltages in power systems. This work uses numerical simulation to model the overvoltage wave caused by negative lightning propagating down the transmission line. The drift-diffusion-reaction equations for electrons, positively charged ions, and negative ions are used to predict the corona's impact.

Yingyi Liu [12] et al. have the introduced corona current is a key element in describing the corona discharge on high-voltage direct current (HVDC) transmission lines. The spectrum components for corona current have a significant relationship with a number of corona phenomena, particularly auditory noise. It is crucial to research corona current's frequency-domain features. Here, the relationship between the DC component and also the spectrum components for corona current in the 2–20 kHz region on HVDC transmission lines was investigated. First, a significant quantity of corona current data was gathered at two HVDC experiment locations. Then, a formula was created to show the connection between the DC component and also spectral components of corona current across the frequency range of 2–20 kHz, utilizing the maximum surface nominal electrical field strength of a conductor as just a middle variable. Finally, it was determined that the relationship found was accurate and useful. The results of this research provide the framework for a unique technique for indirectly gathering audible noise in the future, which relies on the DC component of coronal current as well as its spectrum components in the region of 2 to 20 kHz. They also define the characteristics of corona discharge.

Kelin Li [13] et al. have corona discharges on high-voltage transmission lines raise issues with energy waste and electromagnetic interference. Previous studies on negative DC corona discharges have mainly concentrated on the effects of various environmental factors on the corona inception voltage, Trichel pulse frequency, and other variables. Very few research have been done on the Trichel pulses-pulseless glowing mode transition, and little is known about the transition mechanisms involved. This article describes the construction of a vacuum vessel that can accurately alter the humidity and pressure in order to replicate corona discharges under varied climatic conditions. While the pressure varies from 50 to 101 KPA, the relative humidity (RH) from 10 to 90%. A needle-plane electrode with such a changeable radius of curvature is used to produce negative corona discharges. It has been shown that when RH and air pressure rise, the transition voltage increases as well. High humidity elevates the temperature of the gases around the needle electrode and results in the production of hydrated ions that are less mobile. The results of the trials demonstrate that the effect of reduced ion mobility is greater than the impact of increased gas temperature. The transition between the discharge modes, when the Trichel pulses as well as the pulseless light coexist together, also causes the needle electrode with a greater radius of curvature to generate an intermediate process.

Gernot Komar [14] et al. have electricity transmission lines but also substations are addressed, and their status is often checked. Most often occurring defects in power transmission equipment manifest as corona or thermal impacts. As a result, the vast majority of issues with power transmission infrastructure may be discovered using only an IR camera and just a sun-blind UV camera. The majority of manual inspections have historically been used by many network operators. However, in recent years, accessible human and unmanned aerial inspection technologies, whose are much more time efficient, have grown in popularity. Relevant measurement results must take into account a variety of factors, which may be difficult to obtain using conventional, static measurements. In the case of extremely dynamic measurement methods, the relationship between velocity and distance presents additional challenges (airborne or vehicle-based). The primary focus of this study is on the UV and IR sensors' dynamic detecting capabilities. To do this, experiments were carried out using a conventional IR and UV/corona camera over various distances from created flaws. A machine learning-based method is also offered for automatically assessing UV and IR data.

Bo Chen [15] et al. explained that corona discharge from HVDC transmission cables could result in ion flow fields. The HVDC transmission line's surface becomes rougher due to wind-borne sand and friction, which decreases the corona starting energy. As a consequence, the surface micro-geometry of this type of transmission line directly affects the ion flow field. To simulate the impact of wind-blown sand on transmission lines, sand particles were placed to wire samples with varied degrees of roughness in this investigation. Based on light sectioning, the micro morphology of the wire sample's surface was investigated, and the roughness of cable samples were calculated. The electric field of such a wire surface with different surface microgeometry was calculated using FEM. The number of spiky protrusions and the maximum electric field of the wire surface both increase as the roughness does. The initial corona voltage of the wire sample also was obtained using the corona cage method. It was shown that the surface roughness of wire corresponds with the roughness coefficient inside the Peek formula. As the amount of roughness increases, the roughness factor should decrease. The correlation is used in ion flow field predictive analytics. The hardness coefficient was also defined by the observed surface roughness to increase the reliability of the expression of a micro-geometry of a wire surface.

DISCUSSION

Corona phenomenon plays a significant influence in the construction of an overhead line for transmission. Important Corona Analysis Parameters As a result, the terminology listed below are employed while analyzing corona effects:

Critical Disruptive Voltage, or CDV: The "Critical Disruptive Voltage" is the lowest phase-neutral voltage during which corona occurs.

Now imagine two conductors with a radius of "r" cm and a distance of "d" cm between them. Given by is the potential gradient 'g' there at conductor surface:

$$g = \frac{V}{r \log_e \frac{d}{r}} \text{ volts / cm}$$

Where, V is the phase-neutral potential. For corona to develop, the value of g must be adjusted to match the air's breakdown strength. At 76 cm of pressure and 25 °C, the breakdown strength of air is 30 kV/cm (max) or 212 kV/cm (r.m.s.), and this value is represented by the symbol go. If Vc is the phase-neutral potential necessary in these circumstances to create corona, then,

$$g_o = \frac{V_c}{r \log_e \frac{d}{r}}$$

Therefore, Critical disruptive voltage is:

$$V_c = g_o r \log_e \frac{d}{r}$$

Air density has a direct relationship with the value of go. As a result, the breakdown strength of air at quite a temperature of t 0C and a barometric pressure of b cm of mercury is:

$$\delta = \text{air density factor} = \frac{3 \cdot 92b}{273 + t}$$

Under normal circumstances, the value of Equals 1.

Vc = go r loge (d/r) is known as the critical disruptive voltage.

The conductor's surface quality also affects the corona effect. The above equation is multiplied to account for the irregularity factor mo. Vc = mo go r loge (d/r) kV/phase, critical disruptive voltage in Table 1.

Where mho's value is provided as:

Table 1: Illustrates the factor value of irregularity of conductor surface.

Conductor surface	Value of irregularity factor
Polished conductors	1

Dirty conductors	0.92 - 0.98
Stranded conductor	0.8 - 0.87

Visual Critical Voltage: The light of the corona does not develop along the conductors at disruptive voltage Vc; instead, it does so at visual critical voltage, which is a greater voltage. The following formula may be used to calculate the visual critical voltage's phase-neutral effective value:

$$V_v = m_v g_o \delta r \left(1 + \frac{0 \cdot 3}{\sqrt{\delta r}}\right) \log_e \frac{d}{r} \text{ kV/phase}$$

Another irregularity element is m v in this case. Its value ranges from 0.72 to 0.82 for conductors with a rough surface to 1 when the surface is polished.

3. Corona-Related Power Loss: Energy is lost during the development of the corona, and this energy is released as light, heat, sound, and chemical activity. The power loss caused by corona whenever disruptive voltage is surpassed is given by:

$$P = 242 \cdot 2 \left(\frac{f + 25}{\delta}\right) \sqrt{\frac{r}{d}} \left(V - V_c\right)^2 \times 10^{-5} \text{ kW / km / phase}$$

Where,

f = supply frequency in Hz

V = phase-neutral voltage (r.m.s.)

Vc = disruptive voltage (r.m.s.) per phase

To ensure both a decrease in energy loss and an increase in system safety, electrical corona discharge is a significant element in transmission and sub-transmission systems that should be taken into consideration. The signal integrity of data transmission is threatened by the corona effect, which results in corrosion at the conductor's surface. The corona effect has been somewhat mitigated using a variety of methods. The diameter of the conductor may be increased, the transmission line conductors may be spaced apart, hollow conductors may be used, and corona rings may be used, among other modern techniques. For lines over 230 kV and for 500 kV, it is generally advised to utilize aluminum corona rings at the conductor end of the string insulators and on both ends of the insulator. Engineers must have a solid grasp of conductor material in order to create effective methods for reducing the negative impacts of electrical corona. In the conclusion, it is important to take into account the conducting line's design in addition to the variables impacting corona discharge, such as the AC line's resistance and current capacity.

Corona Effect declines

The strong corona effects have been shown to occur at operating voltages of 33 kV or higher. If careful engineering is not done to decrease the corona effect, highly ionized air may induce

flash-over in the insulators or between the phases on substations or bus-bars designed for 33 kV and greater voltages, seriously damaging the equipment. The following techniques may be used to lessen the corona effect

By Expanding the Conductor

By enlarging the conductor, the voltage at which corona develops may be boosted. Thus, the corona effect could be diminished. This is one of the explanations for why transmission lines employ ACSR conductors with bigger cross-sectional areas.

By Expanding the Space between Conductors

By expanding the space between conductors, which elevates the voltage at which corona develops, the corona effect may be removed. The price of the supporting structure, which includes larger cross arms and supports to go along with the increase in conductor spacing, limits the amount of conductor spacing that may be increased.

With the Corona Ring

At the location where the conductor curvature is acute, there is a strong electric field. As a result, the sharp points, edges, and corners are where corona discharge initially appears. Corona rings are used at the terminals of extremely high voltage equipment to reduce electric field.The ends of bushings and insulator strings were fastened with corona rings, which are metallic rings with a toroidal form. Due to its smooth, rounded form, which greatly lowers the potential gradient there at conductor's surface below the crucial disruptive value and prevents corona discharge, this metallic ring disperses the charge across a larger region.

CONCLUSION

Even under normal circumstances, the air includes several free electrons and ions since it is not a perfect insulator. These ions and free electrons are pressed onto them when an electric field intensity develops between the conductors. The ions and charged particles are accelerated and transported in the reverse direction as a result of this impact. During their travel, the charged particles clash not only with one another but also with the very slow moving uncharged macromolecules. As a result, the quantity of charged particles keeps growing quickly. As a result, there is an increase in air conduction between the electrodes and a breakdown. As a result, an arc forms between the conductors.

References

[1] A. Abugalia, “Effect Of Corona On The Wave Propagation Along Overhead Transmission Lines,” *Acta Electron. Malaysia*, 2019, doi: 10.26480/aem.01.2019.06.09.

[2] I. Kitta, S. Manjang, I. Rachmaniar, and F. Maricar, “Tropical climate effects on corona power losses on 275 kv transmission lines in the south sulawesi system,” *Prz. Elektrotechniczny*, 2019, doi: 10.15199/48.2019.01.48.

[3] K. Vyas and J. G. Jamnani, “Cost effective design of extra high voltage transmission lines for minimizing transmission congestion problems,” *Int. J. Innov. Technol. Explor. Eng.*, 2019, doi: 10.35940/ijitee.J9455.0981119.

[4] K. Zhu, W. K. Lee, and P. W. T. Pong, "Non-Contact Voltage Monitoring of HVDC Transmission Lines Based on Electromagnetic Fields," *IEEE Sens. J.*, 2019, doi: 10.1109/JSEN.2019.2892498.

[5] S. Hedtke, M. Pfeiffer, and C. M. Franck, "Corona discharge pulse pattern and audible noise on hybrid AC/DC transmission lines under electric field bias, ripple and ion coupling," *J. Electrostat.*, 2019, doi: 10.1016/j.elstat.2019.103373.

[6] Z. Li and X. Zhao, "Calculation of ion flow field of monopolar transmission line in corona cage including the effect of wind," *Energies*, 2019, doi: 10.3390/en12203924.

[7] K. Vyas and J. G. Jamnani, "Optimal design of 1200 KV UHV AC transmission lines in India using newly developed standalone MATLAB GUI," *Int. J. Recent Technol. Eng.*, 2019, doi: 10.35940/ijrte.B3820.078219.

[8] K. Vyas, V. Joshi, D. Shah, K. Gopani, and S. Shah, "A Novel GUI Based Approach for Computation of Extremely Low Frequency Fields and Corona Effects for UHVAC Transmission Line," 2019. doi: 10.1109/i-PACT44901.2019.8960142.

[9] C. Tejada-Martinez, F. P. Espino-Cortes, S. Ilhan, and A. Ozdemir, "Optimization of radio interference levels for 500 and 600 kV bipolar HVDC transmission lines †," *Energies*, 2019, doi: 10.3390/en12163187.

[10] L. Wang, S. Chen, and F. Wang, "Kinetic Modelling of Atmospheric Pressure Corona Discharges in Humid Air," *Plasma Chem. Plasma Process.*, 2019, doi: 10.1007/s11090-019-10006-9.

[11] M. Ignjatović, J. Cvetić, and D. Pavlović, "The influence of corona on the lightning surge propagation along transmission lines," *Microw. Rev.*, 2019.

[12] Y. Liu, Y. Liu, Y. Cui, H. Yuan, and J. Lv, "Analysis of the relationship between DC component and spectral components of corona current on HVDC transmission lines," *IET Gener. Transm. Distrib.*, 2019, doi: 10.1049/iet-gtd.2018.6839.

[13] S. Chen, K. Li, F. Wang, Q. Sun, and L. Zhong, "Effect of humidity and air pressure on the discharge modes transition characteristics of negative DC corona," *IET Sci. Meas. Technol.*, 2019, doi: 10.1049/iet-smt.2019.0032.

[14] G. Komar, O. Pischler, U. Schichler, and R.-L. Vieriu, "Performance of UV and IR Sensors for Inspections of Power Equipment," *Proc. Nord. Insul. Symp.*, 2019, doi: 10.5324/nordis.v0i26.3283.

[15] B. Chen, T. Lu, P. Xu, D. Wang, and X. Li, "Characterization of Surface Roughness of HVDC Transmission Lines in Ion Flow Field Models," *Gaodianya Jishu/High Volt. Eng.*, 2019, doi: 10.13336/j.1003-6520.hve.20190410011.

CHAPTER 9

ROLE AND DESIGN OF TRANSMISSION LINE

Dr. Vikram Singh, Associate Professor
Department of Computer Science Engineering, Sanskriti University, Mathura, Uttar Pradesh, India
Email Id- vikrams.soeit@sanskriti.edu.in

Abstract:

Lattice steel and tubular steel towers are typically the two alternatives for overhead transmission line towers for high voltage lines. More popular and typical are lattice steel towers, which come in a variety of well-known forms and dimensions.

Keywords:

Distribution Lines,Power, Tower, Transmission Line.

INTRODUCTION

Understanding the background and surroundings of the transmission and distribution lines is essential to gaining a thorough understanding of the issue. First of all, the lines function as a component of power transmission, which means that they are no longer functional in the absence of a worldwide network that connects producers and consumers. In light of that, we will now present the idea of a grid. Either 230-kilovolt (kV) or 500-kV alternating current lines make up the majority of the country's major transmission lines. 115-kV wires are used on occasion. Lower voltages are much less effective in transporting electricity across distances of hundreds or thousands of kilometers without suffering major energy losses. The greater the voltage, the more space is required between the conductors and other things like trees, buildings, or even the ground for safety purposes.

Although the height of overhead high-voltage transmission lines varies considerably depending on the topography and the line's voltage, they are normally at least 30 feet above the ground. Lattice steel and tubular steel towers are typically the two alternatives for overhead transmission line towers for high voltage lines. More popular and typical are lattice steel towers, which come in a variety of well-known forms and dimensions. Four concrete foundations, or perhaps a combination thereof concrete pavers and guide wires, can support them. Depending about whether the transmission line is single circuits (three wires) or double circuit, the number of conductors amongst each tower will vary (six wires). A single steel pole that is fixed to the ground makes up tubular steel towers, which are relatively new. Although traditionally they have been more expensive to construct and may require more care than contemporary lattice steel counterparts, these can be more aesthetically pleasing.

Power from generating stations is transmitted at high voltage (such as 132, 220, or 400 kV) over great distances to the major load facilities, and then the power is distributed across different power stations located at different locations and localities though the distribution lines. Generation & distribution lines are crucial links between generating stations and consumers. The need for power has multiplied due to the rapid industrial expansion. As a result, it is crucial that

the transfer and distribution of electricity from the producing stations towards the various customers be done with the least amount of loss and disruption. This goal can only be accomplished if the transmission and distribution system is built in a way that makes it effective, technically sound, and dependable. In order to transmit the needed power over a certain distance without an excessive voltage drop nor overheating, the line should have enough current carrying capacity. The insulation of both the line should be sufficient to handle the system voltage, as well as the line losses should really be minimal. The line should be mechanically strong enough to withstand the worst conceivable (but not necessarily worst likely) weather conditions and offer excellent service for a long time without the need for excessive maintenance.

Conductor Configurations:

There are several different conductor arrangements, but the three that are most frequently used are the triangular configuration, and vertical configuration, as well as the horizontal configuration (or horizontally placement of conductors). There really is no apparent benefit to employing the symmetrical delta or triangle shape, and mechanical considerations typically lead to the usage of flat horizontal or vertical arrangements, especially when suspension insulators are involved. All of the conductors are positioned across one cross-arm with horizontal form. Even if a bigger right of way is required for such a conductor configuration, it still requires supports that are less tall. The conductors are arranged vertically in particular crowded regions where it is impossible to position them horizontally (along the length of pole one below the other). Vertical formations have the disadvantages of higher towers and increased lightning threats. There are locations where both vertical and horizontal formations are used. Conductors that are arranged asymmetrically are often transposed between regular intervals to rebalance the electrical properties of the different phases and avoid inductive interference with nearby data transmission. Experience has shown that for the double circuit lines, the vertical layout is the most cost-effective, whereas for single circuit lines, a horizontal or L-type arrangement preferable.

Conductor Spacing's:

Considerations that are somewhat mechanical and partially electrical define how far apart the conductors should be. The voltage drop increases with increasing line inductance, therefore conductors should be just as close together as possible while still preventing corona to keep the voltage drop within a safe range. The most important factor to keep in mind while determining the minimum distance between conductors would be that the electrical clearances amongst conductors in the worst circumstances, such as the highest temperature and wind speed, must not be less than the safe limits, especially at the mid spans. Due to the conductor's propensity to move in an elliptical pattern due to the influence of strong winds, the minimum clearance to structural columns for suspension insulators should indeed be calculated with such a 45° swing of the suspension strings in the direction of the structure.

Span Lengths of Transmission Lines:

It is important to notice that there is one specific figure for the span length that would yield the minimal total cost of the line, ignoring the determining impact of local variables like the requirement of following the contiguity of roads, canals, or railroads. Costs reduce as span lengthens because fewer insulators and supports are needed, but this is offset by increasing costs as the height of a support must be raised to accommodate more sag and the length of a cross-arms must be lengthened to accommodate wider spacing. Additionally, the working voltage

determines how long the span will be; the higher the operating voltage, the longer the span will be economically since insulators and supports are more expensive relative to each other.

Additionally, the weakest link in a transmission line is its insulators, therefore dependability of the line is increased by using longer spans and fewer towers per kilometer. As a result, it is impossible to provide a firm recommendation for the ideal span length to use; the only way to do so is to compute the total cost per kilometer for a variety of alternative span lengths and then plot the results to identify the one that is the most cost-effective. When the conductor size predicted by electrical calculations is fairly small, it is often possible to lower the overall cost of the line by choosing a thicker, stronger conductor and extending the span. It might not always be possible to calculate the height of the line support as well as span length just based on line cost since lightning dangers significantly rise as conductor height above ground increases.

LITERATURE REVIEW

Rafael Rodrigues [1] et al. stated the significance of bolt slippage on the structural behavior of TL towers. Despite these developments, the structural design—which is performed using commercial computer programs that use a linear or a geometrically nonlinear elastic analysis still ignores this impact. As a result, differences exist between the model's predictions and the tower's actual behavior. Furthermore, the tower topology, which is defined by the engineer expertise, has a significant impact on its size. In this context, it is obvious that the bolt slippage effect is still a problem that has to be resolved from the standpoint of technical application. It would be easier to follow a set of design topology guidelines able to reduce the impact of the connections on structural tower behavior rather than incorporating it in the mechanical model. Consequently, 72 models of the same self-supporting 230 kV actual structure are built using a FEM model that incorporates the nonlinear bolt slippage and matches the experimental findings from the CIGRE (2009) study. The most prevalent characteristics used in the sector are represented by these topological variants. Topology design advice are given since each one's impact is separated and evaluated (qualitatively and statistically) independently, enabling the structural behavior to get a great deal closer to the linear one. The influence of each variation decision on the final tower weight is then critically evaluated.

Koki Matsuishi [2] et al. designing of a transmission line, it may be necessary to seek a solution that concurrently fulfills many performance criteria, including competing demands for electrical, mechanical, and thermal performance. This work makes a fresh effort to introduce Preference Set-Based Design (PSD), a multi-objective acceptable design technique, to the design of a transmission line connected to a mesh ground plane. This paper illustrates how the PSD technique may be used for multiple-objective transmission line design while taking into account the SI and EMI performances. PSD is effective in obtaining the design parameters for a straightforward transmission line that are referred to the mesh ground plane and fulfill the necessary performance. The effectiveness of the suggested technique is shown.

R. B. Spielman [3] et al. Zflow evaluation of magnetically insulated transmission system and also the theory of magnetic insulation (MITLs). Here, we outline a unique design procedure for a real-world MITL for z-pinch reasonable means on the Zflow model of electromagnetic insulation utilizing the circuit code screamer. We construct a 15-TW, 10-MA, 100-ns double-disk transmission line specifically utilizing circuit modeling software and MITL Zflow analysis. The MITL design takes into account important factors including current loss towards the anode during the installation of magnetic insulation and the change from a non-emitting pressure power

source to an MITL. We are now able to investigate cutting-edge MITL designs, such as variable-impedance MITLs, for the first time. These devices provide a much-reduced total inductance and enhanced energy delivery to the load. The laborious process of using highly resolved 2D and 3D electromagnetism particle-in-cell codes to simulate the final MITL design happens as a validation step rather than as part of the design process.

According to the Xinmin Yu [4] et al. transmission line design has essentially attained intelligent integration, however China's present management design level in this area is archaic and ineffective. In order to facilitate the application of transmission line 3D design and to create the interface with expert line 3D design software, it's indeed necessary to develop a power transmission 3D design application system that is based on the grid GIS cloud platform with both the benefits of web cross platform even without installing plug-ins. This will enable the seamless operation of GIS elevation but also image information. Experiments show that the grid GIS cloud platform-based construction of transmission line three-dimensional design system application offers a set of straightforward, quick, practical, intelligent, and effective three-dimensional design assistance for planners and designers. It is a powerful tool for contemporary power firms to raise the bar for management design and increase productivity, and it has enormous economic and social advantages.

Robert G. Olsen [5] et al. spatial distribution of electric fields between the phase conductors is one of the most crucial electrical design requirements for lengthy (i.e., stability restricted) high voltage overhead transmission lines. Because of this, while constructing a lengthy transmission line, altering one design parameter also affects the others. It is shown how comprehension of these connections may provide information about the layout of these transmission lines as well as the trade-offs that must be made. More precisely, a more uniform electric field across space suggests a higher power capacity over long transmission lines, but it also lowers the critical flashover voltage therefore boosts capacitance per unit length.

Changsong Cai [6] et al. designs a unique magnetic resonant coupling-based wireless power transfer system that monitors equipment charging on a 110-kV high-voltage transmission line. An overall plan is presented via installation location, coupling structure, and drive topology design, taking into account the operating environment on electrical transmission tower and transmission line. Related optimization techniques such limiting the power flow channel, raising the quality factor, and coupling have been employed to increase the system's adaptability in high-voltage environments. The magnetic field dispersion is constrained by the addition of a barrel-shaped high-permeability material layer because the coupling coils are mounted at both ends of an insulator string. Additionally, the effects between the charging system and the transmission line are examined. Electric distribution of an insulator string with the charge controller was simulated, and the impact of a power frequency magnetic field mostly on charging system is determined. The findings of the analysis suggest that cross effects may be insignificant. Results from experiments show that the planned charging system can work steadily under high-voltage conditions and that the transmit power can satisfy power supply needs.

Kallol Roy [7] et al. Using several simulations, which may take an absurd amount of time, circuit designers have mostly relied on their domain knowledge when designing microwave architectures and tweaking parameters. The idea behind the inverse problem method is to work backwards from the intended output's qualities to identify the design parameters. In this paper, we offer a revolutionary machine learning architecture that, by using a Lifelong Learning Architecture, avoids the conventional design process for given quality of ocular attributes. For

the inverse mapping of power transmission geometry from eye features, our suggested machine learning architecture is a large-scale linked training system in which many predictions and classifications are done together. Utilizing intra-task outcomes, a shared Knowledge Base (KB), and coupling restrictions, and our model is trained in a guided way. Our inverse design approach is generic and applicable to numerous applications.

Yujiro Kushiyama [8] et al. the design of a composite right/left-handed (CRLH) leaky-wave antenna (LWA) based on a power transmission resonator is shown. In our design, matching portions are created using a bandpass filter synthesis approach to increase input impedance bandwidth. A 40% fractional bandwidth LWA is created and constructed. An LWA with such a slightly distinct parameters value is also created, and the results are compared, in order to talk about the sensitivity to fabrication faults.

Rotgerink [9] et al. necessary to consider risk while designing the cabling for an airplane, as well as when optimizing cable bundles, estimating crosstalk effectively, and determining the dependence of crosstalk on designable factors. The analysis of crosstalk in multi-conductor transmission lines using a low-frequency method is described. A closed-form equation for crosstalk in a certain cabling design is the outcome of this investigation. The method has been tested by measurements, and it is used in two scenarios using two wire pairs near and in free space from a ground plane. Both scenarios result in low-frequency closed-form formulas for near-end crosstalk that directly link any designable parameter with crosstalk levels. Additionally, these formulations make it evident how the instances both with and without a ground plane vary from one another. For couples near to the ground, the reduction in crosstalk caused by doubling frequency separation distance was 24 dB, but it is 12 dB in free space. The sensitivities of crosstalk to any and all designable parameters for the both setups are compiled using the closed-form equations. When applied to more complicated non-uniform transmission lines, the low-frequency approximations of a chain characteristics result in calculations that are more than 20 times quicker than those produced by full MTL simulations.

Tsai and Lin Chuan [10] transformers are studied using recently proposed novel formulations of the basic load impedance circuit inside the Z-plane. Serial lines in a transformer setup have three sections. Transfer function prototypes, parametric modeling strategies, and optimization approaches are used in the design processes, and dual-band uncorrelated frequencies of Fourier transform there at normalizing frequency () are investigated. The PCB FR4 substrate used for this transformer's design has a permittivity of 4.4, a loss tangent of 0.0245, and a thickness of 1.6 mm. Complex load impedance may be balanced at two uncorrelated frequencies, according to modeling and test findings. By using optimization methods, transmission lines' characteristic impedance values are modified in accordance with the autoregressive process. The experimental findings and theoretical values are well congruent.

Jun Zhang [11] et al. ground wires within transmission lines are designed using the reliability design technique to achieve the consistency of design requirements under international standards. The reliability indices of ground wires are confirmed to fulfill safety standards depending on the reliability calibration required by the Chinese national standard. The goal reliability index then determines the load and impedance partial coefficients of ground potential in the final condition. When the reliability theory-based design approach is used, analysis and optimization may be used to determine the proposed partial coefficients for ground wires. This approach makes reliability theory more widely used for developing transmission line ground wires.

DISCUSSION

With rising power demand, electric energy transmission between power plants to substation centers is expanding nowadays. Over the years, transmission systems have grown, and it seems that any extra capacity on transmission lines is either used up by system expansion or by transmission customers coming up with more cost-effective ways to fulfill system demand. More consumption results from the growth, which further encourages it. Engineers will gain insight into how this impacts operations and dependability by understanding the factors and restrictions associated in designing transmission systems.

Transmission Constraints

Users require an increasing amount of energy as a result of expansion growth to meet their demands. Congestion in energy transmission occurs when it can no longer handle the increasing power flow. The causes of transmission congestion might vary, but the usual demand problems prevent the flow of electricity on a particular route without endangering the route's dependability. Let's list typical limitations and the effects that result from them.

Thermal Constraints

Transmission lines have a certain thermal limit that, if exceeded, may cause sagging lines. This may cause a line fault, which may cause electric arcing to occur near neighboring plants, buildings, and of course the earth. When this occurs, protective transmission components cut the defective line to prevent significant harm to the terminal equipment. Other transmission lines get additional loads to make up for the loss when the line is removed for repair. Overloading may occur, which might cause thermal limitations to surpass their operating bounds. The other lines making up for the loss may encounter exactly the same predicament as in Figure 1 if this issue is not appropriately handled soon.

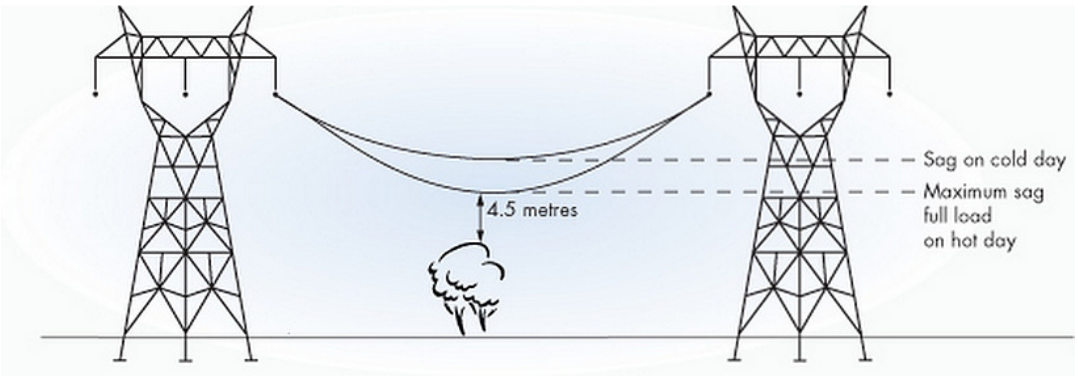

Figure 1: Illustrates to calculate the distance between the two towers.

Recognizing that energy transmission cables might still exceed their heat limit and that this temporary repair is intended for emergency situations. Because of this, emergency ratings are often assigned to energy transmission networks. In order to reduce the likelihood of reaching the thermal limit, this rating specifies a period of time during which larger load transfers are permitted.

Voltage Constraints

Typically, the voltage applied at the beginning end is significantly greater than the reactance of the energy transmission line at the receiving ends. Larger voltage fluctuations above or below the

normal voltage value may harm the provider's or the customer's equipment. Which explains why maintaining operations that satisfy standards requires an operating voltage restriction. In places with dispersed and protracted energy transmission lines, this restriction is even more crucial.

Operating Constraints

Loads are continually changing, and these variations might be slight or significant. Whenever mechanical power on the generating side adjusts to electrical demand, loads often shift only little. The link between systems may stay in synchronization as long as the fluctuation is minimal. As long as the loads do not increase in size and oscillate at low frequencies, the system would stay stable. These oscillations may result in unstable voltages and frequency problems, which may result in outages. Large oscillations happen as a result of maintenance, flaws, or interruptions in the energy transmission cables. Non-steady-state instability may occur as a consequence of unpredictable circumstances that are brought on by larger frequency ranges. To reduce the likelihood of instability, preventative actions are required. When systems are subjected to greater reactive power fluxes, voltage instability occurs. The voltage differential between the line's beginning and receiving ends is what causes this. Voltage dips occur at the receiving end as a consequence. Lower voltages cause current to rise and thus exacerbate losses. The eventual result is voltage breakdown damage to equipment and potential power interruptions.

The design of transmission lines takes a variety of factors into account. Transmission lines for energy are defined by a number of factors. These variables affect how the effects on the environment. The fundamental parameters are:

- Nominal Voltage Line Length
- Height Range

Planned Loads

The line voltage would be almost the same as the nominal voltage. The actual voltage changes according to the line's electrical performance, resistance, and factors such as distance and connected devices. In general, altitude range refers to the forecasted weather and topography. Weather is taken into account while creating design loads. For instance, the design load that wind and ice place on the towers and lines used for electricity transmission. This has an impact on the tower's size, height, design, mechanical strength, and wind dampening.

Tower Design Specifications

Conduits are kept apart from the surrounding area and from one another by transmission towers. The separation distance must be bigger as the energy transmission voltages increase. A fault to ground scenario occurs when an arc may leap from a transmission line towards the ground. When electricity is transferred to the surroundings, something occurs. The conductors themselves may also experience this. The fault described here is a phase-to-phase fault. The distance between both the conductors, the tower, and any possible arcing structures is the first design factor to take into account. This gives a broad sense of the tower's actual measurements. This contains the mounting insulator length, conductor spacing, and tower height. The tower frame's structural strength is the next design factor to be taken into account in order to maintain the initial design criteria. This considers the component, the environment, and any potential effect loads. Providing the appropriate foundation to sustain the tower and the prescribed design loads in Figure 2 is the last design consideration.

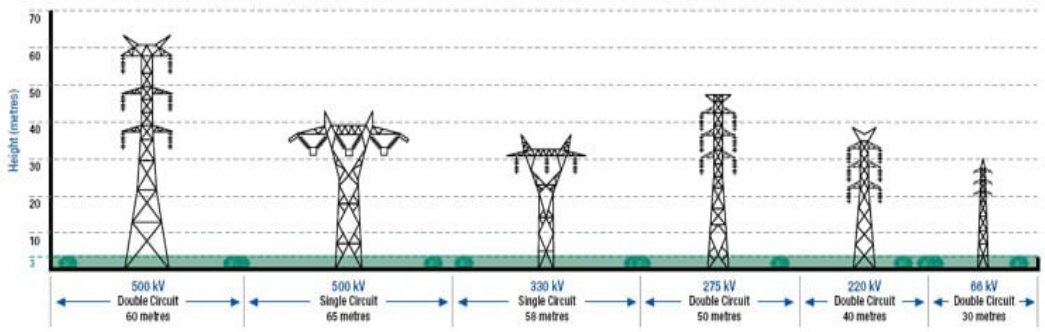

Figure 2: Illustrates the designing different types of tower.

Clearance Design Parameters

The tower's primary purpose is to keep conductors apart from their environment, other conductors, and any possible arcing structures. Phase-to-tower, phase-to-phase, but also phase-to-ground tolerances. Insulator strings are often used to maintain phase-to-tower clearances, and they must take conductor motion into consideration. In order to reduce line temperature and the possibility of line sag, as well as to manage vegetation and possible arcing structures, the phase-to-ground clearances is depending on the tower height. Figure 3 restricting line motion and tower shape regulate phase-to-phase separation.

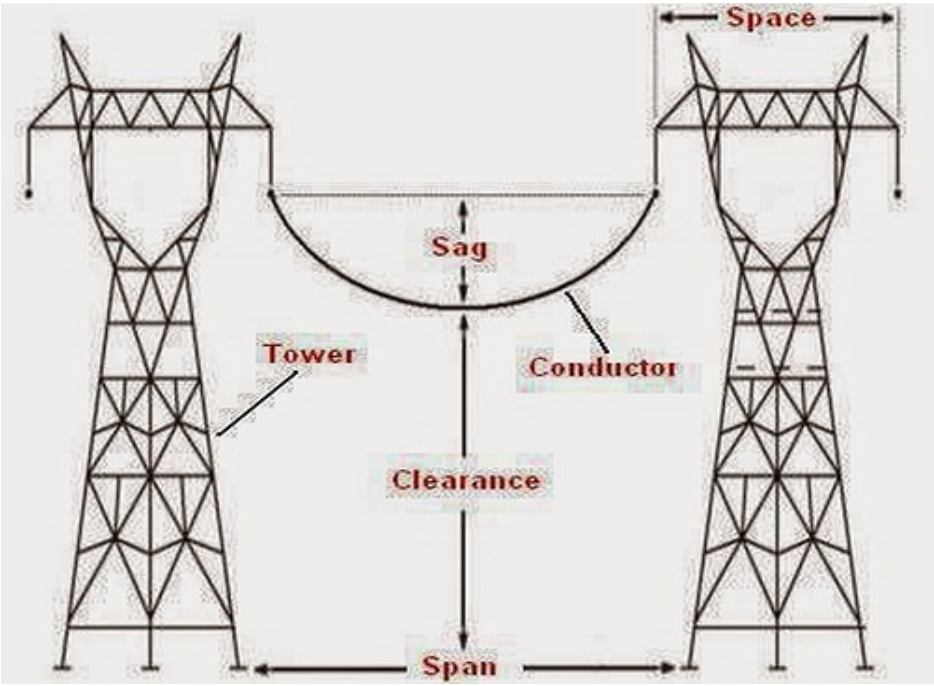

Figure 3: Illustrates the sag between the two standard towers.

Designing for Lightning Protection

The likelihood of a lightning strike increases with tower height. Energy transmission systems and consumer electronics are particularly vulnerable to harm from lightning strikes. An additional set of wires are stretched from the top of the tower towards the ground therefore for lightning to follow in order to reduce the damage caused by lightning strikes. These are often known as shield wires, and they aid in preventing device failure in Figure 4.

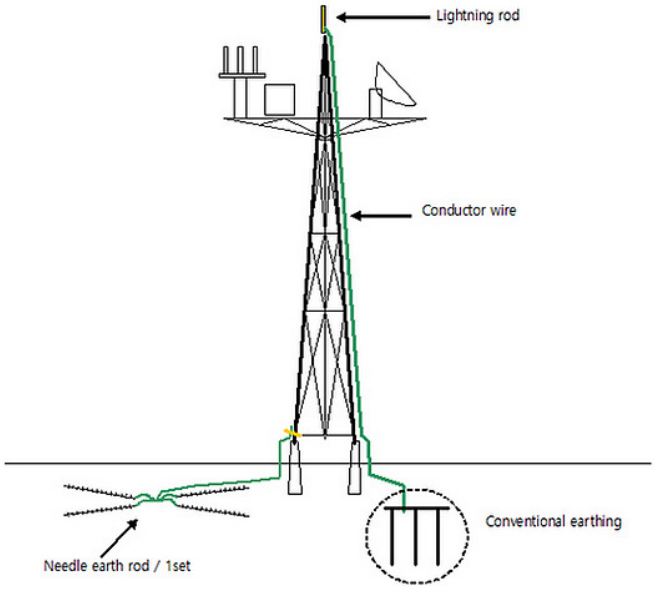

Figure 4: Illustrates the Lightning strikes can cause considerable damage to energy transmission and consumer equipment.

Designing to Reduce Conductor Motion

Equipment used for energy transmission might possibly be harmed by weathering processes that induce conductor motion. The Stockbridge damper is the most used kind of energy transfer damper. These are situated close to the conductors' attachment point to the tower, underneath the conductors. The transmission structure's damper design may be determined with the use of an adequate forecast for weathering effects. These stop the weathering's vibratory impacts from possibly harming utility equipment.

Layout of the physical design cables

Cable enables a comprehensive platform that combines a flexible mix of mechanical and electrical CAD. Designing energy transmission lines, substation connections, and transmission towers will be made simple and straightforward thanks to the tools and features that will be made available. Gives you the tools you need to maintain the geometric requirements for mechanical constructions while preventing designs from clashing. Provides simple drag and drop snap in capabilities that make it possible to create interconnecting system panels and transmission lines. Using input parameters depending on customer demand, create a simple, error-free design. A few of the following are provided.

Makes Panel Controllers Physically Representable

- Verify Design Rules
- Conflict Recognition
- Prevention of Placement Errors
- Bridge for 3D Routing

The 3D routing bridge makes it simple to switch between the most popular MCAD programs available today and the routing and design of energy transmission lines. To estimate the length and diameter of the energy transmission line for design parameters, just upload MCAD files into

the E3.3D routing bridge. This offers a transitional phase before combining the electrical and mechanical engineering components in a single, user-friendly program. In order to meet operational engineering requirements, 3D routing bridges provide a better picture of the linkages between conductor, energy transmission and distribution, and insulators.

CONCLUSION

Linear elastic models are used in the present industry practice of designing transmission line (TL) towers (or geometrically nonlinear, for guyed towers). However, design engineers and academics have noted that some significant nonlinear behavior may occur, apparent even at mild load levels, based on observation of a tower's failure during prototype testing (i.e., in design region for pre-collapse loads). In this instance, the particular behavior of the links is linked to the primary cause of nonlinearity. In comparison to above, subterranean needs less right-of-way since it is not as exposed. This may bring the total installation costs of two techniques closer together, along with the reality that public opposition to overhead is likely to be considerably larger than that to subterranean. This lesser gap could be acceptable, especially if installing an overhead line is just impossible owing to opposition from the general population.

References:

[1] R. R. de Souza, L. F. Fadel Miguel, J. Kaminski, and R. H. Lopez, "Topology design recommendations of transmission line towers to minimize the bolt slippage effect," *Eng. Struct.*, 2019, doi: 10.1016/j.engstruct.2018.10.032.

[2] K. Matsuishi, Y. Kayano, F. Xiao, and Y. Kami, "Multi-Objective Design of Transmission Line Referenced to Meshed Ground Planes by Preference Set-based Design," 2019. doi: 10.1109/EMCEurope.2019.8872115.

[3] R. B. Spielman and D. B. Reisman, "On the design of magnetically insulated transmission lines for z -pinch loads," *Matter Radiat. Extrem.*, 2019, doi: 10.1063/1.5089765.

[4] X. Yu, T. Zhong, X. Wang, K. Nie, and J. Lv, "Research on Application System of Three-Dimensional Design of Transmission Line Based on Grid GIS Cloud Platform," 2019. doi: 10.1051/e3sconf/201913601037.

[5] R. G. Olsen and C. Zhuang, "The Spatial Distribution of Electric Field as a Unifying Idea in Transmission Line Design," *IEEE Trans. Power Deliv.*, 2019, doi: 10.1109/TPWRD.2018.2884879.

[6] C. Cai *et al.*, "Resonant wireless charging system design for 110-kV High-voltage transmission line monitoring equipment," *IEEE Trans. Ind. Electron.*, 2019, doi: 10.1109/TIE.2018.2808904.

[7] K. Roy, M. A. Dolatsara, H. M. Torun, R. Trinchero, and M. Swaminathan, "Inverse Design of Transmission Lines with Deep Learning," 2019. doi: 10.1109/EPEPS47316.2019.193220.

[8] Y. Kushiyama, T. Arima, and T. Uno, "Design of transmission line resonator based CRLH leaky-wave antenna," 2019. doi: 10.23919/APMC.2018.8617260.

[9] J. L. Rotgerink, H. Schippers, and F. Leferink, "Low-frequency analysis of multiconductor transmission lines for crosstalk design rules," *IEEE Trans. Electromagn. Compat.*, 2019, doi: 10.1109/TEMC.2018.2868985.

[10] L. C. Tsai, "Design and Implementation of a Three-Section Transmission Line Transformer," *Iran. J. Sci. Technol. - Trans. Electr. Eng.*, 2019, doi: 10.1007/s40998-018-0131-z.

[11] J. Zhang, L. Zhou, L. Yang, and Y. Zhang, "Reliability Design Method of Ground Wires in Transmission Lines," 2019. doi: 10.1088/1755-1315/304/3/032012.

CHAPTER 10

STUDY ON THE SAG AND TENSION OF TRANSMISSION LINES

Dr. Vikas Sharma, Assistant Professor
Department of Computer Science Engineering, Sanskriti University, Mathura, Uttar Pradesh, India
Email Id- vikass.soeit@sanskriti.edu.in

Abstract:

The conductors' ground clearance there at highest temperature and lowest loading level should be maintained because safety reasons. Again for continuity and efficiency of electrical supply, assessment of the sag and tension in the transmission system is crucial. The conductor may break if the stress is raised over a certain point, which would disrupt the system's power transmission. In this chapter author discusses parameters of sag and tension of transmission lines.

Keywords:

Electrical Supply, Sag, Tension, Transmission Lines.

INTRODUCTION

The mechanical structures that support overhead wires are made up of parts like insulation, cross-arms, poles or buildings, etc. Even during the harshest weather, there shouldn't be any mechanical breakdown of the line due to the strength among these components. Forces acting on the conductor include wind pressure, tension, as well as the conductor's own weight. A conductor stretched among both two supports will also have an ultimate strength after which it will fail, as well as the kind of conductor material used only for overhead lines determines the conductor's strength properties. It is vital to allow an appropriate safety factor whenever stringing overhead wires in regards to the stress that the conductor is susceptible to.

Even with a 12.7 mm radial covering of ice and wind pressure upon that order of 380 N/m2, the stress throughout the conductor is often anticipated to be a little than 50% of its own maximum tensile strength. The circumference of a conductor, the distance between supports, the material of the transmission line, the amount of sag in the transmission line, wind pressure, and temperature all affect the tension in that conductor. Temperature changes and loading circumstances have an impact on the connection between tension and sag. For example, as the temperature drops, there has been a corresponding decrease throughout sag and the tension rises. Stretching of both the conductor due to icing of the connection and wind loads is regulated by line tension.

Sag:

When stretched between the fixed supports at about the same level, a completely flexible wire with a homogeneous cross section will create a catenary. The form of the curve, however, resembles a parabola if indeed the sag is relatively tiny in comparison to the span. Sag is the differential in level here between lowest point mostly on conductors and the support points. The elements influencing an overhead line's sag are listed below in Figure 1:

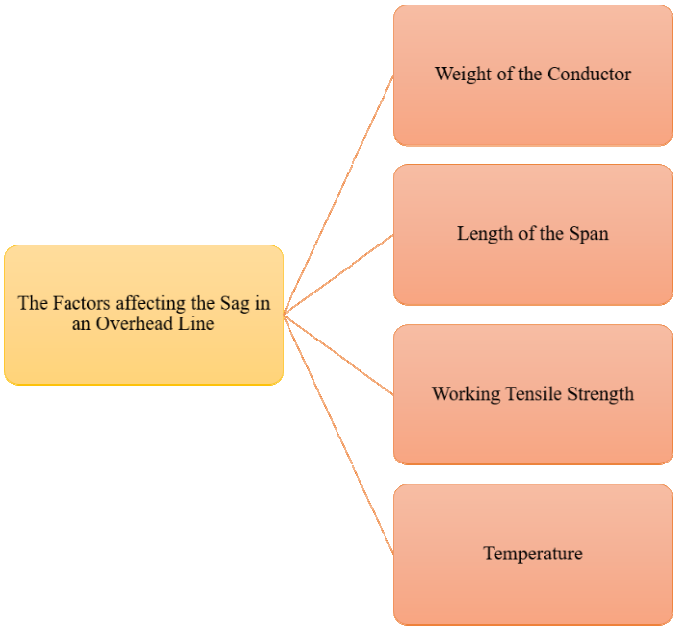

Figure 1: Illustrates the Factors affecting the Sag in an Overhead Line.

Weight of the Conductor:

The sag is directly impacted by this. Greater sag results from heavier conductors. This will also result in an increase throughout the sag in areas where the conductor is forming ice.

Length of the Span:

This impacts the sag as well, The Square of the span length is exactly proportional towards the sag [1]. As a result, even with other factors like the kind of conductor, operating stress, temperature, etc. staying constant, a segment with a longer span will experience significantly more sag.

Working Tensile Strength:

If other factors like temperature, span length, etc. don't change, the sag is inverse proportion towards the working strength properties of the conductor. The conductor's operational tensile strength is calculated by multiplying the maximum stress by the square of the x-section plus dividing by either a safety factor.

Temperature:

As a result of the fact that all metallic objects expand as the temperature rises, the lengths of the conductor also grow as a result, along with the sag. Inside the design of an overhead wire, the sag is crucial. Offering either a too-high or too-low sag has drawbacks [2]. If the sag is too high, additional conductor material will be needed, more weight will need to be supported by the supports, higher supports will be required, and that there is a possibility that the swing-amplitude will be increased owing to wind load. On the other hand, if somehow the sag is too low, the conductor is under more tension and is therefore more likely to break under extra stress, such as that caused by line vibration or a drop in temperature.

Normally two conditions should be investigated, when making sag-tension calculations:

At Minimum Temperature:

Whenever the temperature is the lowest as well as the wind is the strongest, the conductor section sags the least and has the most stress. Under these circumstances, the tension upon that conductor shouldn't be greater than the conductor's breakdown strength divided by such a safety factor of 2.5.

At Maximum Temperature:

However, maximum sag happens when temperatures are at their highest and that there is no wind pressure.

Below are approximated formulas for calculating sag:

$S = wL2/T$

Where,

w = conductor's mass in kilograms per meter of length,

L = Measurement of the span in meters, and

T = kilograms of conductor tension.

LITERATURE REVIEW

Dicky Novriandi [3] et al. in order to calculate the sag and tension analysis upon that 275 kV transmission line conductors, this study will create a catenary technique. The weight of the conductor, the maximum tensile tension of the conducting wire, the length of a span, and the maximum sag of a conductor are all factors in the catenary method equation. With the model being created using the AutoCAD program, the approach will be utilized to calculate the values of sag and tension. The study's findings show that the identical tower sags at 6.86 m, 4610.83 kg of tension, and 401.06 m of conductor length, but the tower sags at 8.14 m, 4612.84 kg of suspense, and 401.06 m of conductor length changes. When the lowest current sag value is 6.9828 m as well as the maximum current sag number rises to 8.44 m, an increase in current results in an increase in the sag value. The present lowest pressure is 4531.27 kg, and the maximum pressure is 3749.728 kg. As the tension decreases, the temperature rises. The ambient temperature has an impact on both sag and tension as well. Sags are 6.8621 m just at lowest temperature and climb to 7.793492 m at the highest temperature of 40 °C. Whenever the temperature is 20 °C at the lowest, the tension is 4610.538 kg. When the temperature is 40 °C at the maximum, the tension is lowered to 4062.345 kg.

Michal Wydra [4] et al. for overhead transmission lines (OTLs), dynamic line rating (DLR) solutions are presently being researched. While sensors must be mounted directly on wires, DLR systems often depend on observations of the weather, temperature, inclination, and current to determine tension and sag. These technologies provide excellent precision and dependability for calculating the maximum permitted current. However, its installation can need disabling the transmission line from use. DLR sensors detecting wire temperature or tension should indeed be put at several sites of OTL in order to get exact data about the actual operating conditions for the entire transmission line. Each stress section and essential spans should be covered by the smallest number of installation points, which will raise installation costs. Utilizing a vision system built around cameras is an alternate approach that enables OTL monitoring. Cameras

mounted on the OTLs' poles may capture pictures that, when properly analyzed, can provide information about the sag and temperature of wires without requiring OTL to stop operating for installation or further maintenance. Because it eliminates the need for measurement data to be communicated from the sensor station put on the wire towards the base station situated on the pole, such a vision system also simplifies data transmission (for instance, via radio). This article seeks to introduce the idea of a vision system that employs long-range (LoRa) wireless connection and data transfer to monitor the temperature and sag on overhead transmission lines (OTLs). A camera and a microprocessor with a LoRa communication module make up the created system. The whole system takes photographs, processes them for wire sag-temperature estimate, and sends the data to the manufacturer's Supervisory Control and Data Acquisition system to monitor OTLs' spans (SCADA). When keeping track of the whole OTL, the system highly efficient is also put out and researched.

Pradeep Kumar [5] et al. stated an important factor in the functioning of the power system is the mechanical sag of the overhead transmission line (OTL). However, the conductor's distant positions restrict the amount of sag that may be seen. Distributed (DMS) or point measurement systems (PMS) are employed to monitor sag. However, PMS is favored since DMS cannot employ the ruling span approach. Every tower must have sensors for PMS, which raises the bar for sensor and data transmission requirements. This study makes an effort to lessen the sensor need and calculate the leveling span sag. A linear integer programming-based optimum sensor placement strategy is provided in order to decrease the number of sensors and locate them while maintaining redundancy. To estimate the sag in a leveled span arrangement, a reduced order, least-square based state estimate is presented. The estimator takes as input the temperature and tension of the conductor at one end of the span. Despite being created based on the ideal leveled span arrangement, it is discovered to function in real-world operational situations. The performance of the suggested estimator is examined using simulations using PLS-CADDTM to verify the sag and tension data. Additionally, a sensitivity-based bad data removal strategy is offered to get rid of the problematic data. It enables the replacement of flawed data with almost accurate values. The results demonstrate how reliable the suggested method is.

Mohammad Hadi Jalali [6] et al. the design and nondestructive examination of electrical transmission lines, guyed towers, and bridges are all impacted by interactions between cables and structures. An analytical model that may be used to different applications is described for a beam-cable system on an electric pole. Two stranded cables are joined to a cantilever beam. Euler-Bernoulli tensioned beams are used to simulate the cables in order to account for self-weight-related sagging. The equations of motion are calculated using Hamilton's principle, and the pole is also represented as a cantilever Euler-Bernoulli beam. A setup was created to precisely test the bending stiffness of a stranded cable under tension, and the model was verified using a reduced-scale system inside the lab. It is determined that the dynamics of beam-cable constructions are significantly influenced by the bending stiffness but also sag of the cable. In the system's eigenvalue solution, various hybrid modes appear when the cable is added to the pole structure. Modes with symmetric cable motion are reliant on the cable sag, while modes with asymmetric and symmetric cable motion are sag-independent. When the cables' bending stiffness is greater, sag's impact on natural frequencies is much more noticeable.

Wolfgang Troppauer [7] et al. objective was to provide research on a sophisticated icing mechanism for the transmission grid. The research that has been launched is a two-level procedure that, in the first step, alerts system operators whenever the conditions are right for the

production of ice on conductors. The radius and mass of the anticipated ice layer are then predicted using a mathematical model. The computation of the conductor's expansion (tension) and ultimate length over a fixed span distance depends on the mathematical connection between the conductor's tensile force and sag. The precision of data for conductor temperatures and angle/sag has a significant impact on the accuracy of ice thickness estimations. The OTLM-ICE program gives the transmission network's operator the ability to track sag and clearance changes on a conductor that has experienced ice overloads. In order to avoid damage during the first stages of ice rain, the operator may optimize and choose the appropriate ampacity of transmission lines. The second level of the system uses line-monitoring sensors to monitor the ice development on the phase conductors, giving the system operators accurate information about the state of the line. Additionally, the methodology's workings are examined; these findings are also given via case studies. As a HORIZON 2020 project, FLEXITRANTORE seeks to provide an integrated platform for the flexible power transmission system of the future.

Elvira Fernandez [8] et al. Stress-strain and metallurgical creep tests are the foundation for estimations of the sag-tension of gap-type overhead conductors based on experimental conductor creep testing. Although both the core and the whole conductor are subjected to these tests for bi-metallic conductors, the aluminum metallurgical creep is often ignored and the full conductor metallurgical creep is not performed for gap-type overhead conductors. The work that is being presented aims to validate these computation techniques. Field measurements were taken in an operational pilot line for this purpose. During the first three years of line operation, the installation of gap-type conductors was measured, and component creep was observed. A flexible sag-tension calculation approach has been employed to represent important events such as the pre-sagging but also sagging stages during the installation, as well as ice and wind events during in the operation. Additionally, the widely-used graphical sag-tension approach has been assessed and produced outcomes that are comparable to those of the flexible method. The tension-decrease serves as a creep indication. The tension-decrease values estimated and measured are similar. As a result, it is determined that the sag-tension estimates based on experimental conductor creep testing are accurate representations of the conductor's real creep while it is in use.

Sandeep Gupta [9] et al. whenever a conductor for a transmission line is built between two towers, the weight of the conductor causes the line to droop rather than run straight between the two sites, which is known as a sag. It is closest to the ground and the lowest point between the two towers. Sag in transmission lines has both benefits and drawbacks since it keeps the safe tension level in check on the one hand, and necessitates the construction of higher towers to maintain the necessary ground clearance and increased ampacity on the other. This study explains many elements that contribute to transmission line sag. The main goal of this work is to calculate the sag caused by transmission lines utilizing several conductor types, including ACSR, ACCC, and ACSS, under various situations. A comparison of the conductors in which sag occurs is also made. In this research, the impact of loading on the emergence of conductor sag will also be discussed. The simulation results, modeling, and findings of the comparison analysis across different conductors are all done using MATLAB programming in this work. This research is significant because it will aid in choosing the kind of conductor to be utilized for a certain power system design, particularly for the transmission network with sag.

Davide Poli [10] et al. to determine a transmission line's real capacity, Dynamic Thermal Rating (DTR) keeps track of the conductor temperatures or forecasts weather and load using historical

data. DTR gives Transmission System Operators (TSOs) more dispatching flexibility and aids in decision-making in the event of grid congestion, particularly in terms of the quantity and timing of necessary re-dispatching procedures. This is done by fully utilizing the real performances of conductors in accordance with the current weather conditions. DTR is thus being utilized more often for power system reliability and security analysis. In order to take into account, the stochastic character of meteorological factors, there has recently been an increase in interest in the scientific literature for the use of probabilistic approaches to weather-based DTR processes. In reality, it is clear that the accuracy of weather forecasting is the weak point in projecting the ampacity of a transmission system for the next hours.

This study proposes a Monte Carlo technique to generate weather scenarios with Probability Distribution Functions (PDFs) which have been carefully pre-tuned, for each meteorological measurement, according to the actual weather forecasting mistakes made in the line's vicinity. This technique is used to generate weather scenarios. In order to assess the influence of weather uncertainty mostly on confidence interval of thermal and mechanical outputs (conductor's temperatures, tensions, and sags), the weather scenarios thus derived are next processed by a thermo-mechanical model of the transmission line. The traditional technique of merely modeling meteorological variables using predetermined Gaussian PDFs is often debated and contrasted with this strategy. The resilience of a deterministic DTR process the authors have developed over the last several years is then tested using it.

The DTR procedure being tested combines the CIGRE thermal model of conductors with a sophisticated multi-span mechanical model of a transmission line; in fact, it accounts for the mechanical interaction between spans caused by the potential rotation of strings of insulators as well as the fact that conductor temperature can vary from span to span depending on the weather. On the basis of meteorological data obtained close to the same overhead power lines where the Italian TSO is benefiting significantly from the above-mentioned DTR technique, particularly in terms of an increase in the quantity of dispatch able wind energy, many research findings are addressed.

Jian Hu [11] et al. critical state variable of the dynamic capacity incensement, sag, and tension calculations is the operating temperature for overhead transmission lines. Current transmission line temperatures calculation standards always regard the conductor as an isothermal segment when calculating the conductor surfaces or average temperature.

The line stress and sag calculation in addition to the transmission system safety evaluation may suffer from poor effectiveness if these factors are ignored. In fact, there is a temperature gradient dissemination and different response in the cross-section of the conductor, which are directly impacted by such factors as the skin effect, external thermal conduction, and different twisted materials. The gradient distribution and differential in temperature response of the conductor cross-section must thus be precisely analyzed and calculated. By concentrating on both radial and circumferential thermal transfer channels in conductor cross-section, a thermally network model is first created.

Then, using nonlinear iteration and parameters identification, two calculation techniques for conductor radial and circumference temperature are created. The method using parameter identification can successfully resolve the issue of uncertain model parameters brought on by thermal deformation of the conductor under conduction and convection. The method using nonlinear iteration can fully account for the influence of transient thermal characteristics as

properties of materials, convective heat resistance, and radiation heat inside the process of heat transfer. Finally, a test platform verifies the reliability and correctness of the suggested thermal network model and computation methodologies.

Shashi KantVij [12] et al. difference in level between the points of support and the conductor's lowest point is known as sag in transmission lines. Conductors are not entirely stretched; rather, they are permitted to have sag in order to provide for safe tension inside the conductor. Sag is thus necessary for the suspension of transmission line conductors. Thus, the main focus of this paper is on calculating the sag caused by transmission lines under various conditions, such as with supports at the same level in airplane, supports at different levels in mountains, river crossings between and without wind and ice loads, etc., for various physical parameters. In this work, many variables that cause transmission line sag are described. In this research, the impact of loading on the emergence of conductor sag will additionally be discussed. Then, using the output of MATLAB programming, the mathematical formulation accountable for the sags of a parabolic and catenary shapes is presented, and the magnitude difference between them has been examined.

DISCUSSION

Electricity is a need since it may be utilized in every industry and because it is necessary. Despite the fact that the electric power grid is made up of several subsystems, transmission and distribution are indeed the areas that experience the most problems. As a result, the most crucial components of the overall power transmission system are the power transmission lines. By monitoring any changes on the line, it is able to ensure the energy's quality, consistency, and safety. There are several ways to find electricity transmission line defects. Using LSTM network

s identified transmission line failures. Rain, wind, lightning, sun, and other natural and manmade occurrences like fires all have an ongoing impact on power transmission lines. In addition to bird assaults, landslides and floods, they are also susceptible. Unbalanced load demands also maintain steady pressure on the energy transmission cables in addition to these consequences. Thus, it is essential to maintain continual control over the transmission lines and to constantly upgrade the technological infrastructure. Today, it is well recognized that land conditions account for the majority of power transmission line failures. Other issues include short circuits brought on by birds or other natural events, lightning, uneven load distribution, and unidentified causes. These failures could raise the temperature of a transmission cables. It should be seen as the first indication of failure. Even if there are studies for locating the problem in power transmission lines, it is even more crucial to take preventative measures beforehand. Power loss, drooping, and conductor temperature during overcrowding of a power transmission lines all are influenced by the electrical and mechanical qualities of the lines. Measurement of the electricity transmission cables' temperature is crucial for this reason. Continuous monitoring of a transmission wires is necessary since ice and sag have dangerous impacts on them. The transmission lines are photographed using a camera, and the picture is then processed. Sagging, tension, and temperature are determined while ice is recognized using image processing (Open CV and Python). NRF transmission is used to transmit this data to the monitoring station.

Transmission line icing

In ice conditions, electrical power systems have serious issues. Power networks span vast distances and go over farmland, mountains, and rivers. The weight of the ice puts extra stress and

burden on systems, which increases the risk of a power failure during icing. Most often, temperatures between +2°C and -3°C are used to examine the ice on transmission lines. Electric strength decreases in insulators where ice has collected, leading to icing flashover and a smaller air gap between ice conductors but also ground wires. Icing must be identified in order to perform de-icing.

Transmission line sag and tension

The sag is indeed the difference in elevation between the conductor's lowest point and its points of support. It's crucial to position the transmission line cables with the proper sag. The conductor could break owing to significant mechanical stress if the sag amount is minimal. Large wind amplitudes may cause conductor swing, which might come into contact with neighboring conductors, if indeed the sag amount is high. The transmission line was stated to have a reduced sag when the conductor was tight and stress is high. The transmission line is considered to have more sag when the conductor is slack and the tension is loose.

The transmission line's sag is identified.

The sag of the transmission line S = (28*T*)

Where w=weight per length and L=span length this transmission line's S-sag Transmission line supports A and B were measured by the following parameters: T (horizontal tension), l (cable length), and x (distance between support A as well as any point here on cable).

Detection of Icing

Icing may increase the weight of the transmission line per unit length, which leads to conductor galloping, short circuits, and power outages. Therefore, it is necessary to regularly monitor transmission lines in order to spot ice at its earliest phases.

The camera, which is positioned at the front of the transmission line, records a picture of it. The frosting is identified by picture processing. There are two ways to find it: PSNR cross-correlation that is normalized

Using PSNR to find icing

Peak Signal to Noise Ratio (PSNR), which measures the picture quality in decibels, is employed (dB). The contrast between the two photos is better the higher the PSNR value. Peak noise to signal ratio is employed in this case to determine whether or not ice is present upon that transmission line. The PSNR value was 100 dB when there is no ice present, and ranges from 100 to 0 dB in all other circumstances. The flowchart for utilizing PSNR to detect ice. The Canny edge detection method is the initial stage.

Many edge detection methods exist, including Sobel, Roberts, Canny, and Prewitt. However, other approaches have the drawback of noise, so anticipate Canny. These approaches will treat noise as an edge when it is represented in a picture, and in certain circumstances, the actual edges might not be recognized. The operator that uses a multi-stage method to identify a range of edges is known as canny edge detection in Figure 1.

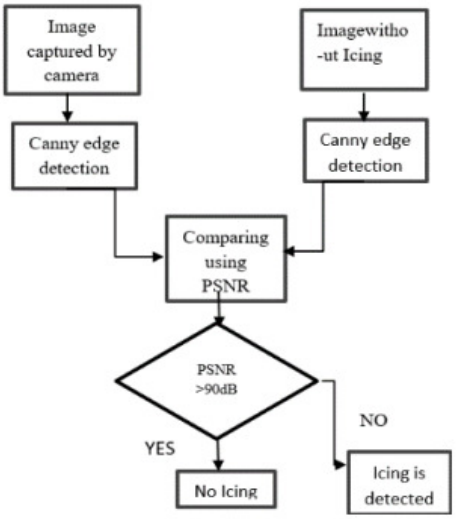

Figure 1: Illustrates the operator that uses a multi-stage method to identify a range of edges.

The operator that uses a multi-stage method to identify a range of edges is known as canny edge detection. By using the Gaussian filter preceding masking, Canny gets over this drawback and significantly reduces noise. The flowchart for detection of canny edges is shown in Figure 4.

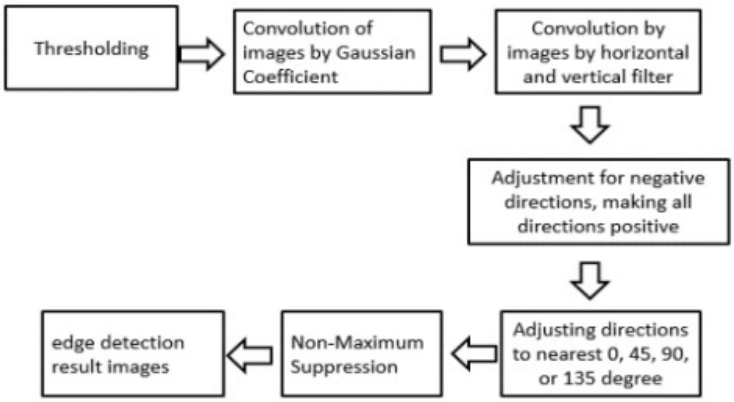

Figure 4: Illustrates the flowchart for detection of canny edges.

In order to acquire the gradient in canny edge detection, either horizontal or vertical filters are used in the first stage of convolution of pictures with canny edge coefficients. The direction is then discovered using arcane (Gx Gy). To clarify the fuzzy edges, non-maximum suppression is used next. Later, the edge strength of the central pixel is compared towards the pixel in a positive gradient's negative gradient direction, and the gradient direction is rounded off to the nearest. If indeed the current pixel's edge strength is higher, keep it; otherwise, delete it. Hysteresis thresholding is then employed to eliminate any remaining sounds. Hysteresis thresholding is indeed a technique that use a hysteresis loop to get a connected outcome. Typically, in the thresholding process, an image becomes white when a pixel value above the threshold and black when it is below it. However, with this procedure, if a pixel's value above the threshold, it becomes white as well as the pixels around it are recursively examined. When neighboring pixels' pixel values exceed a certain threshold, they become white.

Detection of Icing Using Normalized Cross Correlation

One approach of picture matching is normalized cross-correlation. It is insensitive to changes in linear brightness and contrast. Using the original picture as a wire image and also the icing image as both a template. It is feasible to identify ice when the template and the original picture match. The flowchart for utilizing normalized cross-correlation to find ice. The process of swiping the template in the picture region and determining the value X within this image area is known as normalized cross correlation. In this procedure, each template pixel is multiplied by the pixel of the overlaying picture, and the results of each of the templates pixel multiplications are then added together. The place in the original picture where the template fits it best is indicated by the highest value for X. The area of interest must be included in the template picture.

CONCLUSION

Temperature measurements were being taken as the transmission line robot moved along at a consistent pace. The temperature profile offers useful information for spotting certain issues that might develop soon. It assists in taking safeguards by providing early alerts for overload, environmental conditions, and physical wear. In the experiment, a section of the line that had been heated artificially was found and shown on the temperature map. Future research will examine the connection between temperature change and different fault types. As a result, a self-sufficient system for failure early detection may be created. A temperature sensor upon that line robot was used to gauge the surrounding temperature. The idea that changing temperature along a line can be mapped has been demonstrated. There is no provision for verifying the recorded temperature using an outside sensor.

References:

[1] D. A. Douglass and F. R. Thrash, “Sag and Tension of Conductor,” in *Electric Power Generation, Transmission, and Distribution: The Electric Power Engineering Handbook*, 2019. doi: 10.1201/9781315222424-15.

[2] Y. V. Bladyko, “Mechanical calculation of flexible wires of overhead lines with aerial barrage balls in different climatic regimes,” *Energ. Proc. CIS High. Educ. Institutions Power Eng. Assoc.*, 2019, doi: 10.21122/1029-7448-2019-62-1-24-36.

[3] D. Novriandi, A. A. Zakri, and E. Ervianto, “Sag and Tension of 275 kV Transmission Line using Catenary,” *Int. J. Electr. Energy Power Syst. Eng.*, 2019, doi: 10.31258/ijeepse.2.3.15-20.

[4] M. Wydra, P. Kubaczynski, K. Mazur, and B. Ksiezopolski, “Time-aware monitoring of overhead transmission line sag and temperature with lora communication,” *Energies*, 2019, doi: 10.3390/en12030505.

[5] P. Kumar and A. K. Singh, “Optimal mechanical sag estimator for leveled span overhead transmission line conductor,” *Meas. J. Int. Meas. Confed.*, 2019, doi: 10.1016/j.measurement.2019.01.067.

[6] M. H. Jalali and G. Rideout, “Analytical and experimental investigation of cable–beam system dynamics,” *JVC/Journal Vib. Control*, 2019, doi: 10.1177/1077546319867171.

[7] W. Troppauer, V. Lovrenčić, N. Gubeljak, B. Nemeth, M. Kovač, and G. Gocsei, "Advanced monitoring of icing and prevention against icing on overhead power lines," *Int. Work. Atmos. Icing Struct. 2019*, 2019.

[8] E. Fernandez, I. Albizu, M. T. Bedialauneta, A. J. Mazon, and A. Etxegarai, "Field validation of gap-type overhead conductor creep," *Int. J. Electr. Power Energy Syst.*, 2019, doi: 10.1016/j.ijepes.2018.09.006.

[9] S. Gupta and S. K. Vij, "Transmission line sag calculation with ampacities of different conductors," *Commun. Comput. Inf. Sci.*, 2019, doi: 10.1007/978-981-13-2035-4_19.

[10] D. Poli, P. Pelacchi, G. Lutzemberger, T. Baffa Scirocco, F. Bassi, and G. Bruno, "The possible impact of weather uncertainty on the Dynamic Thermal Rating of transmission power lines: A Monte Carlo error-based approach," *Electr. Power Syst. Res.*, 2019, doi: 10.1016/j.epsr.2019.01.026.

[11] J. Hu, X. Xiong, and J. Wang, "Radial and Circumferential Temperature Calculation Method of Overhead Transmission Lines Based on Thermal Network Model," *Diangong Jishu Xuebao/Transactions China Electrotech. Soc.*, 2019, doi: 10.19595/j.cnki.1000-6753.tces.180398.

[12] S. Gupta and S. K. Vij, "Sag calculations in transmission line with different case studies," 2019. doi: 10.1007/978-981-13-2372-0_55.

CHAPTER 11

AN EXPLORATIVE STUDY ON THE ELECTRICAL POWER DISTRIBUTION SYSTEM

Dr. Rajbhadur Singh, Assistant Professor
Department of Computer Science Engineering, Sanskriti University, Mathura, Uttar Pradesh, India
Email Id-rajbhadurs.soeit@sanskriti.edu.in

Abstract:

A distribution system starts at a distribution substation which consists of the wires, poles, transformers, as well as other machinery required to provide the client with electricity at the necessary voltages. In this chapter author is discusses state of the art isolated Direct Current (DC/DC) converters, topology of the quad-active-bridge converter.

Keywords:

Converter, Power Distribution, Electricity, Transmission Line.

INTRODUCTION

Through a network of transmission and distribution networks, the electrical energy produced by power plants is delivered to customers. Major sub-stations receive the electrical energy produced by the power plants through transmission. Electrical power is distributed from the big sub-stations to the bulk power consumers through high voltage distribution systems, whilst it is distributed to the minor consumers via low voltage distribution systems. In order to effectively and inexpensively distribute energy (electricity) among users, the electrical power distribution system needs be carefully thought out. The electrical power distribution system is the portion of the power system that distributes electricity to different customers for local usage. The electrical power distribution system, in general, is that portion of the power system that transfers electric power (or energy) from significant sub-stations (provided by transmission lines) to customers in accordance with their needs. Figure 1 depicts a low-tension distribution system that consists of feeders, distributors, and service mains.

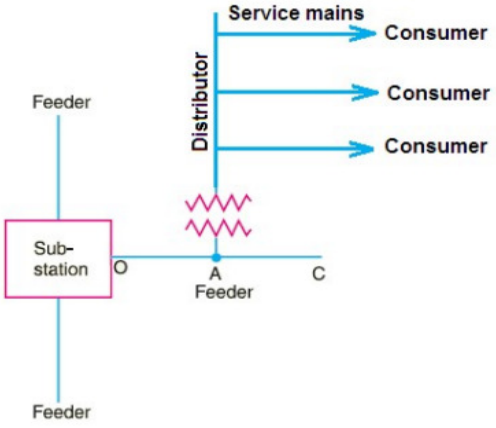

Figure 1: Illustrates a low-tension distribution system is shown in the figure which comprises of feeders, distributors and service mains.

Feeder: The feeder is the conductor or line that links the distributor and the main sub-station. Its purpose is to supply the distributor with electrical power (or energy). The feeder typically maintains the same current along its entire length because no tapping is taken from it. The primary factor considered when designing a feeder is the current carrying capacity.

Distributor:

The distributor is a conductor that is connected to by service mains from various clients. To distribute electricity (or energy) to many customers, several taps are made into the distributor. As a consequence, it carries different currents over its whole length. The most important aspect to consider when developing a distributor is the voltage drop throughout its length. This is because voltage fluctuations at consumer terminals shouldn't go over predetermined limitations.

Main Services:

Service mains are the conductors or cables that link the consumer and distributor. It is made in accordance with the consumer's connected load.

Classification Considering the nature of the supply:

Electricity comes in two flavors: AC power and DC electricity. The distribution systems are divided into AC distribution systems and DC Distribution systems based on the kind of electricity they utilise.

Distribution of AC:

The majority of the time, the load or power consumer needs AC electricity. As a result, AC power is used to produce, transfer, and distribute electricity. Because a transformer makes it simple to step up and step down an AC voltage. The AC distribution system is further divided into two types: Primary distribution system and Secondary distribution system, depending on the voltage level.

Initially Distributed System:

A major distribution system's voltage level is greater than its usage voltage level. Most of the time, the main distribution system is a three-phase, three-wire setup with voltages between 3.3 kV and 11 kV. Large users including businesses, shopping malls, and other commercial complexes get electricity from the main distribution system. A step-down transformer steps down the voltage level at the usage level. This transformer is situated close to the customer's location.

Secondary Distribution System: Power is distributed according to use in a secondary distribution system. At the end of the main distribution network is a transformer that transforms 11 kV into 415 V. And the tiny users get this electricity immediately. To provide a ground terminal, this transformer's main winding is often linked in a delta connection and secondary winding in a star connection. Consequently, a three-phase, four-wire system is used for the secondary distribution system. Any phase with a neutral terminal and a voltage of 230 V or 120 V is used to create a single-phase supply (according to country standards). A single-phase supply is utilised for homes and small businesses. Some users, such as small businesses, wheat mills, etc., need three-phase electricity. This kind of consumer makes use of the R, Y, B, as well as N terminals to connect to a three-phase supply. The secondary distribution network's configuration.

LITERATURE REVIEW

Giampaolo Buticchi [1] et al. stated effective and adaptable electrical distribution is envisioned under the More Electric Aircraft (MEA) concept. In reality, there would be significant weight reduction advantages by upgrading the electrical systems aboard board without overdesigning their generators. For safety purposes, it is preferable to have the generators galvanic ally separated from one another. Multiple DC sources that need to share energy have been successfully used quadruple active bridges (QABs), which also preserve flexibility in control and galvanic isolation. The usage in the MEA hasn't yet been investigated. This study demonstrates how the QAB may be effectively implemented to manage the distribution system inside the situation of varied powers available from of the generators (bus priority) but also load/source disconnection as the MEA would have a DC distribution system with numerous loads and sources. On a lab prototype, simulations and tests demonstrate how coupled magnetic structures offer flexible control without extra redundancy.

Sandro Gunter [2] et al. idea of a more electric airplane attempts to boost the number and efficiency of the electrical subsystems on the upcoming generation of aircraft. The fact that the electric power is produced using electrical generators attached to the jet turbine shaft presents one of the biggest difficulties in this framework. The generators are larger, increasing weight and operating costs, in order to meet peak power demand and overload scenarios. Reduce the size of a generator and use storage devices to provide the peak power as potential solutions to this issue. Solid-state switches may be used as an option to impose load-shedding during periods of high demand. This study suggests an alternative method for controlling the load: changing the distribution's dc voltage. A precise digital identification method is suggested to accomplish this goal. The presented load identification and management approach successfully controls a power curtailment scenario without load-shedding or storage devices, as shown by theoretical simulation and analysis results on even a study-case distribution system. Power hardware inside the loop simulations on such a multiport power converter-equipped dc micro grid support the simulation analysis.

Reyhaneh Taheri [3] has proposed to use a simple methodology for line independence-based modeling of electrical power distribution networks. For the purpose of estimating line currents and bus voltages, the suggested approach may identify the distribution systems' backward and forward sweeping pathways. The approach does this by sequentially identifying the separate lines. A distribution system line that is independent means that it doesn't rely on the current of other lines to operate. It is necessary to complete the suggested line independence-based network modeling only once, before the load flow analysis. The suggested method's output, which is appropriate for backward/forward load flow analysis, consists of matrices that specify the system's steps, the arrangement of its lines, and its beginning and ending points for the hierarchical computation of currents and voltages. Since the forward/backward technique is appropriate for radial distribution systems with load variation, it is employed in this article as the load-flow algorithm. The suggested approach is used to analyze load flow in two IEEE distribution systems, and the results demonstrate its effectiveness.

K. Shashidhar Reddy [4] et al. stated potential harm from fault stress and the expenses related to power outages are the two main issues with today's electrical distribution system. The quickest possible fault clearance is the best strategy for reducing fault stress. Unfortunately, repairing the problem as quickly as possible can compromise coordination and cause worse power outages. Zone Selective Interlocking Coordination ensures that faults for excess currents and voltages

with various faults may persist. The open and shut operations are essential to the circuit breaker's functioning and concept in order to maintain supply and service. Consideration should be given to produce energy during fault circumstances, and its coordination should be examined, in order to lessen the stress just on system.

Daranpob Yodphet [5] et al. conducted a research on Salp Swarm Technique (SSA), a revolutionary optimization algorithm, has recently been discovered to be successful in solving optimization issues. However, optimum system reconfiguration using SSA hasn't yet been shown in the literature. In order to reduce power loss, this study suggests a network redesign of an electrical distribution system depending on the SSA. The distribution systems for buses 33 and 69 are the main focus of the network reconfiguration. The SSA simulation results are contrasted to those of the well-known techniques Genetic Algorithm and Evolutionary Algorithms. In terms of the quality of a resolution and the typical elapsed time, it is discovered that the performance of such an electricity distribution system reconfigured using SSA is reconfigured well compared to other approaches. So SSA becomes an excellent option for electrical distribution network power loss reduction.

Aditya Tiwary [6] has to forecast a system, component, or element's availability and other pertinent indices, reliability assessment is crucial. Reliability is a metric that indicates how long a system will be available under ideal operating circumstances. This study does a reliability assessment of an electrical power distribution system and evaluates several parameters. The electrical power transmission system chosen for investigation is a radial transmission system.

Ali Basim Mohammed [7] et al. investigated the dynamic voltage restorer in order to enhance the electrical distribution system's power quality. Power quality concerns have continuously become worse over the last 50 years. To combat these challenges, equipment including the distribution static compensator (D-STATCOM), solid-state transformer (SST), uninterruptible power supply (UPS), and dynamic voltage restorer have been installed (DVR). One of the cost-effective ways to deal with voltage disturbances like harmonics and voltage sag/swell is to use a DVR. It is often used in global power distribution system, particularly in the medium and low-voltage distribution networks, to reduce voltage disturbances. This essay intends to examine the DVR's integration into a system that uses renewable energy sources. This is crucial since the electrical industry's future is shifting toward renewable energy sources, and it also offers a full analysis of the common components, controllers, compensation strategies, and DVR application. The in-depth analysis of the technology intends to facilitate and hasten the evolution of the DVR in the near future.

In study Redaksi Tim [8] et al. demand for power will keep rising every time, and this is because PLN's client base will also keep expanding annually. As a result, the increase in the quantity of power that must be streamed is precisely proportionate to this. The supplier (PLN) must raise the quantity of energy supplied in tandem with the growth in PLN's client base. The effectiveness of electrical power has always been a major concern in the age of globalization, for both users and suppliers. As a result, the key problem will also be the dependability of the electrical power distribution system. SAIDI (System Average Interruption Duration Index) and SAIFI are the indexes that demonstrate the dependability of the distribution system for electrical power (System Average Interruption Frequency Index). As low as the index values are, SAIDI and SAIFI are more dependable, indicating that the distribution system's efficiency is excellent (high efficiency). The investigation of the Cahaya feeder's SAIDI and SAIFI values, as well as methods for reducing their values, would be covered in this study. Continuity index in the

calendar year 2017, SAIDI and SAIFI along Cahaya Feeder is 2.277 hours/costumers/year and 2.406 time/costumers/years.

Hejun Yang [9] et al. examines the best TOU electricity pricing model as well as its functions for enhancing power quality and lowering power loss in the electrical distribution system since time of use (TOU) methods may directly impact the power flow distribution of a system. First, a moving boundary technique-based optimum period partitioning method is suggested for segmenting a day into its several phases. Second, by reducing the peak-valley difference, the voltage fluctuations, and the power loss, an ideal TOU electricity pricing model is suggested. The suggested optimization problem is solved using the particle swarm optimization (PSO) technique, which converts the multi-objective restricted optimization issue into the single objective unconstrained optimization process. Thirdly, two new indices for characterizing voltage fluctuation and power loss are established in order to take the effects of TOU techniques into account while enhancing power quality and decreasing power loss. Finally, the accuracy and efficiency of the suggested technique are confirmed using an IEEE 14-bus system. The results demonstrate that the algorithm suggested in this study has a significant impact on enhancing the power quality and the financial advantages of the electrical distribution system.

Adil Khan [10] et al. In order to assure stability and sustainability, the power distribution grid needs a new operation and planning tool. This is due to the growing integration with distributed energy resources. The proposed system, in particular the system characteristics and topology, often influences the present planning and operation. The distribution grid, however, lacks or contains erroneous information about the system. Due to the continuing installation of sophisticated metering infrastructure, measurement data are now widely available. These metrics may be a clear option for estimating the distribution grid's structure and parameters. Due to the nonlinearity of the power injection calculations with respect to voltage magnitude and phase angle estimation of line parameters under a noisy environment is challenging. In this study, input and output mistakes have been correctly modeled concurrently using the error within variable (EIV) model. The line parameters have been estimated using an efficient variance approximation approach. In addition to the parameter estimation, an iterative topology estimation method has also been applied. The IEEE 33-bus distribution testing feeder has been used to evaluate the performance of the suggested solution. With the collected data, the approach's superiority and efficacy have been examined.

DISCUSSION

In recent years, the transportation sector has seen unheard-of expansion; in particular, the aviation business has seen a constant rise in the volume of passengers, mail, and products. Given the high level of market demand, increasing efficiency and lowering maintenance costs provide opportunities to save expenses while fostering future growth. The propulsion, hydraulics, electronics, and controls of an airplane are interconnected systems. The primary engines, whether jet- or propeller-based, generate thrust via the burning of fossil fuels, while the utility subsystems get their power either from the mechanical shaft or the turbine. The primary subsystems include the following: Hydraulic actuation system, powered by backup hydraulic pumps connected to the main engine shaft.

De-icing systems, avionics, fuel pumps; Cabin Pressurization System, which is powered by a bleed valve upon that main engine which provides high-pressure air.A bleed-less system is used since the primary engine's bleed valve reduces efficiency. The electrical power

required to run an air compressor again for environmental systems is created by electrical generators connected to the primary engine. Additionally, electrical pumps provided by electrical generators may be used to power hydraulic pumps. So because utility systems are essentially powered by identical electric generators, this architecture makes the mechanical system architecture simpler while also significantly increasing the installed electrical energy on board. More Electric Aircraft (MEA) is the name of a framework, as well as the electrical power distribution system (EPDS) is significant in this context. The hydraulic system and the requirement for redundant hydraulic distribution are significant factors given the growing size of aircraft.

Contribution of weight. Technical complexity of the EPDS would increase if electro-hydrostatic actuators (EHA), self-contained devices that use a local electric pump to operate a hydraulic actuator instead of a hydraulic actuator, gradually replaced hydraulic actuators. For aircraft applications, great dependability and high efficiency remain the primary design objectives. Solutions based on monolithic DC/DC converters or variable frequency AC transmission have been suggested in this context, however they have drawbacks in terms of distribution and overall efficiency. For these reasons, the MIL-STD-704 standard calls for a multi-bus transmission system in which several buses are powered by electrical generators that are linked to the main engine. For starting reasons, an extra bus for the Auxiliary Power Unit is employed, and a network of solid-state breakers enables the connection of various grid components. The EPDS cannot be reconfigured since the electrical generators are designed for peak consumption and also have limited overloading capabilities. This requires the designer must equalize the bus consumptions. The necessity for over-designing the machines would be reduced if the loads could draw support from of the two buses, improving the usage of the available power.

In this study, the feasibility of realizing the aircraft EPDS with a DC distribution system based on interface converters called quadruple-active bridges is discussed. Increased functionality may be achieved without redundant hardware thanks to the ability to route power across several HV/L buses since redundant routes are made possible by magnetic coupling. This study was given in condensed form at the 2017 Electrics conference. A decentralized control is developed, and simulations and tests show that it can function well when load priorities change.

State of the art of isolated DC/DC converters

High efficiency, galvanic isolation (for safety purposes), and complete controllability of a power are the main characteristics of DC/DC converters for the MEA (in order to handle re-generation and load change). The following provides a quick overview of the primary topologies that meet these characteristics. The Full-Bridge DC/DC converter was the very first high frequency DC/DC converter used in an isolated application (FBC). The bidirectional variant is also conceivable, albeit it was previously only used in its unidirectional form (with a diode bridge rectifier just on secondary side). Pulse-width modulation (PWM) and duty-cycle control were first suggested for the converter, which had the benefit of easy and efficient output voltage control. However, the FBC's hard-switching function has a significant influence on the converter's efficiency. Therefore, order to obtain zero voltage during the semiconductors com- mutation (ZVS) of a main side bridge and increase efficiency, a phase-shift modulation of a FBC converter has been adopted. The name of this converter is Zero-Voltage-Switching Phase-Shift Full-Bridge converter in the

literature (ZVS- PS-FB). The need for large filters, which lowers energy capacity, hard-switching of secondary side electronics, and circulating power during idle periods, which lowers efficiency, may be listed as the key drawbacks.

High efficiency and high-power density were presented as problems that might be solved by the Dual-Active-Bridge (DAB) converter. Although there are several modulation strategies, the phase-shift technique is the most popular because of its simplicity and efficiency. With this modulation method, the power flow is regulated by a displacement phase between the main and secondary side bridges, which operate with such a fixed duty-cycle of half of the switching time. Additionally, during commutation, the voltage across the semiconductors is negative, resulting in soft-switching activity on the semiconductors in each of the converter's bridges. Additionally, the quasi-square shape of the current waveform just on stray inductance of the transformer results in low rms values and, as a result, lower conduction losses on the semiconductors but also transformer. The DAB converter's key benefits are soft-switching operation, less energy storage demand on the magnetic components, and straightforward regulation of power flow and output voltage. On the other hand, the significant current ripple on the converter's output capacitor necessitates a large capacitance bank and has a direct influence on the battery capacity of converter. The DAB converter delivers excellent efficiency and high specific power if it is constructed appropriately.

The active bridge is made into a three-phase bridge by adding one more leg, and a three-phase HF transformer is used to create a three-phase version of the DAB. A lot of research was done on this converter. The output current ripple reduction, which results in a smaller output capacitor bank, is this structure's key benefit over the traditional DAB. In terms of the voltage and current stress here on semiconductors and transformer, both converters operate identically. The transformer's intricate construction and large number of parts are a drawback. In fact, high current applications are where this converter is most often employed. The lower needs for the capacitance for the three-phase DAB are a major attribute, making it a great choice for high-power (i.e., compressor) operations on the MEA, where electrolytic capacitors are prohibited for safety reasons.

Many single-input single-output DC/DC converters may be used if multiple buses need to be linked, such as in aerospace or marine systems. Use of a multi-port power converter is an option, as reported. Three active bridges are coupled to an identical high frequency multi-winding transformers in this converter, which is an upgrade to the Dual-Active-Bridge converter. It was given the moniker Triple-Active-Bridge converter because it has three active bridges (TAB). The Quad-Active-Bridge (QAB), an expanded version with four active bridges, was also suggested in to combine dispersed generating and storage systems to a solid-state transformer.

With the added benefit of integrating multiple power sources or loads with the fewest DC/DC conversion stages, these systems provide the same qualities and benefits as the DAB converter with a greater power density. Additionally, the phase-shift angle between the active bridges may be used to simply manage the power flow just on converter. The QAB still has the same drawback as the DAB in terms of the high current ripple inside the capacitors, and a three-phase version is impractical due to the complicated design of the transformer. These factors make the multiple-active-bridge converter an excellent option for use as a power management component in the MEA's low-power sector (Figure 1).

Some of these converters' excellent efficacy has previously been shown.

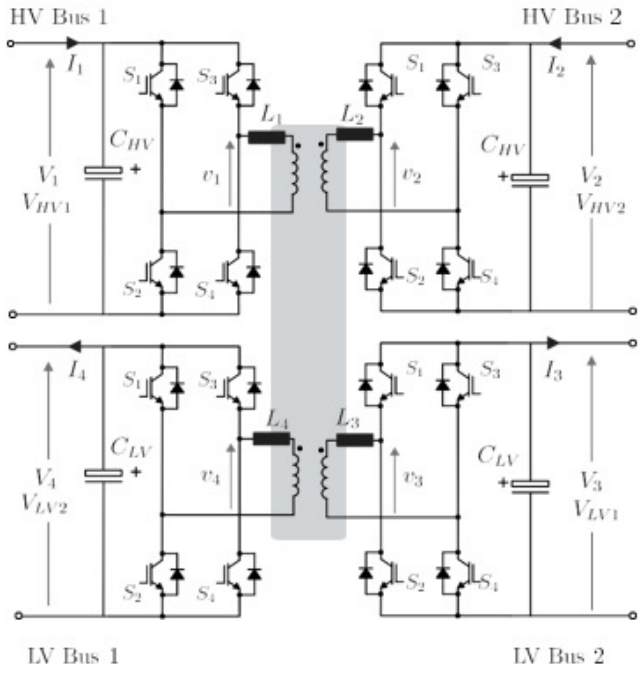

Figure1:TopologyoftheQuad-Active-Bridge(QAB)converter.

Multi-port based electrical distribution

A single-input single-output unit does not support the transmission of power across numerous buses, and the lack of galvanic isolation makes connecting the buses with solid-state breakers undesirable. The main objective of this study is to replace single-input, single-output devices with multiple-input, multiple-output devices that provide power transfer across numerous ports. Although any combinations of HV or LV ports may be used with this method, in the analysis that follows it is assumed that there are two HV ports and two LV ports. This potential connection, in which the ports are denoted by the numbers 1-4 as well as their particular connection (HV1-2, LV1-2). Adopting a 2-DAB solution is the most straightforward way to implement a four-port unit, however this topology prevents power transmission across the HV buses, rendering a whole DAB unit worthless in the event of an HV bus malfunction. The QAB solution contains the same number of components as the 2-DAB solution, and the power exchange is made possible by the magnetic connection. Another option for enabling a robust electrical distribution with 2-port power converters is to use a 3-DAB architecture. However, since two H-bridges and an extra HF transformer are required, the component count is 50% greater. This is the reason why this option won't be further examined. This section will examine the QAB solution. The chosen control is a phase-shift control, which indicates that each full-bridge is powered with a 50% duty cycle and that the power transfer is determined by shifting between the voltage square waves. A delta-equivalent model of a HF transformer may be used to show how each port transfers power with every other port according to the individual phase-shift. The phase shift will be employed in the following using a 2 normalization for simplicity. The voltage waveform with phase shift modulation for the QAB, star, and delta models. Equation (1), where the

inductances and voltages are connected to port 1, describes the total power that is handled by a single port. Lij = Lji is the equivalent inductance between ports I and j, ni is the turn ratio between ports I and 1, and dij is the normalized phase shift. This inductance is made up of all series linked inductances as well as the leakage inductance of the transformer. It is customary to include external series inductance since transformers are typically designed for little leakage.

Aviation standards for electrical stress, software, and hardware must be followed for use aboard airplanes due to strict safety regulations. Redundancy is necessary to prevent single point failure events. This implies that, from the perspective of safety engineering, the safe state is the off state. The power electronics has to be able to recognize the defective occurrence and shut down appropriately, which is the design requirement. The multi-port distribution paradigm provides for power sharing across the many buses, as opposed to the single-input, single-output converter paradigm. Commercial airplanes currently use DC/DC converters, therefore multi-port power converters may use numerous approved methods for fault isolation and detection as well as for the converter enclosure.

A multi-port power converter's key distinction is that a partial operation (i.e., using 3 ports instead of 4) is still theoretically viable and anticipated. In fact, even with a malfunctioning H-bridge, the converter may still function as a power router. To provide a sufficient safety level, these failure modes should be more carefully and thoroughly addressed. To provide spatial separation in the event of a destructive failure, separate PCBs again for H-bridge, for instance, might be utilized. Additionally, fuses could be installed at the transformer terminals or input/output for isolation. The most important factor is an undiagnosed malfunction that causes the converter to operate at an undesirable operation point, such as overloading a section of the EPDS by transferring too much power from one bridge to the other. This fault may not be noticed if the currents and voltages remain within the operating limit since the converter is programmed to maintain some functionality after a fault. Additional sensors and surveillance logic should be designed in order to boost detection likelihood and greatly reduce the likelihood of the aforementioned event. Future study will be conducted on these topics and will not be covered in length in this publication, which is only concerned with the control element.

CONCLUSION

The conductors are fixed to poles made of steel, concrete, or wood. The distribution network's traditional system is another name for this system. In comparison to an underground distribution system, where the conductor is installed, there are greater opportunities for faults and dangers. The overhead system, however, has a lower startup cost. When compared to the subterranean system, the overhead communication network is more adaptable. Since once installed, this system cannot be moved. As a result, expanding the load and establishing a new line are simple tasks. On top of the surface, the conductors are positioned. As a result, this system does not have a nice look for an underground distribution system. The conductors are positioned in the overhead system with enough room. As a result, the air serves as a medium for insulation. Therefore, special insulated wires are not needed. In comparison to the subterranean system, the overhead system currently has a larger carrying capacity.

References

[1] G. Buticchi, L. F. Costa, and M. Liserre, “Multi-port DC/DC converter for the electrical power

distribution system of the more electric aircraft," *Math. Comput. Simul.*, 2019, doi: 10.1016/j.matcom.2018.09.019.

[2] S. Gunter *et al.*, "Load Control for the DC Electrical Power Distribution System of the More Electric Aircraft," *IEEE Trans. Power Electron.*, 2019, doi: 10.1109/TPEL.2018.2856534.

[3] R. Taheri, A. Khajezadeh, M. H. Rezaeian Koochi, and A. Sharifi Nasab Anari, "Line independency-based network modelling for backward/forward load flow analysis of electrical power distribution systems," *Turkish J. Electr. Eng. Comput. Sci.*, 2019, doi: 10.3906/ELK-1812-137.

[4] K. S. Reddy, M. L. Swarupa, and D. Mamtha, "Application of Zone Selective Interlocking in Electrical Power Distribution System," *Int. J. Eng. Adv. Technol.*, 2019, doi: 10.35940/ijeat.b3622.129219.

[5] D. Yodphet, A. Onlam, A. Siritaratiwat, and P. Khunkitti, "Electrical distribution system reconfiguration for power loss reduction by the Salp Swarm algorithm," *Int. J. Smart Grid Clean Energy*, 2019, doi: 10.12720/sgce.8.2.156-163.

[6] A. Tiwary, "Reliability evaluation of radial distribution system – A case study," *Reliab. Theory Appl.*, 2019, doi: 10.24411/1932-2321-2019-14001.

[7] A. B. Mohammed, M. A. M. Ariff, and S. N. Ramli, "Power quality improvement using dynamic voltage restorer in electrical distribution system: An overview," *Indonesian Journal of Electrical Engineering and Computer Science*. 2019. doi: 10.11591/ijeecs.v17.i1.pp86-93.

[8] R. T. Jurnal, "Analisa Nilai Saidi Saifi Sebagai Indeks Keandalan Penyediaan Tenaga Listrik Pada Penyulang Cahaya Pt. Pln (Persero) Area Ciputat," *Energi & Kelistrikan*, 2019, doi: 10.33322/energi.v10i1.330.

[9] H. Yang, L. Wang, and Y. Ma, "Optimal time of use electricity pricing model and its application to electrical distribution system," *IEEE Access*, 2019, doi: 10.1109/ACCESS.2019.2938415.

[10] A. Khan, S. Chakrabarti, A. Sharma, and M. N. Alam, "Parameter and Topology Estimation for Electrical Power Distribution System," 2019. doi: 10.1109/ICPS48983.2019.9067609.

CHAPTER 12

OVERVIEW ON SUBSTATIONS KEY PERFORMANCE INDEX

Dr. Devendra Singh, Assistant Professor
Department of Computer Science Engineering, Sanskriti University, Mathura, Uttar Pradesh, India
Email Id-devendras.soeit@sanskri.edu.in

***Abstract*:**

Key performance indicator, or KPI, is a quantitative measurement of performance over time for a certain goal. KPIs provide goals for teams to strive towards, benchmarks to evaluate progress, and insights that aid individuals across the business in making better choices. In this chapter author is discusses general description of urban rail system, and energy use for urban train system.

***Keywords*:**

Energy, Key Performance Index, Urban Train.

INTRODUCTION

The need for energy is currently increasing, and power-producing substations can provide that demand. There are several different types of power-producing substations, such as thermal, atomic, and hydroelectric. Depending on the resources available, substations are being erected all throughout, however these sites may not be near to load centers. The load centre is capable of doing the actual power utilization. Transporting power from the substation to the locations of the load centers is essential. Therefore, high-capacity, long-distance transmission networks are required for this role. While it is feasible to create electricity at low voltage levels, it is less expensive to deliver it at high voltage levels. To maintain high and low voltage levels, a number of switching and transformation stations must be constructed between the generating station and the consumer ends. Electrical substations are the usual name for the two stations. In this article, the many substation kinds are explored. A substation is a high-voltage electrical system that may be utilised for electronic devices, generators, and other technological devices. AC (alternating current) to DC conversion is the main purpose of the substations (direct current). A transformer and switches are already present within certain tiny substation designs. A range of transformers, tools, equipment, circuit breakers, as well as switches are found in other, larger substation types.

Substation types:

There are several different substation types, including Type Substation, Underground Distribution, Step-down Transformer, Distribution, Switchyard, Customer Substation, and System Station. This particular substation gets its power from a neighboring industrial facility. In this substation, power may be transmitted via a transmission bus linked to transmission lines. The producing facility's incoming power may likewise be hampered by this substation. Equipment utilised in the plant may be powered by the electricity that is obtained. A substation contains circuit breakers that allow it to switch generating and transmission circuits that can be turned on and off as needed.

Substation for Users:

A certain client company's primary energy supply is this form of substation. Client requirements have a significant impact on both the technical specifications and the business case. System Stations: The substation in question, also referred to as a system station, is responsible for transferring a sizable amount of electricity throughout the station. Despite the fact that certain stations can also switch between voltages, some stations only provide power transformers. These stations often provide electrical power to circuits that support transformer stations as well as the places where transmission lines that start in switchyards terminate. They are essential for long-term consistency. The construction and upkeep of these stations are very expensive and of strategic importance. Substations for distribution type are located where the primary voltage distributions were stepped-down in order to deliver voltages to consumers using a distribution network. A voltage of 400 volts will exist between any two components, while 230 volts will exist between any phase and neutrality.

Step-down Type Substation: This type of substation is distributed throughout an electrical network in various locations. They may connect different network nodes and act as a source of sub- or distribution lines. Using this kind of substation, the transmission voltage may be changed into a sub-transmission voltage (69kV). The converted voltage lines may serve as source and distribution substations. Electricity is sometimes pulled from the transmission line and utilised temporarily for industrial uses. Otherwise, power will be sent to a distribution substation.

Underground Distribution Substation: Urban centers often lack the space necessary to build a substation because they lack the necessary amount of land. Burying the substation eliminates the requirement for space and clears the surface for other projects, such as buildings and commercial centers, to address this problem. An underground substation's main objective is to deliver the best conventional substation while occupying less space above ground. Switchyard: The switchyard maintains a steady voltage and acts as a link between the transmission and generation. The main goal of this is to provide the nearby transmission line or power grid with energy generated at the power plant at the desired level of voltage.

An 11 kV substation's primary job is to gather high-voltage energy being transmitted from the producing station, reduce it to a level suitable for local distribution, and provide switching capabilities. A step-down transformer, isolation, lightning arrester, CT metering, circuit breaker, and capacitor bank are all included in this substation.

20 kV Substation: This step-down transformer in the substation is showing the highest apparent power that a step-down transformer can supply by employing its 220 kVA power capability. The received voltage level for this substation would be 220 kV.

132 kV Substation: The step-down transformer is rated at 132kV and has a 132kV primary voltage as well. These transformers are frequently used in transmitting type power stations where another voltage needs to be stepped-down for increased distribution.

LITERATURE REVIEW

A. Waleed [1] et al. whole electrical system has been rapidly evolving. The distribution of power production to innumerable sites has been accelerated by the quick advancement of renewable energies (which are always susceptible to changes). The conventional model of electricity's

unidirectional flow tends to favor multidirectional flows. The electrical power system's transportation infrastructure and manner of operation need to be significantly changed in order to address this issue. The management of power supply and demand is becoming smarter and more structured thanks to technological improvements. The value chain for intelligent transport, generation, and storage must be included in this evolution, together with contemporary monitoring, control, and communication technologies. Thousands of sensors are integrated into digital substations, which increase comfort, independence, availability, and safety while lowering costs, risks, and environmental harm. Digital connectivity, remote monitoring & control, and user involvement are absent from conventional power systems. Fiber-optic wiring in digital substations would enable remote maintenance in addition to real-time data transfer. Along with the most recent developments in smart protection, this paper also compares traditional and digital substations. The flexibility to manage and monitor the digital substations will be improved by electronic protection but also control devices based on a microprocessor and connecting with cloud servers. A sizable quantity of data produced by electrical substation components will enable more advanced monitoring, diagnostic, protection, and optimization capabilities for the facilities. The objective of the study of these developments is to create a smart electrical system that is more effective and offers a better user experience.

N. V. P. R. Durga Prasad and C. Radhakrishna[2]stated the efficiency of the substations that serve the final customers determines how well the electrical distribution utilities perform. Consumer needs are generally focused on the constant supply of affordable, high-quality electricity. The efficient and effective functioning of substations satisfies these objectives. To raise their overall performance and achieve utility level customer-related goals, substations use a variety of asset management methods and efficient maintenance management procedures. These measurements must be focused on to determine their efficacy if performance is to be tracked and improved. Indicators based on dependability are suggested in the literature as a way to evaluate substation performance. Although these indices provide some insight into the general substation condition, they lack the overall performance-centric indicator that shows the substation's operating (maintenance) efficacy and efficiency. The performance of the switchgear is measured in this study using a novel performance metric termed Overall Substation Effectiveness (OSE), which is based on Total Productive Maintenance (TPM) and Equipment Effectiveness (OEE). OSE will give the information necessary for enterprises to spot process improvement possibilities.

T. S. Ustun[3] et al. the Active Distribution Network Management is now becoming fairly difficult as a result of the integration of Distributed Energy Resources (DERs) into to the distribution systems. Distribution substations are used to incorporate DERs into distribution channels. Substation communication networks built on standardized communications are being used to automate substations for better management and operation. Because to its object-oriented modeling and communication characteristics, IEC 61850 has become the most widely used standard. The performance standards for intra-substation communication must be assessed in order to guarantee the smooth and effective functioning of the substation automation system. This study covers IEC 61850 compliant modeling of data flow in the substation and provides simulation and experimental setup validation. For performance validation in the experimental setting, a real bay is reproduced in the lab. The resulting simulation results have been used to verify the method for VLAN and priority tagging implementation.

According to the J. Zhang[4] et al. one collapse in the power system might result from tampering, falsification, and theft of a control and measurement signals in a smart grid. However, communications inside intelligent substations are not protected by any security measures. When implementing security measures, it is important to take into account the high real-time performance requirements for communication services in quite an intelligent substation. The security needs of telecommunications services in intelligent power stations are examined in this study, along with the security strengths and weaknesses of IEC 62351, and a unique security plan for communications in intelligent substations is suggested. Internal and tele control communication are covered by this security plan, which takes into account how each security measure performs in real time. The security precautions of the generic object-oriented substation event, segmented measure value, but also manufacturing message requirements in IEC 62351 are enhanced to meet the real-time requirements of a messages in addition to provide new security features to resist revocation. Certificate less public key cryptography (CLPKC) is used in this scheme to avoid the latency of credential exchange in certificate-based cryptosystems and the issue of key escrow in identity-based cryptosystems. Additionally, a CLPKC implementation in an automated substation is shown. In this research, we combine theoretical analysis and simulation to study the end-to-end latency of protected services and evaluate the security features of the system. The findings show that the suggested plan satisfies the security and real-time performance standards of telecommunications in intelligent substations.

Y. Kwon et al. [5] transmission control protocol/internet protocol (TCP/IP) and Ethernet infrastructures are two examples of digital information technologies that are starting to be included into the infrastructure of the electric power system. With the adoption, network and system management (NSM) solutions with an information systems focus are utilized to control the electric devices and intermediary communication systems within digital substations. However, there is currently no technology available to track serial communication for just a digital substation including cyber-physical System (CPS) data for intelligent electronic devices (IEDs). In this paper, we propose methodologies for a cyber-physical analysis of a digital substation system, focusing on issues such as (1) IEC 62351-7-based network and system management, (2) behavior assessment of the CPS, (3) cyber-physical anomaly detection systems, and (4) a testing ground for a digital substation. A cyber security testbed again for digital substation has indeed been created in collaboration with the Electric Power Research Institute (EPRI) to execute the use cases and assess possible security risks. It is anticipated that newly integrated information management approaches would increase the safety and dependability of the CPS of electric power power grid.

F. S. J. Pereira[6] et al. due to its hazardous environment, building electric power substations involves a significant number of dangers. This study's goal was to assess how construction workers perceive risk, as well as the ways they use to assess and manage the hazards to to which they are exposed. This research conducted a qualitative & quantitative investigation during the installation of a second 100 MVA power transformer to one electric substation. And used the preliminary risk analysis, the hazards were located and analyzed (PRA). In addition, a questionnaire on accident prevention was developed and given to each of the 27 construction employees. The findings revealed what actions are involved in building a power substation, what hazards are there, and how to control them. The PRA and Checklists were discovered to be the most often utilized analytical tools out of a number of others. The relationship between training and risk perception was discovered later. Noise, height-related labor, electric shocks, auto

accidents, dangerous animals, dust, fire, and explosions were among the perceived threats. According to the study's findings, there are a lot of safety concerns associated with building electric power substations, but these risks may be managed effectively by training personnel, which can also lower the frequency of accidents associated with this kind of work.

A. Leal and J. F. Botero [7] Modern power substation communication networks have become more complicated and large in recent years, necessitating the greatest standards of dependability. However, as each end user implements their unique topology or the topology recommended by a vendor in accordance with IEC 61850 standard standards, there is no single criteria to determine the structure of the topology in these kinds of networks. In this study, a technique for constructing a trustworthy network topology in the context of software-defined power substations is proposed utilizing integer linear programming. Utilizing graph metrics, end-to-end time delay performances, and terminal reliability approaches, the veracity of the attained solution is assessed. According to the improves the network requirements indicated by the IEC 61850 standard and the improves the network requirements offered by the IEC 62439 standard, the obtained findings support the idea that the proposed network architecture is extremely reliable to be applied in power substations. We also provide loop-based topologies in the suggested network topology software defined networking-based solutions, which are theoretically impossible to implement using conventional network protocols. These solutions include techniques to address issues with multicast traffic dispersion and dependability, as well as concerns with containing broadcast traffic.

H. Liu[8] et al. compared to system-level and substation-level loads, the load on transformers exhibits more instability and unpredictability. A two-stage short-Term load forecasting (STLF) model of power transformers is suggested in this research. 1) Three current- By using historical load, weather, and calendar data as inputs, state-of-the-art methods are used to anticipate the aggregated substation-level demand. Since no unique STLF model needs to be created at this time, forecasters may choose the most accurate prediction outcomes for predicting transformer-level load. 2) The ratio of the transformer demand towards the substation capacity is known as the load distribution factor (LDF). Under various substation operating circumstances, the link between LDF and also substation load is represented by nonlinear regression functions, and the load within each parallel transformer is forecasted using these non - linear regression functions. Even with little historical load data and erratic operating circumstances, any nonlinear function may be reliably constructed. The efficiency and logic of the suggested approach are shown by three application scenarios. The final illustration shows that STLF of power transformer is required since it offers crucial data for improving substation operating strategies and equipment maintenance schedules.

J. Ma[9] et al. future power systems are expected to be enabled by DC grid, according to certain experts. The multi-terminal dc node (MTDN) is the essential element for voltage/power conversion and fault prevention inside the DC grid. In this study, several MTDN configurations are investigated. MTDN's resemblance to a traditional ac substation is first noted, and three series of "dc substations" based on traditional ac substation architecture have been created. The suggested configurations are contrasted under a four-terminal dc node instance to assess the impact of various "power conversion technology" and "system structure" on dc substation performance. Investigated are possible dc/dc converter uses in dc substations, and each configuration's cost, effectiveness, and dependability are assessed.

K. J. Son[10] et al. that research, the impact of temporal synchronization mistake on collaborative LAN-based protection techniques is investigated. This study suggests a substation model that is built using IEEE 1588 Precision Time Protocol (PTP) enabled intelligent electronic devices in order to calculate the effects of time synchronization. To explore the impact of time synchronization error using two standard substation protection algorithms, namely current differential-based substation prevention and distance protection algorithms, the suggested model is employed as an example of a target platform. It was clear from the examined and simulated findings that time synchronization inaccuracy is a substantial error-causing element for both protection methods, leading to inaccurate fault detection and inaccurate fault distance estimate, respectively. The findings of the investigation presented in this article should serve as a useful blueprint for building the future LAN-based digital power substation having perfect time synchronization.

M. Turski[11] et al. stated the extensive the using district heating systems is one method to reduce air pollution brought on by low emissions. A substantial source-end-users heat demand disparity is a key issue for the effectiveness of district heating systems. The temperature of the return water rises as a result. Modern heat storage techniques are a way to lessen that disparity. The purpose of this research was to increase the efficiency of the district heating system and ascertain the effect of a new component—a phase change material energy accumulator—on the distribution of return water temperature in the substation. This led to the district heating substation doing an examination of the choice and usage of a heat accumulator. There has also been a technique described for calculating the heat buildup rate. For a thermal substation with a thermal output of 150 kW, two cases—without and with the usage of a heat accumulator—were compared using the TRNSYS program. The difference in average return sea surface temperatures were decreased from 7.15 K to 2.29 K after employing the PCM heat accumulator. This made it possible to build up 69.5% of the excess heat and increase the efficiency of the overall heating system by 22%.

DISCUSSION

One-fourth of the total CO2 emissions generated by the transport sector in the European Union (EU), which makes up around 7% of all greenhouse gas (GHG) emissions in the EU, are attributable to urban mobility. Additionally, the prevalence of private automobiles in urban areas contributes to high levels of traffic congestion, noise, and air pollution, which has a significant negative impact on the quality of life in many cities throughout the globe. To address the growing urbanization, while lowering GHG emissions and improving living conditions in cities, it is crucial to develop and promote the usage of integrated, accessible, and environmentally friendly public transport systems. Given its great capacity, safety, dependability, and lack of local emissions, urban rail is ideally suited to serve as the foundation of such sustainable public transportation networks. Additionally, compared to competing modes of transportation, it often produces proportionately less GHG emissions, however this relies on variables like passenger load factors and the mix of the electrical production. However, given the increasing need for capacity and the expense of energy, as well as the fact that competing modes are greatly improving their environmental performance, it is imperative that urban rail minimize its energy usage while also improving the quality of its services. Urban rail systems' energy use is determined by a broad variety of interrelated elements that include the infrastructure, operations, and the cars. Therefore, the development of effective energy efficiency programs requires a

thorough knowledge of the energy fluxes within the system. A organized, logical technique that helps operators and designers evaluate various energy-saving options is also necessary for optimizing the energy consumption in urban train systems. Such a system must include at its heart a thorough collection of KEPIs that are concerned with energy usage. It should thus include a number of measurable factors that provide a complete knowledge of the system's real energy usage, making it easier to pinpoint areas with a high potential for energy savings. Additionally, KEPIs will offer useful data for decision makers to choose the best choice among various energy efficiency techniques if they are further connected to business indicators, for example by providing benefit-cost analyses. They will also be helpful for tracking and assessing the applied energy saving measures.

General description of urban rail systems

Different railway systems that provide public transportation services within of metropolitan regions are referred to as "urban rail." This often comprises tramways, light rail networks, metros (metro is a rail rapid transit network), and commuter or regional railroads [34]. Although many urban rail systems have unique qualities, especially in terms of capacity and quality of service, they all share a few fundamental traits. In tramways and commuter rail, the distance between stations is thus quite low, ranging from 250 to 500 meters to 1 to 5 kilometers. In addition, every urban rail system runs on electricity, with the exception of a few regional routes that use diesel propulsion and are beyond the purview of this effort. Urban train systems have strong operational capabilities, minimal levels of noise, and little localized air pollution. Urban rail also stands out for its high capacity, frequency, level of safety and timeliness, potential for automation, and little surface area requirements. However, compared to non-rail transit modalities, they often demand more expenditure.

Energy use for urban train

Traction and non-traction consumptions are the primary categories used to describe energy usage in urban train systems. The first one, which includes propulsion and on-board auxiliary systems, refers to the energy needed to run the rolling stock across the whole system. The latter takes into account the energy used at stations, depots, and other subsystems, such as groundwater pumps, tunnel illumination and ventilation, and signaling. An illustration of the usual distribution of electrical energy in urban train network. Common connection points (CCPs) are the points where systems connect to the public grid; the initial component of the system's power distribution network is a step-down transformer. 1 Numerous sub-stations are positioned along the track to condition the electricity generation from this system to the needs of feeding rolling stock. The majority of urban rail systems employ step-down transformers and rectifiers because their rolling stock is powered by direct current (DC), often at 600/750 V, 1500 V, or 3000 V. These substations provide power to the traction services to meet the needs, which is often made up of conductor rails or overhead lines (catenary) (third rail). The rolling stock subsequently uses current collector shoe in third-rail systems and pantographs on overhead power cables to gather this energy. The running rails or, less commonly, an additional conductor rail are the usual routes for electric power to transfer to the traction substations (fourth rail). Non-traction loads are often supplied via particular transformers that condition the electricity from the distribution system as needed. These transformers are separate from traction sub-stations, however they are often placed next to one another.

Traction energy consumptions

A typical traction energy flow chart for urban train systems that was created by combining several sources from the literature. This includes estimates for the breakdown of energy consumption in general metro systems and regional rail-roads, findings from studies on the energy efficiency of urban rail systems like Elec Rail and Mod Urban, and energy data from specific systems like the. Because particular systems may vary greatly, it should only be used as an illustration of the usual energy distribution in urban rail. The energy flows throughout the traction system's power supply are shown in red colors in this picture, while the energy distribution inside the rolling stock is depicted in green shades, continuing the color scheme established. The supply voltage and traffic load will be the two main determinants of the energy losses in the power supply system (i.e., from the CCP to the pantograph/collector shoes). In 600V-DC networks, they may be as high as 22%, and as low as 6% in 3000V-DC systems. Respect to the energy fluxes inside the rolling stock itself, braking consumes about half of the energy that enters the rolling stock. This percentage will, however, mostly rely on the number of stops, which is higher for tramways and metros than for local services. A significant portion of the braking energy may be recovered since electric motors can also function as generators. In order to run on-board auxiliary systems, this regenerated energy may be kept in onboard energy storage devices (such as batteries and supercapacitors), or it may be sent back into the power grid to be utilized by other vehicles. However, around a third percent braking energy is irrevocably lost, mostly as a result of losses in the motors, conversions, and transmission system. Losses may also happen during the actual traction process, which is another significant area. As a result, the following energy performances have been recorded: 96–98% for the transmission network, 90–94% for DC and inducement motors, which are the most often used in urban rail, and 98–99% for converters. Most of the traction energy is normally used by on-board auxiliary equipment. The equipment that keeps on-board conditions favorable includes auxiliary systems, which include HVAC, lighting, and information systems as well as traction air conditioners, compressors, and other components that support the vehicle's operating capability. The majority of this consumption is often caused by HVAC equipment, however this varies significantly dependent on the weather conditions under which each system runs. The rolling stock's motion resistance, which includes both mechanical and aerodynamics resistances, is the focus of the remaining energy entering it. Given the relatively slow speeds of urban rail services, mechanical friction between both the rails and rotors often accounts for the majority of the resistance, with the mass of the rolling stock having a significant impact on the total effect.

Non-traction energy consumptions

The energy used at passenger stations, depots, and other infrastructure-related facilities, including such tunnel air conditioning systems, groundwater pumps, tunnel illumination, signaling, as well as the cooling equipment in technical rooms, is referred to as non-traction power consumption. Although certain thermal systems, mainly gas-fired boilers to just provide heating and hot water, are present at stations and depots, the bulk of the aforementioned systems are electrically driven. Lighting, HVAC, escalators, elevators, and information displays are often the stations' top energy consumers. Since temperatures at subterranean stations may rise to very high levels as a result of train operations, the HVAC equipment often accounts for the majority of energy usage. As a result, tunnel ventilation systems are essential for enhancing the train stock's and subway stations' thermal comfort. The inspection, repair, and cleaning of automobiles

account for the majority of the energy usage at depots. This includes the energy used by the on-board auxiliary systems that have to be left on while vehicles are parked, either to aid the aforementioned procedures or during stabling periods, in addition to the energy needed to operate the depot facilities themselves. The kind of system and weather conditions have a significant impact on the percentage of non-traction energy usage. As a result, it will be far less in tramways than in subterranean metros, where it typically accounts for around one third of the entire energy usage.

List of Key Performance Indicators (KPIs)

KPI01 – Specific CO_2 emissions

This indicator shows the annual quantity of CO_2 equivalent emissions (CO_{2e}) linked to the system's overall energy consumption per transportation unit. It may be used to assess the environmental effect of various urban rail systems to one another or to other forms of transportation. It is quantified in kg CO_{2e} per passenger-km. Its computation needs knowledge of the overall energy consumption per source type in the system E(- sys)(i) (such as electricity, gas, renewable energies, etc.) plus the associated CO_2 conversion factors f CO_{2i}, which in the case of the UK may be acquired from the UK Government. It may be evaluated using Eq. (1), wherein NP(sys) is the system's annual total of passengers and d(sys) is the system's annual total of miles traveled by all trains.

$$\mathrm{KPI}_{01} = \frac{\sum_i E_{(i)(sys)} \cdot f_{(\mathrm{CO_2})(i)}}{\mathrm{NP}_{(sys)} \cdot d_{(sys)}}$$

KPI02 – Specific energy consumption

This indicator provides data on the system's total annual energy consumption per passenger-km, which comprises both electrical and thermal energy, or E(el)(sys) and E(th)(sys), correspondingly. This indication gauges the system's overall efficiency. It should be highlighted that E(el)(sys) includes all energy produced inside the appropriate system, whether it comes from renewable or fossil fuels, in addition to the power pulled from the public network via the CCP. The amount of energy pulled from the wireless site must be computed at the CCP as inflow minus outflows power, or, more specifically, as outflow for the portion of the regenerated braking power that is delivered back to the public grid. Usually, generic performance comparisons across various transport modalities are established using this KPI. However, because to the distinctive variables that determine each urban rail system's performance, it is restricted in its ability to compare them. Additionally, since it relies on the degree of occupancy, one such indicator is not the best one to use to evaluate the effectiveness of certain energy-saving measures, necessitating the definition of more precise KPIs.

$$\mathrm{KPI}_{02} = \frac{E_{(el)(sys)} + E_{(th)(sys)}}{\mathrm{NP}_{(sys)} \cdot d_{(sys)}}$$

KPI03 – Share of renewable energy

The proportion of the system's annual energy consumption that is provided by renewable energy sources produced inside the system itself is represented by this metric. It is directly related to KPI01 and may be seen as an indicator of the system's efforts to lessen its environmental effect,

which, if successful, might be utilized to improve its reputation. It is necessary to consider both the electrical and thermal energy that originates from renewable sources (E(el)(sys)(ren) but also E(th)(sys)(ren), respectively).

$$\mathrm{KPI}_{03} = \frac{E_{(el)(sys)(ren)} + E_{(th)(sys)(ren)}}{E_{(el)(sys)} + E_{(th)(sys)}} \times 100$$

KPI05 – Traction power supply efficiency

This indicator measures the effectiveness of the distribution system of electricity and substations that make up the traction system that supplies power. To put it another way, it takes into account the energy losses between the CCP and the place at which the traction power supply grid connects to the new trains (pantograph or collector shoes). It is defined as the annual difference between the total energy used for locomotive purposes as assessed at the substation level and the net2 power consumption of any and all trains in the system when they are in operation.

$$\mathrm{KPI}_{05} = \frac{E_{(el)(sys)(veh)(net)}}{E_{(el)(sys)} - E_{(el)(sys)(non-trac)}} \times 100$$

KPI06 – In-service traction energy consumption

By omitting the consumption of on-board auxiliary systems, this KPI measures the amount of energy primarily utilized for traction in the system each year and per component of transportation. E(el)(sys)(veh)(aux). (Eq. (6)). It is meant to represent the energy savings brought about at the system level by various energy measures implemented on the traction system of the vehicle. Comparing the fleet energy efficiency of different systems may also be helpful, but it's important to take into account the impact of factors like the track profile and the frequency of stops.

$$\mathrm{KPI}_{06} = \frac{E_{(el)(sys)(veh)(net)} - E_{(el)(sys)(veh)(aux)}}{\mathrm{NP}_{(sys)} \cdot d_{(sys)}}$$

CONCLUSION

KPIs assist management in understanding particular issues; its data-driven methodology offers measurable data helpful in strategic planning and assuring operational excellence. KPIs assist in holding workers responsible. KPIs can't discriminate amongst workers since they are scientifically backed and don't depend on sentiments or emotions. When applied properly, KPIs may boost employee morale since salespeople may become aware that their performance is being actively watched. Additionally, KPIs serve as a link between real company activities and objectives. A corporation may create objectives, but without the capacity to monitor results, the plans serve little to no value. KPIs, on the other hand, enable businesses to establish goals and track their success.

References:

[1] A. Waleed *et al.*, “Effectiveness and comparison of digital substations over conventional substations,” *Adv. Sci. Technol. Eng. Syst.*, 2019, doi: 10.25046/aj040452.

[2] N. V. P. R. Durga Prasad and C. Radhakrishna, "Key performance index for overall substation performance," *Int. J. Recent Technol. Eng.*, 2019, doi: 10.35940/ijrte.B3797.078219.

[3] T. S. Ustun, M. A. Aftab, I. Ali, and S. M. S. Hussain, "A novel scheme for performance evaluation of an iec 61850-based active distribution system substation," *IEEE Access*, 2019, doi: 10.1109/ACCESS.2019.2937971.

[4] J. Zhang, J. Li, X. Chen, M. Ni, T. Wang, and J. Luo, "A security scheme for intelligent substation communications considering real-time performance," *J. Mod. Power Syst. Clean Energy*, 2019, doi: 10.1007/s40565-019-0498-5.

[5] Y. Kwon, S. Lee, R. King, J. I. Lim, and H. K. Kim, "Behavior analysis and anomaly detection for a digital substation on cyber-physical system," *Electron.*, 2019, doi: 10.3390/electronics8030326.

[6] F. S. J. Pereira, W. de Albuquerque Soares, E. H. D. Fittipaldi, T. Zlatar, and B. B. Junior, "Risk management during construction of electric power substations," *Gest. e Prod.*, 2019, doi: 10.1590/0104-530X4639-19.

[7] A. Leal and J. F. Botero, "Defining a Reliable Network Topology in Software-Defined Power Substations," *IEEE Access*, 2019, doi: 10.1109/ACCESS.2019.2893114.

[8] H. Liu, Y. Wang, C. Wei, J. Li, and Y. Lin, "Two-Stage Short-Term Load Forecasting for Power Transformers under Different Substation Operating Conditions," *IEEE Access*, 2019, doi: 10.1109/ACCESS.2019.2951422.

[9] J. Ma, M. Zhu, X. Cai, and Y. W. Li, "DC Substation for DC Grid - Part I: Comparative Evaluation of DC Substation Configurations," *IEEE Trans. Power Electron.*, 2019, doi: 10.1109/TPEL.2019.2895043.

[10] K. J. Son, T. G. Chang, and S. H. Kang, "The effect of time synchronization error in LAN-based digital substation," *Sensors (Switzerland)*, 2019, doi: 10.3390/s19092044.

[11] M. Turski, K. Nogaj, and R. Sekret, "The use of a PCM heat accumulator to improve the efficiency of the district heating substation," *Energy*, 2019, doi: 10.1016/j.energy.2019.115885.

CHAPTER 13

ELECTRICAL DISTRIBUTION SYSTEM OVERHEAD CABLES

Dr. Abhishek Kumar Sharma, Assistant Professor
Department of Computer Science Engineering, Sanskriti University, Mathura, Uttar Pradesh, India
Email Id-abhishek.sharma@sanskriti.edu.in

***Abstract*:**

A power system has the adaptability to continuously meet future needs in addition to being able to handle the current load. The whole system must be maintained operational continually without major failures in order to secure the optimum return on the significant investment in the equipment that makes up the power system and also to keep users delighted with dependable service. In this chapter author is discusses the factor of electrical distribution system in overhead cable.

***Keywords*:**

Electrical Distribution, Energy, Overhead Cable, Transmission Line.

INTRODUCTION

Almost all facets of the typical man's everyday activities are impacted by the prevalence of electrical energy. The production, transmission, distribution, and use components of the electrical power system are the most common divisions. One of the essential components of an electrical power system that is often directly connected towards the load center is the distribution network. Through the electricity distribution network of a utility, the electrical energy that is produced and subsequently delivered is provided to consumers. Electrical distribution substations that step-down transmission line voltage levels around 69 kV and 765 kV to distributing voltage levels, often 35 kV or less, make up the distribution system network. According to Indian norms, the voltage level is typically 33 kV/11 kV. Both subterranean cable systems and above electrical wires can be used in distribution networks. Voltages at utilities customer delivery locations may need to be further reduced or stepped down to a voltage of 400 V (three phase) or 230 V using either utility transformer or customer-owned as well as operated transformer (single phase).

Power system engineers are presently very interested in the design and operation of distribution systems once the idea of integrating both dispersed and sources of renewable energy there at distribution level is created. The demand from end customers of energy for higher electrical power reliability and more reliable services has more increased the interest and difficulty of operating the distribution system. According to one of the World Bank's estimates, India loses 4% of its GDP to inefficient power distribution, placing it 80th out of 137 economies when it comes of the dependability of its power supply. One of the highest rates in the world, India has the unfortunate distinction of losing 20% of its power during transmission and distribution, which comes to almost Rs 8,500 crore annually. Numerous unique methods have been introduced in the form of electric distribution systems as a result of the paradigm shift, which has improved system reliability and efficiency overall. Through appropriate changes and the use of

cutting-edge technical breakthroughs, the problem of T&D losses may be solved. Both subterranean cables and overhead transmission lines can be used to deliver electric electricity. Therefore, careful cable selection inside this distribution network is essential to ensure the appropriate degree of operational dependability while taking into account the cost element.

Cables and their selection:

Cables have insulation, which sets them apart from naked overhead conductors in this regard. As a result, the aspect of relative safety may be guaranteed. The need is often the basis for the cable design. Electricity cables are assemblies of one or more electrical conductors that have been individually insulated and are often kept together by an overall sheath in order to transmit and distribute power. These electrical cables may be installed as permanent wire in structures, run above or exposed to the atmosphere while being buried in the ground. Flexible power cables are used by portable machines, equipment, and electronics. The rated voltage, power, maximum working temperature, and intended uses of the client are taken into consideration throughout the design and production of these cables.

Construction of power cables:

Generally, a typical power cable consists of the following:

The component of the cable that carries power happens to be conductors. Copper and aluminum-based conductors are fairly prevalent due to their great qualities favorable to improved conductivity, even though the conductors can be formed of a variety of materials. In recent years, various materials such as cadmium-copper alloys, phosphor bronze, galvanized steel, steel core cooper, and steel core aluminum are also being exploited as conductors thanks to developments in the field of material science. The conductor size is typically determined by the conductor resistance. Based on the requirements of the final use, the conductors can be further divided into solid, flexible, ultra-flexible, and stranded conductors.

Insulation:

Depending on the operating temperature as well as the cable's voltage and current rating, several insulating materials are chosen for usage in cables.

Beheading:

A cable is given extra mechanical strength through the process of beading. Beading can occasionally be utilized for earthing purposes.

Armoring:

The technique of armoring provides an earthing shield towards the conductors that transport current. For safety reasons, armoring is also utilized to ground the wire. If the cable is appropriately earthed, the fault current has sufficient pathways to pass through the armor in the event that the conductor's insulation fails.

Outer Sheath:

This is the cable's outermost cover, which protects it from mechanical, weather, chemicals, and electrical hazards. Typically, rubber and PVC (Poly Vinyl Chloride) are used for the exterior sheath (Various Types of Rubber).

Underground and overhead cables:

Most people are aware that overhead wires are hidden aloft while subterranean cables are buried beneath the earth. But aside from this, each of these types of cables have a number of important characteristics from the standpoints of the transmission of electricity but rather distribution. Technology advances have also made the process of choosing the right cable for a given application more versatile. In the new scenario of the power system design, specifically the distribution system, the connections and their features have become very selective.

Overhead Cables:

In the past, electrical power transmission and distribution have been done via overhead cables or bare wires. These have a straightforward layout and are often activated via towers or poles. Although copper wires are occasionally used in medium modern power system and low-voltage interconnections to customer premises, the bare wire components upon that line are often composed of aluminum (either plain and strengthened with steel or fiber - reinforced composites like as carbon and glass fiber). There are various issues with the system's dependability and safety because the conductors are continually exposed to the elements. The longevity of these conductors might be negatively impacted by unfavorable weather circumstances such intense rain, wind, snowstorm, humid air, and salty substances, which could pose major electrical safety risks. However, the most distinctive benefits, such as lower conductor costs due to the need for less insulation, simpler fault detection because to the conductors' clear visibility, comparably lower installation costs, and ease of expansion, are among the overhead conductors' general benefits. These benefits are supported by a number of additional technical benefits as well, such as independence from the proximity effect, substantially lower conductor sizes, and a significantly greater life expectancy. However, the recent advancements in cable technology and the altered sense of how to perceive various locations from an aesthetic perspective having made the deployment of subterranean cables for power distribution or even transmission increasingly alluring recently. Apart from their unsightly look, the overhead wires also have several other serious drawbacks that account for this. Due to corona discharge, overhead wires frequently cause radio interference. High-voltage overhead wires make hissing or humming noises.

LITERATURE REVIEW

S. V. Khond and G. A. Dhomane[1] In the case of a failure at the loads linked to the distribution system, strong fault currents flow. Circuit breakers and relays must be placed in the right locations and coordinated properly in order to safeguard these loads. This study looks into the effect of time multiplier settings (TMS) of directional overcurrent relays in a framework with combined overhead lines and underground cables in order to determine the ideal relay setting needed for the shortest amount of time to interrupt power supply and prevent relay discoordination. For optimization, a linear programming problem (LPP) technique is applied.

Given that subterranean cables vary from above lines in terms of their features, it is interesting to learn about the quantitative changes in TMS.

O. Lennerhag[2] et al. when lightning hits a shield wire (back flashover) or even a pole conductor, HVDC cable systems linked to HVDC overhead lines are susceptible to quick front overvoltages coming from the line (shielding failure). For HVDC cable networks, representative fast forward overvoltage values are often determined without taking into account their statistical properties. Prior research led to the development of a statistical approach to assess overvoltages in relation to the permissible mean time between failures (MTBF) for the cable system. The technique takes into consideration both the attenuation of the overvoltage wave brought on by corona discharges on the line, which predominate for system voltages up to roughly 320 kV, and the statistical distribution for lightning current magnitudes. This article provides an updated statistical technique that further takes into consideration surge attenuation via resistive effects, soil electrification, and statistical handling of overvoltages caused by shielding failures, making the method applicable for larger system voltages as well. The enhanced approach is used in a case study for a 525 kV DC line to demonstrate its use.

R. B. Kalombo[3] et al. in order to assess the fatigue effectiveness of two overhead wires composed of various kinds of pure aluminum, this paper offers an experimental comparison research. Two cables constructed of 100% aluminum (AA 1350 and AA 1120, respectively) with the names Orchid and AAAC 1120 823 MCM through a battery of seventeen fatigue tests. One of the primary causes of failure brought on by Aeolian vibration is cable fatigue. The clamping force, bending stress, and mean stress resulting from the cable stretching stress are the three forms of loading that the cable experiences via wind. The ratio of the horizontal extending load H to the cable's linear weight w, or H/w, is used to represent this stretching load. The H/w parameter of power line cable design against causing significant to Aeolian vibration has been recommended by the CIGRÉ organization. Two S-N curves were produced at the same H/w value of 1820 m during fatigue testing for cable/suspension clamp systems. For each cable, a single curve was produced. The obtained S-N curves demonstrated that, given the assumed value of H/w, the AA 1120 cable could withstand more cycles before fatigue failure than for the AA 1350. Furthermore, a failure map was created to identify the wire break's morphology. The microscopic examination revealed that the fretted markings served as the origin of the fissures. For the fatigue design of overhead wires against Aeolian vibration, the study's data will be useful.

C. E. Mueller [4] et al. the opposition of locals to the development of new high-voltage overhead transmission lines, potential negative expectations, as well as a lack of public support are common issues that governments and energy providers must deal with. Building subterranean cables instead of overhead wires is an often-mentioned solution to these problems. However, there is currently no empirical support for the claim that replacing overhead power lines with subterranean cables would really lessen protest or alter public perceptions of danger. By comparing citizens' risk expectations, attitude, and protest activity seen at two when their locations in Germany using a quasi-experiment, this research helps close this gap. Both grid expansion projects—an overhead line project in Lower Saxony as well as an underground cable development in Hesse—were at the same stage of the legally prescribed planning and approval process at the time these data were gathered. Results showed that there are either no changes in risk expectations, attitudes, or protest activity of locals questioned at the two project locations

after adjusting for a number of possible confounders. The conclusion drawn from our research is that installing underground cables does not inevitably lead to an improvement in risk expectations, attitudes, or protest activity.

A. De Conti and O. E. S. Leal[5] the goal of the research presented in this article is to determine how an insulating layer protecting an overhead wire affects the transient overvoltages brought on by adjacent lightning strikes. For various load circumstances, the research is conducted taking into account or omitting the existence of an insulating layer. It is shown that, if mismatched loads are taken into account at the line ends, it may be necessary to include an insulating layer in order to adequately define the tail of the ensuing transient overvoltages. On the other hand, the insulating layer has almost little impact on estimated peak voltages.

M. G. Ippolito[6] et al. the building of new transmission overhead wires is becoming more challenging due to strict environmental restrictions. In contrast, cable lines may now be used for high (HV) and extra-high (EHV) voltage systems. When the electrical system is operating under steady-state and transient circumstances, the arrangement of the so-called mixed lines may cause various issues. When examining the dynamic response for power systems, one of the primary issues is in particular the system stability. In this research, the analysis of angular stability of the system with a mixed line is provided; a particular control logic applied towards the mixed line's shunt reactors is suggested as a way to increase the stability of the system as a whole. First, a theoretical discussion of the suggested switching logic is presented, and it is then tested using two separate testing methods. The 400 kV power grid that Sicily uses to connect to the rest of continental Europe is then used as a case study for the use of the suggested switching technique. The results of many simulations run in the power system modeling program NEPLAN360 demonstrate the critical impact timing of control actions given to the shunt reactors plays in maintaining the stability of the system. The suggested control works well to protect the system from major eventualities by making a concerted effort to prevent angular separation between regions and so maintain the system's stability.

P. Zavaleta[7] et al. one of the greatest fire risks in nuclear power facilities is electrical cabinet fire. Four fire experiments were conducted as part of the OECD PRISME-2 project to examine how a fire spread from such an open-doors electrical cabinet to overhead network trays and other cabinets in a restricted and mechanically ventilated space. The same cabinet (fire source) and three overhead cable trays were employed in these experiments, which were designated CFS-5 through CFS-7 and CORE-6. For CFS-5, the trays included a halogenated flame-retardant connection type, and for the other three tests, a halogen-free cable type. Additionally, whereas CORE-6 test featured two extra cabinets close to the fire source, CFS-7 test employed fire dampers. For the purpose of determining how a fire spread, measurements including such flame and gas temperatures, gas concentration, weight loss rate, and heat release rate were taken. Cable trays used for the CFS-5 and CFS-6 tests were damaged by a cabinet fire. For CFS-5, three quick and brief cable tray fires were shown; for CFS-6, a sluggish and lengthy cable tray fire was emphasized. In contrast, the overhead wires were not ignited because the fire dampers were switched off during the CFS-7 test. The higher wires were not ignited during the CORE-6 test, but the cabinet resulting fire to the nearby cabinets.

X. Liu[8] et al. this work proposes an effective approach for measuring the voltages caused by lightning on single-conductor overhead lines and subterranean cables. By fully taking into account the inherent relationship between the frequency-dependent surface load resistance per

unit-length (p.u.l.) and admittance p.u.l., the numerical evaluation of something like the temporal convolution caused by the lossy ground is simplified in this method. Predicated on this, it is possible to implement the assessment of a lightning-induced voltages on to an overhead line or buried cable network inside an effective manner. By separating the lightning channels base current into high-frequency and low-frequency components, the frequency-domain approach of evaluating the lightning horizontal electromagnetic current either above or below the ground surface is changed to further increase efficiency. To verify the suggested technique, certain numerical examples are run on the MATLAB platform, and the effectiveness is examined.

B. d'Andréa-Novel, I. Moyano, and L. Rosier[9] the topic of the work is the stabilization of a hybrid PDE-ODE system over finite time, which may be used to simulate the motion of the overhead crane with a please indicate the extent. The wave equation having constant coefficients is thought to adequately represent the dynamics of a flexible cable. We demonstrate that a finite-time stabilization occurs for the whole system platform + cable that used a nonlinear feedback rule that is modeled after those provided by Haimo (SIAM J Control Optim 24(4):760–770, 1986) for a second-order ODE. The concept of nonlinear semigroups is also used to demonstrate the system's overall well-pawedness.

J. Ding[10] et al. has in comparison to subterranean cables, overhead lines have a distinct characteristic impedance value. There are drawbacks to current traveling wave-based fault-finding techniques for mixed power transmission systems, such as location inaccuracy brought on by wave velocity and challenges determining wave arrival time. Installing wire-based sensors all along power line is a workable way to address these issues since it will improve the amount of information that is accessible from various places. This work introduces a traveling wave-based fault location technique that uses current data collected at the junction site and the overhead line's midway. The wire-based current sensor we created measures the information at these two points. These two sensors separate the whole power transmission system into three sections. The post fault current measurements at the two measuring devices are first recorded as part of the suggested procedure. Second, the defective section may be found by contrasting the current's amplitudes and polarity at these two measurement locations. After determining the post-fault wave propagation routes and obtaining correct wave velocity estimates for the overhead line and subterranean cable, the fault spot may then be identified without the use of time synchronization.

J. R. Villar-Uribe[11] has aerial cable car systems have been implemented in densely populated outlying areas in many cities in Latin America as part of attempts to modernize public transportation. But might these modernization efforts signal the end of impromptu transportation services that help certain outlying residents with their everyday mobility needs. This study used a mixed-methods approach to examine how the Transmissible (TMC) system's installation in Bogota, Colombia, affected the use of informal transportation services. The findings demonstrated that the introduction of the TMC system had little to no impact on the informal transportation (IT) service, and on the contrary, it promoted the development of a new route that links Ciudad Bolvar's rural region with the TMC system. Additionally, it was discovered that informal transportation handles a sizable number of daily trips to the Ciudad Bolvar district's inner surface that formal public transportation mechanisms do not adequately address. This finding reflects the "urban maturation" process that is happening in urban peripheral settlements throughout Latin America, which necessitates a new strategy for planning and overseeing public transportation in these areas.

DISCUSSION

Current is quickly increased when shunt faults in power distribution systems occur. This abrupt spike in current value is a good sign that a system issue has occurred. In power systems, protection techniques are used to separate a defective portion from a healthy section. For the protection of power systems, overcurrent protection techniques are most often utilized. In certain protection plans, the sole kind of network protection is overcurrent relay protection. Each main relay safeguards a certain zone. The backup protection relay is offered to clear the fault if the main relay is unable to isolate the defective portion. To safeguard the whole system under examination, a power system often contains a number of equipment pieces and protective relays. Relay coordination is crucial in protective mechanisms because of this. The operation of the main and backup relays will malfunction if they are not properly coordinated with one another. Therefore, it is crucial to coordinate the functioning of overcurrent relays when constructing suitable safety methods for any power system network. Getting adequate overall coordination between a large number of main and backup relays becomes a challenging task as network capacity grows. In order to improve coordination of both directional and non-directional overcurrent relays, various researchers have reported using artificial intelligence-based methods such as Teaching Learning Based Machine learning, Fuzzy Logic, Nature Inspired Algorithms (NIA), Smart Computing Rules Forethought, Particle Swarm Optimization (PSO), Honey Bee Automated system, Harmony Search Algorithm, Artificial Bees Vassal state, etc.

Fault current but also load current only flow in one direction inside a radial electricity system with a single source of generation. If directed relays are employed, they won't need to coordinate with the relays before them since they will act if fault current flows in the designated direction of tripping. Coordination between the main and backup relays is required because, in the event of a primary relay failure, the backup relay must run to separate the malfunctioning part from the healthy section. Due to the high current flowing and inductance of subterranean cables in radial distributed generators with mixed overhead lines and underground cables, coordination between the main and backup unidirectional overcurrent protection becomes crucial. Underground cable's charging current, which could be as high as a significant portion of the load current, rises with increasing capacitance. The minimum relay settings are constrained as a result. There is a flow of fault conditions and load current in both directions whenever the mode of operation is altered, such as in a power system with several sources of generation or even a ring main system. As a result, the relays employed in protection methods for such a system are sensitive to fault currents traveling in both directions, necessitating the combination of directed and non-directional overcurrent protection at the proper locations. The directional relays will be in the opposite direction of the corresponding bus. The operating time of the relay that came before it, the operating time of something like the circuit breaker connected to it, and the overshoot time of a relay under examination are all taken into account when determining the actual operating time for every directional and non-directional relay. Since non-directional overcurrent relays are utilized in these systems, coordination between both the relays at the distant end of the line and the relays behind them is necessary. The optimization issue may be framed using the above-mentioned model for coordinating between the relays, and it can be solved using the linear programming approach. Therefore, creating the best relay coordination method employing directional overcurrent relays for distribution systems with mixed overhead lines and subterranean cables may be seen as a constrained optimization issue that is addressed as a linear

programming challenge without constraints. Such issues may be resolved using a variety of techniques, such as simplex, dual simplex, or two - phase flow simplex methodology.

Faults Occurrences

The nature of a fault just defined as any abnormal condition, which causes decreases the insulation strength between phase conductors, earth, and any earthed screens adjacent to the conductors. The fault usually occurs due to the breakdown of the insulator between live conductors. This breakdown may be caused by any one or more of numerous factors, for example, mechanical damage, overheating, voltage surges caused by lightning, ionization of air, and misuse of equipment. In practice a reduction is not regarded as a fault until is it is detectable that is until it results either in an excess current or in a reduction of the impedance between conductors and earth to a value below that of the lowest load impedance normal to the circuit. Thus a higher degree of pollution on an insulator string, though it decreases the insulation strength, and affected phase does not become a fault up to a flashover produces excess current or other visible abnormality. The fault current releases a huge amount of thermal energy, not cleared rapidly may cause fire hazards, extensive damage to equipment, and risk to human life. The types of fault causes are similar, but the proportions are different in different boundary those are:

Grounding System

This system can be divided into two parts those are an effectively grounded system (including solidly grounded and low resistance grounded system) and a non-effectively grounded system (including ungrounded, high resistance grounded, and resonant grounded). Conductor Type The fault origin in overhead line, this fault is protected by overhead conductor and underground cable in the power distribution system. The overhead line and the underground cable are the most commonly used in power distribution systems.

Geographical Environment

The fault causes in natural and forestry are different, but tree-caused and animal-caused fault in forestry areas would be more.

Weather Season

The summer of a lighting fault is maximum in this case to break down protective equipment in the power distribution system. The most cause of fault in the power distribution system are: Lightning Many electrical faults occur on overhead power transmission lines are caused by lightning.

Pollution

Pollution is usually deposited dust or cement powder in industrial areas and silt deposited by wind borne sea spray in coastline areas. It causes a flashover rope to decrease extra current or other visible abnormality example, abnormal current flow in the power distribution system.

Fires

The incidence of fire under transmission lines is responsible for an excessive number of line outages in many countries. An extra problem rising from burning is the pollution of the insulators due to the gathering of particles of dust on their surfaces. In this case, the line insulation requirements should be determined in such a way that the outages under fire could be reduced to a minimum. Additional causes of faults on the above lines are trees, birds, aircraft, ice, snow loading, broken insulators, open circuit conductors and nonstandard loading.

Power System Protection

These definitions that follow are generally used in relation to power system protection. Protection System: a complete arrangement of protection equipment and other devices required to achieve a specified function based on a protection principalprotection equipment: a collection of protection devices such as (relays, fuses, Current Transformers and Circuit Breakers. Protection Scheme: a collection of protection equipment providing a defined function and including all equipment required to make the scheme. The purpose of the power protection system is: (i) to keep and minimize damage of electrical equipment, (ii) To isolate the fault portion system to healthy portion of the system,(iii) Provided reliable power supply distributed to the consumers,(iv) Securing from the risk sits for the electricity to persons. The function of a protective device for power protection system is minimize damage to the system and its components to limit the duration of service interruption, whenever apparatus failure, human error, and lighting stork occur on any portion of the system. The overcurrent relay is a sensor fault that sends the signal to the circuit breaker is the trip fault. The electrical power engineer in the power protection system, one of the power problems is solved differentiating faulted and health parts from of the power distribution system. This problem is solved significantly by the power system to protect humans or any components from assist injury. Power protection systems detect and isolate the faulty party automatically. Some abnormal conditions are happening in the power protection system that cannot connect one system to the anthers system.

Protection Device

When the selection of overcurrent protection devices in the protection system deepened up on fault current. Protection for the electric system is an art as well as science and should be modeled with the following objectives in mind Prevent or minimize damage to equipment. Minimize the effect of the disturbance on the uninterrupted portion of the system both in its extent and duration. Minimize interruption of power. Minimize the effect on the utility system. Prevent injury to personnel. The separation of short circuits needs the application of protective apparatus which will sense an abnormal current flow and eliminate the affected portion from the system. The sensing and interrupting device may be separately interconnected only through external control wiring, they may be the same device and isolated devices mechanically coupled to function as a single device. The equipment used for the protection system is a relay, fuse, and circuit breaker. The following part is clarified each overcurrent protective device in detail.

Relay

The purpose of the protective relay is to the quick elimination fault from a part of the power protection system. When it begins to operate in an abnormal manner that might cause damage or

otherwise interfere with the effective operation in the rest of the system. Over current relay is one of the major overcurrent protective devices. In distribution feeders, they play a more significant role and there may be simply protection provided. The power protection system primary protective devices fail, then a backup of the protective device is the clear fault. In any power system, protective devices are coordinated in such a way that protects the adjacent equipment [9]. Over Current Relays (OCR) are normally applied in the power protection system can prevent overcurrent, short circuit, and phase failures. An overcurrent protective device was created to diminish damage to the transformer, electrical device, and support to operate the power distribution system [10]. According to [11] power protection system in high voltage transmission uses more overcurrent relay and ground fault relay as limited backup protection. Over current relay is works when the current exceeds the predetermined setting. The ground fault is disturbances in transmission lines because the transmission line is air insulation, so it is very susceptible to soil disturbance. To detect any current flowing from the power system to the ground is called the residual current. Ground fault relay is a working relay based on the amount of residual current flowing from the system. According to [12] the significant appearances of an overcurrent relay are selectivity, reliability, and discrimination. For any kind of fault occur in the protection system to be either symmetrical or unsymmetrical fault during this time the overcurrent relay has to operate efficiently and provide correct discrimination. Moreover, these relays must operate after a certain time delay and act as backup protection for other relays. The directional overcurrent relays modeled to sense the actual operating situations on an electrical circuit and trip circuit breakers when a fault is detected. The phase relationship of voltage and current is used to limit the direction of a fault. The relay first discriminates the fault is sited in front or behind the relay. If the fault is placed behind the relay is no operation will take place. When the fault happens in front of the relay during this time comparison of fault level and position of current will take place to decide whether to operate or not.

CONCLUSION

Despite recent developments in wire materials that have enhanced the appeal of subterranean systems, overhead distribution is still frequently employed. Although overhead wires are less costly to construct and operate, they are vulnerable to several weather-related issues. Due to their placement, underground lines are shielded from extreme weather, but they are more costly to construct and operate. Due to the soil conditions in several areas of the nation, subterranean distribution is all but impossible. Strong options for overhead distribution will always include low-lying areas, flood plains, and rock strata. Underground installation and maintenance still cost utilities more money than overhead, even under perfect circumstances.

References:

[1] S. V. Khond and G. A. Dhomane, “Optimum coordination of directional overcurrent relays for combined overhead/cable distribution system with linear programming technique,” *Prot. Control Mod. Power Syst.*, 2019, doi: 10.1186/s41601-019-0124-6.

[2] O. Lennerhag, J. Lundquist, C. Engelbrecht, T. Karmokar, and M. H. J. Bollen, “An improved statistical method for calculating lightning overvoltages in HVDC overhead line/cable systems,” *Energies*, 2019, doi: 10.3390/en12163121.

[3] R. B. Kalombo, G. Reinke, T. B. Miranda, J. L. A. Ferreira, C. R. M. Da Silva, and J. A. Araújo, "Experimental Study of the Fatigue Performance of Overhead Pure Aluminium Cables," 2019. doi: 10.1016/j.prostr.2019.12.075.

[4] C. E. Mueller, S. I. Keil, and C. Bauer, "Underground cables vs. overhead lines: Quasi-experimental evidence for the effects on public risk expectations, attitudes, and protest behavior," *Energy Policy*, 2019, doi: 10.1016/j.enpol.2018.10.053.

[5] A. De Conti and O. E. S. Leal, "Lightning-Induced Voltage Calculations on an Overhead Insulated Cable," 2019. doi: 10.1109/SIPDA47030.2019.8951575.

[6] M. G. Ippolito, F. Massaro, and R. Musca, "Improving angle stability by switching shunt reactors in mixed overhead cable lines. An Italian 400 kV case study," *Energies*, 2019, doi: 10.3390/en12071187.

[7] P. Zavaleta, S. Suard, and L. Audouin, "Fire spread from an open-doors electrical cabinet to neighboring targets in a confined and mechanically ventilated facility," 2019. doi: 10.1002/fam.2685.

[8] X. Liu, M. Zhang, T. Wang, and Y. Ge, "Fast evaluation of lightning-induced voltages of overhead line and buried cable considering the lossy ground," *IET Sci. Meas. Technol.*, vol. 13, no. 1, pp. 67–73, 2019, doi: 10.1049/iet-smt.2018.5078.

[9] B. d'Andréa-Novel, I. Moyano, and L. Rosier, "Finite-time stabilization of an overhead crane with a flexible cable," *Math. Control. Signals, Syst.*, 2019, doi: 10.1007/s00498-019-0235-7.

[10] J. Ding, X. Wang, Y. Zheng, and L. Li, "A novel fault location algorithm for mixed overhead-cable transmission system using unsynchronized current data," *IEEJ Trans. Electr. Electron. Eng.*, 2019, doi: 10.1002/tee.22930.

[11] J. R. Villar-Uribe, "Public transport modernization in the urban periphery: Is the end of informal transport? Case study: Overhead cable system 'TransMiCable' in Ciudad Bolívar district, Bogotá - Colombia," *Urbe*, 2019, doi: 10.1590/2175-3369.013.E20190367.

CHAPTER 14

ELECTRICAL DISTRIBUTION SYSTEM UNDERGROUND CABLE

Dr. Govind Singh, Assistant Professor
Department of Computer Science Engineering, Sanskriti University, Mathura, Uttar Pradesh, India
Email Id-govind@sanskriti.edu.in

Abstract:

A cable that has been buried underground is known as an underground cable. They deliver telecommunication or electricity generation. Overhead cables, which are located many kilometers above the ground, may be substituted with these cables. Underground cables are frequently employed in lieu of above wires. In this chapter author is discusses the power transmission about 132kV underground cable.

Keywords:

Electrical Distribution, Power System, Underground Cable.

INTRODUCTION

In addition to the overhead lines, we see every day, underground cables may also be used to transport and distribute electrical power. Of course, these subterranean connections have their own set of benefits and restrictions. Other benefits include improved overall look and less disruption of other facilities, as well as fewer voltage dips and a lower likelihood of faults occurring. However, because of their greater manufacture and installation costs, they are employed in places where overhead lines are impractical or dangerous to use. As a result, we use them in certain locations, such as over lake bodies and in metropolitan regions with significant people concentrations (as submarine cables). As shown in Figure 1, a typical subterranean cable will have a conductor or conductors wrapped in various insulating and protecting layers.

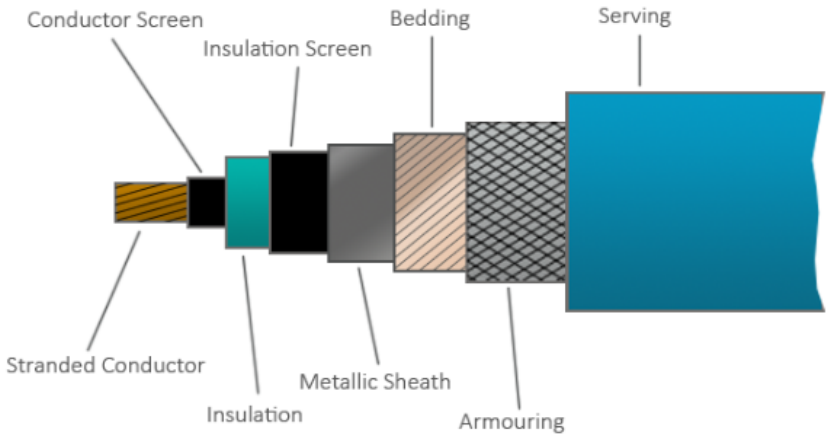

Figure 1: Illustrates the component of underground cable.

Conductor: Depending on the application, 1 or 3 conductors are often utilized. These conductors were stranded to minimize the proximity effect, skin effect, and to maintain flexibility.

Aluminum or pure electrolytic grade copper are used to make conductors.A semi-conductive tape or extrusion layer of the semi-conductive substance is a conductor screen. In MV but also HV cables, conductor screening is often employed to maintain a consistent electric field and reduce electrostatic strains.To resist the electrostatic stress, insulation is offered. Depending on the applied voltage, many kinds (and thicknesses) of insulators are used, including VIR (Vulcanized India Rubber), saturated paper, PVC (polyvinyl chloride), and XLPE (cross-linked polyethylene).A semi-conductive layer of material often used in MV but also HV lines is an insulation screen. It accomplishes the same goal as a conductor screen.

Metallic Sheath: It shields the cable from moisture as well as other chemicals (acids or alkalies) found in the air or soil. Typically, lead or aluminum are used to make it. Because the sheath is empirically grounded while others appear at one end of the cable, it also offers a channel for fault but also leakage currents.

Bedding: A low-grade insulator, such as jute or hessian, shields the metallic sheath from rust and damage caused by armoring's mechanical properties.

Armoring: It offers mechanical defense against the numerous pressures that a cable could encounter during installation and use. A steel tape is often looped around the mattress layer.

Serving: To further protect the steel from air pollutants and agents, another layer of low-grade insulation like Jute or Hessian or even a thermoplastic material like PVC is again given.

LITERATURE REVIEW

G. Tiwaria and S. Sainib [1]discussed the engineers working on power systems are interested in With the introduction of cross-linked polyethylene (XLPE) insulated cables with high capacity for transmitting electricity, the Indian Power System has boosted its usage of subterranean cables. In highly populated areas where environmental restrictions and right of way provide significant challenges, underground cables are recommended. Given that the cables are buried under the earth, the main constraint of underground cable is the inability to discover and detect various defects. On account of protection concerns, the error must be fixed as quickly as possible. This study employs intelligent strategies for quick and more derived from the information and categorization of faults in subterranean cables since standard methods for doing so take a long time. The task was completed in three parts overall, the first of which was to create a MATLAB/Simulink model of an underground cable distribution system with a provision for fault development. For defect detection and classification in the second stage, an Artificial Neural Network (ANN) employing DWT is utilized. To enhance its performance, ANN is hybridized with fuzzy systems and discrete wavelet transform (DWT) techniques in the third stage. The energy components of the three stages of a cable under fault (used as inputs), the fault type, or various distances of cable faults are the training sets for the adaptive neuro fuzzy inference system (ANFIS) (used as outputs). The MATLAB/ SIMULINK environment was used for all simulations.

C. E. Mueller[2] et al. the opposition of locals to the development of new high-voltage overhead transmission lines, negative risk perceptions, and a lack of public support are common issues that governments and energy providers must deal with. Building subterranean cables rather than just overhead wires is an often-mentioned solution to these problems. However, there is currently no empirical support for the claim that replacing overhead power lines with subterranean cables

would really lessen protest or alter public perceptions of danger. By comparing citizens' risk expectations, sentiments, and protest activity seen at two there should locations in Germany using a quasi-experiment, this research helps close this gap. Both grid expansion projects—an overhead line project from Lower Saxony as well as an underground cable project in Hesse—were in the same stage of the legally prescribed planning and approval process at the time the data were gathered. Results showed that there are either no changes in risk expectations, attitudes, or protest activity of locals questioned at the two project locations after adjusting for a number of possible confounders. The conclusion drawn from our research is that installing underground cables does not inevitably lead to an improvement in risk expectations, attitudes, or protest activity.

H. Zhao[3] et al. have an essential component of power line communication (PLC) systems is a power line's characteristic impedance. To understand the properties of power line impedance and achieve impedance matching, use this parameter. In this work, we concentrated on the medium-voltage (MV) cables' characteristic impedance matrices (CIMs). The grounded shields as well as armors, which are often disregarded in current study, were specifically taken into account while examining the computation and features of the CIMs. The experimental measurements used to verify the calculated findings. The findings demonstrate that the forward and backward CIMs of MV subterranean cables with numerous grounding sites are often non-equal unless the whole cable construction is longitudinally symmetrical. After then, the CIMs' resonance phenomena was examined. The resonance inherent inside the CIMs should be of concern inside the resonant frequency of the PLC systems, as we discovered that the grounding of the shields but also armors not just to influenced their own characteristic impedance matching and yet also the characteristics of the cores. Controlled experiments were used to investigate the effects of the grounding resistances, cables lengths, grounded point quantities, and cable branch numbers upon that CIMs of the MV subterranean cables.

J. Zhao [4] et al. urban underground cable wells, as a crucial piece of infrastructure, support efficient urban operations and planned urban growth. The enormous volume of data and intricate structure of the subterranean pipeline, however, make it very challenging to manage, show, and analyze. Point cloud data are progressively being incorporated into the area of building reverse reconstruction with the advancement of LiDAR technology, which is characterized by high-speed, non-contact, high-density, and high-precision. The use of point cloud data to recreate underground cable wells in three dimensions has progressively gained popularity. It is suggested that an approach for topological reconstruction from underground cable well models with holes be employed to address the issues of model incompleteness and modeling inefficiency that arise when triangular networks are constructed directly using point clouds as the data source. The construction of the 3D model uses a novel hybrid model-CSG-BREP (constructive solid geometry-boundary representation) topological model, which is distinct from the widely utilized pipe-lined subterranean pipe network structure. This new model more accurately expresses the internal hierarchical architecture of the underground cable well enough by segmenting the wells into walls, cables, wellbore, etc. Through the addition of the point-surface relationship between tubing holes but also walls as well as the line-surface relationship between pipes and facades to the point-line and line-surface interaction of conventional pipe networks, experimental results demonstrate that the proposed algorithm is capable of reconstructing many different types of walls topologically. The model performs well in the project's test for cable management.

U. Garro[5] et al. Obtaining the cable failure time posterior distribution is necessary for the online Remaining Useful Life (RUL) assessment of subterranean cables and their reliability analysis. In order to provide realistic RUL expectation values and confidence intervals for the findings, Monte Carlo (MC) simulations of complicated thermal heating but also electro-thermal deterioration models must take uncertainties into account. Large simulation sets must be run as part of the process, which is based on historical load or temperature observations and load estimates for the future. Although FPGAs speed up simulations for real-time analysis, the related thermal models are too complicated to be implemented directly in hardware logic. Based on MC simulation, a novel standalone FPGA infrastructure has been presented for the quick and on-site study of underground cable deterioration and dependability. From the findings, the impact of load uncertainties on the anticipated cable End of Life (EOL) has indeed been examined.

M. Majidi[6] et al. In an overhead line with an underground cable, a hybrid fault location approach is suggested in this work. The transient voltage signals collected at a single end are transformed using the time-time (TT-) and S-transforms to extract information. The support vector machine (SVM) that detects whether the fault occurred in the first or the second half of the subterranean cable or overhead line is trained using this information. The SVM parameters are improved using particle swarm optimization to improve classification accuracy (PSO). Using the converted voltage signal and Begley's lattice diagram, the defect is then found. The effectiveness of the suggested strategy is evaluated using a number of factors, including fault type, resistance, inception angle, and position. The excellent accuracy of the suggested strategy in detecting the problematic portion and pinpointing the issue is confirmed by simulation results. Additionally, it is shown that the suggested strategy works better than other techniques in the literature.

I. A. Al-Baldawi[7] et al. the study of thermal fields inside the soil has drawn a lot of interest in the rapidly developing area of buried structures due to the expansion of subterranean systems and technologies. The processes for heat transmission in subterranean cable installations have been discussed in this paper. This study examines a system of an underground cable with such a copper conductor with XLPE insulation that is 12/20 (24) kV single core cable and was installed in one of three experiment types (sand, PVC pipe, and an aluminum pipe). A wooden box was utilized in the laboratory model, and the cable was inserted inside the box through burying the cable using three separate designs and utilizing the soil found in Iraq. This produced successful results, and comparisons being done at each model.

[8] This study involves using a microcontroller and the internet of things to identify faults in subterranean wires (IOT). The microcontroller notifies the user remotely through IOT after it has located the underground cable issue. Through the use of the suggested technology, fault incidence up to a certain distance may be explored. The system has a display device that shows electrical parameters like voltage and current as well as the location of the defect. The fault detection monitors the voltage and current of subterranean cables, and if there is a significant discrepancy in the voltage and current at two of the detector's terminals, the detector will remotely warn the user without having to approach the cable.

M. Jannati [9] et al. electric stress and cable aging are common causes of early failures in subterranean cables. Permanent faults may develop if such defects manifest as brief current surges. Furthermore, due of detection delays, incipient failures may interfere with electrical shipments; as a result, accurate, timely protection judgments cannot be taken. As a result, it is

crucial for utilities to distinguish these sorts of failures from other circumstances as quickly as possible throughout the monitoring process. An accurate method based on Cumulative SUM and Adaptive Linear Neuron has already been presented in this work. The suggested approach's actual online implementation is straightforward and has high-speed detection capabilities. The simulation findings in the EMTP Works environment show that the suggested technique is highly capable of separating cable incipient failures from other distribution system circumstances that are comparable.

S. Bustamante [10] et al. current interest in the issue of dynamic control of electric power distribution lines is high. Dynamic management requires a basic understanding of cable ampacity. This research estimated the ampacity of buried cables at various soil resistivity's and depths. For the purpose of simulating the operational circumstances of a buried wire, a small-scale model was created in the lab. The experimental findings were used to verify a computational model using the finite element technique to assess the capacities determined by two standards. The ampacities produced from the simulated model were compared to those estimated from the IEC 60287-1 and UNE 211435 standards. Additionally, a comparison of the steady-state temperatures for each computed ampacity was done. The ampacity computation technique of the IEC 60287-1 standards when drying-out of the soil happens is the most accurate, according to the findings of the simulated model design, and it has the least chance of surpassing the maximum permitted cable temperature.

DISCUSSION

Appropriate analysis of power systems, the setting of safety relays, and other processes depend on accurate measurement of the electrical constants of power transmission and distribution systems, often known as line constants. There are two types of line constants: main constants derived from the former, such as propagating constant and characteristic impedance, and secondary constants derived from the former, including as per-unit-length impedance and admittance. Line constants are also frequency dependent, meaning that they change due to skin and conductivity and earth proximity effects. For R.M.S. value-based analysis of electricity systems, protective relay configuration, etc., primary line constants for power frequency (commercial frequency) are required. As in the case of overvoltage analysis, secondary line constants are necessary for electromagnetic transient-based analysis, which is primarily relevant to equipment design. This article suggests a technique for determining the subterranean cables' major line constants at power frequency. Manufacturers of cable frequently measure line constants prior to launching subterranean cable transmission lines. Primary line constants, such as positive-sequence admittance, zero-sequence inductances, and positive-sequence capacitance, are the measuring objects. Underground cable line constants have been determined since the 1930s7, although there aren't many technical literatures in this area. For instance, the literature describes a scenario of measuring high-frequency impedance inside a long-distance AC wire. 8 Prior to recent years, multiple connection lines were frequently laid in a single service passageway or transit point along the same routes, but also induction effects from these other parallel lines started to occur from the very beginning.

Originally, impedance has been measured via current flowing under the application of the power-frequency voltage (commissioning). It is challenging to conduct measurements utilizing conveniently transportable instruments, in particular while measuring power-frequency impedance, since voltage and current are subject to induction effects off transformers as well as

other substation machinery even when there are no parallel lines nearby. The authors presented a technique to estimate power-frequency impedance, with a relatively high accuracy, utilizing high-frequency characteristics to use an impedance analyzer, with the goal of accurate impedance measurement with just an easily transportable device even under such circumstances. 9 However, the strength of electromagnetic induction significantly rises when more parallel lines are present, making measurement with impedance analyzers running on voltages on the order of 1 V impractical. In this regard, the authors created a technique for measuring subterranean cable positive- and zero-sequence susceptibility that completely eliminates the effects of electromagnetic induction, even in the presence of other parallel lines. That used a variable frequency supply with only an output of several kVA, current waveforms have been measured whilst also voltage is applied at such a frequency apart from power frequency, as well as impedance at the resonant load is acquired through Fourier series development to distinguish between applied-frequency current and power-frequency current resulting from electromagnetic induction from those other lines. The applied frequency is set between 100 and 200 Hz, while power frequency susceptibility is therefore determined using a linear approximation from observed values. The suggested approach may scarcely be regarded as an easily transportable system when used with an impedance analyzer since it needs a variable frequency source with an output from several kVA. However, it is not necessary to produce current that is so intense that power frequency current produced from other lines might be disregarded, and the necessary power supply can still be thought of as transportable.

132-kV underground cable transmission line

They had the chance to test the line constants of a bulk power system component underground cable transmission line (voltage class: 132 kV, frequency: 60 Hz, solidly-grounded). Two channels are used to link the two transmission substations along this 10-km underground cable transmission network. Employed were independent phase (nontriplex) cables with a conductor cross-section of 2000 mm2 and cross-linked polyethylene (CV) insulation. Gas insulated switchgear (GIS) types transmission substations are used on both ends, and cables with section lengths of several hundred meters to the several kilometers were installed via service tunnels and conduits. Additional underground cable transmission lines have been installed in some of these areas, using the same service tunnel or conduit.

Induced magnetically by other parallel lines

In certain portions, the underground cable transmission line getting tested was installed alongside other subterranean lines. When currents in those lines flow, they create magnetic flux that connects to the line being tested and causes electromagnetic induction. Since the source's impedance is low, induced current superimposes here on current generated by the applied voltage whenever measuring measured impedance of subterranean cable transmission lines through current flowing under voltage. On the other hand, induced voltage superimposes here on voltage generated by injected current when the voltage generated by current injection from a current source is utilized for measurement since the source impedance is high. In either scenario, the superimposition of induced voltage or voltage causes mistakes in measured impedance. Line constants from underground cable transmission lines were measured for each circuit, and it is possible to test a circuit's line constants while the remaining circuits are still in use. From the perspective of line constant measurement, evaluation there at circuit level is more understandable. For convenience, circuits of additional underground cable transmission lines

installed alongside the transmission line under test as well as control systems of the line under test in addition to the one being currently measured are referred to as "other parallel lines. Induced circulation currents were measured in the 132-kV underground cable transmission line undergoing test to assess the effects of electromagnetic induction from these other parallel lines. In order to measure the line constant, a technique that relies on current flowing under the applied voltage from a voltage source has been used; as a result, measurement errors were caused by the induced current. Because of this, circulating currents within circuits #1 and #2 were measured with the measuring and distant ends three-phase shorted, as illustrated in Figure 2.

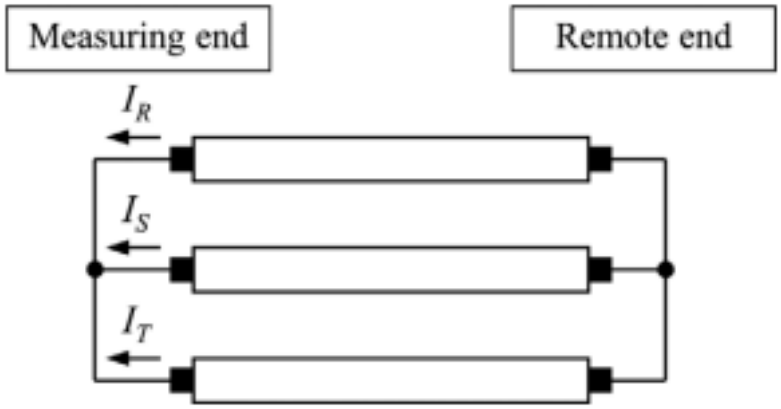

Figure 2: Illustrates the Circuit for measuring circulating currents generated by electromagnetic induction.

The measured values used to determine impedance are superimposed by these currents, which are generated by electromagnetic induction from these other parallel lines. Figures 3A and 3B show the measured outcomes for circuits 1 and 2, respectively. Additionally, each phase's r.m.s. values for the circulating currents have been provided. Unless the quantity of current flowing under the voltage supplied from such a voltage source is considerably bigger than the frequency variation, measured values for impedance are altered by electromagnetic induction.

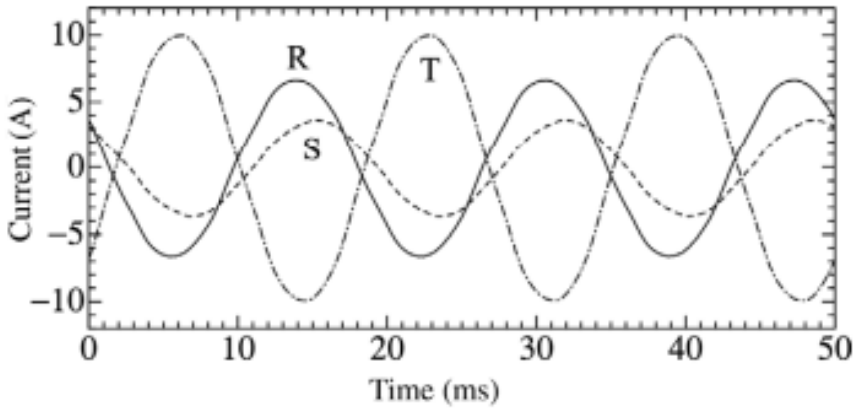

Figure 3A: Illustrates the measured outcome of circulating currents generated by electromagnetic induction.

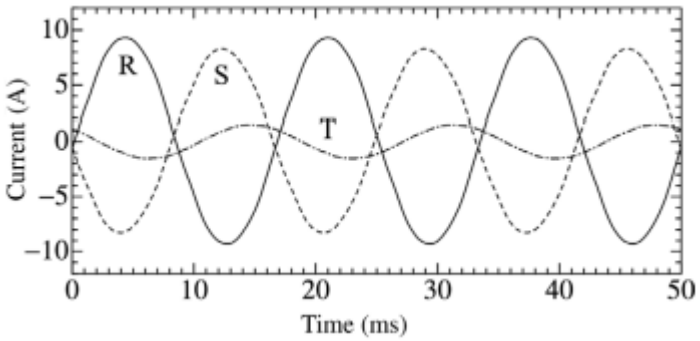

Figure 3B: Illustrates the measured outcome of circulating currents generated by electromagnetic induction.

Impact of electromagnetic induction on circulating currents

A circuit for determining the impedance between phases R and S (the "two-phase approach," which will be detailed later); by connecting the subterranean cable transmission line under test to this measurement circuit (under 60-Hz sinusoidal voltage). The measured results seem satisfactory, and the voltage and current waveforms aren't excessively noisy. However, as was mentioned in the preceding section, this current waveform also has an induced component throughout addition towards the current created by the applied voltage. Since both currents share a frequency of 60 Hz, it is theoretically impossible to separate them. Regarding the observed findings, the power source output is around 300 VA; a portable power supply cannot be anticipated to provide two or three times as much output. The current waveform of has an induced current of an order superimposed on it, hence one may deduce that precise system increases cannot be determined from the observed measurements.

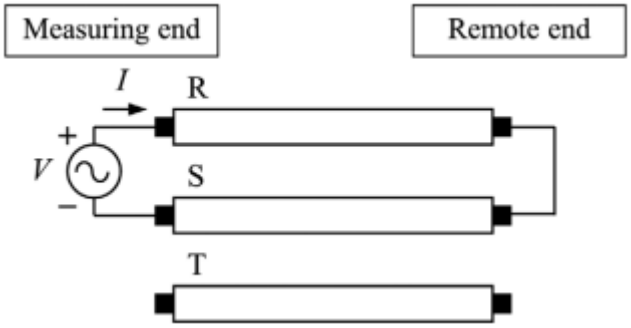

Figure 4: Illustrates the circuit of measuring impedance from both end.

CONCLUSION

The preceding components are taken out, and electromagnetic induction's impact on impedance is disregarded. Next, utilizing two measurement locations near power frequency and a linear approximation, impedance values at power frequency were also determined. In order to show that positive- and zero-sequence susceptibility can be precisely measured even in a real environment with a substantial effect from electromagnetic induction, the suggested approach was applied to a 132-kV underground cable transmission system with a length of roughly 10 km in this study. Additionally, these findings are removed here since the capacitance of the identical

cable transmission line being effectively measured by measuring current which flew under voltage under power frequency provided by such a voltage source.

References:

[1] G. Tiwaria and S. Sainib, "Neuro-fuzzy access for detection of faults in an underground cable distribution system," *Int. J. Recent Technol. Eng.*, 2019, doi: 10.35940/ijrte.B1103.0882S819.

[2] C. E. Mueller, S. I. Keil, and C. Bauer, "Underground cables vs. overhead lines: Quasi-experimental evidence for the effects on public risk expectations, attitudes, and protest behavior," *Energy Policy*, 2019, doi: 10.1016/j.enpol.2018.10.053.

[3] H. Zhao, W. Zhang, and Y. Wang, "Characteristic impedance analysis of medium-voltage underground cables with grounded shields and armors for power line communication," *Electron.*, 2019, doi: 10.3390/electronics8050571.

[4] J. Zhao, Y. Dong, M. Huang, X. Zhang, S. Ma, and M. Sun, "Topological Reconstruction of Underground Cable Well Model with Holes," *Wuhan Daxue Xuebao (Xinxi Kexue Ban)/Geomatics Inf. Sci. Wuhan Univ.*, 2019, doi: 10.13203/j.whugis20180126.

[5] U. Garro, E. Muxika, J. I. Aizpurua, and M. Mendicute, "FPGA-based degradation and reliability monitor for underground cables," *Sensors (Switzerland)*, 2019, doi: 10.3390/s19091995.

[6] O. A. Gashteroodkhani, M. Majidi, M. Etezadi-Amoli, A. F. Nematollahi, and B. Vahidi, "A hybrid SVM-TT transform-based method for fault location in hybrid transmission lines with underground cables," *Electr. Power Syst. Res.*, 2019, doi: 10.1016/j.epsr.2019.01.023.

[7] I. A. Al-Baldawi, S. R. Alsakini, and M. S. Abed, "The effects of sand and pipes on the temperature distributions of the underground cable," 2019. doi: 10.1088/1757-899X/518/4/042012.

[8] "Fault Detection System of Underground Cables," *Int. J. Innov. Technol. Explor. Eng.*, 2019, doi: 10.35940/ijitee.l1036.10812s19.

[9] M. Jannati, B. Vahidi, and S. H. Hosseinian, "Incipient Faults Monitoring in Underground Medium Voltage Cables of Distribution Systems Based on a Two-Step Strategy," *IEEE Trans. Power Deliv.*, 2019, doi: 10.1109/TPWRD.2019.2917268.

[10] S. Bustamante *et al.*, "Thermal behaviour of medium-voltage underground cables under high-load operating conditions," *Appl. Therm. Eng.*, 2019, doi: 10.1016/j.applthermaleng.2019.04.083.

CHAPTER 15

OVERVIEW ON CLASSIFICATION OF DISTRIBUTION SYSTEM

Mr. Harsh Shrivastava, Assistant Professor,
Department of Electrical Engineering, Jaipur National University, Jaipur, India,
Email Id-ershrivastava@jnujaipur.ac.in

Abstract:

A distribution system contains the wires, poles, transformers, and other machinery necessary to supply electrical power to the consumer at the proper voltages, and it is located at a distribution substation. In this chapter author discusses feeder power, and wind speed modelling.

Keywords:

Distribution System, Feeder, Wind Speed Modelling.

INTRODUCTION

According to the connection technique, the distribution system is divided into three categories: radial system, ring main system, and linked distribution system.

Radial System:

Each location in a radial system receives power from either the substation via a different feeder. Additionally, this feeder only supplies electricity in one direction to a distributor. The radial system's architecture is straightforward, making it simple to incorporate in the system. When compared to other systems, this system has a lower startup cost. But this system has a very poor level of dependability. The entire system will come to a standstill if one feeder is running out of pace. Only short-distance distribution systems employ this kind of mechanism. When the load changes, the consumer farther from the feeder can experience poor voltage control and voltage volatility. This sort of system is really only employed to deliver loads that are close to the feeder as a result of this benefit. Figure 1 displays the radial system's single line diagram.

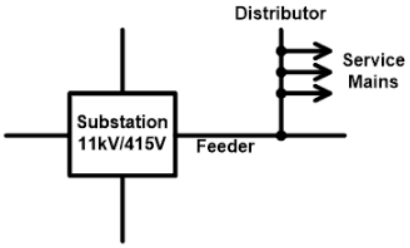

Figure 1: Illustrates the single line diagram of the radial system.

Ring Main System

The distribution transformer is a device in a loop and fed by a substation from one end of the ring main system. It implies that there are two distinct ways for each transmission system to

connect towards the substation. Figure 2 displays a single-line schematic of the ring main system.

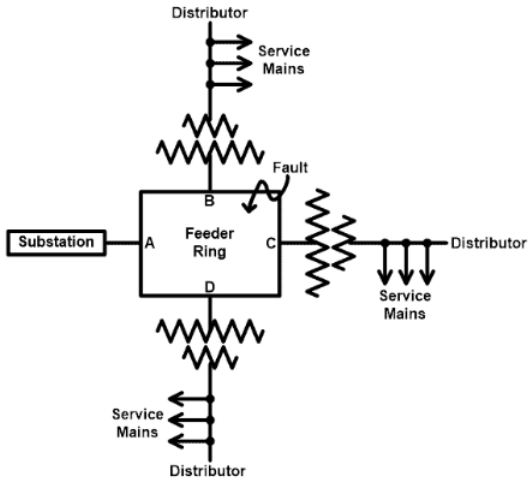

Figure 2: Illustrates the single-line diagram of the ring main system.

This configuration is comparable to two feeds that are linked in parallel. Assume a fault develops between locations B and C. The region between B and C will isolate from either the system in this scenario. Additionally, substations provide electricity in two separate ways. It increases the system's dependability. At the consumer's end, there is also reduced voltage fluctuation. Less current flows across each ring component. Consequently, less conductor material is needed than with a radial arrangement.

Interconnected Distribution System

A loop in an integrated distribution system is fed at various places by many substations. A grid distribution network is another name for this technology. Figure 3 displays the linked system's single-line diagram.

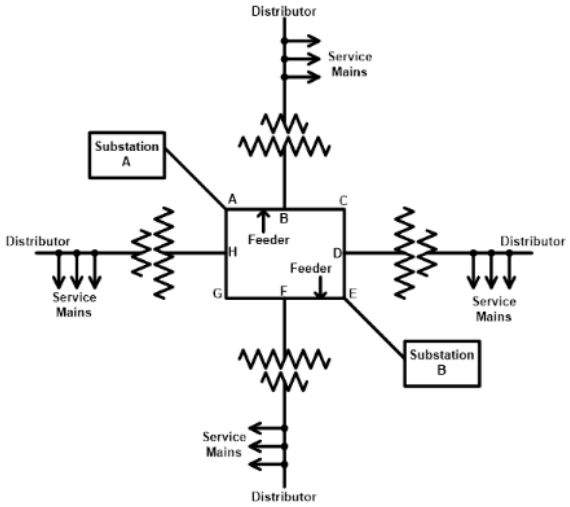

Figure 3: Illustrates the single-line diagram of the interconnected system.

At sites A and E, two substations supply the loop ABCDEFGHA. Comparing the system towards the ring main and radial system, this sort of layout boosts system dependability. Given that more substations are needed in a system, the design of the linked system is extremely challenging and expensive at first. However, this method has the benefit of having better power quality and being more effective. This system lowers the capability for reserve power.

LITERATURE REVIEW

A. Dallmeyer [1] et al. dynamic vegetation models provide the fractional coverage of a few plant functional classes as a means of simulating the global vegetation (PFTs). Although these models often have similar concepts, they vary in terms of the quantity and kind of PFTs, making it difficult to compare the simulated vegetation patterns. Initially, the only type of pollen-based vegetation reconstructions that is accessible is a time series of distinct individual species. Therefore, the modeling results and pollen-based vegetation reconstructions must be transformed into a similar format in order to assess simulated vegetation distributions. The traditional strategy is called biomisation, although until recently, PFT-based biomisation approaches were only accessible for single models. By categorizing PFT distributions into nine mega-biomes using just hypotheses about the minimal PFT cover percentages and a limited number of bioclimatic constraints, they present and assess a straightforward, globally applicable approach (based on the 2 m temperature). These restrictions mostly adhere to the limiting guidelines used in the traditional biome models (here BIOME4). We evaluate the methodology using six cutting-edge dynamic vegetation models that really are part of Earth system approaches that are based on simulations from the pre-industrial, mid-Holocene, and Last Glacial Maximum. Regardless of the geographical resolution or the complexity of the models, the procedure is effective. Large biome belts (such tropical forests) are often more well-represented than limited regional biomes (warm-temperate forest, savanna). The PFT-based biomisation is also capable of keeping up with the conventional technique, as shown by the comparison with biome distributions inferred using the classical biomisation methodology of driving biome models (here BIOME1) with the simulated climatic conditions. The conventional technique, on the other hand, is unable to directly compare and evaluate simulated vegetation distributions because it does not take into account the PFT distributions that the Earth system models have actually generated. Thus, the new approach offers a potent tool for the overall assessment of Earth system models.

According to the K. P. Swain and M. De[2] the voltage profile, a critical performance component in any power system, must be contained within a predetermined tolerance range with regard to the nominal voltage value. In this study, a unique electrical proximity index is used to suggest a voltage control mechanism for smart distribution systems. The dynamics of a system load have no bearing on this index. The approach relies on the electrical closeness of the control units, such as flexible loads and distributed energy resources (DER), starting from the point where voltage control must be included. The impact of these units on voltage variation is computed for various time steps spanning day when depending on the distance of control units from of the place of operation. The control units that are electrically near to the point of voltage variation have their generation or demand adjusted. The control strategy is made quicker and more efficient for managing system voltage profile by using electrical proximity in the selection of control units. The efficiency of the suggested method is shown and assessed for various distribution networks.

According to the S. K. Sudabattula and K. Muniswamy[3] presented an efficient technique for the distribution system (DS (conventional)'s (Gas turbines) and renewable-based distributed

generators (solar, wind) optimum allocation. The goals are to reduce actual reactive power losses and source-generated emissions. Initially, the voltage stability factor (VSF) concept is used to determine the ideal places for DG deployment. By using a search-based dragonfly algorithm, the size and quantity of solar, wind, and gas turbines appropriate to these sites are calculated (DFA). Weibull but also beta probability distribution functions (PDF) adequately characterize the generating uncertainties associated with wind and solar-based DGs to ascertain the precise output power. In this research, two separate scenarios optimal allocation and the mix of various kinds of DERs in the distribution system are taken into account. On IEEE 33 and 69 bus distribution systems, the devised approach is put to the test. The results demonstrate its efficiency in terms of resolving the relevant objective function.

K. H. Choi[4] et al. the class of distributions known as phase-type distributions is exceedingly diverse. Numerous stochastic modeling applications, including those in telecommunications, banking, queueing theory, logistic regression, and inventory systems, have employed them. The contribution of queueing inventory systems (QIS) using phase-type service distributions towards inventory management is reviewed in this research. We have categorized QIS as characteristics in inventory systems including such review policy, replenishment policy, with stock-out assumption in addition to queueing models such as vacation, customer regulation, and customer behavior. Through a literature analysis, we also provide recommendations for upcoming projects that have not received much attention in the past. The literature review's structure in this article gives a clear overview of queueing inventory systems and may be utilized as a springboard for subsequent research.

V. Haldar[5] in a sixty-nine bus micro grid type radial distribution system, this work proposes customer-based multi-objective capacitor allocations and DG integrations taking into account total cost, power losses, SAIFI, SAIDI, and AENS. Here, an evolutionary method called Fish Electrolocation Optimization has been used to tackle multi-objective optimization (FEO). After employing evolutionary multi-objective optimization, non-dominated solutions were obtained, and TOPSIS approach for customer-based decision making was used to examine them. For the purposes of this study, customers from the commercial, industrial, and office/building sectors have been taken into account. The outcomes of the simulation for various clients are optimistic and filled with promise.

M. Khasanov[6] et al. in order to reduce overall power losses, this study suggests a joint optimization approach for determining the best size and placement of several Distributed Generations (DGs) of various sorts in distribution networks. The tree growth algorithm (TGA) and power loss sensitivity factor make up the suggested approach (PLSF). The fight between trees for food and light is what inspired TGA. Intensification and diversification are the two key phases. PLSF is used to shorten computation times and shrink the search space. The suggested method has been developed using M-file MATLAB and tested using a typical IEEE 69-bus test setup. The outcomes of the suggested strategy are contrasted with those of other optimization methods described in the literature. The outcomes demonstrate the computational efficiency, dependability, and ability of the suggested strategy to address the best placement and size of the DG issue.

O. M. Awe[7] et al. everywhere in the globe, water is an essential and fundamental component of nutrition. In order to assess the viability of Water distribution systems (WDSs) and their capacity to function effectively, real-world scenarios must be modeled in order to take into account the

necessity for water distribution systems to meet both rising demand and stringent quality criteria. Various licensed professional and freeware products are readily available for the design and model of various types of WDSs, ranging from basic to complicated, realistic and even hypothetical, according to the assessment of the analysis of modeling software but also performance analysis. Software with licensing, as opposed to software that is available to everyone, gives more adaptability, flexibility, and accuracy when modelling different kinds of hydraulic models. Therefore, the choice of software for designing water distribution systems depends on the degree of software accuracy, the total project cost, the data needed by the program, the complexity of the system, and the aspect of the system to be simulated (quality, demand, valve operation and location etc.) computational and hydrological criteria, as well as software specifics pertaining to the sorts of distribution systems that it can control.

A. Ameen[8] et al. the ability of all-air ventilation systems to run in both cooling and heating mode is a crucial necessity. In contrast to a mixing type air distribution system, two newly developed air distribution systems corner impinging jet (CIJV) and hybrid displacement ventilation (HDV)are experimentally investigated in this study. When running in heating mode, these three separate systems are compared and studied to see how well they perform in terms of local thermal comfort and ventilation efficiency. Two workstations are present in the office setting of the evaluation test room. Three windows on one office wall face a room with a cool temperature. The findings demonstrate that, in terms of ventilation efficacy near to the workstations, CIJV and HDV function similarly to a mixed ventilation. In terms of evaluating local thermal comfort, the findings indicate a little advantage for CIJV in the occupied zone. The average draught rate (DR) inside the occupied zone for C2-CIJV and C2-CMV, respectively, is 0.3% for C2-CIJV and 5.3% for C2-CMV, with the maximum difference reaching up to 10% at a height of 1.7 m. The findings suggest that when employed in workplaces that demand modest heating, these systems may perform just as well as mixed ventilation. The findings also indicate that the overall airflow overall temperature distribution in the space is significantly impacted by the downdraught from the windows.

G. L. Augusto and A. B. Culaba[9]stated the distribution network that distributes chilled water to several buildings at set rates for comfort cooling is the most costly part of a large-scale district cooling system. A comprehensive analysis would be needed to correctly construct the network since the pipe system requires a significant initial expenditure. An approach for the best district cooling distribution network design using a loop-type system is required to get the answer. By calculating the system pressure difference, system volumetric flow rate, but also volumetric flow rate for every building, a district cooling distributed generation model with a loop-type system was examined in this research. Based on a design temperature difference of 9°C as well as a supply temperature of 4.5°C, frictional pressure identification, system modeling, and optimization were carried out. Mass conservation, the performance curve of a variable primary flow pumping system, energy equations resulting from pipe friction, and an equation stating that the algebraic total of head losses around in any closed loop would have to be zero made up the governing equations. The elements of a solution vector were found using the singular-value decomposition technique, and the system of nonlinear equations was then solved using the multivariable Newton-Raphson method. The objective function was solved using an exhaustive search approach, which was then utilized to identify the pipe network design criterion that results in the lowest total cost. Additionally, numerical findings were contrasted with those using

conventional techniques, and they revealed some agreement in terms of pipe sizes with the exception of pressure drop values greater than 100 Pa/m.

T. Patcharoen and A. Ngaopitakkul[10] study suggested a technique for classifying failure types in a distribution system with many distributed generations (DGs). The research also evaluated how DGs' signal characteristics changed when various failure categories occurred in the distribution system. A classification method and decision tree have been built using discrete wavelet transform (DWT)-based signal processing to categorize different fault kinds. The three-phase current signal is used as the algorithm's input data both in normal operation and when a problem occurs. These signals are captured from the DG bus, load, and substation. On a simulation system that's been based on a portion of Thailand's 22 kV distribution network and had a 2-MW wind power production as the DG connected to the transmission line via PSCAD software, the performance of the suggested classifying algorithm was assessed. To assess the performance of the suggested algorithm under different circumstances, the following factors were taken into account: fault kind, fault location, location of DG(s), and number of DGs. The simulation's outcome showed that inserting DGs would significantly alter the properties of the current signal. Additionally, when used on a distribution system with numerous DGs, the suggested approach has shown adequate accuracy in terms of recognizing and categorizing fault kinds.

DISCUSSION

From the standpoint of total fuel consumption, wind power is a desirable renewable energy source from an environmental standpoint. Wind energy will have enormous potential if it can be made available to customers at fair costs without compromising the security and dependability of the distribution system. The intermittent nature of wind power production presents unique technological and financial problems in reaching this aim, which must be overcome if wind power is to be successfully absorbed into the electrical supply. The amount of fluctuation in the electricity produced by wind-based distributed generation (DG) is the highest of all DG methods. One of the biggest problems that the system planners face is distribution system planning, particularly when wind-based DG units (with their intermittent nature) are included in the system. The proper placement of DG units inside the current distribution system is essential for enhancing system efficiency; as a result, optimum DG placement is one of the most vital factors in DG planning. Hereford Ranch method was used to reduce system losses under the restriction of total power penetration from DG units. The location of DG units on the electrical grid may be determined using an iterative method that was proposed in. to locate DG units in the distribution system and reduce system losses, a Tabu Search approach was used. For the distribution system's DG unit allocation, the research used an iterative process. To determine the ideal locations for DG unit placement in the distribution system, they conducted analysis of power flow equations that included both voltage sensitivity and loss sensitivity.

A heuristic method for DG capacity investment planning in a market power auction with competition. A cost-benefit analysis from of the viewpoint of a distribution firm was used to determine the best distribution of DG units. An evolutionary method to choose the best placement of the DG units inside the distribution system is described in order to reduce system losses. Using voltage stability sensitivity in relation to variations in the reactive and active power injected at load buses to efficiently distribute DG units inside the radial distribution system and reduce power losses, an analytical approach is suggested. The suggested method took into

account various load profiles with time-varying loads and DG output. For the best placement of DG units inside the distribution system, a genetic algorithm (GA) was used while taking into account technical limitations such feeder capacity restrictions and feeder voltage profile. Use of a decision theory-based heuristic optimization approach was made to manage the impact of the uncertainties related to DG penetration and protection. The analysis therefore reveals that a lot of effort has been made towards distributing DG units, but much of the work given presupposes that the output of a DG is dispatch able and under control. The intermittent character of the output cannot be modeled using the current techniques.

Feeder power

Owing to the environmental concerns and fuel cost uncertainties associated with the use of conventional energy sources, attention has been directed towards implementing renewable DG units in distribution systems. Therefore, in Canada, based on Ontario's Standard Offer Program (SOP), local distribution companies (LDCs) are required to accept a given percentage of customer-owned wind-based DG units in their system. Consequently, LDCs must select the allocations that will maximize benefits. In general, benefit maximization in any normal planning problem means minimizing cost while maintaining the performance of the system within acceptable limits. Costs include the following: Capital cost: In this case, the capital cost of the wind-based DG units is the sole responsibility of the customer. Running cost (operation and maintenance cost): As with the capital cost, operation and maintenance are the sole responsibilities of the customer. Cost of unserved energy because of interruption (maximizing the system reliability): Based on the current practice of deploying DG units in distribution systems, this cost represents the impact of renewable DG on the reliability of such distribution systems. In this regard, the following should be noted: A distribution network is fed from a transmission network, and when the connection to the transmission system is lost, that is, the distribution network is islanded, all DG units are required to shut down for loss-of-main protection. This practice is normal, and DG therefore does not play a role in increasing the reliability of the supply. If islanding is allowed, the system cannot rely solely on renewable DG units to supply the island's load. Renewable DG units are characterized by high levels of random power fluctuation that result in power mismatch issues, causing stability problems with respect to voltage and frequency.

Conversely, renewable DG has the potential to increase the reliability of the system from the perspective of relieving substation transformers and main feeders during peak load periods. This relief may result in extending the usable lifetime of the transformer and reducing the probability of premature failure because of overloading. However, this potential increase in reliability does not depend on the placement of the DG units on the feeders and is therefore outside the scope of this study. Thus, for the purposes of this study, it is assumed that the location of renewable DG units on a given feeder has no direct influence on the reliability of the distribution system. Feeder power losses: Network losses are a key consideration in the planning problem for the following reasons: Although DG may unload lines and reduce losses, if they are improperly allocated, the reverse power flows from larger DG units can give rise to excessive losses and can overheat feeders. Minimizing system power losses has a positive impact on relieving the feeders, reducing the voltage drop and improving the voltage profile and has other environmental and economic benefits. Therefore, based on these considerations, the objective of the proposed planning problem is, for all possible operating conditions, to minimize the annual energy losses of the system without violating system constraints.

Wind speed modelling

The Rayleigh probability density function is indeed a highly useful equation often used to predict the behavior of wind speed (pdf). The shape index for the Rayleigh pdf, a specific instance of the Weibull pdf, is equal to,

$$f(v) = \left(\frac{2v}{c^2}\right) \exp\left[-\left(\frac{v}{c}\right)^2\right]$$

C is referred to as the scale index. The scaling index c may be determined if the mean wind speed at the a place is known,

$$v_m = \int_0^\infty v f(v)\, dv = \int_0^\infty \left(\frac{2v^2}{c^2}\right) \exp\left[-\left(\frac{v}{c}\right)^2\right] dv = \frac{\sqrt{\pi}}{2} c$$

$$c \simeq 1.128 v_m$$

The continuous pdf has been split into states when the wind speed is within certain limitations in order to integrate the output power of a wind-based DG units as a multi-state variable inside the planned formulation. The Rayleigh distribution's state count is carefully chosen since a low state count reduces accuracy while a high state count makes the task more difficult.

Load modelling

It will be expected that the system peak load will follow the hourly load shape of the IEEE-RTS in order to continue with an appropriate planning choice. Based on this supposition, the load will be separated into different levels using a clustering method that employs the recently developed central centroid classification process. This procedure verifies which selecting ten equivalent load levels (states), with different probabilities (P(Ly)), will provide a reasonable trade-off between accuracy and also quick numerical evaluation. The 10 load states are shown in Table 1 along with their probability.

Table 1: Illustrates the ten load states accompanied by their probabilities.

Load state (y)	% Peak load	Probability ($P_y(L)$)
1	100	0.01
2	85.3	0.056
3	77.4	0.1057
4	71.3	0.1654
5	65	0.1654
6	58.5	0.163
7	51	0.163
8	45.1	0.0912
9	40.6	0.0473
10	35.1	0.033

Combined generation- load model

The combined wind-load model is created using the previously described wind-based DG electrical output combined load modeling. The wind speed states as well as the load states were presumed to be separate in this study (uncorrelated). In other words, the load and indeed the diurnal and seasonal variations in the wind speed were ignored. If there is just a slight link between the wind speed and indeed the load, this assumption will have minimal impact on the outcomes. However, if there is a significant connection between the two, the kind of correlation will have an impact on the findings' accuracy (either it is positive or negative). The justification for this is that reverse power flow, which happens when the output power of a DG units is greater than the load, is the primary cause of restrictions violations. The quantity of the reverse power flow is anticipated to decrease if there is a positive connection between the wind speed as well as the load, hence the optimum penetration of a DG units was anticipated to be larger than the figure determined using the aforementioned assumption. The ideal DG unit penetration, on the other hand, is anticipated to be lower than the amount determined using the same assumption when a negative correlation occurs. Using the following equation as a foundation, it is possible to determine the probability of any load plus wind-based DG output combination (P (Cg)) by converging the two probabilities.

$$P(\boldsymbol{C}_g) = P_w(G) \times P_y(L)$$

By listing all conceivable combinations between the wind-based DG output power and the load, a generation-load model for wind turbines is created based on this idea. As follows is the whole generation-load model,

$$R = [\{\boldsymbol{C}_g, P(\boldsymbol{C}_g)\}: g = 1{:}N]$$

If m is a collection of all commercially feasible turbines, each of which has a unique power performance curve; R is the m turbines' full yearly generation-load model; All conceivable configurations of a wind output power levels, which correspond towards the available turbines, as well as the load states are included in the m + 1 column matrices C. column m + 1 shows the various load levels, where columns 1 to m reflect the output power of an available m turbines as just a percentage of each turbine's power rating; N is the total number of states within model R, which really is equivalent to the product of the wind velocity states as well as the load states, and P(Cg) is a one-column matrix which reflects the probability corresponding with matrix C.

Particle Swarm Optimization

It offers a particle swarm optimization technique to determine the smallest Time Dial Setting (TDS) for overcurrent relay coordination. The linear programming technique is then contrasted with this approach. The math lab has put the approach to use for radial but also parallel feeder systems. Both methods are used to determine the relay coordination's operational time. Particle swarm optimization outperformed linear programming in terms of results in both situations. The system performance of operating time is also maintained and improved, according to digital relay fractional value for time dial setting. In order to achieve the best coordination of directional overcurrent relays because since inclusion of series compensation, this study develops an efficient form of the particle swarm optimization technique based on time-varying accelerating

coefficients. The effectiveness of the recommended version particle swarm optimization algorithm for addressing the optimum coordination for directional overcurrent relay inside the presence of reactive power compensation is supported by simulation results that are contrasted with those from other methods. Addressing overcurrent relay coordination issues in Particle Swarm Optimization (PSO). To address mis-coordination issues and cut down on relay operation time, particle swarm optimization is an optional solution. Eight bus test systems have been used to successfully test these algorithms. The results of the simulations have demonstrated that the particle swarm optimization approach is to reduce the total time that relays are in operation while also resolving the mis-coordination issue in the power protection system. This method's effectiveness is contrasted with results achieved by employing a genetic algorithm. In both instances, particle swarm optimization outperformed genetic algorithms in terms of results. Power system protection uses modeling to keep a close eye on the system to guarantee maximum supply continuity while protecting the system's hardware. Protection of the power system becomes crucial when power system changes alter its structure. There should be such gadgets that can recognize a defect and separate the faulty area from the maintaining healthy segment if any irregularity or fault develops in this system. Protective relays carry perform this really crucial task. In this effort, this same focus is on determining the optimal time dial setting for the relay stations connected at all configurations using particle swarm optimization algorithms. Relay coordination is indeed the process of selecting the appropriate relay settings namely that their own essential protective function is met underneath the prerequisites of sensitivity, selectivity, serviceability, and speed.

CONCLUSION

After receiving the majority of an electrical energy from of the transmission or sub distribution substation, the main objective of the distribution system for electricity is to provide the energy needs of the client. Primary substations and consumer substations are indeed the two main categories of distribution substations. The customer substation connects towards the low voltage (LV) network, whereas the major substation acts as a load center. Referred to as a customer substation, a distribution room is one that is typically offered by the client. A combination of HV switchgear panels and the transformer needed to connect LV to the consumer incoming switchboard may be accommodated in the distribution room. The distribution system may consist of overhead wires or subterranean cables, depending on the locality. In metropolitan regions, cables are often utilized, whereas rural areas employ overhead lines. There are several network designs that may be used to provide the desired supply dependability.

References:

[1] A. Dallmeyer, M. Claussen, and V. Brovkin, “Harmonising plant functional type distributions for evaluating Earth system models,” *Clim. Past*, 2019, doi: 10.5194/cp-15-335-2019.

[2] K. P. Swain and M. De, “A novel electrical proximity index for voltage control in smart distribution system,” *Electr. Power Syst. Res.*, 2019, doi: 10.1016/j.epsr.2019.03.006.

[3] S. K. Sudabattula and K. Muniswamy, “Optimal allocation of different types of distributed generators in distribution system,” *Gazi Univ. J. Sci.*, 2019.

[4] K. H. Choi, B. K. Yoon, and S. A. Moon, “Queueing Inventory Systems with Phase-type

Service Distributions: A literature review," *Industrial Engineering and Management Systems*. 2019. doi: 10.7232/iems.2019.18.3.330.

[5] V. Haldar, "Customer based Multi-objective Capacitor Allocation and DG Integration in a Microgrid Type Radial Distribution System," 2019. doi: 10.1109/GTDAsia.2019.8715899.

[6] M. Khasanov, K. Xie, S. Kamel, L. Wen, and X. Fan, "Combined Tree Growth Algorithm for Optimal Location and Size of Multiple DGs with Different Types in Distribution Systems," 2019. doi: 10.1109/ISGT-Asia.2019.8881414.

[7] O. M. Awe, S. T. A. Okolie, and O. S. I. Fayomi, "Review of Water Distribution Systems Modelling and Performance Analysis Softwares," 2019. doi: 10.1088/1742-6596/1378/2/022067.

[8] A. Ameen, M. Cehlin, U. Larsson, and T. Karimipanah, "Experimental investigation of ventilation performance of different air distribution systems in an office environment-heating mode," *Energies*, 2019, doi: 10.3390/en12101835.

[9] G. L. Augusto and A. B. Culaba, "Identification of design criteria for district cooling distribution network with loop-type system," 2019. doi: 10.1016/j.egypro.2019.01.610.

[10] T. Patcharoen and A. Ngaopitakkul, "Fault classifications in distribution systems consisting of wind power as distributed generation using discrete wavelet transforms," *Sustain.*, 2019, doi: 10.3390/su11247209.

CHAPTER 16

STRINGING CHART OF TRANSMISSION LINES

Mr. Vivek Jain, Associate Professor,
Department of Electrical Engineering, Jaipur National University, Jaipur, India,
Email Id-vivekkumar@jnujaipur.ac.in

***Abstract*:**

Basically, a stringing chart is a graph relating temperatures, tension, and sag. They want our conductor to have low tension and little sag, however this is impossible since sag is inversely related to tension. This is because a low tension indicates a loose wire with greater sag, while a low tension indicates a tight wire but also low tension. In this chapter author is discusses stringing chart of transmission line and model of the vibration damper.

***Keywords*:**

Energy, Stringing Chart, Stockbridge, Transmission Line.

Introduction

The minimum ground clearance must be maintained under those same conditions and the sag must be calculated for the worst possible circumstances. The designer should be aware of the sag to be permitted and the tension in the lines to be allowed because severe circumstances are not present during erection as well as the temperature is often greater. As a result, there should never be a threat to the line.Determining the sag and tension anywhere at temperature may be done with the use of a stringing chart. This graph provides the information regarding the tension and sag limits at a specific temperature. Calculate the sag and tension upon that conductor in the worst possible conditions, such as the highest wind speed and the coldest temperature, before creating a stringing or sag chart. Assume a sufficient safety factor for determining the conductor's maximum working tension. Now assess the sag and tension throughout a wide temperature range that falls within the operating temperature range[1], [2].

Sag Template of Transmission Lines:

An estimated line profile can be created during the early design phases by surveying the planned path, as shown in Figure 1. When creating such a profile, the horizontal scale is significantly less than the vertical scale (let's say to 1/10).The supports should be positioned so that some horizontal modification is allowed without deviating from the conventional or tangent tower lengths, and this profile should fulfill the minimum clearances requirements.

To achieve the necessary clearance, sag templates that are created at the same scale as even the line profile are used. The sag template is typically created on tracing paper or celluloid. The conductivity line is represented by the higher curve I in the sag template.The lower curve I is uniformly below the middle curve (i.e., curve II) by the specified minimum vertical clearance towards the ground.

Equivalent Span of Transmission Lines:

Because the position of the towers relies on the contour of the terrain during which the transmission line is also to be built, it might not be practicable to construct a transmission line

segment with successive spans of identical length. The towers may also be compelled to be placed to provide spans of various lengths in order to minimize disruption to the usage of the land. Variations in loading or temperature will produce differential changes in tension in the various spans if the succeeding spans are of various lengths.Making sag and tension computations about each and every span separately, then making adjustments as the transmission line is being built, is exceedingly time-consuming. The conductors are stretched out via grab blocks attached towards the support arms and evenly tensioned at both ends of a segment of five or six blocks when a transmission line is being built. Insulator swing keeps the conductors' uniform tension when they are fastened to suspension insulator strings. Because the supports are flexible, equal stress is guaranteed whenever the conductors are attached to pin-type insulators.Calculating sag and tension in terms of a fictitious comparable span and applying that tension to every span in the segment of overhead wire in between the tensioning sites is frequently convenient. If an equivalent span Le is to be supplied for n spans of lengths L1, L2, L3, etc., therefore the strung length of the corresponding line must match those of the individual spans.

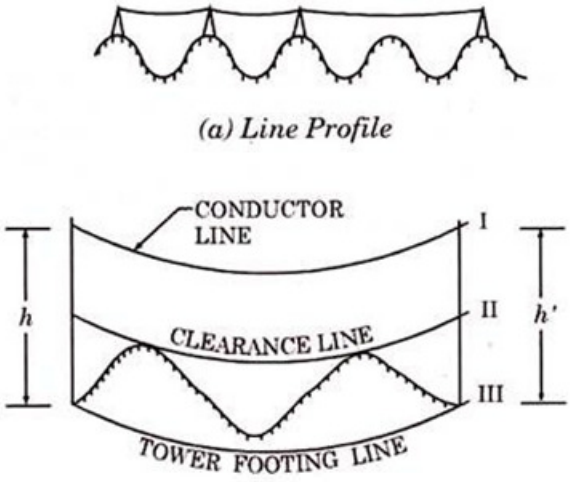

Figure 1: Illustrates the profile is constructed with the horizontal scale much more reduced (say to 1/10) in comparison to vertical scale.

Vibrations and Dampers in Transmission Lines:

In addition to the regular swinging in the wind, the overhead distribution line suffers two forms of vibrations throughout the vertical plane: aeoline vibrations, also known as resonant vibrations as well as high frequency oscillations, while galloping or dancing, also known as low frequency vibrations. Simple conductor swinging is safe as long as there is enough space between them to prevent them from coming too close to one another and sparking. High frequency (5-100 Hz) with low amplitude (20 mm to 50 mm) vibrations are referred to as aeolian vibrations. These are brought on by the vortex phenomena in low-speed (5–20 km/h) winds. The conductors of the line oscillates in various loops.The length of a loop (half-wave length) is determined by the tension T and the conductor's weight w per meter of length. Depending on T, w, and f, the length of the loop can range from 1 through 10 meters. All conductors experience these vibrations, which are rather constant.

The conductor becomes fatigued and finally breaks as a result of these detrimental vibrations at clamps or supports. When sleet storms with a high wind, low frequency vibrations (approximately one Hz) take place. The conductors are considered to "dance" because to the extremely huge amplitude, which is around 6 meters or more. Given that the "dancing" occurs both horizontally and vertically, functioning is all but impossible when the conductors are in close proximity to one another. It is believed that the event occurs as a result of the line conductor receiving an atypical sleet coating.In addition, if the principal axis of an ellipse forms an angle of 45° to the wind, the shape will experience significant aerodynamic lift (or downward push) similar to that experienced by an aerofoil. If somehow the cross-section of the coating is thought to be an ellipse, the line will suffer a drag. Due to the erratic sleet deposition, the conductors will afterwards dance both horizontally and vertically with enormous amplitude and irregularly. These vibrations are also caused by the stranding of wires. The conductor's line of travel resembles an ellipse. These (low-frequency) vibrations cannot be prevented in any way. However, using a horizontal conductor layout might lessen the threat caused by such vibrations. The conductors are shielded from resonant disturbances by dampers, which stop the vibrations before they reach the conductors near clamps or supports. The standard bridge damper is made up of two weights that are fastened to a length of stranded cable that is either 0.3 or 0.5 meters long and secured to the transmission line. The stranded cable absorbs the vibration's energy, quickly reducing the vibration. Another effective damper is made of a box carrying a weight that is supported by a spring. In this instance, the spring takes in vibrational energy. By attaching metal rods or even a length of the exact same conductors towards the main conductor just outside of the clamp, one can reinforce the conductor for a few meters on either side of a clamp to prevent fatigue.

LITERATURE REVIEW

K. Ji[3] et al.stated the maximum bending strain threshold, the tensile detachment criterion, and the shear attachment criterion are three confirmed ice failure criteria that are combined in the numerical investigation of a mechanical de-icing procedure for overhead transmission lines employing shock load. The ice shedding ratios and dynamic reactivity of overhead cables are examined in a total of 25 simulated situations. The objective is to evaluate the relative significance of the main factors that influence both the transient effects and the effectiveness of the shock-load snow clearing technique. The parameters being investigated also include line profile, the ice accumulation characteristics (equivalent thickness and eccentricity ratio), as well as the shock load characteristics (amplitude, time history, and applied position along the span) (height difference of span suspension points and adjacent spans). The investigation yields recommendations for enhancing the shock-load method's de-icing effectiveness and lowering the negative transitory impacts just on line components. A practical tool and useful reference for the design, assessment, and optimization of a range of mechanical de-icing techniques, equipment, and processes is provided by the modeling methodology employed in this work.

A. Panjaitan[4] et al.ACSR type conductors are often used in transmission lines. Because to the rising demand for electricity, efforts are being made to expand the transmission lines' capacity by maximizing the current they can carry. However, this optimization runs into issues due to the rising voltage and conductor portion. In order to build a transmission line structure that is compatible with the mechanical characteristics of the employed conductor, it is important to understand how channel flow instability affects the temperature, section, androgen angle, but also voltage of the conductor. The heat balance equation is used in this study's computation to

determine the conductor temperature. The comparable span length is calculated using the Basic Span Length technique.

T. J. Smith[5] et al. beyond 3 THz, the terahertz frequency range seems to have the promise of revolutionizing a variety of applications, including spectroscopy, imaging, and short-range wireless communication. These include chemical and biological sensors. Although silicon-based THz imagers have made great strides below 1 THz, the absence of solid-state sources throughout this frequency range has stymied technical developments beyond 3 THz. Additionally, the design space beyond 3 THz presents whole new difficulties for the electromagnetic interface and electronics. A vertical through from the top antenna layers to the detector is a dispersed element in the spectral range since the wavelength is so tiny (about 50 m at 3 THz) (transmission line or radiator). In this letter, we describe a methodical circuits-electromagnetics co-design methodology for a hybrid imaging system that consists of a 100-pixel CMOS imager that communicates with a THz quantum cascades laser frequency comb with a mode spacing of 17 GHz and a frequency range of 3.25–3.5 THz. The array chip has an average noise energy equivalent (NEP) (across pixels) of 1260 pW/Hz between 3.25 and 3.5 THz and a predicted NEP of 284 pW/Hz over the design spectrum of 2.7-2.9 THz, despite being intended for optimum performance across this frequency range. Towards the best of our knowledge, we provide the first hybrid quantum cascade laser (QCL)-CMOS demonstration of complete THz imaging. This strategy enables future works to exhibit new technical advancements for systems in the 1–10 THz range by using both QCL and CMOS technology.

According to the T. J. Smith[6] et al. beyond 3 THz, the terahertz frequency range has the promise of revolutionizing a variety of applications, including spectroscopy, imaging, and short-range wireless communication. These include chemical and biological sensors. Although silicon-based THz imagers have made great strides below 1 THz, the absence of solid-state sources in this frequency range has stymied technical developments beyond 3 THz. Additionally, the design space beyond 3 THz presents whole new difficulties for the electromagnetic interface and electronics. Given that the wavelength in this spectral region is so tiny (about 50 m at 3 THz), a vertical through connecting the top antenna layer to the detector is considered a dispersed element (transmission line or radiator). In this letter, we describe a methodical circuits-electromagnetics co-design methodology for a hybrid imaging system that consists of a 100-pixel CMOS imager that communicates with a THz quantum cascade laser frequency comb with a mode spacing of 17 GHz and a frequency range of 3.25–3.5 THz. The array chip exhibits an average noise equivalent power (NEP), while being designed for optimum functioning between 2.7 and 2.9 THz (across pixels). To the best of our knowledge, we provide the first hybrid quantum cascade laser (QCL)-CMOS demonstration of complete THz imaging. This strategy enables future works to exhibit new technical advancements for systems in the 1–10 THz range by using both QCL and CMOS technology.

S. Wood and A. Garcia[7] et al. it may take a lot of time and computing power to do pressure cycle fatigue analysis using a fracture mechanics technique, such the Paris Equation. For large crack populations (>20,000), hours or perhaps even days of calculation time are needed to do a fatigue evaluation on an ILI data set, depending on the resolution and breadth of your pressure spectrum (usually 5psi and 3 months). Pipeline Operators won't compromise accuracy, thus they won't choose the Miners rule's more straightforward S-N-based fatigue relations. By handling the bottleneck step cycle-by-cycle integration via the rain flow counted pressure series to appropriately define the incremental crack progress and stress intensity factor just at crack tip the

Equivalent Load technique overcomes the efficiency problem of the Paris Equation. By recognizing that the loading parameters driving crack progression for one fault may be coupled to another using correction factors that take into account variations in cycle stress, the process can be made simpler. Additionally, keeping the fracture length constant enables accurate numerical approaches for computing the crack depth integral. This shows to be quicker than a cycle-by-cycle method while still producing equivalent outcomes. In this work, the validation research and the calculation of the Equivalent Load correction factors were covered. The error as compared to the cycle-by-cycle integration provided in BS7910 Annex M is also covered. Seven crack the validation research included in-line inspection sets of data from several liquid transmission pipes with a range in age, diameter, and history cycle intensity. With an average variance of 2% from BS7910, the Equivalent Loading Method yields equal remaining life, but in a much less amount of time.

Y. Xie[8] et al. the on-line powering of high voltage transmission lines is extremely promising since tapping electricity from the segmented ground wire of an overhead transmission line offers special benefits like ease of technical implementation and broad application scope. The only things that make this technique feasible are that its tapping power is often low and that it is vulnerable to lightning strikes. First, this same equivalent calculation circuit for power tapping has been proposed based on vortex appointment through the theoretical analysis for electromagnetic induction of the ground wire of typical lines, followed by the Thevenini's equivalent circuit specifications of the commensurate power-tapping port are deduced. In the meanwhile, the impacts of real line characteristics like the span and distribution of tower-footing resistance were examined. And with this information, the necessary power might be easily produced by choosing the right parameters and matching the impedance. Second, using the EMTP-ATP modeling tool, the impact of lightning strikes and methods of protection against them were examined. Finally, field tests for power-tapping power and other parameters were carried out at a 500kV line. Results demonstrate the accuracy of the theoretical calculations and analyses for power tapping. Additionally, the power-tapping tool poses less of a risk to line insulation.

S. Zhao[9] et al. stated Sutong long-span electrical transmission line under consideration is the tallest tower-line system to date with the largest span, making wind load its primary influencing factor. The aero elastic model may be tested in a wind tunnel, which is an efficient technique to learn more about these coupled vibration events caused by the wind. While the construction of both the aero elastic model had to relax the standards for the Froude number for transmission towers owing to the limitations of wind tunnel circumstances and model materials, Davenport's equivalent line model design approach was utilized instead. However, this may result in a mismatch between the tower-line system's reaction and a difference between the aerodynamic damping and mass resemblance ratios. By calculating the exact aerodynamic force similarity ratios of a transmission line modeling, applying other techniques, and increasing overall stiffness matrix despite maintaining the sag of the transmission line framework, the aero elastic model of the transmission tower-line system was created. The developed model was placed in a wind field with the proper calibration, and finite element analysis was employed to determine the impact of gradient wind. Furthermore, a transmission tower model either with or without wires was examined for its reactions to wind-induced motion. It was made clear how the transmission tower and line are coupled with regard to displacement, frequency, damping, and other factors. The results of the tests reveal that the transmission tower's displacement response is at its highest

whenever the angle of inclination is 30 degrees; the coupling here between transmission system and the line alters the dynamic characteristics as well as the transmission tower's wind-induced response component; and indeed, the transmission system and conductors are also both aerodynamically reliable underneath the test wind speed.

C. Liu[10] et al. have introduced the inductors are often employed within PCB electronic systems that frequently serve as radiators for those other analog components. However, since the real physical model for inductors is not accessible due to commercial secrecy, it is challenging to do pre-simulation to anticipate the coupling. With Huygens' equivalent model, the inductor is rebuilt in this research in order to calculate the near-field coupling within analog circuit design. To verify the effectiveness of the equivalent technique, the transmission scattering characteristic S21 of three examples is calculated: 1 nH to a microstrip line, 3.3 uH to a microstrip line, and 3.3 uH to the a WiFi antenna. Inside the frequency range, there are 6 dB differences between the test results and the simulation of Huygens' equivalent model. The practicality offers a potential method for estimating the isolation of the whole channels, such as the inductors, as well as coupling from the transmitting towards the receiving impedance matching channels, the buck converters to the antenna, etc.

O. J. Lynch[11] has although the use of so-called "wood equivalent" steel poles is particularly discouraged by ASCE Standard 48, Development of Steel Transmission Pole Structures, this same practice of building a transmission line using wood poles and then replacing them one for one with pre-engineered steel poles persists. This not only has the potential to lead to an inaccurate design but also is probably not the most cost-effective design. There might be significant cost differences between various classes and lengths of steel or wood poles, leading to vastly different optimum designs. Frequently, a cost-effective wood pole line will produce smaller poles having shorter spans, while a cost-effective steel pole line would produce higher poles with longer spans. This essay will examine three possibilities for a transmission line's optimal design. The transmission line will be first designed with wood poles, then those wood poles are exchanged one by one with steel poles that are "wood comparable," and eventually the transmission line was designed with steel poles. The optimization and economic study utilized actual wood and steel pole utility costs. A life-cycle cost analysis (LCCA), which considers the long-term costs related to the design, fabrication, operation, maintenance, and retirement phases along with a discussion here on resiliency of each design, will be presented in addition to evaluating the implemented costs of each option and also in accordance with ASCE Policy Statement 451.

DISCUSSION

The transmission line may get worn out and eventually fail as a result of Aeolian vibrations. These are the most frequent vibrations seen in transmission lines, and they are brought on by vortex shedding brought on by laminar wind flow. The frequency of the low amplitude vibrations range from 3 to 150 Hz. The conductor cable eventually fails as a result of the vibrations, which are felt in the vertical direction. Aeolian vibrations were the cause of the transmission line's catastrophic breakdown between Cowal Junction and Longwood downtown London. Aeolian vibrations were blamed for a number of further recent events in Ontario and Manitoba. This problem is addressed in their work on cabling vibration suppression. One of the most often utilized dampers for reducing Aeolian vibrations is indeed the Stockbridge damper. Two counter weights are linked by the messenger cable to make up the traditional damper. And

used an aluminum clamp, this assembly is suspended from the conductor cable. Only when the damper's inherent frequencies are set to include the Strouhal frequency range is energy absorption feasible. Because the counter weights across both sides are symmetric, the basic Stockbridge damper created by George H. Stockbridge around 1925 is also known as a 2R damper because it has two resonant frequencies inside the Strouhal frequency range. The contemporary asymmetric Stockbridge damper, also known as the 4R damper, has four resonant frequencies and uneven counterweights. An asymetric Stockbridge damper that is offered for sale. Both the length of a messenger cable on the two sides and the counter weights are uneven. Effectiveness of the Stockbridge damper is one of the main issues while developing new transmission lines. The demand for improved dampers is expanding, and design advancements have drawn a lot of attention. The number of resonant frequencies—natural frequencies lying within the range of the complete Strouhal frequency spectrum—of the Stockbridge damper may be increased, leading to a considerable performance gain, by tuning its counterweights, length, but also cross-section of a messenger cable.

Asymmetric Stockbridge dampers have been the subject of several writers' mathematical development. The most recent of these was created by, in which the authors gave exact equations for the frequency equation with mode forms of an asymmetric Stockbridge damper. The method of empirically deriving the frequency response from of the impedance curves is one that is often used by researchers. The fundamental approach and the direct way of testing are both highlighted in the technical preparatory considerations. The fundamental technique involves attaching the Stockbridge damper to a test span of the cable and measuring the energy loss caused by the damper. The Stockbridge damper is immediately installed on an electrodynamic shaker in the direct technique, in contrast, and only vertical excitation is employed to establish the resonant frequencies. The fundamental approach is preferred for a system-wide examination, according to the sources (cable and damper). Technical and financial factors make the direct technique the preferable option above the basic method. In the studies, a frequency sweep between 2.5 and 35 Hz was utilized with a constant displacement approximately 1 mm peak to peak. With a consistent peak to peak movement of 2.7 mm, in also performed trials comparable to this. Nevertheless, the measurement guidelines, as stated in the criteria and tests for Stockbridge model Aeolian vibration dampers, advise testing any Stockbridge damper at the constant velocity.

Vibration damper

In Figure 2 displays a full-scale, solid model of a vibration damper. There will be a substantial mathematical model for the whole vibration damper. A half-model of the vibration damper was employed in the calculation to make it simpler. The schematic for the vibration damper's half-model is shown in Fig. 3. The O1, O2, and O3 coordinate systems are employed. The system is modeled as having three beams and three masses. The clamp's initial coordinate system, O1, has mass M1 at its opposite end. The masses M2 and M3 are located at the extreme extremities of the third and second coordinates systems, which are located on each side of the mass M1. While masses M2 and M3 are thought to be point masses, mass M1 is thought to rotate along an axis parallel to the length of a messenger wire. In the first, second, and third coordinate systems, correspondingly, W1, W2 and W3 indicate the vibration displacement along of the j coordinate.

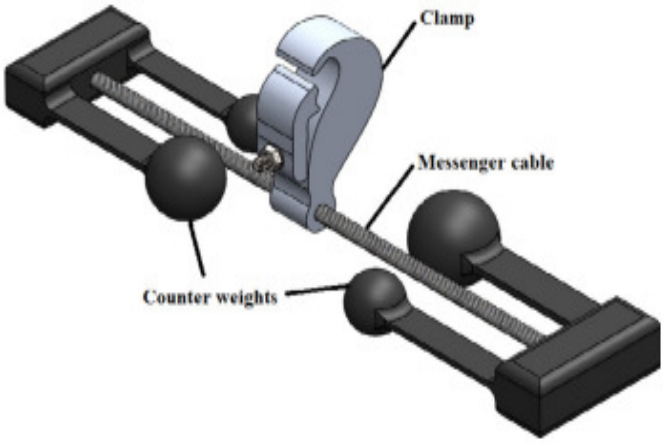

Figure 2: Illustrates a full-scale solid model of the vibration damper.

The kinetic and potential energy of the system are given by Eqs. (1) and (2), respectively,

$$T = \frac{1}{2}m_1\int_0^{L_1}\dot{W}_1^{\,2}(x_1,t)dx + \frac{1}{2}M_1\dot{W}_1^{\,2}(L_1,t) + \frac{1}{2}J\dot{W}_1^{\,\prime 2}(L_1,t) + \frac{1}{2}m_2\int_0^{L_2}\dot{W}_2^{\,2}(x_2,t)dx + \frac{1}{2}M_2\dot{W}_2^{\,2}(L_2,t) + \frac{1}{2}m_3\int_0^{L_3}\dot{W}_3^{\,2}(x_3,t)dx + \frac{1}{2}M_3\dot{W}_3^{\,2}(L_3,t)$$

$$V = \frac{1}{2}EI_1\int_0^{L_1}W_1^{\prime 2}(x_1,t)dx + \frac{1}{2}EI_2\int_0^{L_2}W_2^{\prime 2}(x_2,t)dx + \frac{1}{2}EI_3\int_0^{L_3}W_3^{\prime 2}(x_3,t)dx$$

Differentiation with regard to x is represented using primes in the equations above, while differentiation without with respect to time was represented by dots. E is the Youngs modulus, while I I 1, 2 and I3 are the messenger cable's and the beams' respective area moments of inertia. J is indeed the mass M1's rotational inertia, L1 seems to be the cable's length, and m1 is its mass in terms of its length. The lengths of a beams are L L 2 3 and their relative masses per unit length were m m2 3. The system's equations of motion are derived using Hamilton's principle as,

$$EI_1W_1^{IV} + m_1\ddot{W}_1 = 0$$

$$EI_2W_2^{IV} + m_2\ddot{W}_2 = 0$$

$$EI_3W_3^{IV} + m_3\ddot{W}_3 = 0$$

Stockbridge damper

Due to its dependence on the driving frequency and conductor vibration amplitude there at site of the damper clamp, this same Stockbridge damper is frequently believed to be nonlinear. An analogous viscous damping may be used to mimic the damper's nonlinearity. Based on empirical data, this equivalent damping coefficient is determined as,

$$c_d = \frac{E_d \omega}{\pi V_c^2}$$

where

$$E_d = \frac{P_d}{f} \text{ and } P_d = \frac{1}{2} F V_c \cos \phi_{FV}$$

It is the frequency of the circle in rad/s. f is the excited frequency in Hz, F is the force sent to the shaker either by damper, Vc is indeed the measured velocity there at clamp, while FV is the phase angle between both the force and the velocity. Ed and Pd are indeed the energy but also power wasted by the damper during a full cycle, respectively. The force delivered to the shaker by the dampers, the clamp's velocity, as well as the phase difference between the force and the velocity are all measured using the forced response technique. The experimental setup and methodology were carried out in accordance with IEEE Standard 664.25. The experimental set-schematic up's an electrodynamic shaker supported the Stockbridge damper. An accelerometer (B&K 4382) was positioned at the clamp to measure the damper's velocity, as well as a load cell was inserted between both the shaker and the fixture to quantify the delivered force. The Stockbridge damper has the following features: The mass per unit length was mm 14 0.25 kg/m, and the flexural rigidity was Em Im 14 31.8 Nm2. The right and left caster wheel each weigh 3.4 kg and 1.46 kg, respectively. The messenger's lengths are LL1/4 0.22 m and LR1/4 0.3 m, respectively. At a steady speed of 100 mm/s, the Stockbridge damper was aroused in the sweep range of wind-induced vibration. Given that now the shaker really wasn't usable at frequencies below 10 Hz, the frequency range were limited to frequencies higher than 10 Hz. Through charge amplifier, a dynamic signal analyzer (PCI-6034E) was linked to both the load cell as well as the accelerometer. Values for the shaker input force, clamp velocity, but also phase angle between both the force and the velocity was collected for every tested frequency. Equation uses the observed frequency, force, plus velocity just at clamp to calculate the Stockbridge damper's equivalent damping ratio. Cd versus the observed frequencies shown. It shows that after reaching a particular peak, the comparable viscous dampening diminishes. It should be observed that the Stockbridge damper's resonant frequencies correlate to the frequencies corresponding to all these peaks.

CONCLUSION

The vibration damper gets represented mathematically, and the numerical model is used to confirm the analytical model's findings. Using a computational model and measurements, the resonance frequency of the asymmetric damper are determined. With the new design, the data clearly reveal a rise in resonant frequencies, which indicates better damping performance than that of the traditional Stockbridge damper. To produce improved damping and resonance capabilities, the geometrical features of the innovative vibration damper may be fine-tuned further. The authors believe that in order to account again for messenger cable's reliance on frequency and vibrations amplitude, future study will concentrate on modeling it using nonlinear curved beam theory.

References:

[1] N. A. Salim, H. Mohamad, Z. M. Yasin, N. F. A. Aziz, and N. A. Rahmat, “Graphical user interface based model for transmission line performance implementation in power

system," *Indones. J. Electr. Eng. Comput. Sci.*, 2019, doi: 10.11591/ijeecs.v16.i1.pp92-100.

[2] O. Menéndez, M. Pérez, and F. Auat Cheein, "Visual-Based Positioning of Aerial Maintenance Platforms on Overhead Transmission Lines," *Appl. Sci.*, vol. 9, no. 1, p. 165, Jan. 2019, doi: 10.3390/app9010165.

[3] K. Ji, B. Liu, Y. Cheng, X. Zhan, and G. McClure, "Evaluation and optimization of a shock load de-icing method for transmission lines with combined ice failure criteria," *Cold Reg. Sci. Technol.*, 2019, doi: 10.1016/j.coldregions.2019.102818.

[4] A. Panjaitan, Usman, and B. Suherman, "A Design of Analysis Influence of Channel Flow Instability Against Andongan on SUTT 150 Kv," in *Journal of Physics: Conference Series*, 2019. doi: 10.1088/1742-6596/1361/1/012045.

[5] T. J. Smith, A. Broome, D. Stanley, J. Westberg, G. Wysocki, and K. Sengupta, "A hybrid THz imaging system with a 100-Pixel CMOS Imager and a 3.25-3.50 THz quantum cascade laser frequency comb," *IEEE Solid-State Circuits Lett.*, 2019, doi: 10.1109/LSSC.2019.2933332.

[6] T. J. Smith, A. Broome, D. Stanley, J. Westberg, G. Wysocki, and K. Sengupta, "A Hybrid THz Imaging System with a 100-Pixel CMOS Imager and a 3.25-3.50 THz Quantum Cascade Laser Frequency Comb," in *ESSCIRC 2019 - IEEE 45th European Solid State Circuits Conference*, 2019. doi: 10.1109/ESSCIRC.2019.8902823.

[7] S. Wood and A. Garcia, "Equivalent load fatigue: An efficient modification to the familiar Paris equation," in *PPIM 2019 - 31st Pipeline Pigging and Integrity Management Proceedings*, 2019.

[8] Y. Xie, X. Jiang, J. Hu, Z. Zhang, S. Fan, and C. Fan, "Study on Power-tapping From Segmented Insulation Ground Wire of Typical Overhead Transmission Line," *Zhongguo Dianji Gongcheng Xuebao/Proceedings Chinese Soc. Electr. Eng.*, 2018, doi: 10.13334/j.0258-8013.pcsee.161783.

[9] S. Zhao, Z. Yan, Z. Li, J. Dong, and Y. Zhong, "Investigation on Wind Tunnel Tests of an Aeroelastic Model of 1000 kV Sutong Long Span Transmission Tower-line System," *Zhongguo Dianji Gongcheng Xuebao/Proceedings Chinese Soc. Electr. Eng.*, 2018, doi: 10.13334/j.0258-8013.pcsee.171688.

[10] C. Liu, G. Zhang, and X. Yu, "Inductor modeling with Huygens's equivalent model to estimate coupling noise," in *2018 IEEE International Symposium on Electromagnetic Compatibility and 2018 IEEE Asia-Pacific Symposium on Electromagnetic Compatibility, EMC/APEMC 2018*, 2018. doi: 10.1109/ISEMC.2018.8393742.

[11] O. J. Lynch, "Wood v. Steel: Dawn of justice," in *Electrical Transmission and Substation Structures 2018: Dedicated to Strengthening our Critical Infrastructure - Proceedings of the 2018 Electrical Transmission and Substation Structures Conference*, 2018. doi: 10.1061/9780784481837.033.

CHAPTER 17

ANALYSIS ON THE ELECTRICAL POWER SYSTEM PROTECTION

Mr. Harsh Shrivastava, Assistant Professor,
Department of Electrical Engineering, Jaipur National University, Jaipur, India,
Email Id-ershrivastava@jnujaipur.ac.in

Abstract:

Power system protection aims to separate a malfunctioning component of the electrical power system from of the remaining live system so that the remaining portion may continue to operate as intended without suffering serious harm from fault current. In this chapter author is discusses functional requirement of protection relay and important components for protecting power system.

Keywords:

Power System Protection, Relay, Transformer, Transmission Line.

Introduction

Almost everything connected to the protection system in the power system is covered in this section of our website, including standard lead and device numbers, terminal strip connection methods, multi-core cable color codes, and execution-related dos and don'ts. It also covers the fundamentals of numerous power system protection systems, including unique ones like differential relays, limited earth fault protection, directional relays, and distance relays, among others. Details on the protection of transformers, generators, transmission lines, and capacitor banks are also provided. It nearly entirely addresses power system protection. Switchgear testing, instrument transformer testing, including testing of current transformers and voltage or potential transformers, as well as testing of related protective relays, are all thoroughly detailed. There may be hundreds of pieces of equipment in a typical industrial power network, and additional protection relays are needed to safeguard the system. The protection system comprises of a variety of relays with varied operating theories to address various fault kinds. Depending on the voltage level and significance, it is often necessary to use two or more relays with various working principles to safeguard the machinery. Coordination is required between each protection relay in the power system and the relays guarding nearby equipment. Thus, coordination of the total protection is quite difficult. Unfortunately, it is almost hard to find a protection setting that can guarantee the coordination between all nearby relays in a real industrial power network. In reality, there are a few coordination blind spots that affect how well the power system is protected. According to their kind, such as overcurrent but also distance protection, protection relays are categorized in the conventional way of coordination for protection, and each type is coordinated separately. Coordination's impact on other protective mechanisms is often overlooked. Work has been done on relay setup coordination for various relay kinds.

Power system protection aims to separate a malfunctioning component of the power system's electrical supply from the remaining live system so that the remaining portion may continue to operate as intended without suffering serious harm from fault current. The circuit breaker really divides the malfunctioning system from the rest of the functioning system, and it immediately opens in the event of a problem thanks to the trip signal it receives from the protective relays.

The basic protection tenet is that no power system prevention can stop fault current from passing through the system; it's only able to stop fault current from traveling further by swiftly cutting off the short circuit route from either the system. The following functional criteria for protection relays should indeed be met in order to achieve this rapid disconnect in Figure 1.

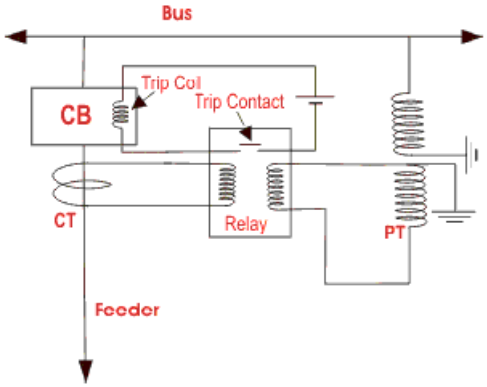

Figure 1: Illustrates the basic connection diagram of protection relay.

LITERATURE REVIEW

Liliana, N. Jalinus[1] et al. purpose of that study is to evaluate how well students learned about electric power system protection after using the research-based learning approach. To meet present and future learning demands, the learning paradigm should be modified. Achieving student learning abilities in each topic, one of which is impacted by the chosen learning methodology. The Research Based Learning model is one of the learning paradigms emerging nowadays that helps students improve their capacity for acquiring academic information. This strategy incorporates research into learning by focusing on students as a learning resource (SCL). A paradigm for research-based learning has been established and is being used in this study. This model has nine steps that are used while teaching about electric power system protection. An improvement in student learning outcomes is assessed in the assessment of effectiveness via formative assessments and summative evaluation after utilizing the research-based learning model in learning.

H. H. Alhelou[2] et al. have Power systems are among the most intricate systems that play a crucial role in contemporary living. They directly affect modernization, as well as the economic, political, and social aspects. There are a number of control and protection approaches needed to run such systems in a stable state. Despite the fact that contemporary systems are outfitted with a number of protective measures intended to prevent unforeseen occurrences and power outages, power systems continue to experience emergencies and malfunctions. The system as a whole or at least a significant portion is at risk during the most serious crises. A blackout might occur if the incident is poorly handled and the electricity system experiences cascade failures. Many nations have research and expert teams that seek to prevent blackouts on their systems because to the repercussions. This report provides a thorough overview of the significant blackouts and cascade incidents that have happened during the last ten years. Given that the US is one of the world's top power producers and since data on previous incidents is readily available, special attention is paid to power system failures in the US and their causes. The report also identifies the underlying factors that contribute to various global blackouts. The effects of blackouts are also examined, as well as blackout and cascading analysis techniques. Additionally, the

shortcomings of the current safety measures and the unresolved research questions on power system blackouts and cascade occurrences are highlighted. Also suggested are future research objectives and concerns for power system blackout investigations.

N. M. Moyo[3] et al. stated the electrical defects or disturbances may have a negative impact on traction power systems. These might disrupt the trains' power supply, impact system performance, and result in significant delays. In order to make decisions that will lead to reduced outage times, precision in fault reporting and problem localization is crucial. To increase system dependability and lower outages and associated costs, traction power failsafe mechanism assessment and analysis has become essential. Because impedance relays are used in protection systems, line impedance measurements are an essential component of fault investigation and distance location. The accuracy of distance protection switches may be increased by undertaking impedance measurements, as shown in this research. Impedance measurements were performed in this study, and the obtained findings were contrasted with the predicted values. The impedance calculations and analyses employed the measurements of the feeder with earth, catenary to earth, and feeder to catenary. All line sections' earth immunities were also measured. A traction power system's protection parameters optimization specifically used the line impedance readings for the computation of the compensation for the earth return factor. The precision of the protective settings has benefitted from this. As a consequence, the protection configuration parameters were altered.

H. S. E. Barkat and B. Mahdad[4] proposed and performs an experimental platform based on an Arduino microcontroller and GSM card for power system protection education. The experimentation was divided into three sections: The purpose of the first section is to show how the Arduino board may be modified and used to measure several electrical characteristics, including voltage, active power, current, and power factor. The focus of the second section is on customizing the Arduino board and utilizing it to show how primary and secondary protections should work together. While the third section attempts to remotely operate a contactor delivering a load in order to imitate the fundamental operation of the SCADA system. A GSM card connected to an Arduino board is used to perform this duty, making it possible to remotely manage the contactor's opening and shutting as well as to identify the defect in the load by sending a message.

S. Chandra Shekar[5] et al. Micro-grids comprise Distributed Energy Resources (DER’s) with low voltage distribution networks having controllable loads those can operate with different voltage levels are connected to the micro-grid and operated in grid mode or islanding mode in a coordinated way of control. DER’s provides clear environment-economic benefits for society and consumer utilities. But their development poses great technical challenges mainly protection of main and micro grid. Protection scheme must have to respond to both the main grid and micro-grid faults. If the fault is occurring on main grid, the response must isolate the DER’s from the main grid rapidly to protect the system loads. If the fault occurs within the micro-grid, the protection scheme must coordinate and isolates the least priority possible part of the grid to eliminate the fault. In order to deal with the bidirectional energy flow due to large numbers of micro sources new protection schemes are required. The system is simulated using MATLAB Wavelet Tool box and Wavelet based Multi-resolution Analysis is considered. Wavelet based Multi-resolution Analysis is used for detection, discrimination and location of faults on transmission network. This paper is discussed a transient current based micro-grid connected power system protection scheme using Wavelet Approach described on wavelet detailed-

coefficients of Mother Biorthogonal 1.5 wavelet. The proposed algorithm is tested in micro-grid connected power systems environment and proved for the detection, discrimination and location of faults which is almost independent of fault impedance, fault inception angle (FIA) and fault distance of feeder line.

N. Bayati[6] et al. in the recent years, using distributed generations (DGs) has increased in order to compensate the load and consumption growth. Although connecting DG resources to power system has many advantages, it might cause some protective problems such as mis-coordination between network protection devices, due to the changing in the short circuit level of power system. In this paper, two methods for restoring the coordination of relays in the presence of DGs by using FCLs are proposed. In both methods, different criteria, such as considering the variation of network topology, optimizing the value and number of FCLs are considered to propose a comprehensive and adaptive protection method. In the first method, an adaptive protection scheme by using FCLs is proposed to active and deactivate FCLs in different topologies to restore the coordination of relays. In addition, the second method proposes a robust method which considers all possible situations and topologies of the power system to maintain the coordination of power system during fault. Finally, the proposed robust and adaptive protection scheme has been compared in terms of cost, the operation time of relays and computation time, and based on the aims of operators in a power system one of these method can be implemented, The proposed methods are implemented on IEEE 14-bus standard network, and all possible topologies of the mentioned network are considered. Simulation results show that the proposed method can maintain the coordination of overcurrent relay protection in the presence of DGs and topology changes. In other words, the proposed method is robust against topologies changes.

T. S. S. Senarathna and K. T. M. Udayanga Hemapala[7] micro-grids are made up of Distributed Energy Resources (DERs) that are linked to low-voltage distribution networks with controlled loads that may run at various voltage levels. These loads can be operated either grid mode or islanding mode under coordinated control. DERs provide society and consumer utilities certain economic and environmental advantages. However, the key technological issue in their creation is the preservation of the main and micro grid. Both failures on the main grid and those on the micro-grid must be addressed by the protection system. To safeguard the system loads if the failure affects the main grid, the reaction must quickly separate the DERs from the power network. If the fault occurs inside the micro-grid, the protection strategy must coordinate and isolate the grid's component with the lowest priority in order to fix the issue. New protection mechanisms are needed to handle the bidirectional energy transfer caused by a high number of micro sources. MATLAB Wavelet Toolbox is used to model the system, and wavelet-based multi-resolution analysis is taken into account. Wavelet-based multi-resolution analysis was used to determine, classify, and locate transmission network defects. In this research, a wavelet-based transient current protection technique for micro-grid-connected power systems is addressed. It is based on Mother Biorthogonal 1.5 wavelet detailed coefficients. The suggested method is evaluated in a micro-grid linked power systems environment and shown to be effective for fault detection, discrimination, and localization that is mostly unaffected by fault impedance, fault inception angle (FIA), but also fault proximity of feeder line.

Liliana[8] et al. utilizing distributed generators (DGs) has risen recently in order to offset the rise in load and consumption. Although there are numerous benefits to linking DG resources to the power system, there may also be some safety issues, such as network protection device mis-

coordinations, as a result of the power system's fluctuating short circuit level. In this study, two methods for leveraging FCLs to restore relay coordination in the presence of DGs are suggested. In both approaches, several factors are taken into account to provide a thorough and flexible protection strategy, including maximizing the value and quantity of FCLs and taking network topology variance into account. In the first way, an FCL-based adaptive protection mechanism is suggested to activate but also deactivate FCLs in various topologies in order to restore relay coordination. In order to sustain the coordination of the power system during faults, the second technique also suggests a resilient strategy that takes into account all potential circumstances and topologies of the power system. Finally, depending on the objectives of operators in a power system, one of these methods may be applied. The suggested robust and adaptive protective strategy has been compared in regards to the cost, the operating time of relays, and computing time. All conceivable network topologies for the IEEE 14-bus standard network, on which the suggested solutions are implemented, are taken into account. Based on the findings of the simulation, it can be concluded that the suggested solution can continue to coordinate overcurrent relay protection inside the presence of DGs and topology changes. In those other words, the suggested technique is resilient to changes in topologies.

K. P. Schneider[9] et al. over the last 10 years, microgrids have drawn a lot of attention and developed into a crucial tool for the energy sector. One of the key factors contributing to the popularity of microgrids is their capacity to incorporate sustainable energy generating techniques into the distribution network. The microgrid is sustainable in both grid-connected and islanded modes while lowering power losses thanks to a range of Distributed Generating (DG), including energy storage, solar generation, and wind and other micro-turbine generation. To fully use the capabilities of microgrids, a number of technological obstacles must be overcome, and protection is just one of them. The introduction of various solutions was sparked by the advancement of defense methods. Adaptive protection is one of the most promising methods for microgrid security. This article provides a thorough analysis of the pros and weaknesses of several applicability variations for adaptive protection of microgrids. Additionally, it examines cutting-edge studies that use computational intelligence to accomplish adaptive defense. With a more adaptable and trustworthy system that will be used internationally, these solutions are about to completely redefine protection solutions.

According to R. Bansal[10] learning model should indeed be modified to meet both the present and future learning requirements. The learning paradigm that is used affects how well students learn in each competence course. Research-based learning (RBL) is one of the instructional strategies that helps students improve their capacity for grasping the subject matter. In this strategy, the students serve as learning resources that incorporate research into the classroom. The purpose of this study is to evaluate how well students learn in courses on electrical power system protection using the RBL model. In order to protect the electrical power system, this study uses the nine-step RBL model, which entails identifying a research topic, goals, and research question as well as research procedures used to collect and intervention, applying theory, research methodology but also design, data processing, results and discussion, and making recommendations for strengthening the research. After using the RBL methodology, there was an improvement in the quantifiable student learning outcomes used to gauge the efficiency of both formative and summative assessments.

J. de Jesús Jaramillo Serna and J. M. López-Lezama[11] the deployment of intelligent systems and equipment that are owned by utilities and non-utility (customer-owned) entities is growing

throughout the globe's electric distribution networks. Distribution automation, microgrids, and self-healing systems are recent utility-owned asset deployments. Solar photovoltaic power, behind-the-meter energy storage devices, and electric cars are examples of non-utility-owned assets. Although these installations provide potential data and management points, the centralized control structures that are now in place lack the adaptability and scalability needed to include the growing number and diversity of devices. These innovative gadgets and systems are unable to be used as active resources due to the communication bandwidth, latency, and scalability of the centralized control architecture. This study provides a standards-based architecture for the decentralized power system management that, by integrating centralized and distributed control systems, enhances operational flexibility. Utilizing a distributed design, the system actively engages both utility and non-utility assets to boost dependability during routine operations and resilience during severe events. Results from laboratory investigations and early field deployments are described, together with information on a current full-scale installation at Duke Energy.

B. Tetteh and K. Awodele[12] stated the smart grids assist in the generation, transmitting, substations, distribution, and consumption of electricity to accomplish a system that really is clean, safe (protected), safeguard, reliable, effective, and sustainable. As distributed generation interconnected transmission power flow becomes bidirectional, it results in network problems. This publication utilizes DIG silent Power Factory to demonstrate the usage of relay technology, instrument transformers, fuses, electrical systems, and transmission line protection configuration. Senior undergraduate and postgraduate students, in addition to researchers studying electrical engineering's fields of power systems, distribution and transmission especially protection systems, are the intended audience.

DISCUSSION

Functional Requirements of Protection Relay

Reliability

Reliability is the most crucial need for a protective relay. They are inactive for a long period before a defect appears, but when one does, the relays must react quickly and accurately.

Selectivity

Only those circumstances, for which relays inside the electrical power system are commissioned, may be used to activate the relay. Protection relays must be able to identify the suitable condition for which they would be operated since there may be certain common fault conditions under which some relays should not be run or operated after a specific amount of time.

Sensitivity

Relaying equipment has to be sensitive enough to function properly when the level of a fault state barely reaches a set threshold.

Speed

The necessary speed must be maintained by the protective relays. The numerous power system protection relays must be properly coordinated so that a problem at one part of the system won't disrupt another healthy part of the system. Given that they are electrically linked, a portion of the

healthy section may experience fault current flow; however, because of this, the healthy portion's relays really shouldn't function any quicker than the faulty portion's relays to prevent an unintended disruption of the healthy system. Once again, if a relay connected to the problematic part of the system is not operated in a timely manner owing to a flaw in it or for any other cause, the fault must be isolated by first operating the relay connected to the healthy part of the system. Therefore, it should neither also be sluggish, which may harm the equipment, nor too rapid, which could cause undesirable functioning.

Important Components for Protecting Power Systems

Bulk oil circuit breakers, minimum oil circuit breakers, SF6 circuit breakers, air blast circuit breakers, and vacuum circuit breakers are the basic components of switchgear. The circuit breaker uses a variety of functioning mechanisms, including solenoids, springs, pneumatics, hydraulics, etc. The essential component of the electricity system's protection mechanism, the circuit breaker immediately isolates the malfunctioning element of the system by opening its connections. Protective Gear consists primarily of relays for power system protection, such as current, voltage, dielectric loss, power, and frequency relays, as well as relays based on the operating parameters, such as definite time, inverse time, and stepped relays, and relays based on specific operating characteristics, such as differential and over fluxing relays. The connected circuit breaker receives a trip signal from the protection relay throughout a fault, causing it to open its connections.

Battery Station

The electrical power system's circuit breakers all seem to be DC (Direct Current) operated. Due to the fact that DC power may be stored in batteries, in the event that there is a complete loss of incoming power, it is still possible to activate the circuit breakers in order to rectify the problem. As a result, the battery is yet another crucial component of the power system. It is often referred to simply as the electrical substation's heart. When there is an AC supply available, an electrical substation battery and essentially a station battery with many cells stores energy. When relays are operating, the battery discharges, tripping the appropriate circuit breaker when the incoming AC power fails.

Gautrain Power Supply System

The national power supplier Eskom provides 88 kV AC, 50 Hz to the Gautrain System, which then steps it down to 50 kV (2 25 kV) AC using four 40 MVA traction transformers. Approximately two phases are linked to each transformer in the three-phase network that supplies the 88 kV AC power, as seen in Figure 1. Redundancy is ensured for the high voltage main power supply by using two distinct Eskom feeds, each of which has adequate capacity to power the full Gautrain network. The Eskom feeders were linked at two distinct substations, each of which has a different kind of power source.

It is a streamlined version of the power supply and distribution (PS&D) system for the Gautrain. The arrangement of the 88 kV: 50 kV (2 x 25 kV) transformers and their connections for feeding the track towards the south and north of the MPS are shown in the diagram. There is a neutral portion outside the MPS upon that OHW to divide the various stages whenever the trains go from the north to the southeast of a MPS and vice versa. In other systems, this is characterized as a phase split. The connections between the catenary, feeder, and OHW as well as the connections

between the autotransformer's neutral as well as the traction transformers' neutral and the traction return circuitry are shown in Figure 1. Out of a maximum of five APS, one is highlighted for simplicity. The smallest APS has one autotransformer, while the largest APS has three autotransformers. There are two APS in the south with three APS in the north. All APSs work identically, but power flow related load flow computations and simulations are used to determine their size and position in relation to the MPS and in relation to other APSs. The shortest and furthest distances between the substations in this instance are 5.14 km and 17.98 km, respectively. Two of the MPS's four transformers power the lines going north to Pretoria, while the other two provide the lines going south to OR Tambo Airport and Park station in Johannesburg.

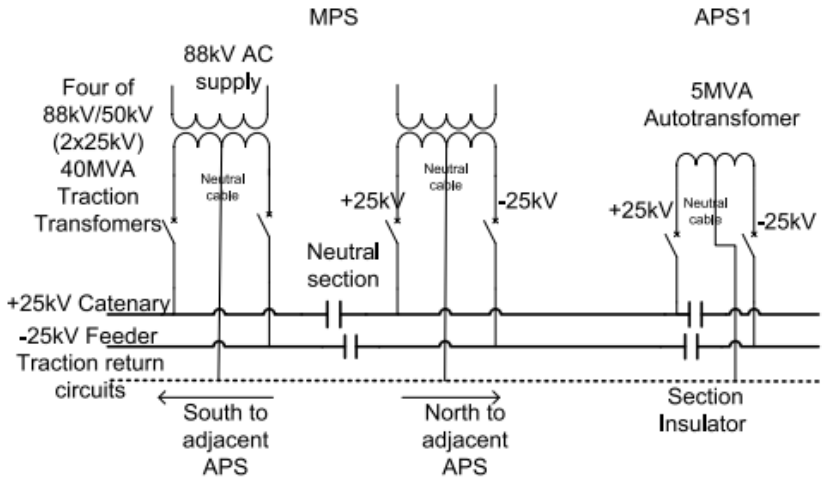

Figure 1: Illustrates the Simplified Gautrain power supply.

One transformer is always in operation in each direction, with the backup transformer being utilized if necessary. In the event that one of the transformers malfunctions or has to be turned off for repair, this design provides an n-1 redundancy within every direction north and south of the MPS. The setup also increases flexibility such that the whole network may be powered by a single transformer that is underutilized and has its neutral section closed. The ability to supply the whole system through either of the two Eskom HV feeds by shutting the bus-section that separates them affords flexibility. The common neutral bus bar, which would be earthed to the MPS ground/earth grid but also linked to the rail and aerial earth components of the OHW, receives power from the neutral terminal mostly on secondary side of each MPS transformer. Similarly to the APS, the earth grid, the rail, and the aerial earth underground cables of an OHW are all linked to a single neutral bus bar via which the neutral terminals of an autotransformers are likewise connected. Figure 2 depicts the OHW configuration. Two conductors (2 25 kV) carrying the 25 kV AC are delivered to the OHW to be used by the trains. Catenary/contact conductors, feeder underground cables, and the earth wire make up the OHW. The rail rails, the AEC, and the BEC—installed all the way down the track—make up the return circuit. The neutral bus bars throughout every substation in addition to the earth networks of a MPS and APSs are all linked to the return circuit. Through the train pantograph, which receives electricity from the contact wire around 25 kV AC, power is continually transmitted to the trains.

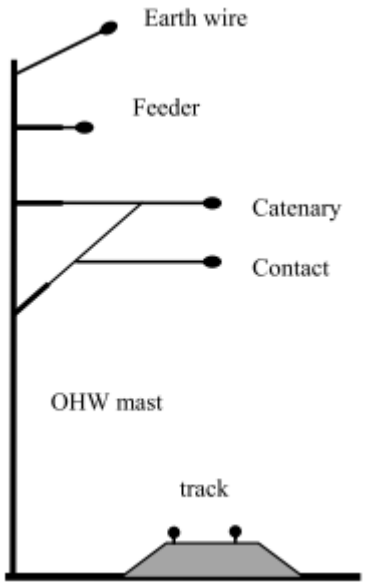

Figure 2: Illustrates the traction overhead wiring OHW arrangement.

Auto-Transformer Paralleling Systems

According to design calculations and load flow calculations, the APSs are placed at far dispersed locations in the system because, as is to be anticipated, there are significant voltage dips throughout the OHW power distribution system. The APSs are made to maintain voltages within the acceptable limits shown in Table 1. At the APS, the return current is equally divided between the two phases, and the voltages between both the catenary as well as the autotransformer neutral, in addition to those between the feeder and the autotransformer neutral, were balanced. The feeder as well as the catenary have a 180 degree phase difference in this setup. The feeder wire is regarded as negative, whereas the catenary cable is positive. The return current in the APS design travels via the AEC, rail, and BEC.

Table 1: Illustrates the APSs are designed to keep voltages in admissible ranges that are given.

Classification	Voltage
Highest Non-permanent Voltage	29 kV
Highest Permanent Voltage	27.5 kV
Nominal Voltage	25 kV
Lowest Permanent Voltage	19 kV
Lowest Non-permanent voltage	17.5 kV

The autotransformer is discovered to be the best suited for this application when compared to those other AC traction power generation systems, such as the boosting transformer system. Its benefits include the ability to be deployed with fewer substations and the use of greater voltages, which increases efficiency by reducing losses. Lower currents, voltage drop, and electromagnetic interference with said communication lines characterize the autotransformer propulsion supply system. APSs are spaced far apart—up to 15–18 km—in contrast to booster installations, which are 3–5 km apart. Because there are 50 kV AC between both the catenary as well as the feeder,

the system's voltage level is thought to be twice that of a booster system, resulting in fewer losses for the identical amount of power pulled from the system as well as smaller voltage dips. Booster transformers only get electrified when a train is nearby, but autotransformers are constantly active. A booster transformer causes an equal amount of electricity to flow through the return circuit and the catenary. The ground leakage current is reduced by this setup. As the APS does not need any HV supply, it is additionally desirable that the HV source of both the 88 kV AC supply would be at one site rather than scattered throughout the system. The tap changers included in the MPS traction transformers are utilized to control any voltage discrepancies. The design eliminates issues with electromagnetic interference (EMI) between the traction and other circuits like communications and signaling.

CONCLUSION

The distance protection parameters rely on human calculations and simulations utilizing conductor data from either the manufacturers without performing line impedance testing. Manufacturers provide the conductor impedance per unit distance, and the overall impedance is subsequently computed. In this study, line and earth impedances were measured and analyzed in order to contrast the findings with theoretical or estimated values provided by the conductors' replacement parts makers. It is evident from the discussion and analysis of the findings that measurements must be made since doing so will increase the precision of the impedance relay protection settings.

References:

[1] Liliana, N. Jalinus, Krismadinata, and B. H. Hayadi, “Application of research based learning (RBL) model in subject of electric power system protection,” *Int. J. Sci. Technol. Res.*, 2019.

[2] H. H. Alhelou, M. E. Hamedani-Golshan, T. C. Njenda, and P. Siano, “A survey on power system blackout and cascading events: Research motivations and challenges,” *Energies*. 2019. doi: 10.3390/en12040682.

[3] N. M. Moyo, R. C. Bansal, R. Naidoo, and W. Sprong, “Line impedance measurement to improve power systems protection of the gautrain 25 kv autotransformer traction power supply system,” *IEEE Access*, 2019, doi: 10.1109/ACCESS.2019.2940894.

[4] H. S. E. Barkat and B. Mahdad, “An Experimental Educational Platform Based Arduino-GSM for Power System Protection,” 2019. doi: 10.1109/CCEE.2018.8634537.

[5] S. Chandra Shekar, G. Ravi Kumar, and S. V. N. L. Lalitha, “A transient current based micro-grid connected power system protection scheme using wavelet approach,” *Int. J. Electr. Comput. Eng.*, 2019, doi: 10.11591/ijece.v9i1.pp14-22.

[6] N. Bayati, F. Aghaee, and S. H. H. Sadeghi, “The adaptive and robust power system protection schemes in the presence of DGs,” *Int. J. Renew. Energy Res.*, 2019, doi: 10.20508/ijrer.v9i2.9154.g7642.

[7] T. S. S. Senarathna and K. T. M. Udayanga Hemapala, “Review of adaptive protection methods for microgrids,” *AIMS Energy*. 2019. doi: 10.3934/energy.2019.5.557.

[8] Liliana, N. Jalinus, and Krismadinata, "The application of Research Based Learning Model in electric power system protection course," 2019. doi: 10.1088/1742-6596/1387/1/012008.

[9] K. P. Schneider *et al.*, "A distributed power system control architecture for improved distribution system resiliency," *IEEE Access*, 2019, doi: 10.1109/ACCESS.2019.2891368.

[10] R. Bansal, *Power System Protection in Smart Grid Environment*. 2019. doi: 10.1201/9780429401756.

[11] J. de Jesús Jaramillo Serna and J. M. López-Lezama, "Alternative methodology to calculate the directional characteristic settings of directional overcurrent relays in transmission and distribution networks," *Energies*, 2019, doi: 10.3390/en12193779.

[12] B. Tetteh and K. Awodele, "Power System Protection Evolutions from Traditional to Smart Grid Protection," 2019. doi: 10.1109/SEGE.2019.8859874.

CHAPTER 18

EXPLORATION ON THE CIRCUIT BREAKER

Mr. M.Sashilal, Associate Professor,
Department of Electrical Engineering, Jaipur National University, Jaipur, India,
Email Id-msashilal@jnujaipur.ac.in

Abstract:

A switching device known as a circuit breaker stops the aberrant or fault current. It is a mechanical apparatus that turns on and off as well as interrupts the passage of large magnitude (fault) current. The circuit breaker's primary purpose is to close or open an electrical circuit, protecting the electrical system in the process. In this chapter author is discusses the indicator state of circuit breaker and their price limit.

Keywords:

Circuit Breaker, Indicator, Network, Switching Device.

INTRODUCTION

Essentially, a circuit breaker is made up of movable and stationary contacts. When the circuit is closed, these contacts are contacting each other and conducting current normally. The electrodes—the current-carrying contacts—engaged with one another when the circuit breaker was closed under the force of a spring. The circuit breaker's arms may be opened or closed during regular operation in order to switch and maintain the system. Only pressure must be given to a trigger in order to release the circuit breaker.

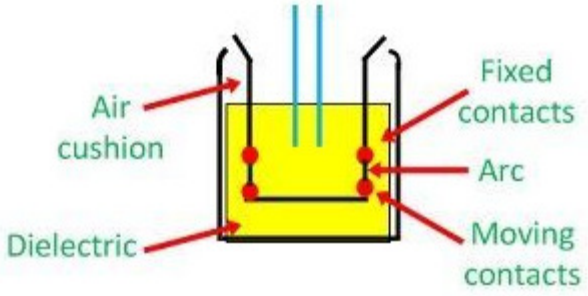

Figure 1: Illustrates the component of circuit breaker.

An electrical circuit breaker is indeed a switching mechanism for managing and safeguarding an electrical power system that may be used both manually and automatically. A circuit breaker should be specially designed to be able to safely stop the arc created during the shutting of a circuit breaker since the contemporary power system deals with extremely high currents. The fundamental description of a circuit breaker was just as follows. The vast power network and many electrical devices it is coupled with make up the contemporary power system. A strong fault current will pass through this equipment in addition to the power network during one short circuit fault or any other sort of electrical fault (including such electric cable problems). The networks and equipment may sustain long-term harm from this high current. The fault current

has to be eliminated as soon as possible from the system in order to protect these items of machinery and the power networks. In order to send dependable, high-quality power towards the receiving ends, the system must quickly return to normal operation when the problem has been fixed. In addition, many switching activities must be carried out for the power system to be controlled properly. Therefore, there must be a unique form of switching devices that can be operated securely under enormous current carrying conditions in order to quickly disconnect and reconnect various elements of the power system network both protection and management. Significant arcing would occur between switching contacts during the cessation of a large current, hence care should be made to safely quench these flames in circuit breakers. The circuit breaker is indeed a unique device that performs all necessary switching activities while there is electricity flowing. This was the fundamental overview of a circuit breaker.

Fixed contacts and movable contacts make up the majority of the circuit breaker. These two contacts were physically linked to one another while the circuit breaker is in its typical "ON" state as a result of the mechanical pressure being exerted to the moving contacts. When a switching signal is applied to a circuit breaker, potential energy that has been accumulated in the working mechanism was released. The potential energy may be stored in the electrical system in a variety of methods, including via hydraulic pressure, compressed air, or compacting metal springs. However, potential energy must be dissipated during operation, regardless of the source. The moving contact slides quickly thanks to the release of electric potential. When a switching pulse energizes the working coils (tripping coils and closure coil) in a circuit breaker and displaces the plunger inside of it, the circuit breaker trips. This operating coil plunger is normally linked to the circuit breaker's operating mechanism. As a result, mechanically stored potential energy in the switchgear mechanism has been released as kinetic energy, which causes the moving contacts to move because they are mechanically connected to the operating mechanism through some kind of gear lever arrangement. After a circuit breaker cycle, the whole energy saved is released, and potential energy is afterwards once again stored in the functioning mechanism of a circuit breaker that used a spring charging motor, an air compressor, or any other method. We have so far spoken about the mechanical operation of a circuit breaker. However, while discussing how a circuit breaker operates, it is also important to take into account its electrical properties. Let's talk about the electrical theory behind circuit breakers. The circuit breaker must handle huge rated power or experience a failure. Due to this significant power, the arcing between the circuit breaker's moving and fixed contacts is constantly at dangerously high levels. As we previously explained, if the dielectric strength between both the circuit breaker's current carrying connections grows quickly during each alternating current zero crossing, the arc inside the circuit breaker may be safely quenched. There are several ways to increase the electrical properties of the media between contacts, including compressing this same ionized arcing media because doing so speeds up the deionization procedure of the media, cooling this same arcing media because doing so increases the resistance of the arcing path, or replacing this same ionized arcing mainstream press with new gasses. Therefore, the functioning of the circuit breaker should include certain arc quenching operations. There are remote control circuit breakers that can be controlled on demand and from a distance, even though circuit breakers typically fulfill their duties autonomously and without supervision.

LITERATURE REVIEW

M. Žarković and Z. Stojković[1]stated the health assessment of high voltage SF6 circuit breakers using advanced artificial intelligence (AI) techniques is presented in this research. The paper

provides a summary of high voltage SF6 circuit breakers' most crucial condition indicators and monitoring and troubleshooting procedures. An emphasis is placed on locating and establishing indication limit values that AI may utilize to develop new health assessments. Fuzzy expert systems that will decide how to maintain circuit breakers have been developed using fuzzy logic, a component of AI. To determine the condition of contacts, the fluid used to put out the electric arc, and the driving mechanism, three fuzzy expert systems were developed. The k-means cluster technique and cluster tree were used to use unsupervised machine learning (UML) to categorize and divide the evaluated high-voltage circuit breakers under groups with a comparable condition and failure probability. In order to forecast the lifespan and accelerated age of tested circuit breakers, an artificial neural network (ANN) is developed as part of supervised machine learning (SML). The high-voltage SF6 circuit breakers' health can be better assessed using the AI techniques that have been described.

S. Liu [2] et al. the primary objective of that study is to simulate a mechanical circuit breaker (MCB) that can reproduce the features of the breaker in a real-world setting. In order to adequately represent the circuit breakers during system analysis studies, the suggested MCB with active current injections is simulated for a system level. The suggested MCB models' external current-voltage characteristics closely resemble those of actual devices. It is well knowledge that in order to prevent converter damage, the DC circuit breaker (DCCB) must intercept DC faults extremely rapidly. The time required to identify the defect, the time required for the DC prevention to instruct the DCCB, and the time it takes the DCCB to clear its arc make up the overall current interruption time. Therefore, before these devices could be deployed and commissioned in reality, it is important to show the performance of the system of connected protective devices via real-time simulation. In this study, a thorough RTDS-based real-time simulation environment model of the mechanical DCCB is presented. Simulations based on PSCAD are used to confirm the model's performance, and defensible conclusions are reached.

A. Heidary[3] et al. the power system is concerned about safeguarding delicate loads against voltage drops. A quick fault current limiter combined circuit breaker may help sensitive loads quickly recover their voltage. The compound form of current limiter and circuit breaker (CLCB) that this study suggests may restrict fault current and quickly break to correct voltage sags at protected buses can also limit fault current. It may also function as a circuit breaker to cut off the problematic line. The series L-C resonance, consisting includes a resonant transformer as well as a series capacitor bank, is the foundation of the proposed CLCB. A diode as well as an IGBT are also included in the CLCB, and they are coupled in series using bus couplers. The suggested structure was simulated in MATLAB to conduct a CLCB performance study. Additionally, an experimental prototype were created, put to the test, and the findings were documented. Comparisons demonstrate that experimental findings and simulation findings were generally in accord, confirming CLCB's capacity to serve as both a fault current limiter and just a circuit breaker.

According to the Y. Wang[4] et al. due to its distinctive qualities, the DC microgrid has gained increasing interest. However, the creation of a DC microgrid is also fraught with difficulties, such as the interruption and isolation from short-circuit fault currents. Therefore, a dc microgrids ability to operate normally is dependent on the dc circuit breaker. The bidirectional flow of energy is made possible in this work by the unique bidirectional dc solid-state electrical system that is provided, ensuring the greater operational efficiency of the dc microgrid. The suggested innovative topology features a simpler construction, a common ground, and fewer elements as

compared to conventional solid-state circuit breakers. First, using simulation findings of the circuit architecture, this study conducts a thorough investigation of the various operating phases of the circuit at the time the failure arises. The criteria for choosing components based on calculations and circuit analysis are then provided in this study. Finally, tests are used to demonstrate how well the unique bidirectional solid-state circuit breaker performs.

S. Wang[5] et al. in that research, a high-voltage direct-current (HVDC) grid protection method is suggested to reduce dc fault currents and avoid overcurrent in the arms of modular multilevel converters (MMCs). The plan is based just on coordination of hybrid dc circuit breakers and half-bridge MMCs (DCCBs). This is accomplished by enabling the temporary bypass of MMC submodules before accessing the DCCBs. The DCCBs will isolate the issue after which the MMCs will resume normal functioning. The effectiveness of the suggested approach is evaluated and contrasted with that of blocking MMCs and the absence of remedial action. In order to do this, a fault detection and classification algorithm is used, and its effects on MMC bypassing are addressed. The suggested technique is illustrated in PSCAD/EMTDC using a four-terminal HVDC system to evaluate its efficacy. According to simulation data, coordination between MMCs and DCCBs may decrease dc fault current and the absorbed current energy by even more than 70% and 90%, respectively, while maintaining low MMC arm currents.

I. M. Sifat and A. Mohamad[6]disused financial markets, there is debate concerning the effectiveness of the circuit breaker, an automatic regulatory tool used to ward off panic, control volatility, and avoid collapses. Advocates assert that it gives traders a favorable break when price levels are under pressure and encourages them to make logical trading selections. Its opponents downplay its strength, calling it a hindrance to the process of laissez-faire price discovery. Researchers have mainly focused on its ability to calm panic, interference throughout trading, volatility transmission, possibility of self-fulfilling prophecy though the gravitational pull itself toward, and delayed information dissemination since it was conceptualized in the 1970s and put into practice in the 1980s. Circuit breakers are a clear favorite among regulators, who discount the credibility of anti-circuit breaker results by blaming, among other things, questionable methodology and a lack of statistical power, despite the fact that financial economists disagree with their utility. The calls for more regulatory engagement in markets became stronger against the background of the 2007–2008 Crisis and the 2010 Flash Crash. Therefore, it is doubtful that protective devices like circuit breakers would wane. Are circuit breakers, however, worthwhile? This paper attempts to explain the regulatory rationale and synthesizes three decades' worth of experimental and theoretical works. It also highlights limitations, issues, but also methodological flaws undermining findings and offers guidance for future research inside an environment where markets are becoming more complex.

S. Zhao[7] et al. natural transition the low losses of mechanical circuit breakers and indeed the quick switching frequency of solid-state circuit breakers are combined in hybrid DC circuit breakers. The success or failure of controlling the current distribution of a DC distribution network is influenced by its overall dependability. Based on the hybrid DC circuit breaker's architecture, the Fault Tree was employed in this study to examine the fundamental parts that contributed to the circuit breaker's failure. In order to determine steady state availability, probability of failure, but also mean time between failures for hybrid DC circuit breakers, the Markov model is added to the reliability modeling process. This foundation is used to examine the redundancy of weak components for hybrid DC circuit breakers using the k/n (G) model and Gamma distribution. Finally, a quantitative analysis is done to determine how various

redundancy components and multiple redundancy methods of weak components affect the dependability of hybrid DC electrical devices. The study techniques and findings may serve as a guide for hybrid DC circuit breakers' system reliability and design.

According to the M. Zhou[8] et al. in a meshed HVDC grid, hybrid high voltage direct-current circuit breakers (DCCBs) can cut off fault current in a matter of milliseconds, although their capital costs are substantial. The capacitor commutated dc circuit breaker is an idea put forward in this research to improve the hybrid DCCBs' economic competitiveness (CCCB). The CCCB primarily consists of a main branch with a series connection of the dc capacitor and diode valves, and an auxiliary branch with a quick disconnector in series with semiconductor technology. The CCCB is described in great depth in this essay. Discussions are held on topology and operating principles. Snubber circuits with stray inductances' effects on the commutation procedure are examined. The CCCB's primary components' basic sizing methodology is described in depth. It is examined how transmission lines close under various operating circumstances. To further cut down on the cost of semiconductors and on-state operating power loss, a number of extended topologies are suggested. Assessments are made on CCCB costs and power loss. The dc fault isolation & reclosing of the CCCB were confirmed by thorough simulations using PSCAD/EMTDC.

S. Li [9] et al. HVDC grid has drawn a lot of interest as the high voltage direct current Transmission (HVDC) industry booms. High voltage direct current circuit breakers (DCCB) are a crucial part of the HVDC grid and need urgent and in-depth research. This research proposes a unique topology for current limiting DCCB (CL-DCCB). The topology is made up of a number of components that fall under the main circuit breaker (MCB) but also branch circuit breaker categories (BCBs). To improve the current limiting impact, it is flexible to choose the numbers of inductor branches. Whenever a suspected fault develops, the CL-DCCB may begin current limiting operation. It may be decided whether to conduct a breaking operation or return to the regular state after the detecting circuit shows what has occurred. This mode ensures that the fault current stays under the system's maximum limit while allowing for lengthier fault detection times and circuit breaker operating delays. In order to explore the design criteria with CL-DCCB, an experiment prototype and simulation model are created. The maximum detection latency, it has been found, may be increased to 12 ms. additionally, by increasing the quantity of inductor branching or the inductance of the each branch, the current limiting impact may be strengthened.

L. Tapia [10] different types of boats may increase their fuel economy and energy efficiency by using electric propulsion and integrated electric hybrid systems. There are various advantages that may be realized if the vessel power system is based on DC grid transmission, including improved generator efficiency and reduced volume and cost. For this type of DC grid-based power system, protective devices still present certain issues. It is difficult because the DC current lacks a natural zero crossing and necessitates quick, programmed breaking times. Although there are several articles discussing DC breaker topologies including their function in DC grids, it might be challenging to get thorough information regarding the DC breaker's design process. The foundation for a DC solid-state circuit breaker (SSCB) with low voltage vessel DC grids is described in this study. In less than 3 seconds, the full-scale prototype of the planned SSCB finds and opens the flaw. Theoretical analysis, design recommendations, modeling and simulation, but also experimental findings are all included in this work.

DISCUSSION

Every power electric system strives to provide a reliable source of energy (PES). The state of the high-voltage equipment has a significant impact on the EPS's capacity to operate reliably. Mechanical, electrical, atmospheric, and chemical stressors alter the properties of high voltage equipment. As a result, there are more electrical losses, more faults, more repairs, and a higher chance of costly equipment being damaged. The purpose of a high-voltage circuit breaker (CB) would be to establish, continuously transmit, and disconnect current. All EPS equipment is protected by the CB, which interrupts short-circuit currents. Because of this, the CB's effective operation is crucial to the PES's dependability. All PES equipment is subject to corrective, preventative, and reliability-based maintenance. Condition and reliability-centered asset management (RCAM) is current in the literature. The challenge with equipment monitoring & diagnostics in PES is figuring out their condition and deciding on the importance of maintenance, repair, or replacement. Although monitoring high-voltage CBs is not as advanced as monitoring the power transformer, it nevertheless offers a wide range of measuring techniques and diagnostic data. These findings of individual monitoring techniques are often used in papers to diagnose CBs without taking into account the overall objective picture of a CB situation. Standards provide maximum values for all CB indicators and parameters but do not suggest how to apply them. Health assessments are not feasible without these constraints, thresholds, and circumstances since they are values. The report refers to the most recent sensors and CB monitoring metrics that are currently available. The article discusses the working group's experience and includes details on the CBs' lifespan. High voltage CB timings are shown. An innovative method for evaluating the CB's life cycle or phases of degradation using data from its control circuit is given in this research. Based on CB's timings, the study assesses the condition index and probability distribution for CB. Through data mining and meaning clustering, decision assistance again for condition-based maintenance of CBs is demonstrated. Based upon operations times OD CB, the articles assess the status of CB. These inputs, timings, only directly reflect trip and close coil performance; they do not reflect the overall CB state. The influence of SF6 gas characteristics on the condition-based maintenance approach of CB is explained in the study. The condition of CB contact wear every interruption is assessed and estimated in this work. The time, moisture, and SF6 pressure-based aging failure model. The signal processing but also contact force monitoring techniques developed by CB are shown. With this procedure, the mechanical properties of the CB are assessed based on timings, contacting movement speed, & contact travel distance. Circuit breaker maintenance priorities should be determined using Rank Boost-based data-driven methodology, and only CB's timings should be used.

Circuit breaker state indicators

The CB must guarantee that the electric circuit is effectively broken and that the electric arc is immediately extinguished with a small amount of switching overvoltage. The arc chambers, the insulator, as well as the drive mechanical mechanism are the three fundamental components of the CB that are crucial for its successful functioning regardless of the type. The CBs are categorized into four categories according on the cooling medium used in an electric arc chamber: oil, pneumatic, vacuum, and SF6. The CB's driving system has three different options: hydraulic, pneumatic, and spring. The CB is subjected to many forms of stress while being used, which reduces its lifespan. Correct diagnostic technique selection results in maintenance tasks that are tailored to the CB's current state. The following diagnostic techniques are used to check high-voltage CBs: insulating resistance measurement, Verify the dielectric oil's strength, the

vacuum level, or the SF6 gas' density. Verify the contacts' position inside the open-closed state, verify the contacts' walk by capturing the space-time diagram. Measurement of the coil's current, measuring the motor mechanism's timing frequency As well as counting activities, gauge contact resistance. The most significant factors affecting the CB lifespan are the quantity of interruption operations and the magnitude of the current in short circuit breakdowns. Depending on the kind of CB and rated voltage, the CB's lifespan varies (Ur).

pneumatic: 41 ± 6 years (110 kV < Ur < 345 kV) and 40 ± 6 years (345 kV < Ur),
oil: 42 ± 6 years (110 kV < Ur < 199 kV), 41 ± 6 years (200 kV < Ur < 275 kV) and 38 ± 5 years (345 kV < Ur) and
SF_6: 43 ± 6 years (110 kV < Ur < 199 kV), 42 ± 6 years (200 kV < Ur < 275 kV) and 42 ± 6 years (345 kV < Ur).

The maximum number consecutive break operations (no), which is established by mechanical testing and is up to 10,000, differs according on the kind of CB. The cumulative break current is frequently measured since the interrupted current is equally significant. The cumulative current is quite helpful since it strongly influences both the state of the cool medium and how quickly the CB contacts deteriorate. The primary purpose of keeping track of switching operations is to assess mechanical damage to the pole contact surfaces. The heat impulse determines the extent of contact damage, and the damage grows exponentially with the square of the current that the poles separate. The quantity of operations and the amplitude of then short-circuit current have a significant impact on the CB's lifespan. Each CB must meet the following roughly required requirement.

$$\Sigma n \cdot I_{sc}^2 \leq 20\,000$$

ISC stands for the short-circuit current in [kA] and n represents the number of interrupted current flow. 50% of CB failure is caused by corrosion, contact degradation, and aging. A thermovision can quickly identify contacts that are in poor condition. Increasing the contacts' resistance causes more warmth and hot patches, which may be distinguished by overheated temperatures. For all three phases, direct current is often used to evaluate contact resistance (RC []). Comparing it to the values from the two remaining phases is the traditional method for estimating the RC. It is important to fix the CB if the deviation (RC) is more than 50%. This measurement, which serves as the main circuit's parameter, is essential for carrying current when the circuit is closed.

The diagnostics does not address this issue because to the minimal number of CB insulation failures, therefore in actual usage, feedback voltage and tg measurements are seldom used. Examining the arc medium's insulating properties receives a lot more focus. The most sophisticated and widely used CBs are SF6 CBs. the evaluation of the SF6 CB's condition. For oil and vacuum CBs, a similar algorithm may be used, but it will need to keep track of various cooling medium properties. The humidity and air concentrations within SF6 gas, gas density, the gas's dielectric strength, temperatures, and gas pressure are the major properties of the SF6 medium. As a result of the interdependence between these features, sensors have been created to monitor the medium's temperature, pressure, and gas leakage. Between 30 °C and 100 °C is the range of probable gas temperature values (SF6). The maximum and minimum temperatures are respectively 40 °C and 110 °C. The permitted annual gas leakage (p) varies from 0.5% to 1%. The thermovision can quickly identify the location of a gas leak during an examination. The

manometer measures the gas pressure (p), which has a typical range of 6.25 bars to 7.77 bars. The 5.98 and 8.05 bar pressure limits are the values. Monitoring the tightness of a SF6 chamber of a CB has a direct relationship to checking leakage but also gas pressure. Additionally, when SF6 gas enters the liquid form at high pressure, it is unable to cool the arc. The density () of SF6 gas is another crucial factor. The density of SF6 gas typically ranges between 45 and 50 kg/m3. Mechanical issues and control circuit issues, not insulation problems, are the most frequent CB defects. The coil's inability to turn on or off is the most frequent CB malfunction. As a result, the coil is monitored with the greatest attention.

The functioning of the drive mechanical component is tested by recording the contacts' motion. The comparison of a recorded curves serves as the foundation for the analysis of a contacts walk. The referenced curves of the health and new CB may be used to compare the recorded curves. This kind of comparison lacks quantifiable data beyond an arbitrary aesthetic assessment. Consider the duration of a contact path location as well as the simultaneity between CB poles instead of interactions walk comparisons. Based on recorded connection travel and contact speed, it is possible to determine the length of a contact walking during the entire CB operation. In online monitoring systems, sensors that detect contact speed (vC [m/s]) are attached. The switching operations' lower and higher speed limits were 3.1 m/s and 5.6 m/s, respectively. The contact routes' maximum allowed lengths (dC [mm]) are 190 mm and 213 mm, correspondingly. Longer dielectric stresses result if one CB pole's break time was shorter than that for the other poles. As a consequence, the electric arc may be restarted. By comparing the opening and shutting timings of all three poles, the compliance and correct operation of CB poles is verified. The manufacturer determines the acceptable deviation times (t [ms]) between both the CB poles. The permitted t for Siemens' manufacturer is 3 ms for releasing and 2 ms for shutting, compared to 5 ms and 3 ms for Areva. The smallest permitted variation of 2 ms is chosen as the maximum limit for the most important parameter in both switching operation scenarios. The motor-driven propulsion's potential energy is used to kick-start the switching mechanism. The primary function of motor-driven propulsion would be to transmit energy from of the springs towards the contacts, allowing them to open and shut at predetermined intervals. The first symptom that the mechanical functioning of the CB is disrupted and leads to an inaccurate arc-extinguishing is any significant departure from the prescribed, nominal period for operation. Contacts that take too long to close show a lack of power inside the motor drive. More mechanical strain strains and potential contact crashes result from more energy. The motor-driven mechanism's reduced energy translates into slower operation, longer switching periods, and less breaking power. The contacts' walk route and switching operation times are both closely connected. The recorded contacts' walk route and speed may be used to determine the CB's response time (tr [ms]). The CB's permitted maximum and minimum response times are 1 ms and 19 ms, respectively. The CB's mechanism time (tm [ms]) is also specified, and the permitted range is 51 to 76 ms. the close coil duration (tC [ms]), which is also measured, is typically recorded between 18 and 40 ms. All of the set time boundaries apply to the contact's closure procedure. O-0.3 s-C-O is the fundamental cycle needed for CB switching operations: open (O) - 0.3 s pause- close (C) - open (O). High voltage (110-400 kV) CB manufacturers' permitted operational time variances include:

For Siemens, the permitted variation is 7 ms closing and 3 ms whenever opening the CB; for Areva, it is 10 ms shutting and 3 ms when opening the CB; and for ABB, it is 2 ms opening time as well as a maximum CB closing duration of 70 ms.

Price limit

A price limit is the most allowed difference from a reference price that may be made. Therefore, price constraints essentially create a range of acceptable prices for a certain time. Price limitations provide a channel of allowed percentages (or ticks) by which price may change, dependent on the reference price, which could be the previous session's or day's settlement price, or the latest executed price within the current session. Before the cash market opens, certain index futures were subject to a price cap defining a deviation band. The terms "limit up" and "limit down" refer to the channel's peak and trough, respectively. Limits may be intraday or daily (interday, static) (dynamic). Some marketplaces are known to use daily and intraday limitations at the same time. Price limits were first used in the 18th century at the Dojima trade in Japan.

Stop trading

A trade stop is the brief cessation of continuous trading for a single asset, a collection of securities, a single exchange, or a collection of exchanges that are typically (but not always; for example, the EU) governed by the same regulator. It is used to correct—or prepare for—market disorder, such as an imminent business statement or piece of news, or to address an unbalanced order. Open orders may be canceled and options may be executed during a pause. Halts may be optional or governed by rules (automatic). For the former, a market operator may choose to pause trading in a security to give investors an equal chance to assess news and base judgments on it—typically prior to significant or pertinent news. Suspicion about questionable price-related conduct may also give rise to it. Contrarily, rule-based halts are invoked when specified conditions are reached. For instance, when a price limit is met, trading in a stock may be immediately suspended. In contrast to discretionary halts, these halts are brief in nature and simpler to foresee, allowing participants to adjust their trading behavior and strategy in light of the possibility of trade suspension. Even though rule-based halts are more frequent and shorter in length than discretionary halts, exchanges have the option to prolong them.

Interruption of volatility

European exchanges started experimenting with a mechanism in the 1990s that stops continuous buying and selling and switches to something like a call auction (or a continuation of a call auction if such an interruption occurs during in the auction) when the next potential price drops outside of a predefined range based on a reference price, in contrast to the circuit breakers that were popularized in North America. Volatility interruption (VI), a component of this process, is distinct from conventional circuit breakers in a number of respects. First of all, VIs are not generally enforced. Instead, they are implemented on certain securities. As a result, just that instrument is affected when a VI is triggered, not the entire market. However, it may have unforeseen repercussions if the security in question is a bellwether or an industry leader. Moreover, posting auction prices and volumes facilitates price discovery during a VI-triggered auction. Last but not least, VIs normally remains no more than a few minutes, unlike halts, which may last for an extended period of time or perhaps the whole trading day. This makes an argument that VI is better suited for index computations and derivatives pricing.

CONCLUSION

In financial economics, the phrase "circuit breaker" refers to a broad range of regulatory tools used by securities market custodians to control volatility, avert collapse situations brought on by

excessive investor overreaction or broken algorithms, and maintain market integrity. Circuit breakers in financial markets halt or finish trades sooner after a significant price movement to give market participants time to reflect on the fundamentals, acquire data, evaluate positions, and make reasoned choices. Additionally, individuals who have not yet entered the market are given the chance to contribute or offer liquidity. Regulators anticipate that this will prevent panic, facilitate price discovery under tense market conditions, and safeguard liquidity providers. Price caps and trade halts are the two most typical types of circuit breakers.

References:

[1] M. Žarković and Z. Stojković, "Artificial intelligence SF6 circuit breaker health assessment," *Electr. Power Syst. Res.*, 2019, doi: 10.1016/j.epsr.2019.105912.

[2] S. Liu, Z. Liu, J. de Jesus Chavez, and M. Popov, "Mechanical DC circuit breaker model for real time simulations," *Int. J. Electr. Power Energy Syst.*, 2019, doi: 10.1016/j.ijepes.2018.11.014.

[3] A. Heidary, H. Radmanesh, A. Bakhshi, K. Rouzbehi, and E. Pouresmaeil, "A compound current limiter and circuit breaker," *Electron.*, 2019, doi: 10.3390/electronics8050551.

[4] Y. Wang, W. Li, X. Wu, and X. Wu, "A novel bidirectional solid-state circuit breaker for DC microgrid," *IEEE Trans. Ind. Electron.*, 2019, doi: 10.1109/TIE.2018.2878191.

[5] S. Wang, C. Li, O. D. Adeuyi, G. Li, C. E. Ugalde-Loo, and J. Liang, "Coordination of MMCs with Hybrid DC Circuit Breakers for HVDC Grid Protection," *IEEE Trans. Power Deliv.*, 2019, doi: 10.1109/TPWRD.2018.2828705.

[6] I. M. Sifat and A. Mohamad, "Circuit breakers as market stability levers: A survey of research, praxis, and challenges," *Int. J. Financ. Econ.*, 2019, doi: 10.1002/ijfe.1709.

[7] S. Zhao, X. Yan, B. Wang, E. Wang, and L. Ma, "Research on reliability evaluation method of DC circuit breaker based on Markov model," *Electr. Power Syst. Res.*, 2019, doi: 10.1016/j.epsr.2019.04.005.

[8] M. Zhou, W. Xiang, W. Zuo, W. Lin, and J. Wen, "A novel HVDC circuit breaker for HVDC application," *Int. J. Electr. Power Energy Syst.*, 2019, doi: 10.1016/j.ijepes.2019.02.045.

[9] S. Li, J. Zhang, J. Xu, and C. Zhao, "A new topology for current limiting HVDC circuit breaker," *Int. J. Electr. Power Energy Syst.*, 2019, doi: 10.1016/j.ijepes.2018.07.042.

[10] L. Tapia, I. Baraia-Etxaburu, J. J. Valera, A. Sanchez-Ruiz, and G. Abad, "Design of a solid-state circuit breaker for a dc grid-based vessel power system," *Electron.*, 2019, doi: 10.3390/electronics8090953.

CHAPTER 19

REVIEW STUDY ON VOLTAGE TRANSFORMER

Mr. Harsh Shrivastava, Assistant Professor,
Department of Electrical Engineering, Jaipur National University, Jaipur, India,
Email Id-ershrivastava@jnujaipur.ac.in

Abstract:

Instrument transformers that are coupled in parallel include voltage transformers (VT), sometimes known as potential transformers (PT). Devices have an exact voltage ratio & phase relationships to permit accurate secondary connection metering, are made to offer a minimal load to the source being monitored, and are intended to do so. In this chapter author discusses types of voltage transformer and potential transformer errors.

Keywords:

Load, Potential Transformer, Power System, Phase Shift.

INTRODUCTION

An electrical power system is a collection of electrical parts that are used to generate, transmit, and utilize electricity. Power is generated by a generator, such as a power plant, transported across transmission and distribution networks, and used in household applications. To guarantee an optimal value is conveyed at different locations throughout the power distribution system, the voltage level should be monitored. This voltage is often quite high, making it impossible to measure with a standard voltmeter. To detect very high voltage and current across the power system, specialized transformers called instrument transformers are used. A high-voltage transformer is known as a voltage transformer, often referred to as a potential transformer, while a high-current transformer is known as a current transformer. The construction, operation, measurement, varieties, and uses of voltage transformers are covered. A secondary station inside the electricity generating, transmission, and distributing system is called an electrical substation, where transformers are used to change voltage from a high value to a low value or the opposite. Between power plants and the customer, electricity travels via a number of substations, where the voltage may be adjusted in stages. Several industrial facilities and residential regions receive and use the voltage produced at a power station or substation. It must be verified that both the voltage produced and the voltage received after transmission across numerous lines have not experienced significant losses. Therefore, it is crucial to monitor these voltages at different locations. Conventional voltmeters are unable to monitor high-level voltages inside power plants and load centers. A potential transformer is indeed a step-down transformer which transforms an input voltage into a lower output voltage that can be monitored by such a voltmeter and is used for monitoring high voltages in the transmission and distribution systems.

A voltage transformer is built using main and secondary windings, much like a standard power transformer. The ratio of the secondary's turns to the primaries determines the voltage generated at the load side. This formula for the voltage transformation is:

V1/V2 = N1/N2

V1: Primary power transformer voltage applied

V2: The voltage generated at the transformer's secondary (load).

N1: The primary's number of turnings.

N2: The number of secondary turns

For instance, a transformer having N1=1 and N2=10 will have a secondary winding voltage of 1V as well as a primary winding voltage (V1) of 10.

For instance, a transformer with N1=1 and N2=10 will have a secondary winding energy of 1V and a primary winding voltage (V1) of 10 in Figure 1.

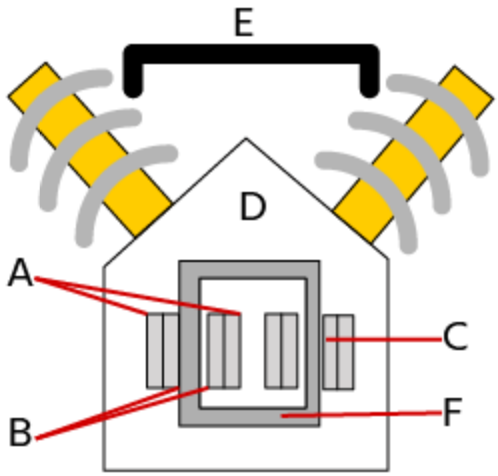

Figure 1: Illustrates the schematic diagram of potential transformer.

A voltage transformer does indeed have a core made of silicon laminations that is much larger than the magnetic core (designated F) of a standard power transformer. Either a core-type or a shell-type magnetic core is possible. Due to how simple it is to insulation a low-voltage winding, the secondary side typically coiled close to the core (labeled B). Using paper tape or cotton insulating (designated C) in between, the secondary winding is coiled over the primary, which is carrying voltage output (labeled A). In high rated voltage transformers, individual windings are submerged in an oil-filled tank (, designated D), which improves insulation (above 7kV). The oil-filled bushings used to extract the high voltage connections from the tank (labeled E).

Voltage transformer working principle

High voltages are often measured using a potential transducer. The transmission line for whom the voltage (132 kV in) is going to be monitored has the primary side of a potential transformer (PT) attached across it. A load named "A" that draws electricity from the transmission line gets connected to the line. The line is always linked in parallel to the potential transformer. A common low-range voltmeter is attached towards the secondary side of a power transformer (labeled V). The line for whom the current has to be measured is always linked in series with such a current transformer. To get a detailed comparison comparing distribution transformer and current transformers, see our article. A voltage is induced upon that secondary winding when a voltage is supplied to the main winding. This voltage is related to the number many windings

upon that secondary and primary sides and is lower than that of the voltage upon that main winding.

LITERATURE REVIEW

A. Arroyo[1] et al. constant state Ferro resonances cause prolonged aberrant system oscillations in isolated neutrality electrical systems, which may harm inductive voltage transformers (IVTs) as well as other system components. This process causes the IVT to become saturated, which causes magneto-striation to modify the ferromagnetic material's properties. The IVT's intrinsic vibration modes are stimulated as a result of this behavior's inherent nonlinearity. The purpose of this work is to use these unusual vibration modes to demonstrate ferro-resonance in IVTs. It is discussed and experimentally shown how to use vibration analysis to discover ferro resonance in IVTs.

K. Wang[2] et al. the high voltage fuses used it to safeguard voltage transformers (VTs) sometimes burn out unnaturally in a neutral ungrounded system, leading to unbalanced VT operation. Additionally, fuses fail to blow off in a timely manner, severely harming the VT. Results from tests on VT fuses' steady-state current, breaking properties, X-ray measurements, fuse corona, and electromagnetic transient impact were presented in this publication. This study offers fresh recommendations for the usage of high voltage fuses in voltage transformers while thoroughly examining and analyzing the quality and electrical performances of VT fuses. This study suggests using fuses with current ratings of 1 A derived from a single fuse that has not readily oxidized and has a wrapped skeleton made of an Ag or Ni melt in 35 and 10 kV systems.

M. Faifer[3] et al. Monitoring voltage harmonics is one of the crucial responsibilities in determining the quality of the electricity. The used instrument transformer in particular is crucial to the attained precision. Its frequency response function is often measured in order to assess its harmonic measurement capability. Nonlinearities, nevertheless, may have a non-negligible effect on measurement errors; for instance, this is true when inductive voltage transformers were taken into account. In this study, a straightforward method for compensating the harmonic distortion caused by the high fundamental primary voltage, which is the most important nonlinear impact, is proposed. The approach is first developed and presented using numerical simulations, and it is then put into practice using an appropriate experimental setup. The results show tremendous accuracy gains when measuring voltage waveforms that are realistic.

Z. Meng[4] et al. one of the most crucial pieces of measuring equipment in the power system is the capacitor voltage transformer (CVT), and the quality of its measurements is crucial for ensuring both the security of the power system and the equity of the energy market. Before running in substations, traditional calibration is performed on CVTs, and the operational CVTs must undergo periodic calibration. This is done to assure the steady-state measurement accuracy. However, even with successful calibrations, CVTs often have considerable measurement error. The explanations for the discrepancy between calibration findings and actual measurement errors were suggested in this research. Three-phase working CVTs, on-site calibration, and laboratory calibration are all modelled in accordance with real-world operating circumstances. Theoretical research and simulation findings both show that there are large discrepancies between the calibration outcomes of CVTs and the actual measurement errors. The findings from the simulations are supported by certain experiments. Finally, several recommendations are made to increase the accuracy of calibration findings.

Acording to the H. Liu[5] et al. it might be difficult to detect insulation deterioration in a voltage transformer winding, but it can eventually lead to the transformer blowing up and causing mishaps like phase-to-phase short circuits. Currently, the insulation condition may be determined online by equipment like power transformers, lightning arresters, and other pieces of machinery. There is, however, no established technique for voltage transformer winding insulating monitoring system. In this paper, a zero-sequence loop-based tiny current disturbance approach is suggested. The insulation status of the winding is assessed using the characteristic characteristics of the low-frequency fluctuation of zero-sequence voltage following a disturbance. A lower frequencies oscillation of around 10 Hz can be observed on the zero-sequence voltage whenever the insulation resistance of something like the voltage current transformer is within the range of 0-40 k, as well as its amplitude as well as duration seem to be proportional to the severity of insulation damage, according to theoretical modeling, virtual environment tests, and field tests. The on-line diagnosis of voltage power transformer insulating faults may thus be done using this as a criteria.

J. Diazdelacruz and M. A. Martin-Delgado[6]suggested when a heat bath at a certain temperature is accessible, a physical system out of thermal equilibrium may be used to generate useful work. Information the machines that employ the renowned Maxwell devils to generalize Szilard cylinders are called heat engines. In this research, we take into account a thermochemical store of electrons that may be converted into work and entropy. In order to create long-range voltage transformers with no electrical nor magnetic interconnections between the main and secondary circuits, qubits are employed as messengers connecting electron reservoirs. The transformers use Carnot cycles to operate while they are at various temperatures. A generalization is made to take an electrical network into account, where quantum approaches may provide more security.

According to the W. Wu [7] et al. line loss is a natural part of the transmission and distribution processes, and it may have an effect on how much money power supply companies make. As a result, it serves as a crucial metric and a reference point for assessing daily line loss rates for areas with low voltage transformers. However, the collection of line loss rates includes significant outliers, and the number of areas is often extremely big. When trained on massive data sets, it is crucial to create a regression model with a high resilience and efficiency. A unique approach based on a resilient neural network (RNN) is suggested in this situation. It is a multi-path network model that incorporates a denoising auto-encoder (DAE), that benefits from Huber loss function, L2 regularization, and dropout. It may provide a variety of results that are used to determine appropriate ranges and benchmark values. The suggested RNN outperforms the tested traditional regression models in terms of accuracy and resilience, according to the comparative findings. In the gathered dataset, there are around 13% outliers, and approximately 45% of areas have outliers within a month, based on the benchmark study. Therefore, there is still room for improvement in the quality of transmission losses rate data.

M. Lahame [8] et al. optimization of a three-phase, tetrahedral-type transformer of high voltage that can power three voltage-doubling cells plus three magnetrons per phase is the subject of this article. An algorithm employed in MATLAB/Simulink to evaluate the impact of transformer geometrical parameters just on electromagnetic functioning of the power supply served as the foundation for the optimization technique. This research will make it possible to discover a transformer with a smaller volume while still adhering to the manufacturer's existing requirements for magnetrons. Magnetrons' powers are calculated to determine the best solution while maintaining the nominal functioning.

In stidy by H. Lian[9] there are issues with substantial monitoring inaccuracy and poor resilience in the conventional approach of electronic voltage transformer condition monitoring. As a result, a brand-new electronic voltage transformer condition monitoring technique based on the L-M algorithm is suggested. Utilizing the Laplace transform, it is possible to determine the connection between the input and output voltages of a capacitor voltage divider in an electronic voltage transformer. Depending on the relationship result with L-M method, the transfer functions model of an electronics voltage transformer is built. The frequency parameters of an electronic voltage transformer as well as the range of typical measurement frequency are analyzed using the transfer function model, and the partial pressure ratios of the electronic voltage transformer underneath the high frequency situation is then obtained. Accordingly, the capacitance value between both the two adjacent coaxial cylindrical fuel tanks of a capacitance divider inside the electronic voltage transformer has been determined by determining the over voltage magnitude on the two sides of the procurement card inside the electronic voltage transformer. This completes the monitoring of the electronic voltage transformer's state. The experimental findings indicate that the suggested approach may significantly increase the dependability of an electronic voltage transformer since it has a low detection mistake and great resilience.

E. Mohns [10] et al. that study describes the configuration of the necessary components as well as the new basic step-up approach for standard voltage power transformer (VTs) there at Physikalisch-Technische Bundesanstalt. The active low-voltage capacitor, with primary and secondary side's voltages among both 5 kV and 800 kV/ 3, is a crucial element. It is made to create capacitive voltage dividers using compressed gas. Low phase errors as well as a minor voltage dependency are characteristics of this divider at 50/60 Hz. A transfer uncertainty once per build-up step of < 110 -6 (k = 2) has been achieved using the additional components, namely a two-stage VT featuring integrated inductive voltage regulator as well as a sampling-based voltage comparison.

DISCUSSION

Types of voltage transformers

Types of voltage transformers based on their construction

There are two main types of potential transformers based on their construction: wound-type and capacitor voltage type.

Wound-type potential transformer

The shell and core type potential transformers are classified as wound-type. The primary and secondary windings are wound on the core limbs with proper insulation. For measuring high voltages (typically greater than 10 kV), the construction becomes complex due to insulation problems. Hence, capacitive potential transformers are used to measure very high voltages.

Capacitive potential transformer

A capacitive potential transformer being connected A capacitive divider and an auxiliary transformers are used in a capacitive potential transformer (Figure 2 labeled A). The need for a high-rated power transformer is removed by the capacitor divider. From across high voltage to somehow be measured is attached a capacitive-divider network (four capacitance) (labeled B). The capacitor begins charging towards the voltage's magnitude whenever it is connected to an AC voltage. The capacitors split the input voltage, bringing down the high voltage level to a minimal figure. Using an auxiliary transformer, the low voltage received from of the capacitive

divider was stepped down (designated D). A capacitive potential transformer, which consists of a capacitor-divider as well as an auxiliary transformer, is described by the darkened area with the letter C in it.

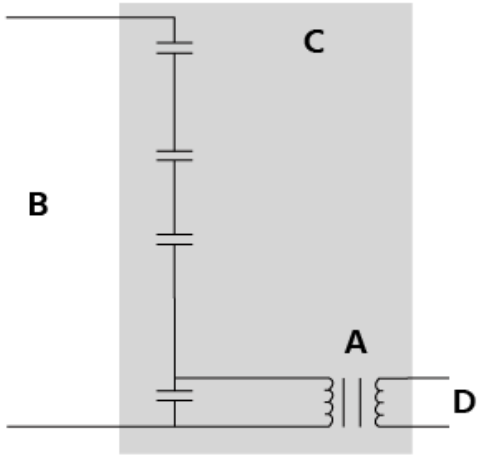

Figure 2: Illustrates the Connecting a capacitive potential transformer.

Voltage transformer types according to operational voltage

Voltage transformers are divided into High-voltage voltage transformers and System voltage transformers depending on the system voltage employed.

Typically, high-voltage potential transformers need an input voltage of at least 69 kV. For monitoring high voltages on distribution transmission lines, these instruments are ideal. Due to the enormous size of the transformer, it is not cost-effective to utilize a single transformer for measure voltages beyond 500 kV. In this situation, two transformer units were cascaded to provide the necessary voltage. Connecting two transformers in parallel is known as cascading. For instance, a transformer with such a turns ratio (number of rotations inside the secondary winding: percentage of turns inside the primary winding) of 1:10000 is necessary to step down a very high voltage of 100 kV to 10V, making the transformer very large. For the same application, two transformers with such a turn's ratio of 1:100 may be employed. The main winding of a second transformers receives a feed of 1 kV, which the first transformer reduces from an input voltage that is 100 kV. The output of the second transformer reduces the 1kV input voltage to 10V. In order to achieve the same voltage conversion as just a single transformer, but now with significantly less size and construction constraints, transformers may be cascaded.

Transformers supporting medium-voltage voltage

According to the IEEE standard, medium voltage is often used to describe realistic voltage levels (incoming voltage) between 5kV and 35kV. High-voltage distribution lines are those that carry a voltage more than 35 kV. After stepping down overall distribution line voltage to a level acceptable for consumer usage, a medium-voltage distribution transformer delivers the last voltage transformation inside a system that distributes electricity. Depending on the amount and range of the input voltage, these transformers are perfect for both outdoor and indoor applications (see Table 1). The system voltage mentioned for various voltage transformer types is provided for informative reasons only; actual values may change depending on the applicable IEEE, IEC, and ANSI standards.

Table 1: Illustrates the various types of voltage transformer specification.

Transformer Type	Construction	Insulation type	System voltage	Indoor/outdoor applications
Low voltage	Single-phase, Three-phase	Resin cast, tape wound	440V	Indoor
Medium voltage	Single pole three-phase, Double pole three-phase	Resin cast	3.3 kV-33kV	Indoor and outdoor
Medium voltage	Single-phase earthed type	Oil-immersed	3.3kV-33kV	Outdoor
High voltage	Single-phase earthed type	Oil-immersed	66kV and above	Outdoor

Transformers for low-voltage voltage

With an input voltage that is less than 600V, a low-voltage transformer can operate. This transformer serves as an auxiliary source of electricity in the motor control panel as well as with measurement or monitoring devices.

Potential Transformer Errors

In a perfect transformer, the main and secondary voltages are in-phase and exactly proportional to the turns ratio of the transformer. However, in practice, the reactance at the primary causes a voltage drop, which leads to phase-shift and voltage ratio errors. Here are a few PT faults that might happen.

Ratio Error

The difference in load causes a change in the voltage ratio, which is the ratio error. Variable load alters the core losses and magnetizing current, which modify the secondary voltage of the PT. Its nominal ratio and real ratio are different, to put it simply. Ratio mistake may be found via.

$$\text{Ratio Error} = (\text{Nominal Ratio} - \text{Actual Ratio}) / \text{Actual Ratio}$$

$$\text{Ratio Error} = (K_n - R)/R$$

$$\% \text{ Ratio Error} = \{(K_n - R)/R\} \times 100$$

Where,

Nominal Ratio = Kn (Rated Ratio)

Actual fundamental to secondary reference voltage is denoted by R.

The rated primary energy to rated secondary reference voltage is known as the nominal ratio.

Error in Voltage Ratio

The discrepancy between both the ideal voltage and the actual voltage is known as the voltage ratio error. The formula for determining voltage ratio error is given below.

$$\text{Voltage Ratio Error} = (V_P - K_n V_S)/ V_P$$

$$\% \text{ Voltage Ratio Error} = \{(V_P - K_n V_S)/ V_P\} \times 100$$

Where,

K_n = Nominal Ratio (Rated Ratio)

V_P = Actual Primary Voltage

V_S = Actual Secondary Voltage

Phase Angle Error

The discrepancy between the main voltage's phase and the inverted secondary voltage is known as that of the phase angle error. The secondary voltage should ideally be in phase with both the main voltage. However, in reality, the reactance of a windings affects the secondary voltage's phase, resulting in phase shift inaccuracy.

Phasor of a Potential Transformer

The potential transformer's phase shift. The primary current IP, primary voltage VP, secondary current IS, and secondary voltage VS are shown in this phasor diagram.The primary flux m serves as the reference for the provided phasor diagram. By subtracting losses brought on by the primary and secondary windings resistance RP and reactance XP, the primary generated voltage is obtained. The reactance of a windings equals IPXP, while the voltage drop resulting from the main windings equals IPRP. The magnetizing potential Im and core loss current IW are added to provide the excitation current Io. The primary current IP is produced by multiplying the turn ratio 1/Kn by the vector sum of the excitation current Io and the reversing secondary winding IS. The main emf will change into in the secondary emf ES inside the secondary windings as a result of mutual inducement. Simply subtract the voltage dips caused by the secondary winding's impedance RS & reactance XS yields the secondary voltage VS something which is seen at the secondary windings' output.

CONCLUSION

An efficient market should not have significant overreaction or under reaction that causes unjustified volatility since participants possess access to all information. A market like this would provide price signals that correspond to changes in the fundamentals. However, markets in the real world have flaws, and ex ante and ex post consequences of news are often illogical. Supply and demand are wildly out of whack, which causes an imbalance in orders and maybe excessive volatility. Price research is hampered. Despite the fact that these flaws are biological in nature—arising from the free will of market agents—the implementation of circuit breakers is indeed a legal requirement. Collars on security prices were introduced as a market stability measure, drawing inspiration from electrical engineers whom employ an automatic switch to safeguard a circuit against current overload.

References:

[1] A. Arroyo, R. Martinez, M. Manana, A. Pigazo, and R. Minguez, "Detection of ferroresonance occurrence in inductive voltage transformers through vibration analysis," *Int. J. Electr. Power Energy Syst.*, 2019, doi: 10.1016/j.ijepes.2018.10.011.

[2] K. Wang, H. Liu, Q. Yang, L. Yin, and J. Huang, "Impact transient characteristics and selection method of voltage transformer fuse," *Energies*, 2019, doi: 10.3390/en12040737.

[3] M. Faifer, C. Laurano, R. Ottoboni, S. Toscani, and M. Zanoni, "Harmonic Distortion Compensation in Voltage Transformers for Improved Power Quality Measurements," *IEEE Trans. Instrum. Meas.*, 2019, doi: 10.1109/TIM.2019.2906990.

[4] Z. Meng, H. Li, C. Zhang, M. Chen, and Q. Chen, "Research on the reliability of capacitor voltage transformers calibration results," *Meas. J. Int. Meas. Confed.*, 2019, doi: 10.1016/j.measurement.2019.07.011.

[5] H. Liu, K. Wang, Q. Yang, L. Yin, and J. Huang, "On-line detection of voltage transformer insulation defects using the low-frequency oscillation amplitude and duration of a zero sequence voltage," *Energies*, 2019, doi: 10.3390/en12040619.

[6] J. Diazdelacruz and M. A. Martin-Delgado, "Quantum information remote carnot engines and voltage transformers," *Entropy*, 2019, doi: 10.3390/e21020127.

[7] W. Wu *et al.*, "Benchmarking daily line loss rates of low voltage transformer regions in power grid based on robust neural network," *Appl. Sci.*, 2019, doi: 10.3390/app9245565.

[8] M. Lahame, M. Chraygane, H. Outzguinrimt, and R. Oumghar, "Optimization of a three-phase tetrahedral high voltage transformer used in the power supply of microwave," *Int. J. Adv. Comput. Sci. Appl.*, 2019, doi: 10.14569/ijacsa.2019.0100534.

[9] H. Lian, "The state monitoring method of electronic voltage transformer based on L-M algorithm," *J. Adv. Comput. Intell. Intell. Informatics*, 2019, doi: 10.20965/jaciii.2019.p0385.

[10] E. Mohns, J. Chunyang, H. Badura, and P. Raether, "A Fundamental Step-Up Method for Standard Voltage Transformers Based on an Active Capacitive High-Voltage Divider," *IEEE Trans. Instrum. Meas.*, 2019, doi: 10.1109/TIM.2018.2880055.

CHAPTER 20

OVERVIEW ON THE ROLE OF CURRENT TRANSFORMER

Mr. Vivek Jain, Associate Professor,
Department of Electrical Engineering, Jaipur National University, Jaipur, India,
Email Id-vivekkumar@jnujaipur.ac.in

Abstract:

The current of another circuits is measured using a Current Transformer (CT). Across national electricity networks, CTs are utilized to monitor high-voltage lines. A CT's secondary winding is made to generate an alternating current proportionate to the main current it is monitoring. The current transformer does this by reducing a high current to something like a lower value, making it possible to safely check the electrical current passing through a transmission line with AC. In this chapter author is discusses

Keywords:

Current Transformer, Equipment, Power System.

INTRODUCTION

Power systems are more complex than first seems. Although we cannot truly see electricity, we can see how it functions. Electrical power is made up of several different components that fit together like a jigsaw, one of which is a current transformer. What you need know about this crucial piece of gear is as follows: A current transformer is an appliance that generates an alternating current proportionate to the AC current inside its primary in its secondary. When a current or voltage becomes too high to monitor directly, this method is often utilized. When the main and secondary circuits are isolated, the generated secondary current is appropriate for measuring devices or processing in electronic equipment. This decrease in high-voltage currents makes it possible to easily and securely use a normal ammeter to measure the actual electrical charge flowing inside a transmission line with AC. A voltage or current transformer has several turns as its main winding, while an electrical CT has only a single or a few. It differs from a current transformer because the main current is regulated by such an external load rather than being reliant on the secondary grid voltage. The number of secondary turns is identical to the CT ratio. Based on the main wire passing through into the transformer window only once, this ratio.

In the contemporary environment of smart grids with a significant penetration for nonlinear loads but also energy generation from renewable sources, the monitoring of harmonics and electrical quality in general is a crucial job. The most widely used current or voltage transducer throughout power systems today, at all voltage levels, are current and voltage instrumentation transformers (CTs and VTs). As a result, CTs and VTs are used in the majority of measuring devices for power system applications, including power/energy measurement, power performance monitoring, phasor measurement units, etc. Even CTs and VTs with high accuracy classes (i.e., accuracy classes greater than 0.5) may experience nonlinearity effects, according to several experimental studies published in recent scientific literature. The amplitude, phase difference, and order of harmonic components of the sinusoidal waveform all have a significant impact on

the accuracy of a CT/VT as a result of these effects. As a result, the accuracy of the harmonics measured by CTs and VTs may be much lower than that of the accuracy class of an instrument transformer employed in the measurement chain. The application of a non - linear mathematical (either analytic or numerical) framework for the instrument transformer that is capable of precisely reconstructing the primary number of units (i.e., current for CTs and voltage for VTs) from of the measured secondary amount of substance is thus required for accurate measurement of harmonics by the CT or VT. In the scientific literature, many methods for numerically expressing the nonlinearity for instrument transformers have indeed been proposed. In essence, these methods are built on models of the saturation and eddy current phenomena within transformers. However, whenever harmonic distortion was present in the main amount, the performances of a strategic planning process have not been confirmed. The distortion induced by the CT there at secondary is thought to be solely reliant on the basic primary amplitude, notwithstanding the absence of sinusoidal operating circumstances.

Constructing Current Transformers

The silicon steel lamination used to construct the current transformer's core. Making cores using Perm alloy or Meatal allows for a great level of precision. The current that has to be measured travels via the primary windings of a distribution transformer and therefore is linked to the main circuit. The secondary windings of both the transformer, which are linked towards the current windings of something like the meters or even the instrumentation, carry a current that is proportionate to the current that has to be measured. The cores as well as the secondary windings were isolated from one another and from the main winding. The main winding, also known as a bar primary, is a single turn wrapping that carries the whole load current. The transformers' secondary winding features a significant number of turns. The current transformer proportion of a circuit is indeed the ratio between the main current as well as the secondary current. The transformer's current ratio is typically high. The secondary performance figures range from 5 to 1 to 0.1 amps. The range of current main ratings is 10A to 3000A or higher. The evocative image of the current transformer. The current transformer operates on a somewhat different premise than the power transformer. In contrast to power transformers, each current transformer seems to have a slightly different load's impedance or strain on the secondary. Thus, secondary circuit conditions must be present for the current transformer to function.

LITERATURE REVIEW

A. J. Collin [1] et al. the most common current transducers in energy systems, current transformers (CTs), will be required to detect and monitor signals with higher degrees of distortions as harmonic sources become more prevalent. The nonlinear behaviour of the CT, which is reliant here on distortion in the measured signal, may have an impact on the measurement's accuracy, but non - linear mathematical models can indeed be employed to correct the observed value. This work uses a frequency domain system based on tensor linearization to represent the complex ratio of the CT and produces a real-valued compensating matrix. To evaluate how well the CT performs in distorted circumstances, a precise measurement setup has indeed been developed. Experimental findings for large commercial CTs with accuracy classes 0.5 and 1 utilizing the suggested compensating approach are given and discussed. It is shown that using the observed CT distorted secondary current, the suggested approach can precisely recreate the harmonic content (up to several kilohertz) of a CT primary current.

J. Duan[2] et al. the analysis and modelling of the protective distribution transformer, particularly under weak transient saturation, are still not adequate for a broad range of current levels. It is required to construct a mathematical tool that makes it possible to represent both steady and transient modes of current transformers. Multiple test levels spanning 6 to 48 kA transients were acquired with the help of the big current transient test carried out on the actual protective current transformers. An enhanced dynamic regional saturation J-A model is recommended in this research, which is dedicated to the investigation of more accurate modeling for protected current transformers. In order to simulate this same secondary output of a current transformer online, it stresses the excess loss of both the core under transient circumstances and proposes a numerical solution again for suggested dynamic regional saturation J-A current transformer model without iteration. The suggested dynamic partitioned saturating J-A model, the static J-A model, and the dynamic J-A model were compared and confirmed using a variety of data that are genuinely saturated inside the transient flow test. Numerous findings support the usefulness of the suggested approach, which can replicate the protective current transformer fluctuation in the real world. Additionally, a broad range test shows that the average inaccuracy is quite steady.

Z. Li [3] et al. nonconventional instrument transformers having received a lot of attention since there is an increasing interest on a worldwide scale in creating future smart grids. The electronic current transformer (ECT), in contrast to the conventional magnetic core current transformer, somehow doesn't show saturation, has a compact volume, and may provide a digital signal that complies with contemporary digital communication standards like the IEC61850. However, the electromagnetic forces created by the bus bar owing to short-circuit currents and the mechanical vibration brought on by the neighboring circuit breakers (CB) action have an impact on the ECT's measurement accuracy. The root mean square of an ECT output current shall not, in accordance with GB/T 20840.8 and IEC 60044-8 standards, rise over 3% of a rated secondary current after just a 5-ms delay after a CB operation or a significant current of a short period. In order to appropriately pinpoint their terminating moment, the existing ECT vibration compliance testing does not correctly link the ECT output current with both the CB and the big current signal. As a result, the results of the present testing method can be erroneous. The condition of the vibration source is concurrently correlated with the ECT output signal in the novel vibration testing platform for ECT proposed in this study. To acquire and compare the CB status as well as the ECT output current in synchrony, a status monitoring circuitry is suggested and put into practice. A fundamental current sensor is moreover created to precisely realize the finish time of any brief, huge current. To accurately pinpoint the CB breaking moments as well as the termination of the huge current, a software platform is created. Extensive simulation and real-world studies are used to confirm the proposed testing platform's superiority and resilience.

M. Bouchahdane and A. Bouzid[4] despite the significant impact that correct transducers have on accounting systems, we consistently see underestimations in all transformer testing. Additionally, checks considerably lessen the chance of mucking up various instrument transformers or associated connections. Tests may also be used to detect damage caused by transit within a transformer. Last but not least, routine testing is crucial for identifying problems that may happen over a transformer's lifespan, including such shorted coils, degradation of class accuracy from material changes, or modifications to the load. The transformer may become useless for protection if the power distribution topology is altered, since transient actions may cause the transformer to become saturated much sooner than planned. In this essay, we will

examine the current transformer testing procedures used by the national electricity and gas company (Sonelgaz Algeria) and demonstrate how the CPC 100 can be used to perform a variety of electrical test results for CTs with a single device, cutting down on testing cost of time and labor.

M. Kaczmarek and E. Stano[5] requirements and assessment standards for the suggested inductive current transformers' transformation accuracy testing for distorted current are presented in the study. Additionally, a detailed description of the testing process and the constructed measurement equipment with its calibration technique is provided. The harmonic components of a composite error recorded by the differential circuit are used to determine the values of ratio and phase errors across harmonic frequencies to guarantee high accuracy of findings. Equations that are needed are provided. Regardless of the main connection and primary converter type, the proposed approach makes it possible to evaluate the accuracy class extensions enabling quality metering of active and passive instrumentation current transformers. Furthermore, the tested CT's rated secondary current values and those of the reference transducer may vary. The demonstrated use of the established approach supports the necessity for extending standard testing since it yields favorable findings for the 0.1 and 0.2 accuracy classes for multi-range reference inductive current transformers intended to convert sinusoidal current of frequency 50 Hz. A brief summary of alternative measurement methods and the criteria for verifying the transformation accuracy of instrument transformers, both both passive and active, are included in the article. Inductive current transformers' transformation accuracy may decline for greater harmonics of deformed current compared to sinusoidal current at their rated frequency under various circumstances, which are also examined.

According to the M. S. Ballal and M. G. Wath[6] power distribution utilities often utilize measuring current transformers (CTs) to measure energy. The current transformer error compensation unit (CTECU), which is specifically designed to provide compensation to all kinds of measurement CTs, is created in this work. The calculated correction factors, which are dependent on the ratio but also phase angle errors data, form the foundation of the proposed CTECU. The creation of the CT error compensation technique is successfully presented in conjunction with the analytical underpinnings. On 1.0 class and 0.5 class of CTs, CTECU is implemented online in the lab. Under a variety of operating situations, the experimental effectiveness is deemed good. The suggested approach is unusual in that it allows for the conversion of CTs through one class to another.

Authors S. Gu[7] et al. all-fiber optical current transformer has a number of benefits, such as compact size, lack of magnetic saturation, high measurement precision, and excellent protection against electromagnetic interference. The all-fiber optical transformer's exorbitant price, however, prevents widespread use in engineering. This work suggests a design strategy for an independently double acquisition loop that utilizes a single optical route for an all-fiber optical current transformer. First, a two-channel sampling signals need for relay protection as well as an independently dual-acquisition loop design strategy for the all-fiber optical distribution transformer are provided. These are based on closed-loop control technique and open-loop control mode, respectively. An examination of system failure effect cost is used to show the scheme's dependability and economic viability. The findings demonstrate that the strategy can successfully integrate the procurement functionality of two distinct all-fiber optoelectronic current transformer product lines onto a single all-fiber current transformer, immensely reducing the cost of the all- fiber optical current transformer throughout engineering applications.

According to L. Cristaldi[8] et al. in order to calibrate current transformers for use in ac power systems, sinusoidal currents are often applied at various frequencies. This method's primary flaw is that it ignores nonlinearities, which might significantly affect how harmonic current is measured. Test currents that are comparable to those encountered in typical working situations should be used to build a more precise characterization. However, this need a suitable current generator that can accurately produce multitoned waveforms, which is uncommon in labs. A waveform generator, a signal conditioning, and a transformer are used in this research to offer a straightforward method for implementing a current generator that permits increasing the output current capability. The intended current waveform may be linearly pre-filtered in order to make up for the device's unequal input-output response. An ideal compensation filter is simple to construct when the generator is used to replicate a certain class of current waveforms, for example those often seen in ac distribution grids. As shown by actual data, this method enables the cancellation of systematic nonlinearities induced by the transformer and the power amplifier, greatly improving accuracy in comparison to a standard frequency response compensation.

F. Naseri[9] et al. the detection and adjustment of current transformer (CT) saturation using a quick and accurate approach based on the Kalman filter (KF) theory is presented in this study. The extended Kalman filter (EKF) and the current sample points are used by the algorithm throughout the unsaturated sections to create a model that accurately captures the behavior of the current signal. The actual current waveform is recreated during the saturated sections using the obtained model. By creating a criterion based on the EKF algorithm's estimate error, the beginning and end locations of the CT saturation intervals were found. The suggested approach is extremely advantageous since it only needs one sample point to identify CT saturation and it can deal with measurement noise and harmonic issues as well. Numerous test cases acquired utilizing the PSCAD/EMTDC software and real-time hardware implementation have shown these benefits.

According to the S. Biswal and M. Biswal[10] the signal delivered by Intelligent Electronic Devices (IED) to/from the external source is crucial to the safe functioning of the smart grid. The efficient functioning of system parts is crucial for this. The accurate functioning of protective devices may be compromised by measurement error caused by the transient response with instrument transformers like current and voltage transformers. The current transformer (CT) saturation interval is determined using an integrated filtering technique in order to reduce this problem and enhance the performance of protective devices. The technique aids in pinpointing the precise saturation period, allowing signal reconstruction or significant delay logic to be used to prevent the estimate error process. Through the use of a built model in the EMTDC/PSCAD platform, the suggested integrated filtering strategy is evaluated for several crucial instances. Real-time digital simulation (RTDS) findings for noisy signals are also shown. The approach is also contrasted with the current method, and it is determined to be more trustworthy and should be used.

DISCUSSION

Burden on a Load

The burden of a current transformer is the value of the load connected across the secondary transformer. It is expressed as the output in volt-amperes (VA). The rated burden is the value of the burden on the nameplate of the CT. The rated burden is the product of the voltage and current

on the secondary when the CT supplies the instrument or relay with its maximum rated value of current.

Effect of Open Secondary Windings of a CT

Under normal operating conditions the secondary winding of a CT is connected to its burden, and it is always closed. When the current flows through the primary windings, it always flows through secondary windings and amperes turns of each winding are subsequently equal and opposite. The secondary turns will be 1% and 2% less than the primary turns and the difference being used in the magnetizing core. Thus, if the secondary winding is opened and the current flows through the primary windings, then there will be no demagnetizing flux due to the secondary current. Due to the absence of the counter ampere turns of the secondary, the unopposed primary MMF will set up an abnormally high flux in the core. This flux will produce core loss with subsequent heating, and a high voltage will be induced across the secondary terminal.

This voltage caused the breakdown of the insulation and also the loss of accuracy in the future may occur because the excessive MMF leaves the residual magnetism in the core. Thus, the secondary of the CT may never be open when the primary is carrying the current.

Phasor Diagram of Current Transformer

The phasor diagram of the current transformer is shown in the figure below. The main flux is taken as a reference. The primary and secondary induced voltages are lagging behind the main flux by 90º. The magnitude of the primary and secondary voltages depends on the number of turns on the windings. The excitation current induces by the components of magnetising and working current. The secondary current lags behinds the secondary induced voltage by an angle θº. The secondary current relocates to the primary side by reversing the secondary current and multiply by the turn ratio. The current flows through the primary is the sum of the exciting current I_0 and the product of the turn ratio and secondary current $K_t I_s$.

Ratio and Phase Angle Errors of CT

The current transformer has two errors – ratio error and a phase angle error.

Current Ratio Errors – The current transformer is mainly due to the energy component of excitation current and is given as

$$Ratio\ Error = \frac{K_t I_s - I_p}{I_p}$$

Where I_p is the primary current. K_t is the turn ratio and is the secondary current.

Phase Angle Error – In an ideal current transformer the vector angle between the primary and reversed secondary current is zero. But in an actual current transformer, there is a phase

difference between the primary and the secondary current because the primary current has also supplied the component of exciting current. Thus, the difference between the two phases is termed as a phase angle error.

Types of current Transformer

The current transformer is mainly classified into three types, i.e., wound current transformer, toroidal current transformer and bar-type transformers.

Wound Transformer

In this transformer the primary winding is composed inside the transformer. The primary winding had a single turn and connected in series with the conductor that measured the current. The wound transformer is mainly used for measuring the current from 1amps to 100 amps (Figure 1).

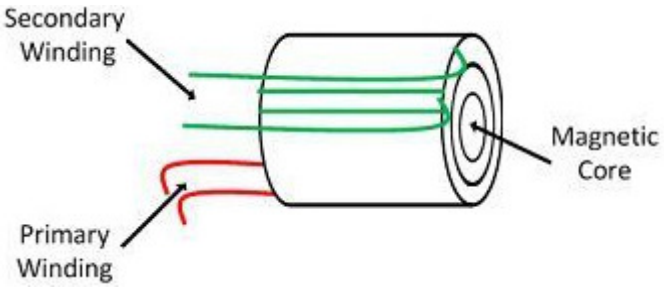

Figure 1: Illustrates the circuit diagram of wound transformer.

Bar-type Current Transformer – The bar type transformer has only secondary windings. The conductor on which the transformer is mounted will act as primary windings of the current transformers in Figure 2.

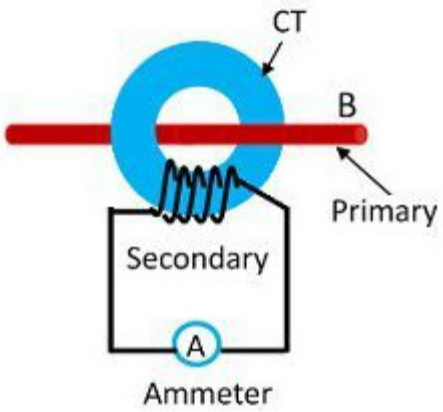

Figure 2: Illustrates the circuit diagram of bar type's current transformer.

Toroidal Current Transformer – This transformer does not contain primary windings. The line through which the current flow in the network is attached through a hole or a window of the transformers. The major advantage of this transformer is that the transformer has a symmetrical shape due to which it has a low leakage flux, thus less electromagnetic interference.

A new age of unconventional instrument transformers and optical communication networks had evolved as a result of the worldwide trend among power utilities to transition from traditional to digital substation automation. Electronic sensors may decrease complicated wiring, do away with laborious specification calculations, improve safety, and make it easier to combine metering, protection, & control into a single device by taking the place of traditional current transformers and voltage transformers. An electronic current transformer (ECT) has a more sophisticated construction than a standard current transformer since it has more parts. When a short-circuit fault occurs and/or a circuit breaker (CB) is operating, this construction is more susceptible to internal deformation and movement of the sensor site owing to external mechanical motion induced by electromagnetic forces. When an optical device is exposed to thermal and mechanical stressors, its birefringence quality changes, depending on whether it is built on magneto-optical glass or fiber optics. As a consequence, the sensor's polarization state will shift, introducing a measurement inaccuracy. The displacement of the conductor owing to a nearby mechanical vibration generator may result in measurement inaccuracy and a failure of the power grid protection system in the case of active ECTs that utilize an air-core coil or a low-power core coil. Additionally, the main conductor and sensor's relative positions will shift as a result of the current-carrying conductors galloping due to unfavorable mechanical vibration, which reduces the precision of the ECT measurement. The literature has suggested a number of methods to lessen the impact of mechanical vibrations here on metering sensors. As an example, there is a proposal for an adaptive vibration canceling method based on linking a solid-state gyroscope with both the metering sensor. The root mean square (rms) of the ECT output current shall not exceed 3% of a rated secondary current after 5-ms after a CB operations, and the highest peak should not exceed 10% of the rated value, in accordance with the Chinese standard GB/T 20840.8 as well as the international standard IEC 60044-8. The effect of mechanical vibration upon that ECT's measurement accuracy was the subject of a research presented by the China Electric Power Research Organization. In this study, the opening and shutting actions of a CB were modelled using a pendulum. However, compared to CB with such a spring mechanism, the vibration frequency and intensity caused by a pendulum motion are very different. However, the impact of short time big current, which is a frequent recurring problem that affects the output of a ECT, has not been mentioned in vibration test for main components mechanically attached to a CB. Additionally, this research did not cover the intricate signal synchronization or the identification of signal mutation locations. A particular technique for identifying the opening and shutting states of the CB was not specified, and the software and hardware components of the suggested test were not presented.

While the Chinese standard GB/T 20840.8 as well as the international standard IEC 60044-8 specify upper and lower threshold limits again for ECT secondary current after that the vibration effect has stopped, they do not take into account the magnitude of that kind of current during in the vibration process or relate the ECT's output to the condition of the vibration source, which could lead to that of an inaccurate evaluation of the ECT's performance. The primary contribution of this study is as follows, based on the debate above: creating a new technology

platform to investigate the performance of a ECT during mechanical motion brought on by short-term large currents in the primary transmission line but also vibration from CB operation; relating resonance reference status information towards the ECT output to precisely monitor the voltage output throughout the vibration process and, in comparison to the current testing practice, determining the ECT's compliance with the standards; creating a primary current sensor that can detect any short-lived big current inside the primary conductor and precisely determine when it ends.

Principle of the Proposed ECT Test System

The status information of the excitation frequency and the merging unit (MU) must be synchronized in order to correctly assess the ECT's vibration properties. Additionally, simultaneous data collection of the ECT's output signal and status information is required. As a result, it is necessary to construct the main current sensor as well as the status monitoring circuit of a CB to continually track, respectively, the short-term high current of the primary conductor and also the closing and opening state of the CB. Figure 3 depicts the suggested vibration platform's architecture. Through the data collection card, the host computer simultaneously gets data from the MU and the vibration generator status monitoring circuitry. To guarantee time synchronization, an external pulse per second signal (PPS) is employed to synchronize both acquisition card as well as the MU. In order to identify the CB disconnection location and the finish times of the big current, the host computer analyzes the two data and simultaneously displays them.

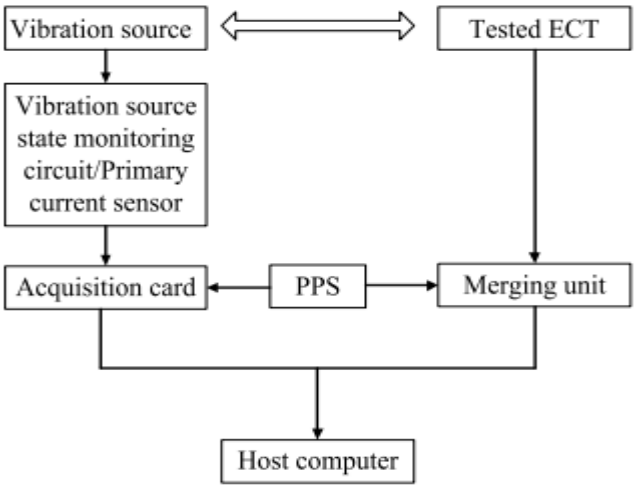

Figure 3: Illustrates the Schematic for the proposed ECT vibration performance test.

CONCLUSION

There is a brand-new platform for assessing ECT vibration performance. To precisely pinpoint the vibration source's terminating point, the suggested testing platform may synchronously link the vibration source's status with the ECT output voltage. Five ECTs from various manufacturers were tested for compliance using the suggested testing platform. Additionally, three ECTs have been used to compare the findings of the new testing platform with the present test method. The

results demonstrate the suggested platform's superiority to the traditional testing methodology, which ignores the vibration source's current condition. The following list contains the main findings of this essay. The novel testing platform has the capacity to thoroughly and precisely evaluate the mechanical vibration characteristics of both the ECT major components under short-term high current of a primary conductor including vibration throughout CB operation.

References:

[1] A. J. Collin, A. D. Femine, D. Gallo, R. Langella, and M. Luiso, "Compensation of current transformers' nonlinearities by tensor linearization," *IEEE Trans. Instrum. Meas.*, 2019, doi: 10.1109/TIM.2019.2905908.

[2] J. Duan, H. Li, and Y. Lei, "Modeling and experimental validation of a dynamic regional saturation J-A model for protective current transformer," *Int. J. Electr. Power Energy Syst.*, 2019, doi: 10.1016/j.ijepes.2018.08.029.

[3] Z. Li *et al.*, "A New Vibration Testing Platform for Electronic Current Transformers," *IEEE Trans. Instrum. Meas.*, 2019, doi: 10.1109/TIM.2018.2854939.

[4] M. Bouchahdane and A. Bouzid, "Testing and protection of current transformer practical experiences in using the cpc 100," *Int. J. Smart Grid Clean Energy*, 2019, doi: 10.12720/sgce.8.2.125-130.

[5] M. Kaczmarek and E. Stano, "Proposal for extension of routine tests of the inductive current transformers to evaluation of transformation accuracy of higher harmonics," *Int. J. Electr. Power Energy Syst.*, 2019, doi: 10.1016/j.ijepes.2019.06.034.

[6] M. S. Ballal and M. G. Wath, "Current Transformer Accuracy Improvement by Digital Compensation Technique," *Mapan - J. Metrol. Soc. India*, 2019, doi: 10.1007/s12647-019-00304-0.

[7] S. Gu, L. Han, D. Liu, W. Yu, Z. Xiao, and T. Feng, "Design and applicability analysis of independent double acquisition circuit of all-fiber optical current transformer," *Glob. Energy Interconnect.*, 2019, doi: 10.1016/j.gloei.2020.01.007.

[8] L. Cristaldi, M. Faifer, C. Laurano, R. Ottoboni, S. Toscani, and M. Zanoni, "A Low-Cost Generator for Testing and Calibrating Current Transformers," *IEEE Trans. Instrum. Meas.*, 2019, doi: 10.1109/TIM.2018.2870264.

[9] F. Naseri, Z. Kazemi, E. Farjah, and T. Ghanbari, "Fast Detection and Compensation of Current Transformer Saturation Using Extended Kalman Filter," *IEEE Trans. Power Deliv.*, 2019, doi: 10.1109/TPWRD.2019.2895802.

[10] S. Biswal and M. Biswal, "Detection of current transformer saturation phenomenon for secured operation of smart power network," *Electr. Power Syst. Res.*, 2019, doi: 10.1016/j.epsr.2019.105926.

CHAPTER 21

RELAY COORDINATION CONCEPT

Mr. Sunil Dubey, Associate Professor,
Department of Electrical Engineering, Jaipur National University, Jaipur, India,
Email Id-sunildubey@jnujaipur.ac.in

Abstract:

Relay coordination is a crucial component of protection system design because coordinating systems must provide quick, accurate, and dependable relay operation can isolate the affected areas of the power system. As a result, the relay coordination issue is stated for the Variable structure simulation of a real-time distribution system. In this chapter author is discusses characteristics of relay co-ordination and equipment co-ordination for protection.

Keywords:

Circuit Breaker, Fault, Power System, Relay Coordination, Substation.

INTRODUCTION

The relay co-ordination is nothing but a tripping of protecting relay in a sequence or order in electrical power system. Relay coordination is very difficult task for relay engineers. Relay co-ordination is required to isolate the faulty part with minimized relay & circuit breaker operation (Figure 1).

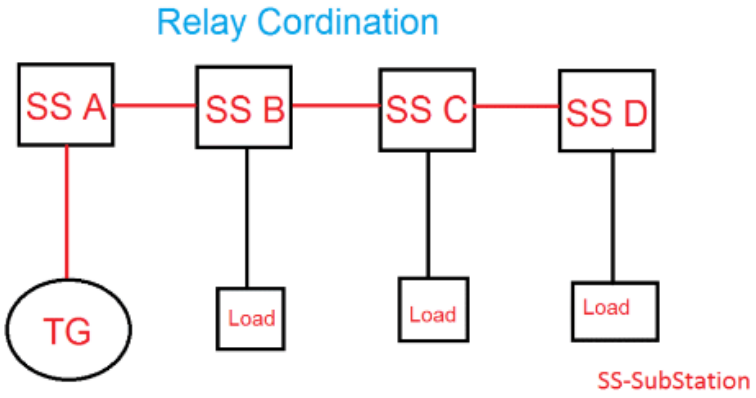

Figure 1: Illustrates the schematic diagram of relay coordination.

Consider four number of substations, Substation A, Substation B, Substation C, Substation D. Here Substation A is generation station and B, C and D are distribution stations. In this, if the fault (short circuit or earth fault) occurs in Substation D means, the substation D relay has to operate, instead of that, the substation a relay operated means such system said to be poor relay coordinated power system. It causes the total power system shutdown or unnecessary zone trips.

Because, there is no fault on substation A, B and C but the substation A operates unnecessarily. In order to avoid such relay operation, we have to set co-ordination between all 4 substations.

Relay co-ordination Procedure for Earth Fault:

All the substation relays current, voltage setting and time setting values will be noted and tabulated.

Check the current setting and operating time of the relay which is associated with the fault. i.e if you are coordinating for earth fault means, you should consider all the earth fault setting.

Adjust the setting i.e the substation D should have minimum operating time and current or voltage setting. Then only substation D operates. If the value is higher than the remaining substation, the substation D relay does not operate under fault condition.

The coordinated setting values would be substation A > Substation B > substation C > Substation D. Also, the setting value of substation should not be exceeded its safe limit.

LITERATURE REVIEW

A. Abbasi [1] et al. the plug-and-play operation of Distributed Generations (DGs) modifies the fault current levels, resulting in Directional Over-Current Relay (DOCR) miss-coordination with subpar tripping times. To combat the negative impacts of DGs on the distribution network, adaptive protection is indeed a fantastic option. While non-adaptive coordination results in long relay operation times, some adaptive protection coordination for any and all DG connection situations necessitates extensive communication infrastructure and equipment modification. The novel adaptive protection idea is presented in this work as a trade-off, where the parameters of a relay are adjusted dependent on the connection to nearby DGs. The suggested sensitivity matrix is calculated in order to determine the number possible Settings Groups (SGs) for each DOCR. Only relays experiencing significant variations in short circuit levels get the SGs. The results of the suggested method's simulation on the IEEE-30 Bus show its potential for effective and ideal construction of adaptive protection systems with suitable SGs allocation.

T. S. Ustun and S. Ayyubi[2] Microgrids, in contrast to traditional grids, may make use of various connections, and the overall topology may change. A new protection concept or system has to be created in light of this in order to ensure safe functioning. In these dynamic microgrid arrangements, maintaining appropriate selective functioning of the relays is a problem in and of itself. Monitoring the connections while adjusting the relays' time delays is necessary to maintain the intended system hierarchy. This research adopts a unique technique in which graph theory is used to represent electrical networks. To automatically identify topology changes and guarantee correct protection operation, clever techniques are used, such as network graph discovery, local manager selection, and differential protection strategy. The hazards connected with central controller-based systems are also reduced by this method's dispersed nature. The created approach offers a distinct implementation in post-disaster recovery and is applicable to everyone power system activities. This self-diagnosis, self-healing system may recognize healthy areas after a tragedy or terrorist assault and operate them alone until help comes. Any healthy portion of the system may be reorganized and used without dependence on any central controller and link since the protective system can be operated as a distributed control.

M. M. Eissa[3] modern power systems are more vulnerable to wide-area disruptions due to the intricacy of their interconnectivity, which has led to a number of system protection failures in both standalone and multi-zone operations. The functioning of the present system protection is negatively impacted by the significant penetration of doubly-fed-induction-generator wind turbines in the power grid, and during fault occurrences the sensing components of the current signals degrade quickly owing to the high crowbar resistance. Relays that run in standalone mode and only rely on current magnitude may be dropped in such circumstances. For the protection of a big, linked grid in the future, standalone relays are an inadequate answer. In order to improve protection schemes, wide area monitoring has indeed been created, but sadly it is only compatible with backup protection applications and does not operate in independent mode. Over 70% of wide-area disruptions are brought on by relay mis-operation as a result of improper protection settings and coordination issues. The notion of the idea acts as a one-zone and is independent of then short-circuit current magnitude. The proposed concept is based on applying differential equations to describe the dynamic behavior of the lines before and following the faults. In a phase-diagram, the orbits are moved to solve the differential equations.

J. Hong[4] et al. in that research, novel domain-based cyber-physical security concepts are proposed for the detection and mitigation of cyber-attacks on substation automation systems. The suggested techniques serve as the framework for a distributed security domain layer which allows substation protection devices to cooperatively fight against cyberattacks. The approaches may execute real-time power system analyses to assess the effects of the control instructions and use protection coordination principles to cross-check protection configuration modifications. To stop data injection attacks using fake sampling values, the transient fault signature (TFS)-based cross-correlation coefficient approach has been suggested. Commercial relays and just a real-time digital simulator was used in a hardware-in-the-loop (HIL) simulation to validate the suggested functionality (RTDS). The effectiveness of the proposed research-grade cyber-attack mitigation capabilities is validated by testing a variety of cyber incursions to determine the effects and repercussions of cyber-attacks on the power grid.

P. Khandare [5] et al. the proposed approach offers a clever method of microgrid protection. This research presents a novel discrete wavelet transform-based method for feature extraction from a faulty current waveform. Additionally, other metrics such as TMS (Time Measurement setting), PSM (Plug setting Multiple), and CTD (coordination time Duration) are calculated from the highlighted defective current. This strategy was used to create a genetic differential algorithm for selecting the best relay pair under the "survival of the fittest" theory. The IEEE 9 bus system is taken into consideration for the various fault kinds for utility-connected and standalone mode. When a main pair of relays is first turned on, the secondary protection kicks in. This research provides an efficient method for a pair of relays to operate quickly and efficiently.

R. Naves [6] et al. In order to use Physical-Layer Network Coding (PLNC) as an interference control method in multi-hop wireless networks, this concept is revisited. We point to one major factor preventing it from becoming a mainstay in big networks as being its close linkage to the Two-Way Relay Channel (TWRC). They present SE-PLNC (Source-Encoded PLNC), a novel PLNC strategy that relies only on one-hop neighbors for coordination and is independent of traffic patterns, making PLNC substantially more practicable to implement in multi-hop wireless connections. In order to achieve this, SE-PLNC implements three innovations: it combines bit-level and physical-level network coding; it transfers the majority of the coding burden from the transmitter to the source of the PLNC scheme; and it takes advantage of the multi-path relaying

opportunities offered by a specific traffic flow. We assess SE-PLNC using simulations, theoretical analysis, including proof-of-concept testing on a Universal Software Radio Peripherals (USRP) testbed. Testbed trials demonstrate its viability in the actual world under several diverse channel circumstances. Big-scale simulations demonstrate that SE-PLNC increases network throughput by over 30% when compared to state-of-the-art PLNC schemes. Theoretical research highlights the adaptability of SE-PLNC and its efficiency across large ad-hoc networks.

A. Łukowa and V. Venkatasubramanian [7] Due to their wide bandwidths, 5G systems are anticipated to employ frequency ranges beyond 6 GHz in the so-called millimeter-wave (mm-Wave) spectrum. Higher carrier carrier frequencies are known to have more route loss attenuation. Furthermore, dynamic obstructions might make it difficult to get enough coverage. Cell densification is thus necessary for millimeter-wave installations in order to achieve large data rates. Densification, however, makes it more difficult to build a system since it need low-cost backhaul. The goal of the wireless self-backhauling (sBH) idea is to provide a backhaul option at a lower price. In order to provide variable, backhaul and access on demand, the self-backhaul system takes use of interconnected access and backhaul (IAB) through each base station. Its performance of in-band self-backhauling featuring integrated accessing and backhaul in a real-world street canyon situation is examined in this article. We take into account central scheduling, which efficiently distributes radio resources for access and backhaul on the time slot based with just a half-duplex limitation. Further cross-interference involving backhaul and access is reduced by the central scheduler employing interference cancellation and beam synchronization. Our findings demonstrate that the suggested relaying paradigm is resilient to user offloading to relay cells and provides substantial user throughput increases for cell edge users. Results further demonstrate that the downlink and backhaul spectral efficiency for IAB deployment may be increased by around 10% using interference cancellation receivers.

P. Sookrod and P. Wirasanti [8] due to the widespread use of distributed generation, the traditional structure of distribution networks is fast changing (DG). DG could have a negative impact on how overcurrent relays coordinate their protection in response to different short circuit levels. By preventing malfunction and unneeded outages of the functioning portion of the system, overcurrent relays are essential to ensuring the dependability of the power system. Depending on the installed DG's capacity and location, the relay settings must be modified. Analyzing all operational circumstances is difficult. In order to sustain coordination for protection, it is necessary to study how the existence of the DG affects the current relays. In this research, an overcurrent relay coordination tool is suggested as a solution to the relay coordination issue. This utility was created utilizing the adaptive protection system approach. Automatic relay setup settings are set in response to shifting systems. Additionally, this suggested tool is appropriate for the intricate future radial distribution systems.

M. M. Eissa [9] has many parallel transmission lines are used in the contemporary power system and the intricately linked smart grid to improve security and dependability. Relay engineers are now facing challenging circumstances regarding system coordination and operation time of the distant relays as a result of the existing complexity of a large-scale power system architecture. Protection of parallel and single lines is provided by a brand-new centralized wide-area monitoring system. On the real, connected, large-scale power grid, a new wide-area primary protection system that is based on phasor measurement units or "PMUs," is installed. The idea's central tenet is based on the use of differential equations to describe the dynamic behavior of

transmission lines during a failure. The movement of routes in a phase diagram may be used to solve the differential calculus. To improve the performance of the three-dimensional (3D)-Phase Surface, the time is introduced as a third axis to the phase diagram. In 3D - Phase Surface, those solution curves that correspond to the pathways are visually displayed. The solution curves might move in close proximity to or far away from the equilibrium point, showing whether or not the transmission lines are faulty. This idea allows for the accurate identification of the line fault. MATLAB/SIMULINK is used to simulate the network of linked systems. The relay demonstrated a solution to the widespread issues with parallel transmission lines for the very first time.

A. Srivastava and S. K. Parida [10] the micro grid idea of distributed generation has been applied rigorously in the electrical grid of today. Distribution systems undergo variations in their short circuit levels when DG penetration levels fluctuate. As a result, each level's relay settings need be updated. In order to achieve overcurrent relay coordination, this study explores the use of the gravitational search algorithm to identify the ideal settings for relays. For real-world scenarios such systems with various DG penetration levels and failure kinds, the relay parameters needed for such an adaptive numerical relay are derived. Simulink platform is used to simulate a four-bus radial system featuring DG and overcurrent safety, while MATLAB software is used for programming.

DISCUSSION

Despite its benefits, DGs adoption in distribution has a negative impact on the protective system. The DOCR parameters need to be changed to accommodate the new fault current patterns enforced from DGs as a result of how DGs contribute to short circuit levels changing. The protection parameters should meet both sensitivity and selectivity including all modes of operation since plug-and-play operation of DGs generates various sets of fault currents. Investigated are the effects of DG penetration on coordination loss, annoyance tripping, and protection blindness. For all DGs connection status modes, DOCRs coordination is employed. To determine the worst coordination constraint, which includes constraints pertaining to all topologies, interval linear programming is employed. The N-1 criterion-based optimum coordination in microgrids is achieved using the optimization framework. A hybrid genetic algorithm-linear programming approach is employed for quick convergence in order to improve the optimization process owing to the large number of constraints coming from various modes of operation. For various topologies, relays having time-current-voltage characteristics are coordinated. Due to the voltage dependent nature of these relays, DGs penetration-related mis-coordination are less likely to occur. In order to combat the impact of DGs on load currents, voltage dependent relays are utilized, where the settings of the relays are adjusted depending on the measure voltage. In an effort to reduce the reliability indices, a novel coordination technique based on the relative position of the DGs and the fault is being investigated. The coordination of overcurrent relays is carried out for various grid operating conditions, such as topology changes and DG plug-and-play.

Due to the excessive operation duration of the relays caused by this method, cables and transformers may be harmed. To reduce the contribution of the DGs and reestablish the coordination of the protection, fault current limiters (FCLs) might be utilized. At the point of connection for the microgrid, a unidirectional fault current limiter was added to stop the microgrid from contributing to upstream grid faults. To cope with DGs connection status

uncertainty and save installation costs, fault current allocation using minimax regret criteria is developed. In a microgrid, fault current limiters are employed to restrict the fault currents that are linked to the grid, and they have a single setting for both modes of operation. FCLs are often put at the DG terminal to restrict the amount of fault current that the DG may inject, preventing the DG from providing reactive power assistance during failures. The DOCRs settings were adjusted depending on the DGs connection state in adaptive protection, which is a fantastic way to deal with DGs connection uncertainties. It is suggested to use a simple adaptive protection where trip characteristics of relays are modified depending on local knowledge. The use of directional interlock with circuit breakers having adjustable tripping curves is recommended as adaptive protection for microgrids. For adaptive protection of the distribution grid, a full communication network including Intelligent Electronic Devices (IEDs) are used, and the settings of the relays are determined for various grid loading conditions and DG penetration. A proposal for online adaptive protection coordination uses the predicted venin equivalent impedance for short circuit calculations. A multi-agent technique is used to adaptively adjust the relay parameters depending on the DG's connection state and control mode. It is also recommended to use a branch contribution factor matrix to reduce the influence of DGs and restore the accuracy of relay settings. We study online adaptive protection including computation of relay settings and fault current. For new operating modes, fault currents associated relay settings were computed; after comparison, these new settings are transmitted to the relays. The minimal fault current and indeed the load current of each mode are conveyed to the protective relays as part of a dynamic adaptive protection scheme to restore the sensitivity of a relays. Distribution grids with low fault currents may also utilize adaptive protection based upon positive and negative sequencing currents. Based upon that probabilistic miss-coordination index, a cooperative multi agent system is developed in for adaptive protection of the microgrid.Relay protection is an important tool in all linked power systems. These programs extract then for a relay protection device is indeed a key component of all linked power systems. These systems use a healthy network to divide fault spots. A defect may be found by keeping an eye on many changes. These include variations in temperature, frequency, current, and voltage. The only thing that can guarantee quick and dependable relay functioning is good relay coordination.

Relay coordination characteristics

The protective relay coordination in a transmission network aids in obtaining sensitivity. Additionally, it facilitates rapid fault removal. Therefore, industries work to get the ideal relay arrangement.

Reliability: A relay system has to function properly. Additionally, it must function properly. Reliability is the level of assurance under these circumstances. In other words, the dependability of the protective system depends on how sound it is.

Selectivity: To be more selective, reduce service gaps, and guarantee continuous service, a protective system must isolate the tiny component of the fault state.

A protective system has to operate quickly. It ought to quickly pinpoint the problematic locations. Thermal stress is reduced as a result. Additionally, it lessens the harm that equipment short circuits do.

A power system protection relay should be straightforward. In a simple system, errors may be rapidly located and fixed.

Sensitivity: A quick and responsive protection system may quickly identify small fault situations. When there is a high impedance problem, sensitivity is crucial.

Economics: Installing a protective system that is effective will be expensive. The ideal scenario would be to maximize protection while keeping costs low.

Equipment Coordination for Protection

They examine the characteristics curves of circuit breakers and fuses during coordination investigation. You then compare them using a log plot. Overlapping curves show mis-coordination if there is any.

Planning and gathering of data:

One must gather certain information before to the coordination research. To gather data and strategize, follow these steps. First, draw a single line schematic of the electrical system that includes information on equipment rating. Gather information about load flow and short circuits. Determine the maximum and lowest defective current value for both an earth fault and a phase fault. These numbers need to apply to every relay site. Obtain information on time-current curves and setting ranges. Gather information on transformer connections and the features of protective devices as well. All power transformers' voltage setting values should be noted down. Obtain information on winding connections as well. Find out the switching circumstances in both normal and emergency situations. Gather information on the impedance of transformers and related networks. Additionally, learn about conductor diameters, types, and installation techniques. This database may be used to save device attributes for later usage.

Coordinating time duration:

To guarantee selectivity while plotting coordination curves, one must have a temporal gap between various protection devices. They take into consideration a number of elements throughout these times. For instance, tolerance in relay features, relay over travel, and breaker interrupting time. For inverse electromagnetic relays, a closing time gap of 0.4 seconds is allowed. But can cut it down to 0.3 seconds if you are using solid-state relays. Verify the variation between their permitted I2t. The excellent I2t of the upstream device ought to be greater than that of the downstream device. When synchronizing the electromagnetic relay with the fuse, a closing time interval of 0.2 seconds may be specified. You may even cut this time for solid-state relays to 0.1 seconds.

Recent trends

Every day, new technological developments take place. So can't depend on standard relay coordination techniques. Thus, attempts are undertaken to improve protective relaying via innovation. It was previously difficult to use electromagnetic equipment to detect a bearing failure. These days, a current spectrum of carrying frequencies is created using neural network algorithms. These frequencies cover both states, i.e., the motor in its normal state and the motor under load. Frequency variations aid in the detection of any malfunction. Similar improvements may be seen in high impedance fault detection and fault localization systems. Multi-functional

microprocessor relays are another option, and they provide other functions in addition to protection. Some of these include remote communication, data recording, and metering data.

Adaptive Protection Coordination

To overcome the various coordination restrictions for various combinations of DGs connections, adaptive protection may be employed. The SGs in DOCRs allow for the usage of various settings when DGs are operating in plug-and-play mode.

Adaptive Protection Formulation

It is possible to describe the best adaptive protection coordination as an optimization problem with a given objective function.

$$\min \sum_{m=1}^{M} \sum_{f=1}^{f_n} \sum_{i=1}^{n} t_{i,f_i}$$

Where tS, TU is the main relay's working time for a near end fault fS, f stands for the near-end and far-end faults, 'I' stands for primary relay indices, and so forth. The DGs connection mode is represented by the indication m, where M = 2X for a network with n DGs. According to (3), the DOCR's operational time in each mode m is just as follows. Where the connection state of the DGs, obtained through binary inputs, is used to identify the active GS. Since there are often fewer SGs than there are total DG connection statuses, clustering and classification algorithms should be applied. Relay characteristic curves are determined by the DOCR's parameters A and B. The working period of the backup relay should lag behind the coordination time interval sufficiently to assure the protection system's selectivity (CTI). The coordination restriction is shown. CTI typically has a value between 200 and 300 ms. A represents the backup relay indices, and B 0i represents the backup relay's operational time. The fault set at the near and distant ends is A.

$$t_{ij}^{f} - t_{i}^{f} \geq CTI \quad for \; \forall \; f \in \Omega$$

Settings Groups Allocation

To meet with coordination needs in various DGs connection statuses, the GSs of DOCRS should be employed cautiously. Two key factors should be taken into account for the best SG allocation and architectural design of the adaptive protection strategy. The contribution of DGs to fault currents is regionally constrained. The DG considerably modifies the fault currents in the region around it, although distant area relays don't suffer any major fault current fluctuation. This idea is demonstrated in where none of the relay parameters are altered adaptively in response to the DG connection state. Because only near relays are engaged in adaptive protection design, there are many SGs needed. Increase of SGs may be avoided without having a negative impact on the protection system, while the other relays can continue to function with only one GS. Depending on each DG's influence, SGs distribution for relays should indeed be handled cautiously. One key signal for GS allocation might be the sensitivity matrix suggested in the preceding section. A threshold determined by the operator's budget. Should be chosen for the creation of an adaptive protection architecture. The following rule may be used to GS allocation with adaptive protection architecture design that focuses on the sensitivity matrix.

$$if|1 - S_{nm}| \geq s_{th}$$

Only relays with a high sensitivity to the connection state of DGs see an increase in SGs. Ef affects the quantity of SGs and the communication channels. Greater numbers of communication lines and more SGs are related with decreased operation times for relays when threshold values are lower.

Principles of Time and Current Grading

There are several methods to take into account the proper relay coordination utilizing time, overcurrent, and just a combination of the two.

Time Discrimination

In this method, each relay controlling a circuit breaker in the power system is given a sufficient time setting such that the breaker closest to the problem opens first. Each protection unit has an overcurrent relay time delay that affects how the current-sensitive component operates. The relay configuration must allow upstream relays to operate and transmit a signal to the circuit breaker which has tripped and cleared the fault at the site of the problem.

Relay for Standard IDMT Overcurrent

Depending on the needed tripping time and the characteristics of other protective devices employed in the system, the present time tripping features of Inverse and Definite Minimum Time (IDMT) relays may need to be changed. The following standard qualities are defined by this purpose: Definite Time, Very Inverse, Extremely Inverse, and Standard Inverse.

Instantaneous high Currently Relay Over

The source impedance is higher than the protected circuit impedance when high-speed components are utilized. The tripping time at fault levels is thus reduced when the source of impedance is smaller than the protect circuit impedance. Additionally, it makes the discriminating curves following the high set instantaneous devices to be lower, which enhances the overall system grading. Reducing the running duration of the circuit protection by the covered area underneath the discriminating curves is one of the benefits of the high set fast devices. When a feeder malfunctions, the source side relay trips, affecting not just the consumers but also the whole customer base. The other feeds from the same source sided relay help with that, and the breaker also loses power. It is crucial that discrimination be supported when there are errors. The following methods may be used to accomplish this: checking just the current level with current grading and time delay operations for time grading.

CONCLUSION

The majority of the methods discussed above optimize a single goal (mono objective) function, such decreasing the overall working time of a relay. While choosing a protective device has not been suggested in some works, multi-objective optimization has been suggested for coordination challenges of the power distribution system. There are no multiple criteria for fault analysis, coordination assessment, or load flow analysis. As a result, this thesis presents goal functions for decreasing the overall working time of overcurrent relays inside the Della system of power distribution while also allocating several objectives for assessing the coordination among overcurrent protection devices. Electrical systems may suffer significant losses if relay

coordination is lacking. Consequently, it is crucial to plan an Electrical system may sustain significant losses if relay coordination is not there. As a result, you should accurately examine the relay coordination.

References:

[1] A. Abbasi, H. K. Karegar, and T. S. Aghdam, "Adaptive protection coordination with setting groups allocation," *Int. J. Renew. Energy Res.*, 2019, doi: 10.20508/ijrer.v9i2.9266.g7647.

[2] T. S. Ustun and S. Ayyubi, "Automated network topology extraction based on graph theory for distributed microgrid protection in dynamic power systems," *Electron.*, 2019, doi: 10.3390/electronics8060655.

[3] M. M. Eissa, "Developing three-dimensional-phase surface-based wide area protection centre in a smart grid with renewable resources," *IET Energy Syst. Integr.*, 2019, doi: 10.1049/iet-esi.2018.0025.

[4] J. Hong, R. F. Nuqui, A. Kondabathini, D. Ishchenko, and A. Martin, "Cyber Attack Resilient Distance Protection and Circuit Breaker Control for Digital Substations," *IEEE Trans. Ind. Informatics*, 2019, doi: 10.1109/TII.2018.2884728.

[5] P. Khandare, S. A. Deokar, and A. M. Dixit, "Differential algorithm based intelligent protection scheme for microgrid," *Int. J. Innov. Technol. Explor. Eng.*, 2019, doi: 10.35940/ijitee.i3026.0789s319.

[6] R. Naves, G. Jakllari, H. Khalifé, V. Conan, and A. L. Beylot, "When analog meets digital: Source-Encoded Physical-Layer Network Coding," *Pervasive Mob. Comput.*, 2019, doi: 10.1016/j.pmcj.2019.05.002.

[7] A. Łukowa and V. Venkatasubramanian, "Dynamic In-band Self-backhauling for 5G Systems with Inter-cell Resource Coordination," *Int. J. Wirel. Inf. Networks*, 2019, doi: 10.1007/s10776-019-00467-2.

[8] P. Sookrod and P. Wirasanti, "Overcurrent relay coordination tool for radial distribution systems with distributed generation," 2018. doi: 10.1109/ICEEE2.2018.8391292.

[9] M. M. Eissa, "A new wide-area protection scheme for single- and double-circuit lines using 3-D-Phase surface," *IEEE Trans. Power Deliv.*, 2018, doi: 10.1109/TPWRD.2018.2808288.

[10] A. Srivastava and S. K. Parida, "Impact of distributed generation penetration level on relay coordination," 2018. doi: 10.1109/ICPES.2017.8387262.